

**Synthetic, Electrochemical, and Structural
Studies on
Diruthenium(II/III) and Dirhodium(II/II) compounds.**

**A thesis presented to the University of London
in partial fulfilment of the requirements
for the degree of Doctor of Philosophy
in the Faculty of Science.**

By

Holly Jane McCarthy.

**The Christopher Ingold Laboratories,
University College London,
February 1990.**

ProQuest Number: 10797756

All rights reserved

INFORMATION TO ALL USERS

The quality of this reproduction is dependent upon the quality of the copy submitted.

In the unlikely event that the author did not send a complete manuscript and there are missing pages, these will be noted. Also, if material had to be removed, a note will indicate the deletion.



ProQuest 10797756

Published by ProQuest LLC (2018). Copyright of the Dissertation is held by the Author.

All rights reserved.

This work is protected against unauthorized copying under Title 17, United States Code
Microform Edition © ProQuest LLC.

ProQuest LLC.
789 East Eisenhower Parkway
P.O. Box 1346
Ann Arbor, MI 48106 – 1346

To Mum and Dad.

With all my love.

Abstract.

This thesis describes the synthetic, structural, and electrochemical studies on compounds containing dirhodium(II/II) and diruthenium(II/III) units.

Chapter two describes the preparation of a range of diruthenium(II/III) compounds with the general formula $[\text{Ru}_2(\text{RNOCR}')_4\text{Cl}]$. Their electrochemical behaviour has been studied in DMSO. The reduction and oxidation potentials of these compounds have been found to be dependent on the identity and the position of the substituent groups attached to the bridging ligands. The effect of adding silver or chloride ions, to the electrochemical cell, on the number and potential of the redox reactions observed has been investigated.

The compound $[\text{Ru}_2(\text{CH}_3\text{C}_3\text{H}_4\text{NNH})_3(\text{CH}_3\text{CO}_2)\text{Cl}]$, has been studied in detail both structurally and electrochemically and this work is reported in Chapter three. The $[\text{Ru}_2]^{5+}$ core of this unusual mixed ligand compound has been reversibly reduced to $[\text{Ru}_2]^{3+}$ in two one-electron steps and reversibly oxidised to $[\text{Ru}_2]^{6+}$. The effect of chloride and silver ions on the electrochemical behaviour of this compound has also been studied.

Turning to rhodium, Chapter four describes attempts to prepare new compounds with the general formula $[\text{Rh}_2(\text{HNOCR})_4\text{L}_2]$. These have been unsuccessful, but compounds have been obtained with the general formula $[\text{Rh}_2(\text{O}_2\text{CR})_n(\text{HNOCR}')_{4-n}\text{L}_2]$ ($n=0,1,2,3$) which have proved interesting in their own right. These compounds have been studied electrochemically in acetonitrile. The effect of altering the substituent groups R and R' has been studied along with varying n for each set of compounds.

Finally, Chapter five investigates a number of dirhodium(II/II) compounds containing mixed bridging and chelating ligands, $[\text{Rh}_2(\text{O}_2\text{CR})_2(\text{R}'\text{COCHCOR}'')_2(\text{C}_5\text{H}_5\text{N})_2]$ ($\text{R}=\text{CH}_3, \text{C}_2\text{H}_5, \text{C}(\text{CH}_3)_3$; $\text{R}', \text{R}''=\text{CH}_3, \text{CF}_3$). These compounds have been fully characterised using infrared, ^1H n.m.r., and ^{19}F n.m.r. spectroscopy, mass spectrometry and microanalysis. Crystal structures of four of these compounds have been reported. The compound, $[\text{Rh}_2(\text{O}_2\text{CCH}_3)_2(\text{CH}_3\text{COCHCOCF}_3)_2(\text{C}_5\text{H}_5\text{N})_2]$, has been separated into *cis* and *trans* isomers using column chromatography. The structures of each of these isomers reveal a coupling between adjacent molecules in the unit cell via Rh-C interactions.

Table of Contents.

Abstract.	3
Contents	4
Acknowledgements.	10
Abbreviations.	11
Chapter One	12
Introduction.	
1.1 Early advances in the field of metal-metal bonding.	13
1.2 The first diruthenium and dirhodium compounds.	15
1.3 A qualitative view of metal-metal bonding.	17
1.3.1 The molecular orbital approach.	17
1.3.2 The hybridisation (directed orbital) approach.	20
1.4 A molecular orbital picture for bonding in diruthenium and dirhodium compounds.	21
1.4.1 Bonds between two ruthenium atoms.	21
1.4.2 Bonds between two rhodium atoms.	21
1.5 The oxidation and reduction of metal-metal bonded compounds.	23
1.6 The historical development of the chemistry of diruthenium compounds.	27
1.6.1 Diruthenium tetracarboxylates.	27
1.6.2 Diruthenium tetraamidates.	33

1.6.3	Diruthenium compounds containing other bridging ligands.	41
1.7	The historical development of the chemistry of dirhodium compounds.	45
1.7.1	Dirhodium tetracarboxylates.	45
1.7.2	Dirhodium tetraamidates.	48
1.7.3	Dirhodium compounds containing other bridging ligands.	52
1.7.4	Dirhodium compounds containing more than one type of bridging ligand.	56
Chapter Two		60
	Ligand Substituent Effects on the Electrochemical Behaviour of Chlorotetrakis(amidato)diruthenium(II/III) Compounds.	
2.1	Introduction.	61
2.2	Preparation and characterisation.	66
2.3	Electrochemical investigation.	70
2.3.1	Results.	70
2.3.2	Electrochemical behaviour - A rationalisation.	74
2.3.3	Ligand Substituent effects.	84
	a) Identity of the substituent group.	84
	b) Position of the substituent group.	85
2.4	Conclusions.	90
2.5	Experimental.	92
2.5.1	Materials and Instrumentation.	92
2.5.2	Synthesis of $[\text{Ru}_2(\text{O}_2\text{CCH}_3)_4\text{Cl}]$.	93
2.5.3	Synthesis of $[\text{Ru}_2(\text{HNOCH})_4\text{Cl}]$.	93
2.5.4	Synthesis of $[\text{Ru}_2(\text{NHOCCH}_3)_4\text{Cl}]$.	93

2.5.5	Synthesis of other $[\text{Ru}_2(\text{RNOCR}')_4\text{Cl}]$ compounds.	94
-------	-------------------------------------------------------------------------	----

Chapter Three		99
----------------------	--	-----------

A synthetic, structural, and electrochemical investigation into the compound $[\text{Ru}_2(\text{O}_2\text{CCH}_3)(\text{CH}_3\text{C}_5\text{H}_3\text{NNH})_3\text{Cl}]$.

3.1	Introduction.	100
3.2	Preparation and characterisation.	102
3.3	The crystal structure of $[\text{Ru}_2(\text{O}_2\text{CCH}_3)(\text{CH}_3\text{C}_5\text{H}_3\text{NNH})_3\text{Cl}]$.	102
3.4	The electrochemical behaviour of $[\text{Ru}_2(\text{O}_2\text{CCH}_3)(\text{CH}_3\text{C}_5\text{H}_3\text{NNH})_3\text{Cl}]$.	108
3.4.1	Behaviour in dimethylsulphoxide.	110
3.4.2	Behaviour in acetonitrile.	116
3.4.3	Electrochemical behaviour - A rationalisation.	120
3.5	Conclusions.	122
3.6	Experimental.	124
3.6.1	Materials and Instrumentation.	124
3.6.2	Synthesis of $[\text{Ru}_2(\text{O}_2\text{CCH}_3)(\text{CH}_3\text{C}_5\text{H}_3\text{NNH})_3\text{Cl}]$.	124
3.6.3	The crystal structure determination of $[\text{Ru}_2(\text{O}_2\text{CCH}_3)(\text{CH}_3\text{C}_5\text{H}_3\text{NNH})_3\text{Cl}]$.	125

Chapter Four		131
---------------------	--	------------

The electrochemical behaviour of Dirhodium(II/II) compounds containing both carboxylate and amidate ligands.

4.1	Introduction.	132
4.2	Preparation and characterisation.	135
4.3	Electrochemical investigation.	136

4.3.1	Results.	136
4.3.1	Electrochemical behaviour - A rationalisation.	141
4.4	Conclusion.	146
4.5	Experimental	149
4.5.1	Materials and Instrumentation.	149
4.5.2	Synthesis of $[\text{Rh}_2(\text{O}_2\text{CCH}_3)_4(\text{CH}_3\text{OH})_2]$.	149
4.5.3	Synthesis of $[\text{Rh}_2(\text{O}_2\text{CC}(\text{CH}_3)_3)_4]$.	149
4.5.4	Synthesis of $[\text{Rh}_2(\text{O}_2\text{CCH}_3)_n(\text{HNOCC}_2\text{H}_5)_{4-n}]$.	149
4.5.5	Synthesis of $[\text{Rh}_2(\text{O}_2\text{CCH}_3)_n(\text{HNOCC}_3\text{H}_7)_{4-n}]$.	150
4.5.6	Synthesis of $[\text{Rh}_2(\text{O}_2\text{CCH}_3)_n(\text{HNOCC}(\text{CH}_3)_3)_{4-n}]$.	150
4.5.7	Synthesis of $[\text{Rh}_2(\text{O}_2\text{CC}(\text{CH}_3)_3)_n(\text{HNOCC}(\text{CH}_3)_3)_{4-n}]$.	150
4.5.8	Synthesis of bispyridine adducts.	151
Chapter Five.		152
A Synthetic and Structural Investigation into the Compounds		
$[\text{Rh}_2(\text{O}_2\text{CR})_2(\text{R}'\text{COCHCOR}'')_2(\text{C}_5\text{H}_5\text{N})_n]$ ($n=1,2$).		
5.1	Introduction.	154
5.2	Preparation and characterisation.	155
5.3	Structural investigations of $[\text{Rh}_2(\text{O}_2\text{CR})_2(\text{CF}_3\text{COCHCOCF}_3)_2(\text{C}_5\text{H}_5\text{N})_2]$.	163
5.4	Investigation of the <i>cis</i> and <i>trans</i> isomers of	168
	$[\text{Rh}_2(\text{O}_2\text{CR})_2(\text{CF}_3\text{COCHCOCH}_3)_2(\text{C}_5\text{H}_5\text{N})_2]$.	
5.4.1	Separation and characterisation of the <i>cis</i> and <i>trans</i> isomers	170
	of the compound $[\text{Rh}_2(\text{O}_2\text{CCH}_3)_2(\text{CF}_3\text{COCHCOCH}_3)_2(\text{C}_5\text{H}_5\text{N})_2]$.	
5.4.2	Structural investigation of the <i>cis</i> and <i>trans</i> isomers	176
	of the compound $[\text{Rh}_2(\text{O}_2\text{CCH}_3)_2(\text{CF}_3\text{COCHCOCH}_3)_2(\text{C}_5\text{H}_5\text{N})]$.	

5.4.3	A rationalisation of the ^1H n.m.r. spectroscopic results to the solid state structures of the <i>cis</i> and <i>trans</i> isomers of $[\text{Rh}_2(\text{O}_2\text{CCH}_3)_2(\text{CF}_3\text{COCHCOCH}_3)_2(\text{C}_5\text{H}_5\text{N})_2]$.	183
5.5	Conclusions.	184
5.6	Experimental.	185
5.6.1	Materials and instrumentation.	185
5.6.2	Synthesis of $[\text{Rh}_2(\text{O}_2\text{CC}_2\text{H}_5)_4]$.	185
5.6.3	Synthesis of $[\text{Rh}_2(\text{O}_2\text{CCH}_3)_2(\text{CH}_3\text{COCHCOCH}_3)_2(\text{C}_5\text{H}_5\text{N})_2]$.	185
5.6.4	Synthesis of $[\text{Rh}_2(\text{O}_2\text{CCH}_3)_2(\text{CF}_3\text{COCHCOCH}_3)_2(\text{C}_5\text{H}_5\text{N})_2]$.	186
5.6.5	Separation of the <i>cis</i> and <i>trans</i> isomers of the compound $[\text{Rh}_2(\text{O}_2\text{CCH}_3)_2(\text{CF}_3\text{COCHCOCH}_3)_2(\text{C}_5\text{H}_5\text{N})_2]$.	187
5.6.6	Synthesis of $[\text{Rh}_2(\text{O}_2\text{CCH}_3)_2(\text{CF}_3\text{COCHCOCF}_3)_2(\text{C}_5\text{H}_5\text{N})_2]$.	189
5.6.7	Synthesis of $[\text{Rh}_2(\text{O}_2\text{CC}_2\text{H}_5)_2(\text{CF}_3\text{COCHCOCH}_3)_2(\text{C}_5\text{H}_5\text{N})_2]$.	189
5.6.8	Synthesis of $[\text{Rh}_2(\text{O}_2\text{CC}_2\text{H}_5)_2(\text{CF}_3\text{COCHCOCF}_3)_2(\text{C}_5\text{H}_5\text{N})_2]$.	191
5.6.9	Synthesis of $[\text{Rh}_2(\text{O}_2\text{CC}(\text{CH}_3)_3)_2(\text{CF}_3\text{COCHCOCH}_3)_2(\text{C}_5\text{H}_5\text{N})_2]$.	191
5.6.10	Synthesis of $[\text{Rh}_2(\text{O}_2\text{CC}(\text{CH}_3)_3)_2(\text{CF}_3\text{COCHCOCF}_3)_2(\text{C}_5\text{H}_5\text{N})_2]$.	192
5.6.11	The crystal structure determination of $[\text{Rh}_2(\text{O}_2\text{CCH}_3)_2(\text{CF}_3\text{COCHCOCF}_3)_2(\text{C}_5\text{H}_5\text{N})_2]$.	193
5.6.12	The crystal structure determination of $[\text{Rh}_2(\text{O}_2\text{CC}(\text{CH}_3)_3)_2(\text{CF}_3\text{COCHCOCF}_3)_2(\text{C}_5\text{H}_5\text{N})_2]$.	194
5.6.13	The crystal structure determination of $[\textit{trans}\text{-Rh}_2(\text{O}_2\text{CCH}_3)_2(\text{CF}_3\text{COCHCOCH}_3)_2(\text{C}_5\text{H}_5\text{N})]$.	194
5.6.14	The crystal structure determination of $[\textit{cis}\text{-Rh}_2(\text{O}_2\text{CCH}_3)_2(\text{CF}_3\text{COCHCOCH}_3)_2(\text{C}_5\text{H}_5\text{N})\cdot 0.5\text{C}_5\text{H}_5\text{N}]$.	195

Appendix One.	229
Cyclic voltammetry.	
A1.1 Introduction	230
A1.2 Instrumentation.	230
A1.3 The basic experiment.	233
A1.4 The characteristics of a cyclic voltammogram.	233
Appendix Two.	235
Linear free energy relationships - Substituent parameters.	
A2.1 Hammett substituent parameters.	236
A2.2 Taft substituent parameters.	236
A2.3 The use of substituent parameters in this study.	237
References.	240
Publications.	249

Acknowledgements.

I would like to thank my supervisor, Dr Derek Tocher for his guidance, encouragement, and discussion, throughout the course of this work and Dr Glyn Williams for his help with ^1H and ^{19}F n.m.r. spectroscopic measurements. All the research students on the fourth floor deserve my thanks for their help and friendship but are too numerous to name. Particular thanks must go to Dr Elizabeth Morrison for her continual support and friendship.

I am indebted to the University of London for the award of a Departmental Research Studentship (Fees) and to the members of academic staff, in particular Professor M.L. McGlashan, who secured financial support for my final year in the form of the Thomas Witherden Batt Scholarship, the Momber Scholarship, and a Sondheimer Bursary.

Finally, to my family, my thanks to them for their love and support cannot be put into words.

Thank you.

Abbreviations.

General abbreviations.

dth = 2,5-dithiahexane, dmg = Dimethylglyoxime,

DMSO = Dimethylsulphoxide, DMF = Dimethylformamide,

HPLC = High performance liquid chromatography,

HOMO = Highest occupied molecular orbital,

LUMO = Lowest unoccupied molecular orbital, Me = Methyl,

Et = Ethyl, n-Pr = n-propyl, PPh₃ = Triphenylphosphine,

Py = Pyridine, THF = Tetrahydrofuran.

Electrolytes.

BTEAC = Benzyltriethylammonium chloride.

TBAC = Tetrabutylammonium chloride.

TBAP = Tetrabutylammonium perchlorate.

TBABF₄ = Tetrabutylammonium tetrafluoroborate.

TEAC = Tetraethylammonium chloride.

TEAP = Tetraethylammonium perchlorate

Spectroscopic abbreviations.

Infrared spectroscopy:

s=strong, m = medium, w = weak, b = broad.

N.m.r. spectroscopy:

s = singlet, d = doublet, t = triplet, q = quartet

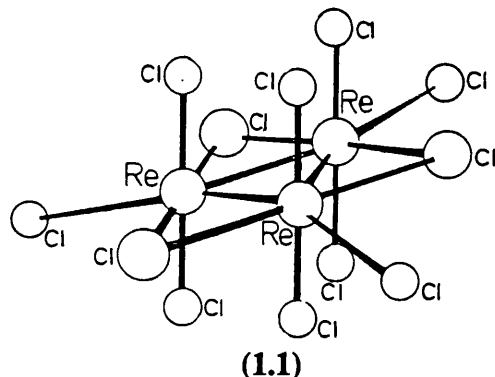
Chapter One.

Introduction.

1.1	Early advances in the field of metal-metal bonding.	13
1.2	The first diruthenium and dirhodium compounds.	15
1.3	A qualitative view of metal-metal bonding.	17
1.3.1	The molecular orbital approach.	17
1.3.2	The hybridisation (directed orbital) approach.	20
1.4	A molecular orbital picture for bonding in diruthenium and dirhodium compounds.	21
1.4.1	Bonds between two ruthenium atoms.	21
1.4.2	Bonds between two rhodium atoms.	21
1.5	The oxidation and reduction of metal-metal bonded compounds.	23
1.6	The historical develop-ment of the chemistry of diruthenium compounds.	27
1.6.1	Diruthenium tetracarboxylates.	27
1.6.2	Diruthenium tetraamidates.	33
1.6.3	Diruthenium compounds containing other bridging ligands.	41
1.7	The historical develop-ment of the chemistry of dirhodium compounds.	45
1.7.1	Dirhodium tetracarboxylates.	45
1.7.2	Dirhodium tetraamidates.	48
1.7.3	Dirhodium compounds containing other bridging ligands.	52
1.7.4	Dirhodium compounds containing more than one type of bridging ligand.	56

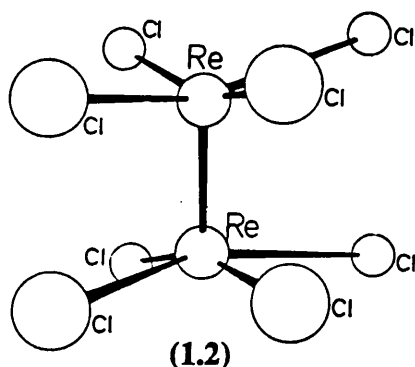
1.1 Early Advances in the Field of Metal-Metal Bonding.

The first evidence supporting the existence of a multiple metal-metal bond was obtained in 1963, when structural studies by two different laboratories^{1,2} on the compound $\text{Cs}[\text{ReCl}_4]$ indicated that this compound contained trimetallic anions $[\text{Re}_3\text{Cl}_{12}]^{3-}$ (1.1). These were suggested to contain triangular Re_3 groups with



two bridging and three axial chloride ions co-ordinated to each rhenium ion, the rhenium ions were linked by double Re-Re bonds (Re-Re 2.477(3) Å)¹. These $\text{Re}=\text{Re}$ bonds were explained by invoking the overlap of the d-orbitals on the metal ions³.

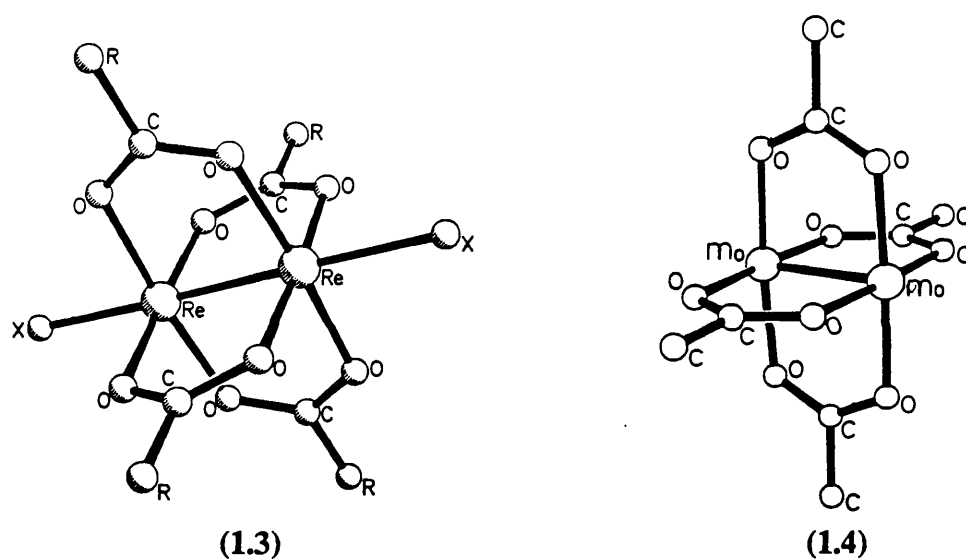
Following a rather confusing report in the Russian literature⁴ of the structure of $[\text{pyH}][\text{HReCl}_4]$, proposing the existence of a $[\text{Re}_2\text{Cl}_8]^{4-}$ anion, work carried out by Cotton and co-workers provided evidence^{5,6} which showed the anion



to be $[\text{Re}_2\text{Cl}_8]^{2-}$ (1.2). This anion contained the first Re-Re quadruple bond to be

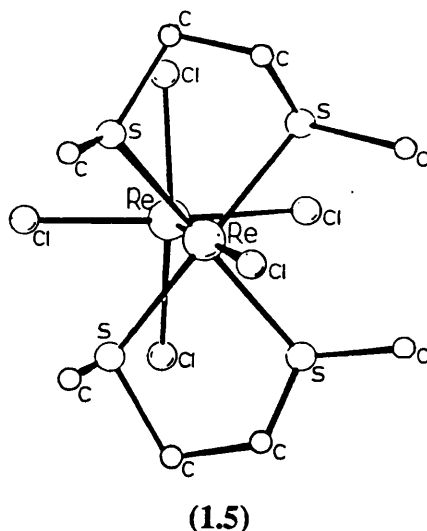
recognised. The structure of the anion, with the chloride ions in an eclipsed configuration, was explained by the fact that d-orbital overlap (leading to δ -bond formation) only occurred if the chloride ions were eclipsed. (The energy of the δ -bond being greater than that arising from the unfavourable steric repulsions, which would give rise to a staggered configuration). A proposal that the Re-Re quadruple bond occurred in compounds of the type $[\text{Re}_2(\text{O}_2\text{CR})_4\text{X}_2]$ (1.3), which were reported at about the same time⁷, was confirmed at a later date⁸.

The recognition of the quadruple Re-Re bond was quickly followed by the publication of the structure of $[\text{Mo}_2(\text{O}_2\text{CCH}_3)_4]^{9,10}$ (1.4) which contained a



quadruple Mo-Mo bond (Mo-Mo = 2.093 Å). Investigations into compounds of technetium were also underway and a structural study of $[(\text{NH}_4)_3\text{Tc}_2\text{Cl}_8 \cdot 2\text{H}_2\text{O}]^{11,12}$ indicated the presence of a $[\text{Tc}_2\text{Cl}_8]^{3-}$ anion (Tc-Tc = 2.13(1) Å), the structure of which was very similar to that reported for $[\text{Re}_2\text{Cl}_8]^{2-}$. The paramagnetic nature of this compound was consistent with an electronic configuration of $\sigma^2\pi^4\delta^2\delta^*$ and a bond order of 3.5.

The structure of an unusual compound $[\text{ReCl}_2(\text{dth})]_n$ (1.5) (prepared by the reaction of 2,5-dithiahexane (dth) and $[\text{Bu}_4\text{N}]_2[\text{Re}_2\text{Cl}_8]$ in acetonitrile) was



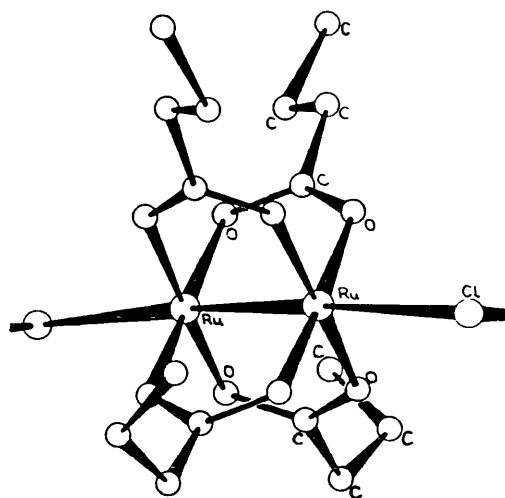
reported in 1966¹³. The staggered rotational configuration of this unsymmetrical molecule indicated the absence of a δ -bond and hence the recognition of the first Re-Re triple bond (Re-Re = 2.293(2) Å).

Following these initial discoveries of multiple metal-metal bonds, work in this area advanced rapidly¹⁴. During this time advances made included the recognition of metal-metal bonds in compounds of diruthenium and dirhodium and it is the study of compounds of these elements which will provide the substance for this thesis.

1.2 The First Diruthenium and Dirhodium Compounds.

As early as 1966¹⁵ the first carboxylates of ruthenium, $[\text{Ru}_2(\text{O}_2\text{CR})_4\text{Cl}]_n$ (R=Me,Et,n-Pr) were prepared. These compounds were unusual in that magnetic susceptibility measurements indicated the presence of three unpaired electrons per diruthenium unit. It was predicted by the authors that the distance between the two ruthenium ions would be too great for a bond to exist and that the two ruthenium ions were in different oxidation states, namely +2 and +3.

The existence of a metal-metal bond in these compounds did not become evident until 1969¹⁶ when the first structure of a chlorotetrakis(carboxylato)

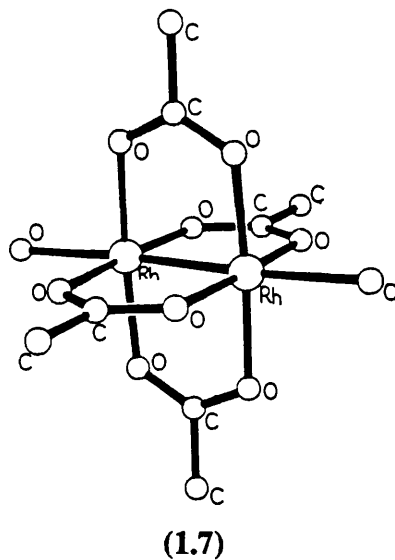


(1.6)

diruthenium(II/III) compound was obtained. The compound, $[\text{Ru}_2(\text{O}_2\text{CC}_3\text{H}_7)_4\text{Cl}]$ (1.6) was found to be polymeric in the solid state with diruthenium units bridged by four n-butyrato groups and linked into chains by axial chloride ions. The Ru-Ru bond distance was 2.281(4) Å, considerably shorter than the shortest contact observed in ruthenium metal (2.65 Å). Structural studies also showed the two ruthenium sites to be structurally, and therefore probably chemically, equivalent, with both rutheniums existing in a non-integer oxidation state of +2.5.

The first tetrakis(carboxylato)dirhodium(II/II) compounds were prepared in the early 1960's¹⁷⁻¹⁹. Structural data on the compound $[\text{Rh}_2(\text{O}_2\text{CCH}_3)_4(\text{H}_2\text{O})_2]$ (1.7), published in 1962²⁰, reported a Rh-Rh distance of 2.45 Å based on two dimensional electron density projections. The accuracy of this report was viewed with some scepticism and in 1970²¹ the structure was reinvestigated. This study reported a considerably shorter Rh-Rh distance of 2.3855(5) Å.

The authors of the two reports^{20,21} viewed the short Rh-Rh distances in



different lights. While one group of authors²⁰ claimed that the bond was a single one, the others²¹ believed the bond length was consistent with a triple bond between the rhodium ions. It was some time before this difference of opinion was settled in favour of the Rh-Rh single bond and the arguments put forward at the time will be discussed more fully in section 1.4.2.

1.3 A Qualitative View of Metal-Metal Bonding.

Before looking in detail at the chemistry of diruthenium and dirhodium compounds it is important to outline the qualitative framework for metal-metal bonding.

1.3.1 The Molecular Orbital Theory Approach.

The most commonly used approach to describe a metal-metal bond in this class of compound is that invoking the overlap of the d-orbitals on the two metal ions.

Five non-zero d-orbital overlaps are possible when two transition metal atoms are brought together. These give rise to five bonding and five antibonding molecular orbitals. The overlap of the d_z orbital from each metal generates a σ -bonding (d_z+d_z) and a σ^* -antibonding (d_z-d_z) orbital. Likewise the overlap of d_{yz} and d_{xz} orbitals generate two degenerate π -bonding ($d_{yz}+d_{yz}$ and $d_{xz}+d_{xz}$) and two degenerate π^* -antibonding ($d_{yz}-d_{yz}$ and $d_{xz}-d_{xz}$) orbitals. Finally overlap of d_{xy} and $d_{x^2-y^2}$ orbitals generate two degenerate δ -bonding ($d_{xy}+d_{xy}$ and $d_{x^2-y^2}+d_{x^2-y^2}$) and two degenerate δ^* -antibonding ($d_{xy}-d_{xy}$ and $d_{x^2-y^2}-d_{x^2-y^2}$) orbitals (Figure 1.1).

The basic concept of the Hückel molecular orbital theory states that orbital energies are proportional to the overlap integrals when the orbitals are of a similar type. Orbital overlap increases in the order $\delta \ll \pi < \sigma$ and hence the order of the molecular orbitals in increasing energy is $\sigma < \pi < \delta < \delta^* < \pi^* < \sigma^*$ (Figure 1.2).

This picture as it stands can only be applied to diatomic M_2 systems. The addition of eight ligand atoms to the system causes a lowering of the symmetry of the molecule. This has no effect on the degeneracy of the π -orbitals but does split the δ -orbitals. This is due to the $d_{x^2-y^2}$ orbitals pointing towards the ligands, whereas the d_{xy} orbitals point between them. Consequently, the $d_{x^2-y^2}$ orbitals become heavily involved in metal-ligand bonding leaving four bonding and four antibonding orbitals to be invoked for metal-metal bonding.

Bond order is defined by the equation

$$\text{Bond order} = \frac{n_b - n_a}{2} \quad \begin{array}{l} n_b = \text{no. of bonding electrons.} \\ n_a = \text{no. of antibonding electrons.} \end{array}$$

This equation can be considered to be a statement of the net number of electron pairs (or fraction thereof) involved in the binding of the two atoms. It does not, except in the broadest sense, give a measure of the bond strength.

Figure 1.1 The five non-zero bonding interactions between the d-orbitals on two transition metal atoms.

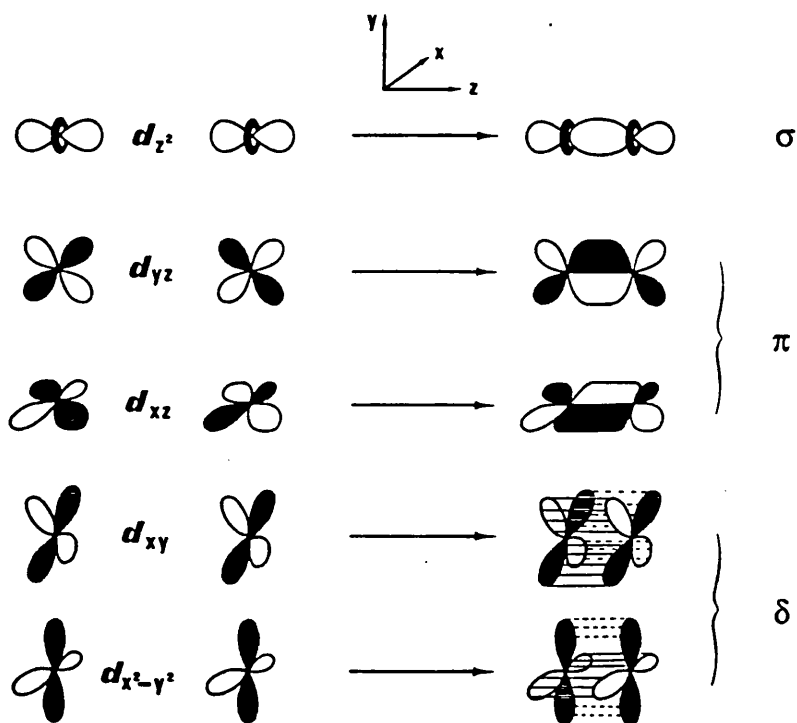
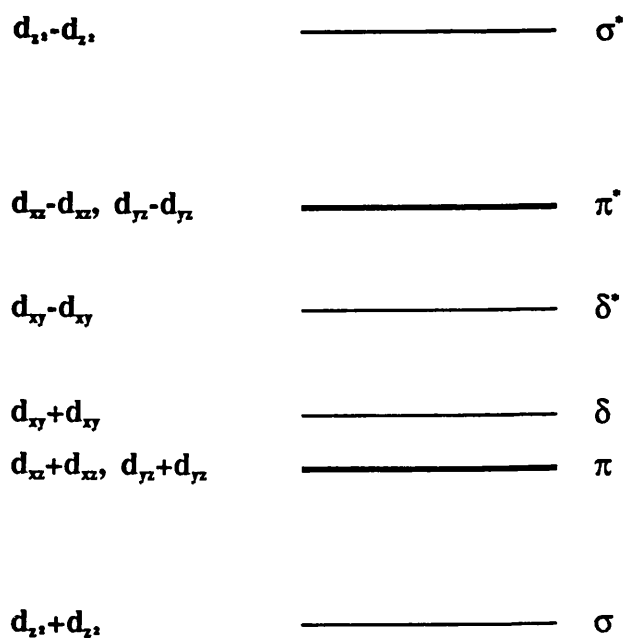


Figure 1.2 The qualitative ordering of the metal-metal bonding and antibonding orbitals.



1.3.2 The Hybridisation (Directed Orbital) Theory Approach.

Valence bond theory, and in particular the hybridisation of atomic orbitals, can also be invoked to describe metal-metal bonding, although this is done less frequently. Using the nine valence shell atomic orbitals a set of hybrid orbitals can be generated (Figure 1.3). The B-type hybrid orbitals are perpendicular to the metal-metal bond and will be used in metal-ligand bonding. The A-type hybrid orbital will be used to bond an axial ligand (if necessary). This leaves the four C-type hybrid orbitals to form up to four "bent" single bonds by orbital overlap with the C-type hybrid orbitals on the adjacent metal atom.

Pauling^{22,23} assumed these bent single bonds to be along the arc of a circle. He used optimum calculated spd bond angles for the angle of the arc, and calculated single bond radii for the arc lengths in order to calculate the expected distance between the two metals (ie the length of the chord corresponding to an arc, twice the single bond radius in length, and at angles equal to the optimum spd bond angles). These chord lengths showed reasonable agreement with the lengths of metal-metal bonds found experimentally. For example the calculated bond length for a quadruple Cr-Cr bond is 1.98 Å (using a single bond radius of 1.235 Å and optimum spd bond angles of 79.24° and 128.8°) compared with 1.975, 1.98, and 2.22 Å found experimentally for $[\text{Li}_4\text{Cr}_2(\text{C}_4\text{H}_8)_4 \cdot 4\text{THF}]$, $[\text{Li}_4\text{Cr}_2(\text{CH}_3)_8 \cdot 4\text{THF}]$, and $[\text{Mg}_2\text{Cr}_2(\text{CO}_3)_4 \cdot 6\text{H}_2\text{O}]$ respectively. The principle failures of this approach are that it does not fully explain the necessity for an eclipsed configuration of ligands when a quadruple bond is invoked and it makes the assumption that the hybrid orbitals are all of equal energy.

1.4 A Molecular Orbital Picture for Bonding in Diruthenium and Dirhodium Compounds.

1.4.1 Bonds Between Two Ruthenium Atoms.

In the case of ruthenium, the metal ions are in the oxidation states II(d⁶) and III(d⁵) therefore supplying a total of 11 electrons to the metal-metal bonding orbitals. The expected electronic configuration from our earlier discussion would be $\sigma^2\pi^4\delta^2\delta^2\pi^*$, with one unpaired electron per diruthenium unit and a net bond order of 2.5. However magnetic susceptibility measurements^{15,24} have indicated the presence of three unpaired electrons per dinuclear unit. SCF-X α -SW calculations²⁵ performed on compounds containing this type of diruthenium unit have shown that the $5_{eg}(\pi^*)$ and the $2_{bu}(\delta^*)$ orbitals are very close in energy and can be considered to be degenerate, consequently the configuration observed is $\sigma^2\pi^4\delta^2\delta^*\pi^2$ (Figure 1.4) with three unpaired electrons per dinuclear unit and a Ru-Ru bond order of 2.5.

1.4.2 Bonds Between Two Rhodium Atoms.

In the dirhodium compounds under discussion here both rhodium atoms are in an oxidation state of II(d⁷), and therefore provide 14 electrons for metal-metal bonding. The electronic configuration predicted based on the simple model is $\sigma^2\pi^4\delta^2\delta^2\pi^*$, giving a bond order of 1.0. This prediction agrees with the bond order proposed by Porai-Koshits and Antsyshkina²⁰ for the compound $[\text{Rh}_2(\text{O}_2\text{CCH}_3)_4(\text{H}_2\text{O})_2]$ and later supported by Dubicki and Martin²⁶, whose extended Hückel calculations indicated a configuration of $\sigma^2\pi^4\delta^2\delta^2\pi^*$, and a bond order of

Figure 1.3 A set of sp³d⁵ hybrid orbitals.

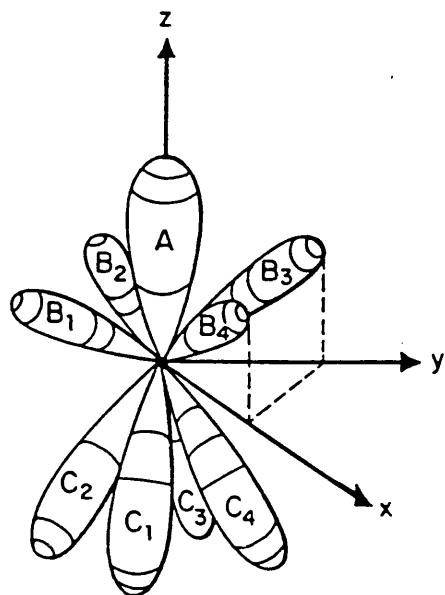
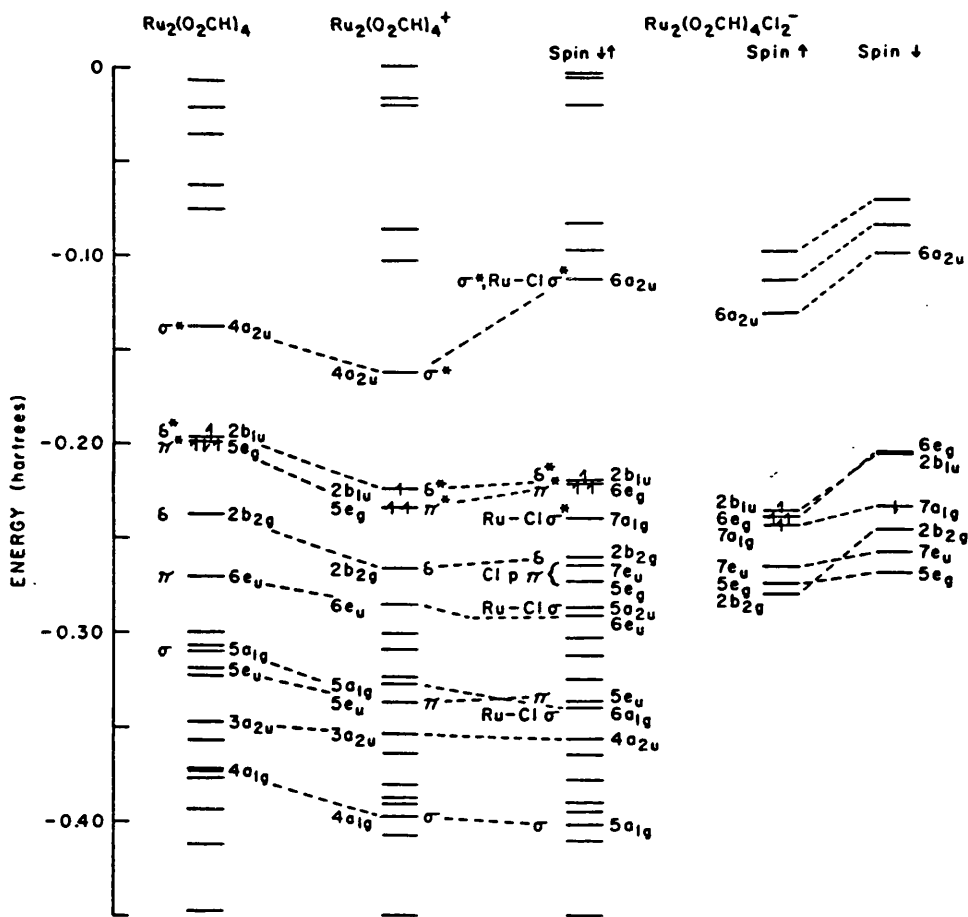


Figure 1.4 The orbital energies for several [Ru₂(O₂CH)₄] species obtained using SCF-X α -SW calculations.



1.0 for this compound.

When $[\text{Rh}_2(\text{O}_2\text{CCH}_3)_4(\text{H}_2\text{O})_2]$ was re-investigated crystallographically by Cotton *et. al.*²¹ the Rh-Rh bond distance was found to be considerably shorter, 2.3855(5) Å, than the originally reported, 2.45(1) Å²⁰. At the time of this study there was only one other structural report on a dirhodium(II) compound, namely $[\text{Rh}_2(\text{dmg})_4(\text{PPh}_3)_2]$ ²⁷, this compound was reported to have a Rh-Rh bond distance of 2.936(2) Å. The 0.5 Å difference in the Rh-Rh bond lengths prompted Cotton *et. al.*^{21,27,28} to propose that the Rh-Rh bond in $[\text{Rh}_2(\text{O}_2\text{CCH}_3)_4(\text{H}_2\text{O})_2]$ must be of a multiplicity greater than one. They put forward the hypothesis that the bond was a triple one and suggested that low lying non-bonding orbitals (mainly Rh 5s and 5p_z) would be filled giving a configuration of $\sigma^2\pi^4\delta^2\sigma_n^2\sigma_n'^2\delta'^2$ (Figure 1.5).

Norman and Kolari²⁹ published the results of SCF-X α -SW calculations on $[\text{Rh}_2(\text{O}_2\text{CH})_4]$ and $[\text{Rh}_2(\text{O}_2\text{CH})_4(\text{H}_2\text{O})_2]$ in 1978 confirming that the correct electronic configuration was $\sigma^2\pi^4\delta^2\pi^*\delta'^2$. The non-bonding orbitals invoked by Cotton *et. al.*²¹ were calculated to be much higher in energy, and unoccupied. The unexpected ordering of the antibonding orbitals was due to an interaction between the d_{xy} orbitals and the π -orbitals of the carboxylate oxygen causing the energy of the δ' -orbital to be greater than that of the π^* -orbitals (Figure 1.6).

1.5 The Oxidation and Reduction of Metal-Metal Bonded Compounds.

Oxidation or reduction of a metal-metal bonded compound will usually have the effect of removing an electron from the highest occupied molecular orbital (HOMO), or adding an electron to the lowest occupied or partially occupied molecular orbital (LUMO), respectively. The addition of an electron to an

Figure 1.5

The qualitative energy level diagram proposed by Cotton *et al.* for $[\text{Rh}_2(\text{O}_2\text{CCH}_3)_4(\text{H}_2\text{O})_2]$.

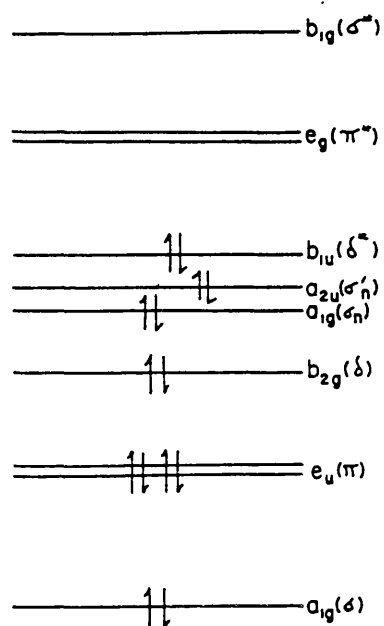
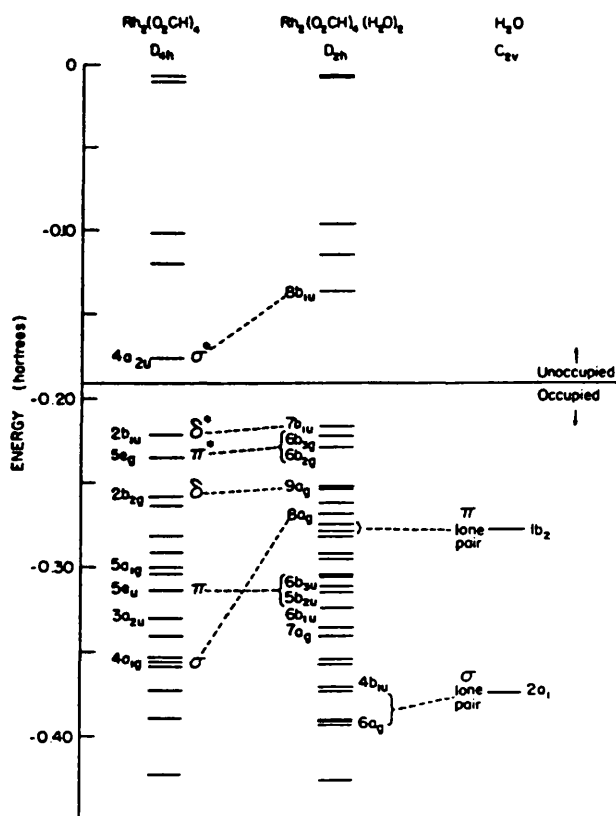


Figure 1.6

The orbital energies for several $[\text{Rh}_2(\text{O}_2\text{CH})_4]$ species obtained using SCF-X α -SW calculations.



antibonding orbital will cause a decrease in the bond order and a consequent weakening of the metal-metal bond, while the addition of an electron to a bonding orbital will have the effect of increasing the bond order and strengthening the metal-metal bond. The removal of an electron would have the opposite effect in each of the above situations.

In diruthenium(II/III) compounds there are three partially filled orbitals as discussed in section 1.4.1. On oxidation an electron will be removed from the highest of these three orbitals while on reduction an electron will be added to the lowest energy orbital. Norman *et.al.*²⁵ studied the compound $[\text{Ru}_2(\text{O}_2\text{CH})_4]^+$ and found that the $2b_{1u}(\delta^*)$ orbital was of higher energy than the $5e_g(\pi^*)$ and so on oxidation an electron would be removed from this orbital. Conversely on reduction an electron would be added to the $5e_g(\pi^*)$ orbital. Since the addition and removal of electrons each involve antibonding orbitals a reduction will cause a decrease in the formal bond order to 2.0, while an oxidation will cause an increase in the formal bond order to 3.0 (Figure 1.7).

In the dirhodium(II) compounds under discussion reduction will add an electron to the $4a_{2u}(\sigma^*)$ orbital, this being the lowest unoccupied molecular orbital. On oxidation an electron would be removed from either the π^* or the δ^* orbital depending on which is at the higher energy. For the compound $[\text{Rh}_2(\text{O}_2\text{CH})_4(\text{H}_2\text{O})_2]$, the $2b_{1u}(\delta^*)$ orbital is of higher energy and so the electron would be removed from there²⁹. Once again the electrons are being added to and removed from antibonding orbitals so a one-electron oxidation will result in an increase in the formal bond order to 1.5 and a one-electron reduction will cause a decrease in the formal bond order to 0.5 (Figure 1.8).

Figure 1.7

Qualitative energy level diagrams illustrating the effect of a one-electron oxidation or reduction on the molecular orbital scheme for a diruthenium(II/III) compound.

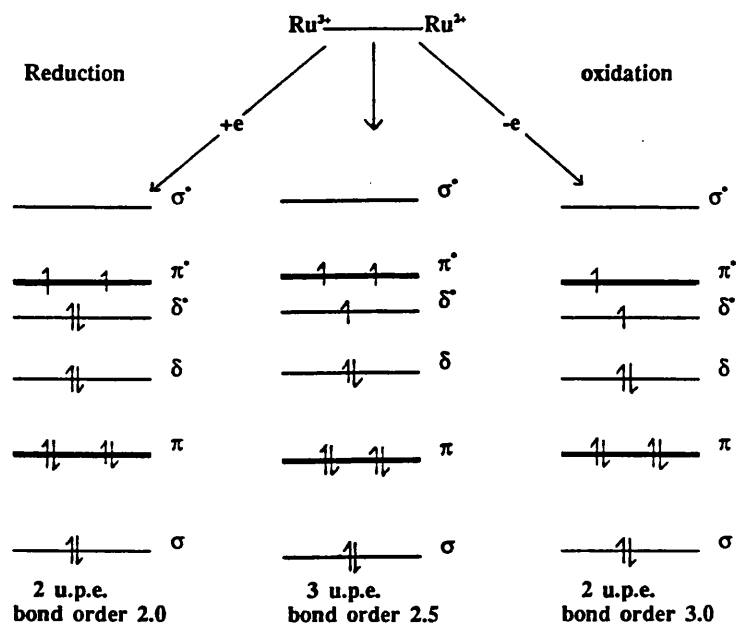
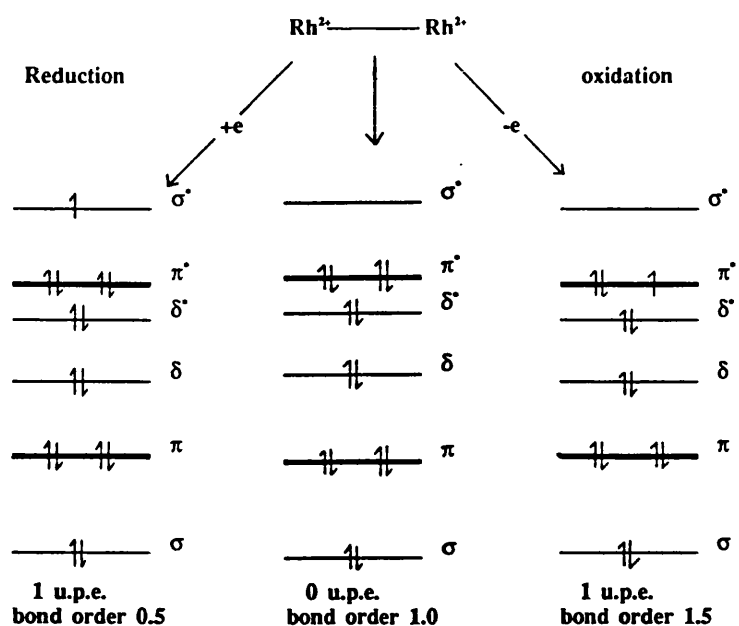


Figure 1.8

Qualitative energy level diagrams illustrating the effect of a one-electron oxidation or reduction on the molecular orbital scheme for a dirhodium(II) compound.



1.6 The Historical Development of the Chemistry of Diruthenium Compounds.

1.6.1 Diruthenium tetracarboxylates.

The initial discoveries of chlorotetrakis(carboxylato)diruthenium(II/III) compounds and the first structural report were discussed in section 1.2. Following this early work there was a gap of several years before the first detailed magnetic and electrochemical studies were reported. Cotton and Pedersen²⁴ investigated the magnetic susceptibility, over a temperature range of 60 to 300 K, and also the electrochemical behaviour in three solvents (CH_2Cl_2 , CH_3CN , $\text{C}_2\text{H}_5\text{OH}$), of the compound $[\text{Ru}_2(\text{O}_2\text{CC}_3\text{H}_7)_4\text{Cl}]$. They confirmed earlier results¹⁵ which indicated three unpaired electrons per diruthenium unit at room temperature and indicated that the magnetic susceptibilities followed a Curie-Weiss temperature dependence in the range 60-300 K.

A one-electron reduction was observed in the potential range 0.00 V to -0.40 V vs. S.C.E. depending on the solvent and electrolyte used. In CH_2Cl_2 (0.1 M TBAP supporting electrolyte) a two step reduction was observed (Figure 1.9) with $E_{1/2}$ values of 0.00 V and -0.34 V. On the addition of chloride ions (TEAC) to the electrochemical cell a decrease in the peak current of the reaction at 0.00 V was observed along with a corresponding increase in the peak current of the reaction at -0.34 V. When the reduction was studied in CH_2Cl_2 (0.1 M TEAC supporting electrolyte) only one reaction was seen at $E_{1/2} = -0.34$ V (Figure 1.10). These results gave the first indication of exchange reactions between the axial chloride ion, and the solvent when these compounds are placed in solution.

The structures of a range of chlorotetrakis(carboxylato)

Figure 1.9

Cyclic voltammogram of $[\text{Ru}_2(\text{O}_2\text{CC}_3\text{H}_7)_4\text{Cl}]$ in CH_2Cl_2
(0.1 M TBAP Supporting electrolyte) scan rate 10 mVs^{-1} .

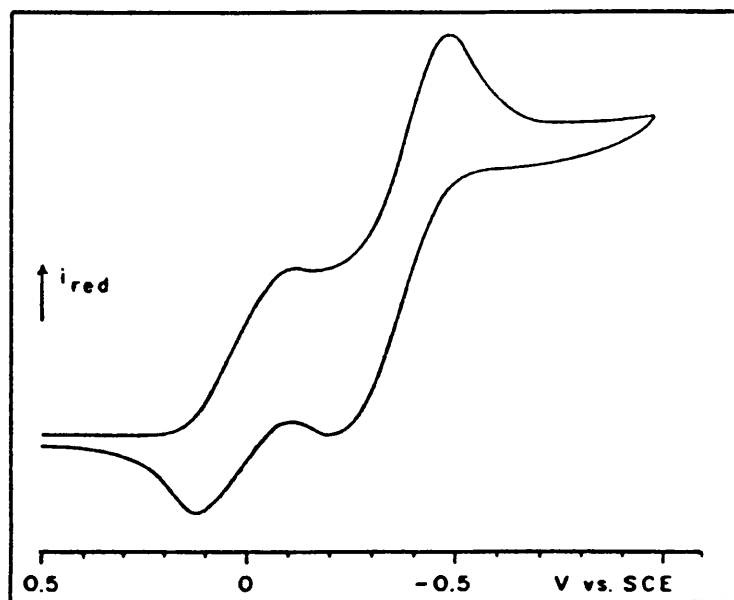
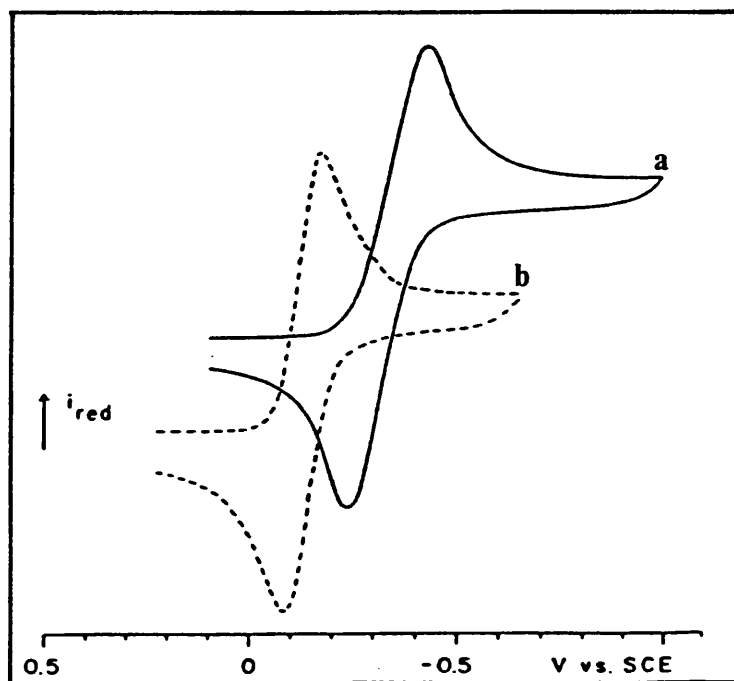


Figure 1.10

Cyclic voltammogram of $[\text{Ru}_2(\text{O}_2\text{CC}_3\text{H}_7)_4\text{Cl}]$ in a) CH_2Cl_2 and
b) EtOH (0.1 M TEAC supporting electrolyte) scan rate 10 mVs^{-1} .



diruthenium(II/III) compounds have been reported. Both discrete dinuclear ionic compounds³⁰, $A[Ru_2(O_2CR)_4X_2]$ ($A=Cs, K, R=CH_3, X=Cl$; $A=K, R=H, X=Cl$; $A=BF_4, R=CH_3, X=H_2O$) and chain polymers $[Ru_2(O_2CR)_4Cl]$ ($R=n-Pr^{16}, Et^{30}, CH_3^{31,32}$) have been reported. These have the same basic structure as $[Ru_2(O_2CC_3H_7)_4Cl]^{16}$ (1.6).

Table 1.1 gives the Ru-Ru and Ru-Cl bond distances and the Ru-Cl-Ru angles found for each of these compounds. The variation observed in the Ru-Ru bond distances were small with the exception of $[Ru_2(O_2CCH_3)_4(H_2O)_2][BF_4]^{30}$ for which the Ru-Ru bond distance, 2.248(1) Å, was considerably shorter than for any of the other compounds. The Ru-Cl bond distances varied depending on whether the compound existed as a linear chain or as a discrete dinuclear units, the latter giving rise to shorter Ru-Cl bond distances³⁰. Examples of linear chain compounds with both straight and angular Ru-Cl-Ru linkages were reported. For one compound, $[Ru_2(O_2CCH_3)_4Cl]$, two crystallographically different forms were reported, one a with linear geometry³², the other with angular linkages³¹.

The electrochemical results of Cotton and Pedersen²⁴ indicated that it should be possible to obtain diruthenium tetracarboxylate complexes containing $[Ru_2]^{4+}$ cores. A range of tetrakis(carboxylato)diruthenium(II/II) complexes^{33,34}, $[Ru_2(O_2CR)_4L_2]$ ($R=H, CH_3, Et, Ph, CH_2Cl$; $L=H_2O, CH_3OH, THF, CH_3CO, CH_3CN$) have recently been prepared and characterised. Magnetic susceptibility measurements³⁴ on each compound indicated the presence of two unpaired electrons per diruthenium unit. Structures have been reported for three of these compounds $[Ru_2(O_2CCH_3)_4L_2]$ ($L=THF^{33}, H_2O^{34}$) and $[Ru_2(O_2CC_2H_5)_4((CH_3)_2CO)_2]^{34}$. The Ru-Ru bond distances are given in Table 1.2. The bond distances observed are somewhat longer than that observed in $[Ru_2(O_2CCH_3)_4(H_2O)_2][BF_4]^{30}$, the analogous $[Ru_2]^{5+}$ compound. This lengthening was expected since an electron has been added to a metal-metal

Table 1.1 Structural data for $[\text{Ru}_2(\text{O}_2\text{CR})_4]^+$ compounds.

Compound	Ru-Ru (Å)	Ru-Cl (Å)	Ru-Cl-Ru (°)	Ref.
$[\text{Ru}_2(\text{O}_2\text{CC}_3\text{H}_7)_4\text{Cl}]$	2.281(4)	2.587(5)	125.4(1)	16
$[\text{Ru}_2(\text{O}_2\text{CCH}_3)_4\text{Cl}\cdot\text{H}_2\text{O}]$	2.267(1)	2.566(1)	180 ^a	30
$[\text{Ru}_2(\text{O}_2\text{CCH}_3)_4(\text{H}_2\text{O})_2][\text{BF}_4]$	2.248(1)	-	-	30
$\text{Cs}[\text{Ru}_2(\text{O}_2\text{CCH}_3)_4\text{Cl}_2]$	2.286(2)	2.521(4)	-	30
$[\text{Ru}_2(\text{O}_2\text{CC}_2\text{H}_5)_4\text{Cl}]$	2.292(7)	2.566(4)	180 ^a	30
$\text{K}[\text{Ru}_2(\text{O}_2\text{CH})_4\text{Cl}_2]$	2.290(1)	2.517(2)	-	30
$[\text{Ru}_2(\text{O}_2\text{CCH}_3)_4\text{Cl}]$	2.281(3)	2.577(1)	127.6 ^b	31
$[\text{Ru}_2(\text{O}_2\text{CCH}_3)_4\text{Cl}]$	2.287(2)	2.577(1)	180 ^a	32

a) Rigorously linear by crystal symmetry.

b) No e.s.d. given.

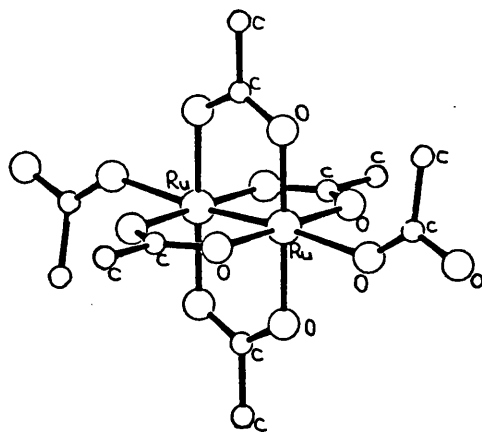
Table 1.2 Structural data for $[\text{Ru}_2(\text{O}_2\text{CR})_4\text{L}_2]$ compounds.

Compound.	Ru-Ru (Å)	Ru-O(axial) (Å)	Ref.
$[\text{Ru}_2(\text{O}_2\text{CCH}_3)_4(\text{THF})_2]$	2.261(3)	2.391(5)	33
$[\text{Ru}_2(\text{O}_2\text{CC}_2\text{H}_5)_4((\text{CH}_3)_2\text{CO})_2]$	2.260(3)	2.363(5)	34
$[\text{Ru}_2(\text{O}_2\text{CCH}_3)_4(\text{H}_2\text{O})_2]$	2.262(3)	2.335(4)	34

antibonding orbital.

The unsolvated species $[\text{Ru}_2(\text{O}_2\text{CR})_4]$ ($\text{R}=\text{H}, \text{CH}_3, \text{Et}, \text{Ph}, \text{CH}_2\text{Cl}$) were studied electrochemically³⁴ in two solvents, THF and acetonitrile, (0.2 M TBABF_4 supporting electrolyte). Each compound showed a single reversible oxidation, in the range +0.34 V to -0.02 V, in acetonitrile, and +0.29 V to -0.05 V, in THF (vs S.C.E.), to generate $[\text{Ru}_2(\text{O}_2\text{CR})_4\text{L}_2]^+$ ($\text{L}=\text{THF}, \text{CH}_3\text{CN}$). In acetonitrile a reversible reduction was observed for each compound at potentials between -1.23 and -1.99 V. The ease of oxidation was found to depend on the electron withdrawing ability of the substituent group, R, and also on the solvent employed.

Although previous work²⁴ had indicated that it was unlikely, McCann and co-workers^{35,36} recently reported two tetrakis(carboxylato)diruthenium(III/III) complexes containing $[\text{Ru}_2]^{6+}$ cores. The crystal structure of the compound $[\text{Ru}_2(\text{O}_2\text{CCH}_3)_4(\text{O}_2\text{CCH}_3)_2 \cdot \text{H}_2\text{O}]$ (1.8) ($\text{Ru}-\text{Ru} = 2.265(1) \text{ \AA}$) was reported in 1988³⁵.



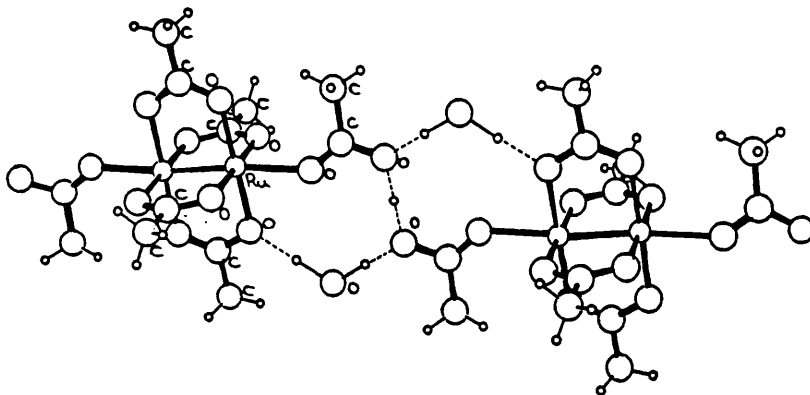
(1.8)

Magnetic susceptibility measurements made on the compound gave a μ_{eff} of $4.5 \mu_{\text{B}}$ per diruthenium unit and electrochemical studies in methanol showed two reversible one-electron reductions at +0.182 V and -0.024 V (vs Ag/AgCl).

The compound $[\text{Ru}_2(\text{O}_2\text{CCH}_3)_2(\text{O}_2\text{CCF}_3)_4(\text{H}_2\text{O})_2]$ ³⁶ was also reported to contain a $[\text{Ru}_2]^{6+}$ core. An electrochemical investigation in methanol showed that

an irreversible reduction occurred at -0.884 V (vs Ag/AgCl), which the authors assigned to the reduction of the $[\text{Ru}_2]^{4+}$ core to decomposition products. The reductions of $[\text{Ru}_2]^{6+}$ to $[\text{Ru}_2]^{5+}$ and $[\text{Ru}_2]^{5+}$ to $[\text{Ru}_2]^{4+}$ were claimed to occur at potentials more positive than $+0.15$ V (the use of a mercury working electrode prevented observation of these reactions).

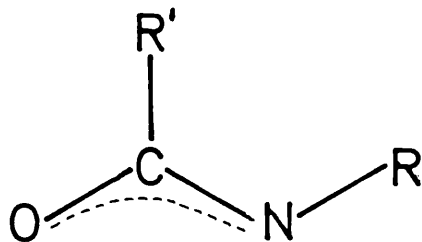
Cotton and co-workers³⁷ attempted to reproduce the synthesis reported by McCann and co-workers^{35,36} and prepare $[\text{Ru}_2(\text{O}_2\text{CC}_2\text{H}_5)_6]$. The material they obtained was identified as $[\text{Ru}_2(\text{O}_2\text{CC}_2\text{H}_5)_5]$. This prompted them to reinvestigate the compounds $[\text{Ru}_2(\text{O}_2\text{CCH}_3)_2(\text{O}_2\text{CCF}_3)_4(\text{H}_2\text{O})_2]$ ³⁶ and $[\text{Ru}_2(\text{O}_2\text{CCH}_3)_6 \cdot 0.7\text{H}_2\text{O}]$ ³⁵. The preparation of the former was found to yield $[\text{Ru}_2(\text{O}_2\text{CCF}_3)_5]$, a $[\text{Ru}_2]^{5+}$ compound. The preparation of the latter yielded the compound previously reported³⁵, but the electrochemical results obtained³⁷ showed a reduction at $E_{1/2} = -0.01$ V (vs Ag/AgCl), a result indicative of a $[\text{Ru}_2]^{5+}$ core. A reinvestigation of the crystal structure of this compound using the original atomic co-ordinates³⁵ revealed the correct formula to be $[\text{Ru}_2(\text{O}_2\text{CCH}_3)_6 \cdot \text{H} \cdot 0.7\text{H}_2\text{O}]$ (1.9), with the extra hydrogen atom located on a crystallographic inversion centre, and hydrogen bonded to the oxygen atoms of the axial acetate groups of two adjacent molecules. This indicated that this compound also contained a $[\text{Ru}_2]^{5+}$ core and hence there is still no evidence for a diruthenium(III/III)tetracarboxylate compound containing a $[\text{Ru}_2]^{6+}$ core.



(1.9)

1.6.2 Diruthenium Tetraamidates.

Amidate ligands (1.10) are known to shift the potentials of oxidations



(1.10)

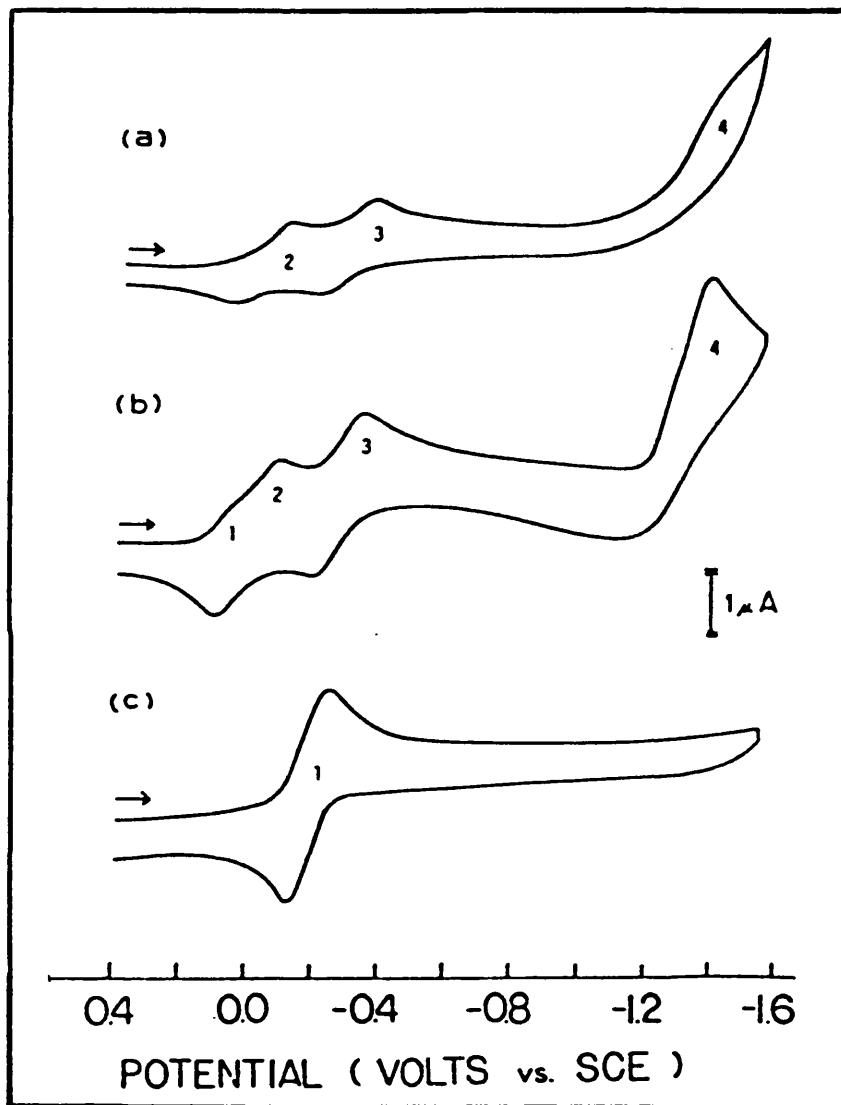
and reductions to more cathodic values than those observed for the analogous carboxylate containing compounds. These ligands also provided the opportunity to vary the substituents at two sites on the bridging group.

The first chlorotetrakis(amidato)diruthenium(II/III) compound, $[\text{Ru}_2(\text{HNOCCF}_3)_4\text{Cl}]^{38}$, was prepared by stirring $[\text{Ru}_2(\text{O}_2\text{CCH}_3)_4\text{Cl}]$ with an excess of CF_3CONH_2 at 127°C , under an inert atmosphere, for a period of 60 hours. After removing the excess ligand by vacuum sublimation, the procedure was repeated with a fresh batch of CF_3CONH_2 . (This method has remained the most commonly used preparative route for compounds of this type). Magnetic susceptibility measurements on $[\text{Ru}_2(\text{HNOCCF}_3)_4\text{Cl}]$ implied the presence of three unpaired electrons per diruthenium unit³⁸.

The electrochemical behaviour of $[\text{Ru}_2(\text{HNOCCF}_3)_4\text{Cl}]$ was studied in eleven non-aqueous solvents, using cyclic voltammetry³⁸. Between one and four reductions were observed in each solvent at potentials of *ca.* 0.00, -0.06, -0.30, and -1.40 V (vs. S.C.E.). The number of reactions and the potentials at which they occurred was dependent on the solvent employed (Figure 1.11). The peak current of

Figure 1.11

Cyclic voltammogram of $[\text{Ru}_2(\text{HNOCCF}_3)_4\text{Cl}]$ in a) CH_2Cl_2 ,
b) CH_3CN and c) DMSO (0.1 M TBAP supporting
electrolyte) scan rate 100 mVs^{-1} .



the fourth reduction wave was approximately equal to the sum of the peak currents of the other three. The addition of chloride ions (TBAC) had the effect of decreasing the peak currents of the first and second reductions while simultaneously increasing the peak current of the third reduction. The addition of silver ions ($\text{Ag}[\text{ClO}_4]$) had the opposite effect. Neither of these additions had any effect on the peak current of the fourth reduction (Figure 1.12).

These results led to the conclusion that in solution an equilibrium reaction between three species was occurring (Scheme 1.1). The position of the equilibrium was dependent on the polarity of the solvent used. A scheme was proposed for the behaviour of $[\text{Ru}_2(\text{HNOCCF}_3)_4\text{Cl}]$ in three of the solvents employed³⁸ (Scheme 1.2).

The compound $[\text{Ru}_2(\text{HNOCCCH}_3)_4\text{Cl}]$ ³⁹ was prepared using a strictly analogous procedure, and its electrochemical behaviour studied in DMSO (0.1 M LiCl supporting electrolyte). Three reactions were observed, one oxidation (the first reported oxidation of a diruthenium(II/III) compound) and two reductions (Figure 1.13). Changes observed in the electronic spectrum observed during controlled potential electrolysis indicated that the oxidation and the first reduction were both metal based processes (Equations 1.1 and 1.2 respectively).

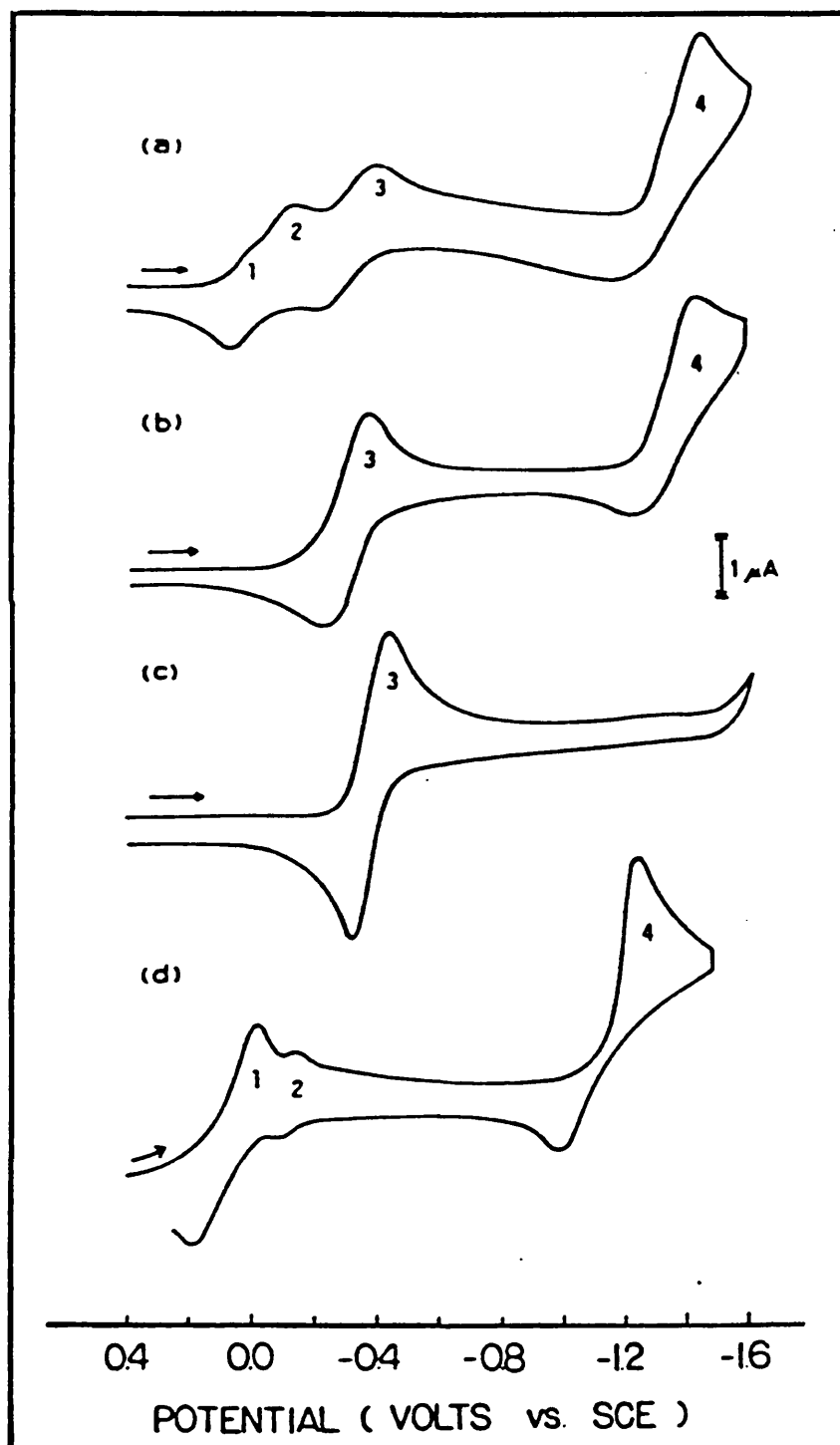


The second reduction could not be assigned since changes observed in the electronic spectrum during electrolysis were small leading to the conclusion that the reduction could be ligand or metal based.

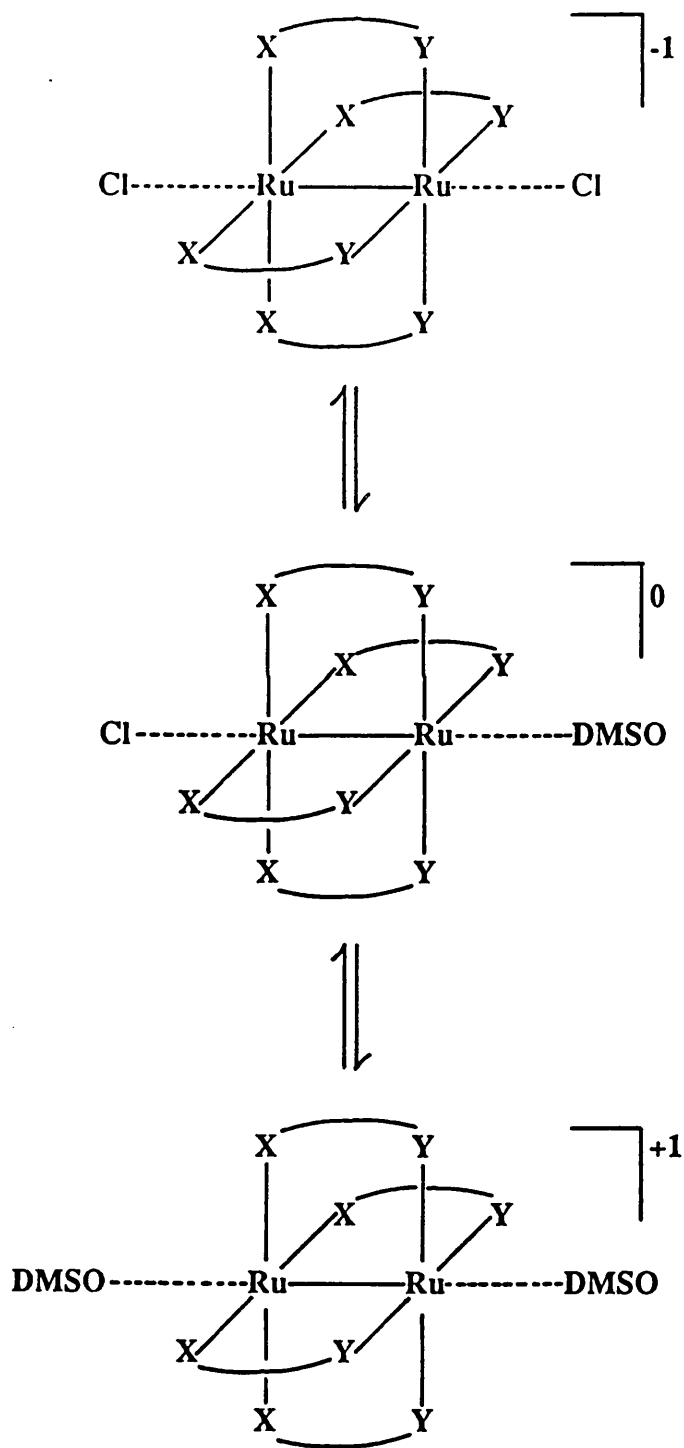
In 1986⁴⁰, the effect of solvent on the electrochemical behaviour of the

Figure 1.12

Cyclic voltammogram of $[\text{Ru}_2(\text{HNOCCF}_3)_4\text{Cl}]$ in CH_3CN (0.1 M TBAP supporting electrolyte) with various ratios of $[\text{Cl}^-]:[\text{Ru}_2(\text{HNOCCF}_3)_4\text{Cl}]$ a) 0:1, b) 1:1, c) 30:1 d) cyclic voltammogram after addition of one equiv. of $[\text{Ag}^+]$ ions.



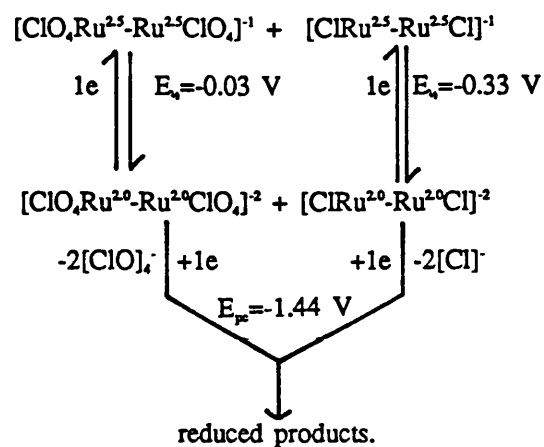
Scheme 1.1 A scheme illustrating the equilibrium existing between different axially ligated tetra-bridged diruthenium(II/III) compounds in solution.



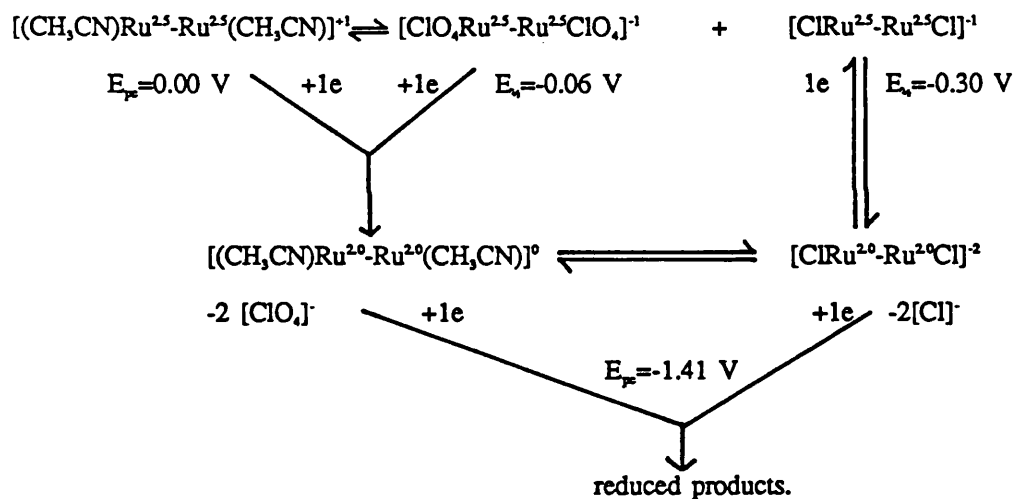
X, Y = O, N

Scheme 1.2 The behaviour of $\text{Ru}_2(\text{HNOCCF}_3)_4\text{Cl}$ in a) CH_2Cl_2 , b) CH_3CN and c) DMSO (0.1 M TBAP supporting electrolyte).

a) CH_2Cl_2



b) CH_3CN



c) DMSO

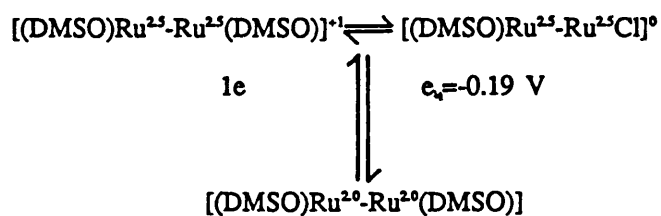
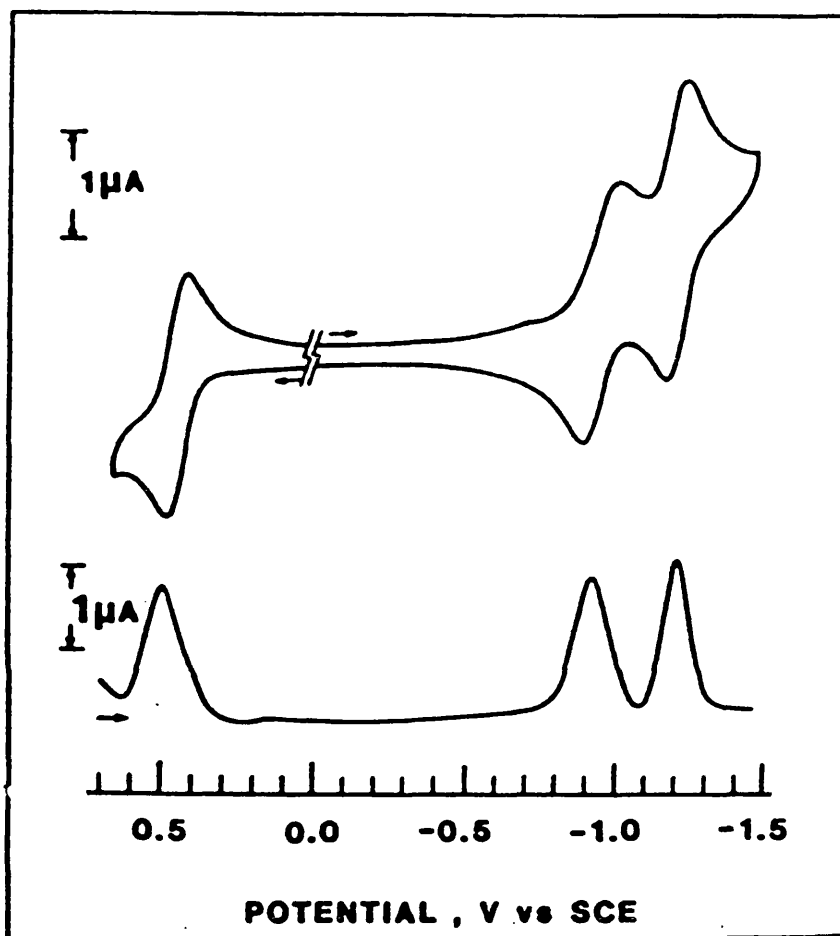
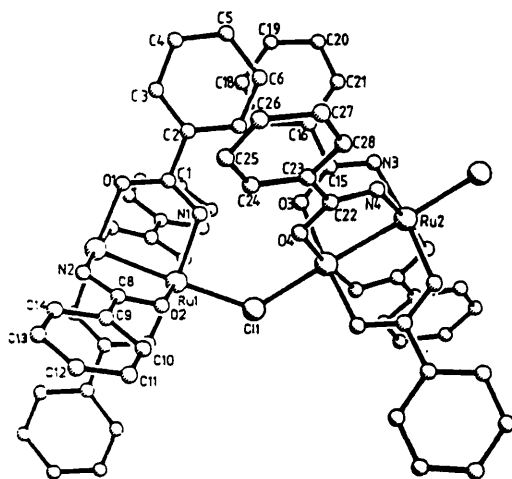


Figure 1.13 Cyclic and differential pulse voltammograms of $[\text{Rh}_2(\text{HNOCCCH}_3)_4\text{Cl}]$ in DMSO (0.1 M LiCl supporting electrolyte) scan rates 50 mVs^{-1} and 4 mVs^{-1} respectively.



the compound $[\text{Ru}_2(\text{HNOCC}(\text{CH}_3)_3)_4\text{Cl}]$ was studied in eleven non-aqueous solvents (0.1 M TBABF_4 supporting electrolyte, except in CH_2Cl_2 (0.25 M TBABF_4)). In contrast to the earlier results³⁸, oxidations were observed instead of reductions. As previously reported^{38,39}, between one and four reactions were observed in each solvent. The number of reactions and their half-wave potentials of the reactions was dependent on the solvent employed, and the peak current of the fourth electrochemical reaction, was approximately equal to the sum of the peak currents of the other three. The addition of chloride ions (BTEAC) had the same effect as observed by Bear, Kadish and co-workers^{38,39} reinforcing the conclusions reached by them that these compounds existed as equilibrium mixtures of three species in solution (scheme 1.1).

Crystallographic studies have been made of two chlorotetrakis (amidato)diruthenium(II/III) complexes, $[\text{Ru}_2(\text{HNOCC}_6\text{H}_5)_4\text{Cl}]^{41}$ ($\text{Ru-Ru} = 2.293(2) \text{ \AA}$)



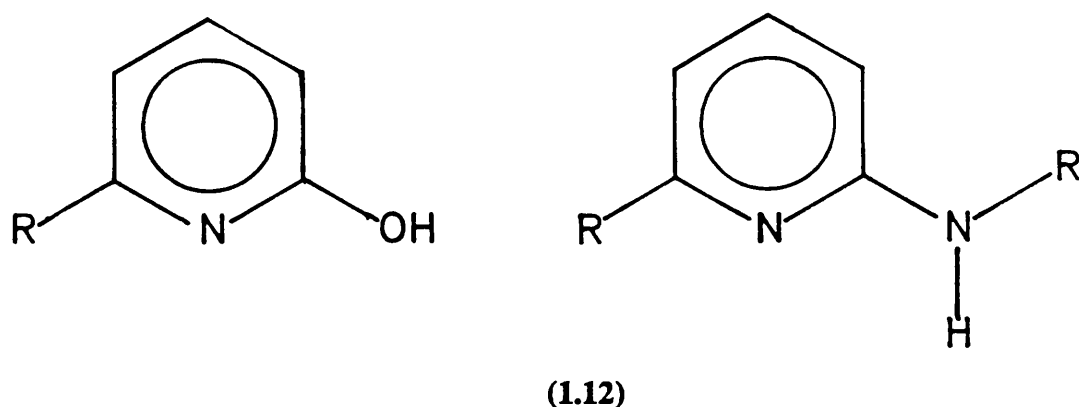
(1.11)

(1.11) and $[\text{Ru}_2(\text{HNOCClC}_6\text{H}_4)_4\text{Cl}]^{42}$ ($\text{Ru-Ru} = 2.296(1) \text{ \AA}$). Both were found to exist as polymers in the solid state. The diruthenium units are bridged by four amidate ligands in a cisoid 2:2 arrangement and linked into chains by angular chloride ion linkages. The Ru-Ru , and Ru-Cl bond distances and the Ru-Cl-Ru bond angles

for the two compounds are essentially identical in the two compounds .

1.6.3 Diruthenium Compounds Containing Other Bridging Ligands.

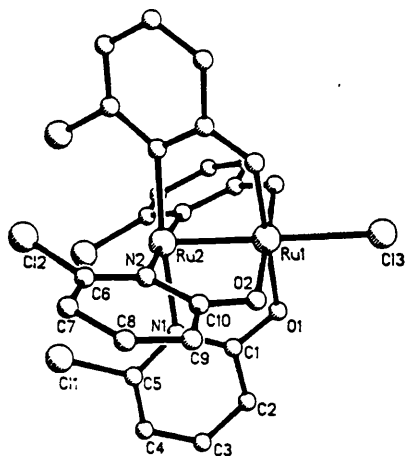
The use of substituted hydroxypyridine and aminopyridine ligands (1.12) has allowed the study of a new range of compounds containing N-C-O bridges and for the first time a range of compounds containing N-C-N bridges.



Three diruthenium compounds have been prepared using substituted hydroxypyridine ligands ($6\text{-RC}_5\text{H}_3\text{NOH}$ $\text{R}=\text{Cl}^{43}, \text{F}^{44}, \text{H}^{45}$) and three using aminopyridine ligands ($\text{C}_5\text{H}_4\text{NN}(\text{H})\text{R}$ $\text{R}=\text{CH}_2\text{C}_6\text{H}_5^{46}, \text{CH}_3^{46}, \text{C}_6\text{H}_5^{45}$) by an analogous procedure to that used to prepare the diruthenium tetraamidate compounds³⁸. A fourth compound containing hydroxypyridine ligands, $[\text{Ru}_2(\text{O}_2\text{CCH}_3)_2(6\text{-CH}_3\text{C}_5\text{H}_3\text{NO})_2\text{Cl}]^{47}$ was prepared by refluxing $[\text{Ru}_2(\text{O}_2\text{CCH}_3)_4\text{Cl}]$ with an excess of 6-methyl-2-hydroxypyridine in methanol for 24 hours, and the compound $[\text{Ru}_2(\text{C}_5\text{H}_4\text{NNC}_6\text{H}_5)_4(\text{C}\equiv\text{CC}_6\text{H}_5)]^{48}$ was prepared by reacting $[\text{Ru}_2(\text{C}_5\text{H}_4\text{NNC}_6\text{H}_5)_4\text{Cl}]$ with an excess of $\text{Li}[\text{C}\equiv\text{CC}_6\text{H}_5]$ in a toluene/THF mixture.

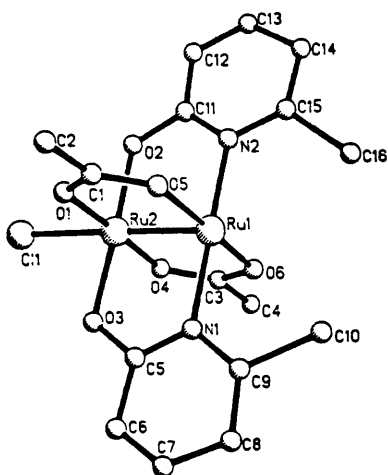
Structural data have been obtained for all four of the compounds prepared containing hydroxypyridine ligands and two chlorotetrakis(aminopyridinato)

diruthenium(II/III) compounds also were studied crystallographically. Table 1.3



(1.13)

presents Ru-Ru and Ru-Cl bond lengths observed. In the compounds containing identical bridging ligands^{43,44} for example $[\text{Ru}_2(\text{ClC}_7\text{H}_3\text{NO})_4\text{Cl}]$ (1.13) the four ligands were orientated in the same direction, blocking one axial site, resulting in polar molecules. In the compound $[\text{Ru}_2(\text{C}_7\text{H}_4\text{NO})_4(\text{C}_7\text{H}_4\text{NOH})\text{Cl}]$ ⁴⁵, the additional neutral ligand was attached to one of the axial sites, the other being occupied by the chloride ion, and hydrogen bonded to the oxygen of one of the bridging ligands. The partially substituted compound $[\text{Ru}_2(\text{O}_2\text{CCH}_3)_2(6\text{-CH}_3\text{C}_7\text{H}_3\text{NO})_2\text{Cl}]$ ⁴⁷ (1.14),

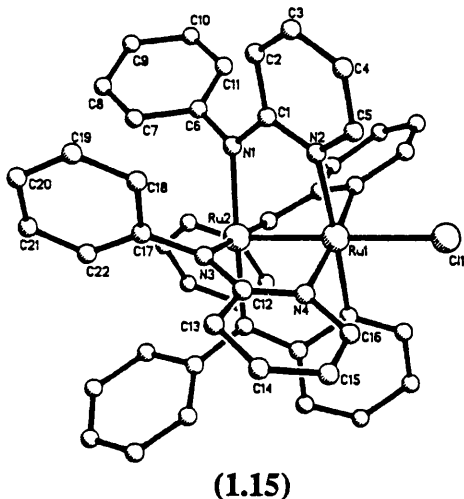


(1.14)

exhibited a 2:2 trans arrangement of the bridging ligands. The two 6-methyl-2-

hydroxypyridine ligands were orientated in the same direction, once again effectively inhibiting coordination to one of the axial sites.

In the compound $[\text{Ru}_2(\text{C}_5\text{H}_4\text{NNC}_6\text{H}_5)_4\text{Cl}]^{45}$ (1.15) the anilinopyridine ligands adopt a polar arrangement about the Ru-Ru bond, with one ruthenium ion



co-ordinated to the four pyridyl nitrogen atoms and the axial chloride ion, while the other ruthenium ion is co-ordinated to the four amine nitrogen atoms. The four pendant phenyl rings effectively block the axial site at that end of the molecule.

The compound $[\text{Ru}_2(\text{C}_5\text{H}_4\text{NNC}_6\text{H}_5)_4(\text{C}\equiv\text{CC}_6\text{H}_5)]^{48}$ was structurally similar to the compound $[\text{Ru}_2(\text{C}_5\text{H}_4\text{NNC}_6\text{H}_5)_4\text{Cl}]^{45}$, except that the axial chloride ion was replaced by a $[\text{C}\equiv\text{CC}_6\text{H}_5]^-$ ligand.

The electrochemical behaviour of these compounds was studied^{44,46-49} and the results obtained are presented in Table 1.4. The oxidations and reductions observed are assigned to metal based processes. The results obtained for the compound $[\text{Ru}_2(\text{C}_5\text{H}_4\text{NNC}_6\text{H}_5)_4(\text{C}\equiv\text{CC}_6\text{H}_5)]^{48}$ are of considerable interest since the reversible oxidation observed ($E_{1/2} = +0.235$ V vs Ag/AgCl) occurs at the most anodic potential for any diruthenium(II/III) compound containing this type of three membered bridge. The ease of oxidation of this compound suggests that it should be possible to generate a $[\text{Ru}_2]^{6+}$ system, from a $[\text{Ru}_2]^{5+}$ one, by chemical oxidation.

Table 1.3 Structural Data for the compounds $[\text{Ru}_2(\text{RC}_5\text{H}_3\text{NX})_4]$ (X=O,N).

Compound.	Ru-Ru (Å)	Ru-Cl (Å)	Ref.
$[\text{Ru}_2(\text{C}_5\text{H}_4\text{NO})_4\text{Cl}(\text{C}_5\text{H}_4\text{NOH})]$	2.278(1)	2.419(5)	45
$[\text{Ru}_2(\text{ClC}_5\text{H}_3\text{NO})_4\text{Cl}]$	2.281(1)	2.443(2)	43
$[\text{Ru}_2(\text{FC}_5\text{H}_3\text{NO})_4\text{Cl}]$	2.284(1)	2.427(3)	44
$[\text{Ru}_2(\text{C}_5\text{H}_4\text{NNCH}_3)_4\text{Cl}]$	2.275(3)	2.437(7)	45
$[\text{Ru}_2(\text{C}_5\text{H}_3\text{NNC}_6\text{H}_5)_4\text{C}\equiv\text{CC}_6\text{H}_5]$	2.319(2)	-	48

Table 1.4 Electrochemical results for the compounds $[\text{Ru}_2(\text{RC}_5\text{H}_3\text{NX})_4]$ (X=O,N).

Compound.	Solvent	Scan Rate mVs^{-1}	$E_{1/2}^d$ V
$[\text{Ru}_2(\text{C}_5\text{H}_4\text{NO})_4\text{Cl}(\text{C}_5\text{H}_4\text{NOH})]^a$	CH_3CN	50-500	-0.29,-1.45 ^e , +0.94,+1.11,+1.48 ^f
$[\text{Ru}_2(\text{ClC}_5\text{H}_3\text{NO})_4\text{Cl}]^a$	CH_2Cl_2	100	-1.70 ^e ,+0.10,+1.13
	CH_3CN	100	-1.70,+0.09,+0.34,+1.61 ^f
$[\text{Ru}_2(\text{FC}_5\text{H}_3\text{NO})_4\text{Cl}]^b$	CH_2Cl_2	100-500	-0.10,+1.68
$[\text{Ru}_2(\text{C}_5\text{H}_4\text{NNCH}_3)_4\text{Cl}]^a$	DMSO	50	-0.78,-1.11,+0.24
$[\text{Ru}_2(\text{C}_5\text{H}_3\text{NNC}_6\text{H}_5)_4\text{Cl}]^a$	CH_2Cl_2	250	-0.75,-1.57 ^e ,+0.50,+1.45
	THF	250	-0.71,-1.57 ^e ,+0.65,+1.20 ^f
$[\text{Ru}_2(\text{C}_5\text{H}_3\text{NNC}_6\text{H}_5)_4\text{C}\equiv\text{CC}_6\text{H}_5]^c$	CH_2Cl_2	100	-0.99,+0.24,+1.05

a) 0.1 M TBABF₄ supporting electrolyte.

b) 0.1 M TEAC supporting electrolyte.

c) 0.1 M TBAPF₆ supporting electrolyte.

d) vs. Ag/AgCl reference.

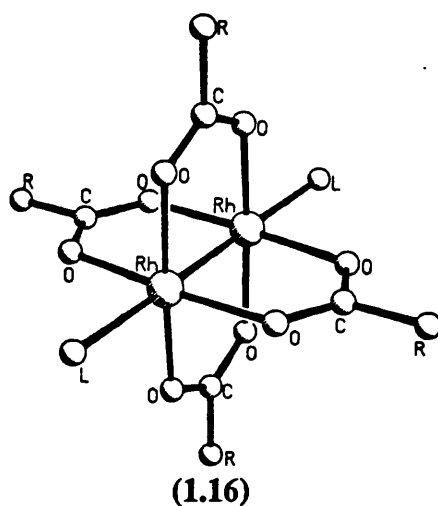
e) value given E_{pc} .f) value given E_{pa} .

1.7 The Historical Development of the Chemistry of Dirhodium Compounds.

The development of the chemistry of dirhodium compounds has followed a parallel path to that of diruthenium chemistry. With this in mind these developments will as far as possible be discussed in an analogous order to those of diruthenium chemistry.

1.7.1 Dirhodium Tetracarboxylates.

The initial discoveries of tetrakis(carboxylato)dirhodium(II/II) compounds and the confusion over the bond multiplicity were discussed in sections 1.2 and 1.4.2. Since these initial results numerous other tetrakis(carboxylato) dirhodium(II/II) compounds have been studied crystallographically⁵⁰⁻⁶⁴ and have been the subject of two comprehensive reviews^{65,66}. Table 1.5 presents the Rh-Rh bond lengths for a selection of these compounds. The structures reported are all similar with the $[\text{Rh}_2]^{4+}$ unit bridged by four carboxylate ligands, and the axial sites filled by neutral molecules (1.16).



Detailed electrochemical investigations into a series of

Table 1.5 Examples of Rh-Rh bond lengths observed for compounds of the general formula $[\text{Rh}_2(\text{O}_2\text{CR})_4\text{L}_2]$.

Compound.	Rh-Rh (Å)	Ref.
$[\text{Rh}_2(\text{O}_2\text{CC}(\text{CH}_3)_3)_4(\text{H}_2\text{O})_2]$	2.371(1)	52
$[\text{Rh}_2(\text{O}_2\text{CCH}_3)_4(\text{CH}_3\text{CN})_2]$	2.384(1)	56
$[\text{Rh}_2(\text{O}_2\text{CCH}_3)_4(\text{H}_2\text{O})_2]$	2.3855(1)	21
$[\text{Rh}_2(\text{O}_2\text{CCH}_3)_4(\text{CH}_3\text{CN})_2]$	2.3963(2)	50
$[\text{Rh}_2(\text{O}_2\text{CCF}_3)_4(\text{DMSO})_2]^b$	2.400(1)	57
$[\text{Rh}_2(\text{O}_2\text{CCF}_3)_4(\text{CH}_3\text{CH}_2\text{OH})_2]$	2.402(2)	63
$[\text{Rh}_2(\text{O}_2\text{CCH}_3)_4(\text{NH}(\text{C}_2\text{H}_5)_2)_2]$	2.4020(7)	51
$[\text{Rh}_2(\text{O}_2\text{CCH}_3)_4(\text{DMSO})_2]^a$	2.406(1)	52
$[\text{Rh}_2(\text{O}_2\text{CC}_2\text{H}_5)_4(\text{DMSO})_2]^a$	2.407(1)	55
$[\text{Rh}_2(\text{O}_2\text{CCH}_3)_4(\text{CO})_2]$	2.4191(3)	60
$[\text{Rh}_2(\text{O}_2\text{CCH}_3)_4(\text{P}(\text{OC}_6\text{H}_5)_3)_2]$	2.4434(6)	58
$[\text{Rh}_2(\text{O}_2\text{CCH}_3)_4(\text{P}(\text{C}_6\text{H}_5)_3)_2]$	2.4505(2)	58
$[\text{Rh}_2(\text{O}_2\text{CCH}_3)_4(\text{P}(\text{OCH}_3)_3)_2]$	2.4556(3)	60
$[\text{Rh}_2(\text{O}_2\text{CCF}_3)_4(\text{P}(\text{OC}_6\text{H}_5)_3)_2]$	2.470(1)	59
$[\text{Rh}_2(\text{O}_2\text{CCF}_3)_4(\text{P}(\text{C}_6\text{H}_5)_3)_2]$	2.486(1)	59

a) Co-ordinates through the sulphur atom.

b) Co-ordinates through the oxygen atom.

tetrakis(carboxylato)dirhodium(II/II) compounds $[\text{Rh}_2(\text{O}_2\text{CR})_4]$ ($\text{R}=\text{C}(\text{CH}_3)_3, \text{C}_4\text{H}_9, \text{C}_3\text{H}_7, \text{C}_2\text{H}_5, \text{CH}_2\text{C}_6\text{H}_5, \text{CH}_2\text{OCH}_3, \text{CH}_2\text{OC}_6\text{H}_5, \text{ClCHCH}_3, \text{CF}_3$) have been reported by Bear and co-workers⁶⁷ and the effect of the substituent group, R, on the electrochemical behaviour of these compounds studied. A reversible one-electron oxidation at half-wave potentials ranging from +0.92 V ($\text{R}=\text{C}(\text{CH}_3)_3$) to +1.28 V ($\text{R}=\text{ClCHCH}_3$) was observed in DMF, and an irreversible multi-electron reduction ($E_{\text{pc}}=-1.04$ V ($\text{R}=\text{CF}_3$) to $E_{\text{pc}}=-1.64$ V ($\text{R}=\text{c-C}_5\text{H}_9$) was observed in DMSO, for each compound.

The electrochemical behaviour of one of the above compounds, $[\text{Rh}_2(\text{O}_2\text{CC}_2\text{H}_5)_4]$, was studied in nine non-aqueous solvents⁶⁷. The investigation was restricted to the one-electron oxidation process observed in the substituent group study. The half-wave potential varied depending on the donicity of the solvent employed, the ease of oxidation increasing with increasing donor power of the solvent.

A second series of tetrakis(carboxylato)dirhodium(II/II) compounds was studied in 1,2-dichloroethane (0.1 M TBAP supporting electrolyte)⁶⁸. Each compound exhibited a quasireversible one-electron oxidation ($E_{1/2}=+1.55$ V to $E_{1/2}=+1.21$ V vs S.C.E.). The half-wave potential was dependent on the identity of the substituent on the carboxylate ligand. Stepwise additions of various substituted pyridines to the electrochemical cell initially caused a decrease in the peak current of the original oxidation and a concomitant increase in the peak current of a second oxidation at a more cathodic potential. Continued additions of Lewis base caused the peak current of this second oxidation to decrease with a simultaneous growth in the peak current of a third oxidation, again at a more cathodic potential. These results indicated that the ease of oxidation increased with increasing axial complexation, a result that agreed well with the earlier findings of Bear and co-workers⁶⁷.

1.7.2 Dirhodium Tetraamidates.

Tetrakis(amidato)dirhodium(II/II) compounds were prepared by an analogous procedure to that used to prepare chlorotetrakis(amidato)diruthenium(II/III) compounds³⁸. The stepwise replacement of the carboxylate ligands with amidate ions during these reactions can potentially give rise to twelve species (Figure 1.14).

Dirhodium(II/II) compounds have been prepared using four different amidate ligands, trifluoroacetamide⁶⁹, acetamide⁷¹, N-phenylacetamide⁷² and benzamide⁷⁰. The reaction of $[\text{Rh}_2(\text{O}_2\text{CCH}_3)_4(\text{CH}_3\text{OH})_2]$ with trifluoroacetamide⁷³ resulted in the formation of three isomers of $[\text{Rh}_2(\text{HNOCCF}_3)_4]$, two of which were identified (IX,XI) by ^{19}F n.m.r. spectroscopy, while the reaction with benzamide⁷⁰ gave rise to a single isomer (IX), which was identified crystallographically. The reaction of $[\text{Rh}_2(\text{O}_2\text{CCH}_3)_4(\text{CH}_3\text{OH})_2]$ with N-phenylacetamide^{72,74} resulted in the preparation of seven of the twelve possible species. Five of these were identified (I,VI,VII,IX,XI) using various spectroscopic techniques. The two remaining species were identified as $[\text{Rh}_2(\text{O}_2\text{CCH}_3)_2(\text{C}_6\text{H}_5\text{NOCCH}_3)_2]$, but they could not be assigned specific geometries. Finally, the reaction with acetamide⁷⁵ resulted in the formation of six species. Three of these were identified (I,VI,IX) using ^1H n.m.r. spectroscopy. The three remaining species, were identified as isomers of $[\text{Rh}_2(\text{O}_2\text{CCH}_3)_2(\text{HNOCCCH}_3)_2]$ but could not be characterised further.

Two isomers of tetrakis(N-phenylacetamidato)dirhodium(II/II) (IX,XI)⁷⁴, and tetrakis(benzamidato)dirhodium(II/II) with two different axial ligands (pyridine (1.17) and triphenylstibine)⁷⁰ were studied crystallographically. Structures of $[\text{Rh}_2(\text{HNOCCF}_3)_4(\text{C}_5\text{H}_5\text{N})_2]$ (IX)⁷³ and $[\text{Rh}_2(\text{HNOCCCH}_3)_4(\text{H}_2\text{O})_2 \cdot 3\text{H}_2\text{O}]$ (IX)⁷⁵ have also been obtained. The Rh-Rh bond lengths for these compounds are presented in Table 1.6. Considerable variation in the Rh-Rh bond lengths was observed

Figure 1.14

The structures of the twelve theoretically isolable

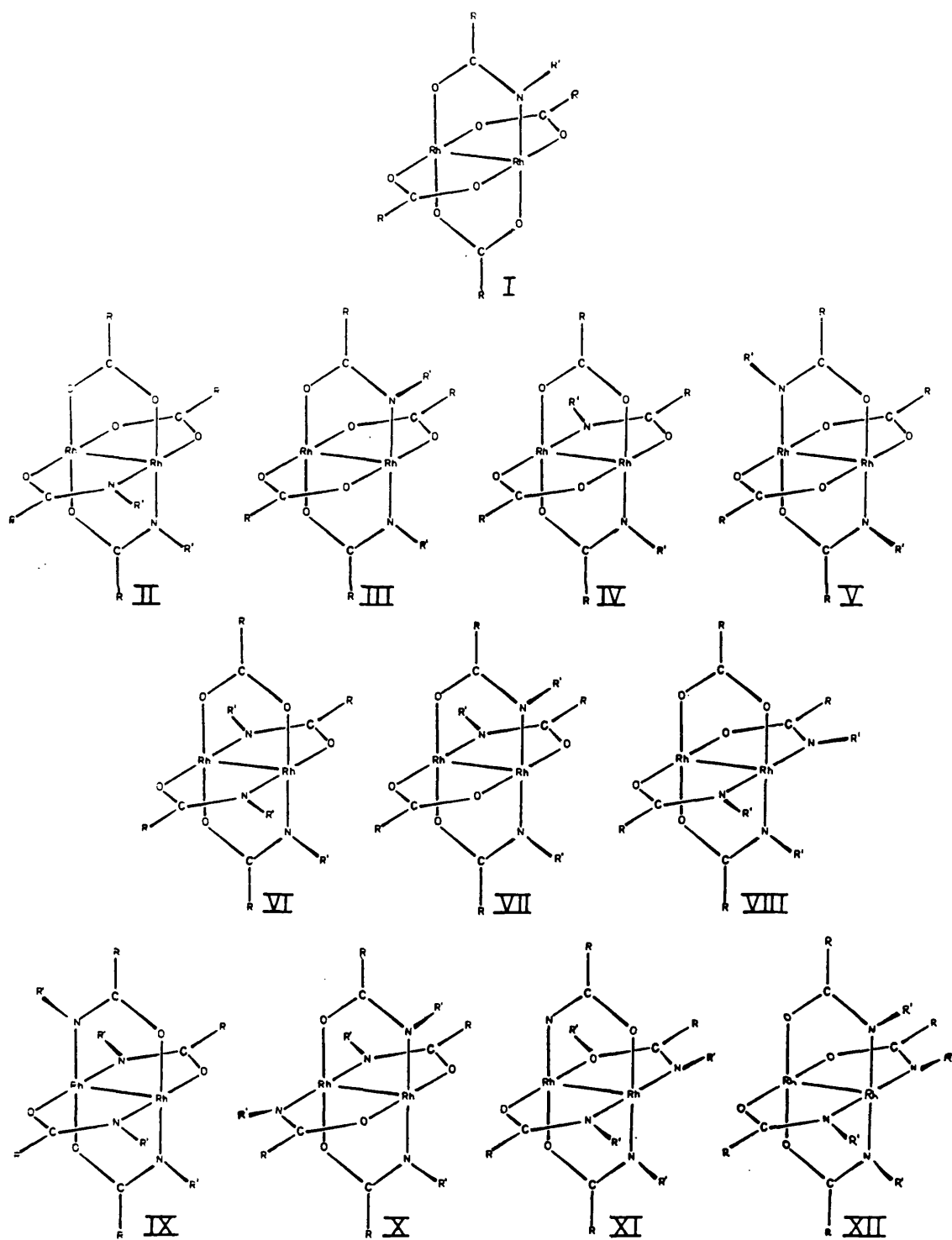
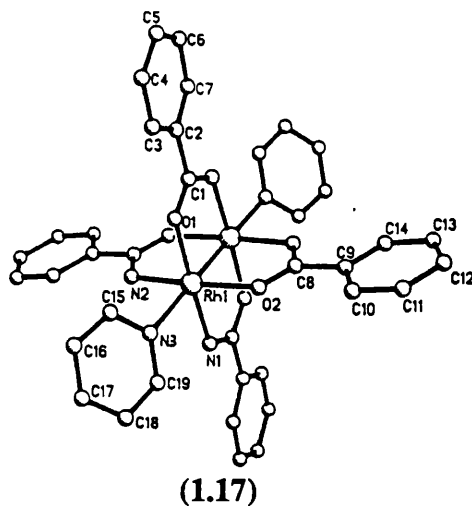
 $[\text{Rh}_2(\text{O}_2\text{CR})_n(\text{R}'\text{NOCR}'')_{4-n}]$ ($n=0,1,2,3$) species.

Table 1.6 Structural data for $[\text{Rh}_2(\text{RNOCR}')_4\text{L}_2]$ compounds.

Compound.	Rh-Rh(Å)	Species ^a	Ref.
$[\text{Rh}_2(\text{HNOCC}_6\text{H}_5)_4(\text{Sb}(\text{C}_6\text{H}_5)_2\cdot\text{CH}_2\text{Cl}_2)]$	2.463(1)	IX	70
$[\text{Rh}_2(\text{HNOCC}_6\text{H}_5)_4(\text{C}_6\text{H}_5\text{N})_2]$	2.437(1)	IX	70
$[\text{Rh}_2(\text{HNOCCF}_3)_4(\text{C}_6\text{H}_5\text{N})_2]$	2.472(3)	IX	73
$[\text{Rh}_2(\text{C}_6\text{H}_5\text{NOCCH}_3)_4(\text{DMSO})_2]$	2.448(1)	IX	74
$[\text{Rh}_2(\text{C}_6\text{H}_5\text{NOCCH}_3)_4(\text{DMSO})]$	2.397(1)	XI	74
$[\text{Rh}_2(\text{HNOCC}_6\text{H}_5)_4(\text{H}_2\text{O})_2\cdot 3\text{H}_2\text{O}]$	2.415(1)	IX	75

a) see Figure 1.14



(2.397(1) Å to 2.472(3) Å) indicating that the Rh-Rh bond distance is dependent on several factors including the identity and arrangement of the bridging ligands and the identity and number of axial substituents.

The electrochemical behaviour of tetrakis(amidato)dirhodium(II/II) compounds, and dirhodium(II/II) compounds containing a combination of carboxylate and amidate ligands has been studied in detail. The compound $[\text{Rh}_2(\text{HNOCCF}_3)_4]^{76}$ was studied in seven non-aqueous solvents. A reversible one-electron oxidation was observed at potentials ranging from +0.91 to +1.15 V (vs S.C.E.) depending on the solvent employed. The electrochemical behaviour of $[\text{Rh}_2(\text{HNOCC}_6\text{H}_5)_4(\text{H}_2\text{NOCC}_6\text{H}_5)_2]$ in four nonaqueous solvents has also been reported⁷⁰. Two closely spaced oxidations were observed in each solvent, the peak current of one being much greater than that of the other. Coulometric measurements indicated that they jointly account for the transfer of one electron per $[\text{Rh}_2]^{4+}$ unit. The addition of triphenylphosphine to the electrochemical cell caused the two oxidations previously observed to merge together, and a second oxidation to appear at a more positive potential. The peak currents for these oxidations were approximately equal. The compound $[\text{Rh}_2(\text{C}_6\text{H}_5\text{NOCCH}_3)_4]$ was studied electrochemically in five solvents⁷⁷. Two reversible one-electron oxidations were observed in each solvent (the first at $E_{1/2} \approx +0.40$ V and the second at $E_{1/2} \approx +1.12$ V vs

S.C.E.).

The three electrochemical investigations^{70,76,77} indicated that the ease of oxidation of these compounds was dependent on the substituent groups on the amidate ligands and on the solvents employed in the investigation. It was also noted that a large cathodic shift in potential occurred on changing from carboxylate to amidate ligands. This was illustrated by an electrochemical study reported in 1984⁷⁸ in which, five compounds $[\text{Rh}_2(\text{O}_2\text{CCH}_3)_n(\text{HNOCCCH}_3)_{4-n}]$ ($n=0,1,2,3,4$) were studied electrochemically in four solvents. In each solvent a stepwise cathodic shift was observed on passing from $[\text{Rh}_2(\text{O}_2\text{CCH}_3)_4]$ to $[\text{Rh}_2(\text{HNOCCCH}_3)_4]$ ($E_{1/2}=1.17$ V and 0.15 V respectively in acetonitrile vs S.C.E.).

1.7.3 Dirhodium Compounds Containing Other Bridging ligands.

Compounds containing hydroxypyridine and aminopyridine ligands were prepared using an analogous procedure to that used to prepare chlorotetrakis (amidato)diruthenium(II/III) compounds³⁸. Crystallographic and electrochemical investigations have been reported for a number of these compounds⁷⁹⁻⁸⁶.

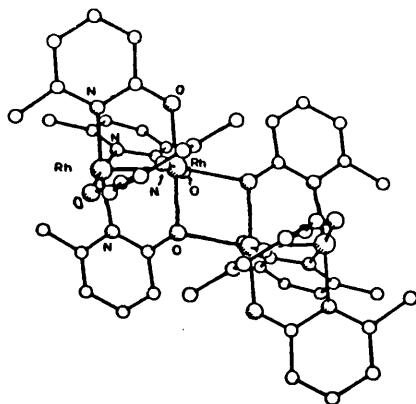
A total of eight crystallographic studies on compounds containing the ligand 6-methyl-2-hydroxypyridine were reported by two laboratories during 1980^{79,80} and 1981⁸¹. Six of the reported structures contain a $[\text{Rh}_2(6\text{-CH}_3\text{C}_5\text{H}_3\text{NO})_4]$ unit⁷⁹⁻⁸¹, and two contained a $[\text{Rh}_2(\text{O}_2\text{CCH}_3)_2(6\text{-CH}_3\text{C}_5\text{H}_3\text{NO})_2]$ unit⁸¹. Structures have also been reported of compounds containing 6-chloro-2-hydroxypyridine ligands and containing 6-fluoro-2-hydroxypyridine ligands. The Rh-Rh bond lengths observed for each compound are given in Table 1.7.

Two of the compounds studied $[\text{Rh}_2(6\text{-CH}_3\text{C}_5\text{H}_3\text{NO})_4]$ ⁷⁹ and $[\text{Rh}_2(6\text{-CH}_3\text{C}_5\text{H}_3\text{NO})_4\cdot\text{H}_2\text{O}]$ ⁸¹ adopt a 2:2 transoid arrangement of ligands, while four

Table 1.7 Structural data for compounds containing $[\text{Rh}_2(\text{RC}_5\text{H}_3\text{NO})_4]$ or $[\text{Rh}_2(\text{RC}_5\text{H}_3\text{NNR}')_4]$ units.

Compound	Rh-Rh(Å)	Ref.
$[\text{Rh}_2(\text{CH}_3\text{C}_5\text{H}_3\text{NO})_4]$	2.359(1)	79
$[\text{Rh}_2(\text{CH}_3\text{C}_5\text{H}_3\text{NO})_4(\text{CH}_3\text{C}_5\text{H}_3\text{NOH})\cdot\text{C}_6\text{H}_5\text{CH}_3]$	2.383(1)	80
$[\text{Rh}_2(\text{CH}_3\text{C}_5\text{H}_3\text{NO})_4\cdot\text{CH}_2\text{Cl}_2]$	2.369(1)	80
$[\text{Rh}_2(\text{CH}_3\text{C}_5\text{H}_3\text{NO})_4\cdot\text{H}_2\text{O}]$	2.367(1)	81
$[\text{Rh}_2(\text{CH}_3\text{C}_5\text{H}_3\text{NO})_4(\text{CH}_3\text{CN})]$	2.372(1)	81
$[\text{Rh}_2(\text{CH}_3\text{C}_5\text{H}_3\text{NO})_4(\text{C}_3\text{H}_4\text{N}_2)\cdot 0.5\text{CH}_3\text{CN}]$	2.384(1)	81
$[\text{Rh}_2(\text{CH}_3\text{C}_5\text{H}_3\text{NO})_2(\text{O}_2\text{CCH}_3)_2(\text{C}_3\text{H}_4\text{N}_2)]$	2.388(2)	81
$[\text{Rh}_2(\text{CH}_3\text{C}_5\text{H}_3\text{NO})_2(\text{O}_2\text{CCH}_3)_2(\text{C}_3\text{H}_4\text{N}_2)\cdot 2\text{CH}_2\text{Cl}_2]$	2.388(1)	81
$[\text{Rh}_2(\text{ClC}_5\text{H}_3\text{NO})_4]$	2.379(1)	81
$[\text{Rh}_2(\text{ClC}_5\text{H}_3\text{NO})_4(\text{C}_3\text{H}_4\text{N}_2)\cdot 2\text{H}_2\text{O}]$	2.385(1)	81
$[\text{Rh}_2(\text{FC}_5\text{H}_3\text{NO})_4(\text{DMSO})]$	2.410(1)	82
$[\text{Rh}_2(\text{C}_6\text{H}_4\text{NNC}_6\text{H}_5)_4(\text{C}_6\text{H}_5\text{CN})]$	2.412(1)	86
$[\text{Rh}_2(\text{C}_6\text{H}_4\text{NNC}_6\text{H}_5)_4\text{Cl}]$	2.406(1)	86

$[\text{Rh}_2(6\text{-CH}_3\text{C}_5\text{H}_3\text{NO})_4(6\text{-CH}_3\text{C}_5\text{H}_3\text{NOH})]^{80}$, $[\text{Rh}_2(6\text{-CH}_3\text{C}_5\text{H}_3\text{NO})_4(\text{C}_3\text{H}_4\text{N}_2).0.5\text{CH}_3\text{CN}]^{81}$, $[\text{Rh}_2(6\text{-CH}_3\text{C}_5\text{H}_3\text{NO})_4(\text{CH}_3\text{CN})]^{80}$, and $[\text{Rh}_2(6\text{-CH}_3\text{C}_5\text{H}_3\text{NO})_4]^{82}$, adopt a 3:1 arrangement of ligands allowing axial ligation only to the rhodium ion co-ordinated by three oxygen atoms and one nitrogen atom. The compound $[\text{Rh}_2(6\text{-CH}_3\text{C}_5\text{H}_3\text{NO})_4]^{80}$ (1.18) was found to have adjacent $[\text{Rh}_2(6\text{-CH}_3\text{C}_5\text{H}_3\text{NO})_4]$ units linked by Rh-O bonds (2.236(3) Å. The final two, $[\text{Rh}_2(\text{O}_2\text{CCH}_3)_2(6\text{-CH}_3\text{C}_5\text{H}_3\text{NO})_2(\text{C}_3\text{H}_4\text{N}_2)]^{81}$, and $[\text{Rh}_2(\text{O}_2\text{CCH}_3)_2(6\text{-CH}_3\text{C}_5\text{H}_3\text{NO})_2(\text{C}_3\text{H}_4\text{N}_2).2\text{CH}_2\text{Cl}_2]^{81}$, both adopt a 2:2 transoid arrangement of bridging ligands. The Rh-Rh bond lengths observed for these two compounds were significantly longer than those observed for compounds containing four 6-methyl-2-hydroxypyridine ligands (Table 1.7).



(1.18)

The compound $[\text{Rh}_2(6\text{-ClC}_5\text{H}_3\text{NO})_4]^{81}$ adopted a 2:2 transoid arrangement of ligands, effectively blocking both axial sites, while for $[\text{Rh}_2(6\text{-ClC}_5\text{H}_3\text{NO})_4(\text{C}_3\text{H}_4\text{N}_2).3\text{H}_2\text{O}]^{81}$ a 3:1 arrangement was observed with the axial ligand attached to the rhodium co-ordinated by three oxygen atoms and a nitrogen atom. In the compound $[\text{Rh}_2(6\text{-F}_3\text{H}_3\text{NO})_4(\text{DMSO})]^{82}$, the 6-fluoro-2-hydroxypyridine ligands adopted a totally polar arrangement about the metal-metal bond with the axial ligand attached to the rhodium co-ordinated by four oxygen atoms.

Crystal structures have been obtained for two compounds containing

aminopyridine ligands, $[\text{Rh}_2(\text{C}_6\text{H}_4\text{NNC}_6\text{H}_5)_4(\text{C}_6\text{H}_5\text{CN})]^{86}$ and $[\text{Rh}_2(\text{C}_6\text{H}_4\text{NNC}_6\text{H}_5)_4\text{Cl}]^{86}$ (a compound containing a $[\text{Rh}_2]^{5+}$ unit, although the authors were unable to determine the origin of the chloride ion). The compound $[\text{Rh}_2(\text{C}_6\text{H}_4\text{NNC}_6\text{H}_5)_4(\text{C}_6\text{H}_5\text{CN})]^{86}$ adopts a 2:2 transoid arrangement of bridging ligands while for the compound $[\text{Rh}_2(\text{C}_6\text{H}_4\text{NNC}_6\text{H}_5)_4\text{Cl}]^{86}$ the bridging ligands adopt a totally polar arrangement about the metal-metal bond.

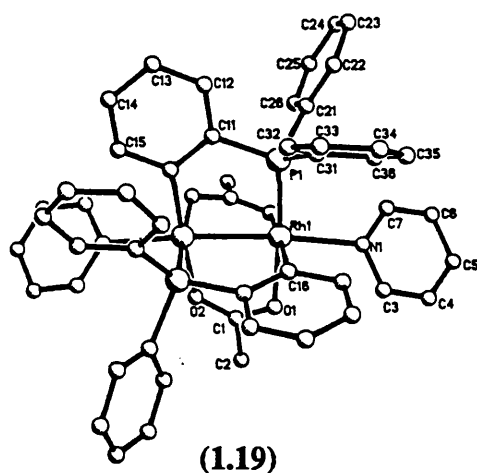
The electrochemical behaviour of three compounds containing hydroxypyridine ligands and two compounds containing aminopyridine ligands have been studied. The compounds $[\text{Rh}_2(\text{RC}_5\text{H}_3\text{NO})_4]$ ($\text{R}=\text{H}, \text{Cl}, \text{CH}_3$) have each been studied electrochemically in nine non-aqueous solvents⁸³. A one-electron oxidation was observed for each compound in all solvents. The potential of the oxidation was found to vary considerably depending on the substituent group R, and on the solvent employed in the measurement. The trends observed mirrored those observed previously for other dirhodium compounds^{67,68}.

The compound $[\text{Rh}_2(\text{C}_6\text{H}_4\text{NNC}_6\text{H}_5)_4]^{84-86}$ was studied electrochemically in dichloromethane by two laboratories who obtained differing results. One laboratory^{84,85} observed two one-electron oxidations ($E_{1/2}=+0.07$ and $+0.72$ V vs Ag/AgCl) and an irreversible reduction ($E_{pc}\approx -1$ V), while the other⁸⁶, observed two one-electron oxidations but at half-wave potentials of $+0.08$ and $+0.82$ V (vs S.C.E.). Two possible reasons were expressed for the difference firstly, that the cell conditions were not the same *ie* different electrolytes and reference systems were used, and secondly, that the two samples could be different isomers.

The electrochemical behaviour of the compound $[\text{Rh}_2(\text{C}_6\text{H}_4\text{NNC}_6\text{H}_5)_4\text{Cl}]^{86}$ was also investigated in dichloromethane (0.1 M TBAP supporting electrolyte). Two one-electron reversible processes were observed, a reduction and an oxidation ($E_{1/2}=-0.38$ and $+0.52$ V vs S.C.E.).

1.7.4 Dirhodium Compounds Containing More Than One Type of Bridging Ligand.

The most extensively studied group of compounds containing more than one type of bridging ligand are those containing orthometallated phosphine ligands. The first of these, $[\text{Rh}_2(\text{O}_2\text{CCH}_3)_2((\text{C}_6\text{H}_5)_2\text{P}(\text{C}_6\text{H}_4))_2 \cdot 2\text{L}]$ ($\text{L}=\text{CH}_3\text{CO}_2\text{H}$ (1.19), $\text{C}_5\text{H}_5\text{N}$) were reported in 1985^{87,88}. Crystallographic studies revealed that the triphenylphosphine ligands were co-ordinated through the phosphorus atom and that orthometallation had occurred at one of the three phenyl rings on each $[\text{P}(\text{C}_6\text{H}_4)(\text{C}_6\text{H}_5)_2]$ ligand. In both compounds the acetate ligands were in a cisoid arrangement.



The electrochemical behaviour of the compound $[\text{Rh}_2(\text{O}_2\text{CCH}_3)_2((\text{C}_6\text{H}_5)_2\text{P}(\text{C}_6\text{H}_4))_2 \cdot 2\text{CH}_3\text{CO}_2\text{H}]$ ⁸⁷, was studied in three solvents, dichloromethane, THF, and methanol (0.1 M TBABF₄ supporting electrolyte). A one-electron oxidation and two ill-defined reductions were observed for each compound in all solvents. The addition of potential donor ligands (pyridine, *p*-dithiane, dimethylphenylphosphine) caused cathodic shifts in the potential of the oxidations, with the magnitude of the shift increasing with increasing donicity of the ligand.

Six further examples of orthometallated dirhodium(II/II) compounds have been reported⁸⁹⁻⁹², using a variety of tertiary phosphine ligands and carboxylates. Crystal structures have been obtained for four of these compounds. Table 1.8 presents the Rh-Rh bond lengths observed. The compound $[\text{Rh}_2(\text{O}_2\text{CCH}_3)_2((\text{C}_6\text{H}_4)\text{P}(\text{C}_6\text{H}_5)_2)((\text{C}_6\text{H}_4)\text{P}(o\text{-ClC}_6\text{H}_4)(\text{C}_6\text{H}_5)).\text{P}(\text{C}_6\text{H}_5)_3]$ ⁹⁰ contains two different phosphine ligands. Both phosphorus atoms are co-ordinated to the same rhodium ion with the orthometallated carbon atoms and the axial triphenylphosphine ligand co-ordinated to the other rhodium ion. This difference in the co-ordination spheres of the two rhodium ions led to the suggestion that this compound formally contains a Rh(I)/Rh(III) core⁹⁰.

The reactivity of one orthometallated dirhodium(II/II) compound $[\text{Rh}_2(\text{O}_2\text{CCH}_3)_2((\text{C}_6\text{H}_5)_2\text{P}(\text{C}_6\text{H}_4))_2.2\text{THF}]$ with monothiocarboxylic acids $(\text{HO}(\text{S})\text{CR})$ $\text{R}=\text{CH}_3, \text{C}_6\text{H}_5, \text{C}(\text{CH}_3)_3$ has been investigated⁹³. These reactions have provided a simple route to the compounds $[\text{Rh}_2(\text{OSCR})_4(\text{P}(\text{C}_6\text{H}_5)_3)_2]$ ⁹³. These compounds were fully characterised and the crystal structure of one, $[\text{Rh}_2(\text{OSCC}(\text{CH}_3)_3)_4(\text{P}(\text{C}_6\text{H}_5)_3)_2]$ reported. The electrochemical behaviour of these compounds was investigated in two solvents, dichloromethane and methanol (0.1 M TBABF₄ supporting electrolyte). A one-electron oxidation was observed for each compound in both solvents, the half-wave potentials being dependent on the substituent group, R. Changing the solvent employed had no observable effect on the electrochemical behaviour suggesting that no significant dissociation of the axial ligand occurred in the solvents employed.

Several other dirhodium(II/II) ^{compounds} containing more than one type of bridging ligand have also been investigated during the last five years. A series of dirhodium(II/II) compounds containing both acetate and 1,8-naphthyridinate ligands were prepared by Ford and co-workers^{94,95} and the crystal structure of one of these, $[\text{Rh}_2(\text{O}_2\text{CCH}_3)_3(\text{C}_{18}\text{H}_{12}\text{N}_4)][\text{PF}_6]$ was reported. The electrochemical behaviour of each

Table 1.8 Structural data for orthometallated dirhodium(II/II) compounds.

Compound.	Rh-Rh (Å)	Ref.
$[\text{Rh}_2(\text{O}_2\text{CCH}_3)_2((\text{C}_6\text{H}_4)\text{P}(\text{C}_6\text{H}_5)_2)_2 \cdot 2\text{CH}_3\text{CO}_2\text{H}]$	2.508(1)	87
$[\text{Rh}_2(\text{O}_2\text{CCH}_3)_2((\text{C}_6\text{H}_4)\text{P}(\text{C}_6\text{H}_5)_2)_2 \cdot 2\text{C}_5\text{H}_5\text{N}]$	2.556(2)	87
$[\text{Rh}_2(\text{O}_2\text{CCH}_3)_2((\text{C}_6\text{H}_4)\text{P}(o\text{-ClC}_6\text{H}_4)(\text{C}_6\text{H}_5))$ $((\text{C}_6\text{H}_4)\text{P}(\text{C}_6\text{H}_5)_2) \cdot \text{P}(\text{C}_6\text{H}_5)]$	2.558(1)	90
$[\text{Rh}_2(\text{O}_2\text{CCH}_3)_2((\text{C}_5\text{H}_5\text{N})\text{P}(\text{C}_6\text{H}_5)_2)_2 \cdot \text{Cl}_2]$	2.518(1)	91
$[\text{Rh}_2(\text{O}_2\text{CC}(\text{CH}_3)_3)_2((\text{C}_6\text{H}_4)\text{P}(\text{CH}_3)(\text{C}_6\text{H}_5)_2)_2 \cdot 2\text{C}_5\text{H}_5\text{N}]$	2.535(5)	92
$[\text{Rh}_2((\text{CH}_3)_2\text{PCH}_2\text{P}(\text{CH}_3)_2)_2((\text{C}_6\text{H}_4)\text{P}(\text{C}_6\text{H}_5)_2)_2 \text{Cl}_2]$	2.770(3)	89

of the compounds was studied in acetonitrile (0.1 M TBAP supporting electrolyte). A one-electron reversible oxidation and either one or two reversible reductions were observed for each compound. The potentials observed ($E_{1/2} \approx +1.30, -0.60$ and -1.20 V vs S.C.E.) were considerably more anodic than those observed for $[\text{Rh}_2(\text{O}_2\text{CCH}_3)_4(\text{CH}_3\text{CN})_2]$ where a reversible one-electron oxidation and an irreversible reduction were observed at $E_{1/2} = +1.02$ and -1.08 V. These results led to the suggestion that the naphthyridine ligands are less electron donating in nature than the acetate ligands, giving rise to an anodic shift in the potentials of both oxidations and reductions.

The electrochemical investigation of a series of compounds $[\text{Rh}_2(\text{O}_2\text{CCH}_3)_n(\text{HNOCH}_3)_{4-n}]$ ($n=0,1,2,3,4$) containing both acetamidate ligands and acetate ligands was discussed in Section 1.7.2⁷⁸. The structure of one of these compounds $[\text{Rh}_2(\text{O}_2\text{CCH}_3)(\text{HNOCH}_3)_3(\text{DMSO})_2 \cdot 2\text{H}_2\text{O}]$ was reported by Bear and co-workers⁹⁶. The axial DMSO ligands were bound to the $[\text{Rh}_2]^{4+}$ unit through the sulphur atom (Rh-Rh = 2.446(0) Å).

The compound $[\text{Rh}_2(\text{O}_2\text{CCF}_3)_2((p\text{-CH}_3\text{C}_6\text{H}_4)_2\text{CH})_2(\text{H}_2\text{O})_2 \cdot 0.5\text{C}_6\text{H}_6]$ was studied crystallographically and electrochemically⁹⁷. The crystal structure revealed that the two trifluoroacetate ligands co-ordinate *cis* to each other (Rh-Rh = 2.425(1) Å). Two reversible one electron oxidations were observed in CH_3CN (0.1 M TEAP supporting electrolyte) and CH_2Cl_2 (0.1 M TBAP supporting electrolyte). These oxidations were assigned to Equations 1.3 and 1.4.



Chapter Two.

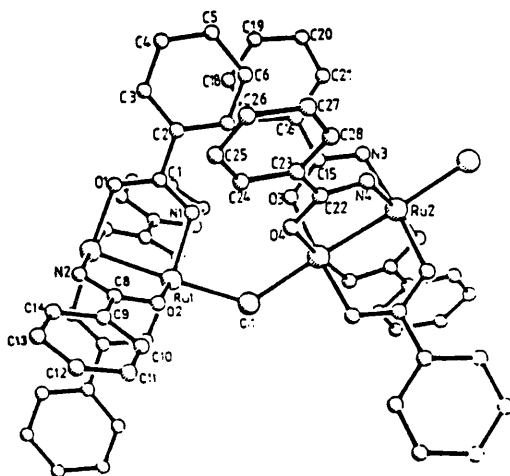
Ligand Substituent Effects on the Electrochemical Behaviour of Chlorotetrakis(amidato)diruthenium(II/III) Compounds.

2.1	Introduction.	61
2.2	Preparation and characterisation.	66
2.3	Electrochemical investigation.	70
2.3.1	Results.	70
2.3.2	Electrochemical behaviour - A rationalisation.	74
2.3.3	Ligand Substituent effects.	84
	a) Identity of the substituent group.	84
	b) Position of the substituent group.	85
2.4	Conclusions.	90
2.5	Experimental.	92
2.5.1	Materials and Instrumentation.	92
2.5.2	Synthesis of $[\text{Ru}_2(\text{O}_2\text{CCH}_3)_4\text{Cl}]$.	93
2.5.3	Synthesis of $[\text{Ru}_2(\text{HNOCH})_4\text{Cl}]$.	93
2.5.4	Synthesis of $[\text{Ru}_2(\text{HNOCCCH}_3)_4\text{Cl}]$.	93
2.5.5	Synthesis of other $[\text{Ru}_2(\text{RNOCR}')_4\text{Cl}]$ compounds.	94

2.1 Introduction.

Five chlorotetrakis(amidato)diruthenium(II/III) compounds

$[\text{Ru}_2(\text{HNOCR}')_4\text{Cl}]$ ($\text{R}' = \text{CH}_3, \text{CF}_3, \text{C}(\text{CH}_3)_3, \text{C}_6\text{H}_5, \text{C}_6\text{H}_4\text{Cl}$) have been reported previously³⁸⁻⁴². Two of these compounds have been studied crystallographically, $[\text{Ru}_2(\text{HNOCC}_6\text{H}_5)_4\text{Cl}]$ ⁴¹(2.1) and $[\text{Ru}_2(\text{HNOCC}_6\text{H}_4\text{Cl})_4\text{Cl}]$ ⁴². The two structures are



(2.1)

very similar, containing a diruthenium(II/III) unit (Ru-Ru 2.293(2) Å and 2.296[1] Å respectively) bridged by four amidato ligands. In both cases the amidato ligands are in a 2:2 cisoid arrangement. The diruthenium(II/III) units are linked into zig-zag chains by chloride ion linkages in the solid state.

The effect of the solvent in which measurements are made on the electrochemical behaviour of two compounds $[\text{Ru}_2(\text{HNOCCF}_3)_4\text{Cl}]$ ³⁸ and $[\text{Ru}_2(\text{HNOCC}(\text{CH}_3)_3)_4\text{Cl}]$ ⁴⁰ has been studied in detail. Between one and four electron transfer reactions were observed for each compound depending on the identity of the solvent. The results obtained are presented in Tables 2.1 and 2.2. The compound $[\text{Ru}_2(\text{HNOCCF}_3)_4\text{Cl}]$ ³⁸ was observed to undergo only reductions while only oxidation reactions were observed for $[\text{Ru}_2(\text{HNOCC}(\text{CH}_3)_3)_4\text{Cl}]$ ⁴⁰. In both series of experiments

**Table 2.1 Electrochemical Data for $[\text{Ru}_2(\text{HNOCCF}_3)_4\text{Cl}]$
(0.1 M TBAP supporting electrolyte).**

Solvent	Red. 1 $E_{1/2}/\text{V}$	Red. 2 $E_{1/2}/\text{V}$	Red.3 $E_{1/2}/\text{V}$	Red. 4 $E_{1/2}/\text{V}$
$\text{C}_2\text{H}_4\text{Cl}_2$	-	-0.02	-0.32	-1.44
CH_2Cl_2	-	-0.03	-0.33	-1.44
n- $\text{C}_3\text{H}_7\text{CN}$	+0.01	-0.04	-0.30	-1.40
CH_3NO_2	-	-0.05	-0.33	-
CH_3CN	0.00	-0.06	-0.30	-1.41
THF	+0.01	-0.07	-0.35	-1.31
CH_3OH	-0.07	-	-	-
$(\text{CH}_3)_2\text{CO}$	-	-0.09	-0.37	-
DMSO	-0.19	-	-	-
DMA	-0.22	-	-	-
DMF	-0.22	-	-	-

Table 2.2 Electrochemical Data for $[\text{Ru}_2(\text{HNOCC}(\text{CH}_3)_3)_4\text{Cl}]$
 (0.1 M TBABF₄ supporting electrolyte).

Solvent	Ox. 1 $E_{1/2}/\text{V}$	Ox. 2 $E_{1/2}/\text{V}$	Ox. 3 $E_{1/2}/\text{V}$	Ox. 4 $E_{1/2}/\text{V}$
DMF	0.67	0.78	0.91	1.14
C ₂ H ₄ Cl ₂	0.61	0.84	1.00	1.23
C ₆ H ₅ CN	0.63	0.85	1.03	1.12
DMSO	-	0.85	-	-
THF	0.55	0.90	1.03	1.32
PC	0.77	0.90	1.04	1.27
CH ₃ CN	0.78	0.92	1.10	1.34
CH ₂ Cl ₂	0.68	0.93	1.09	1.33
CH ₃ NO ₂	0.78	1.00	-	-
C ₂ H ₅ OH	0.97	1.06	-	-
CH ₃ OH	1.01	1.07	-	-

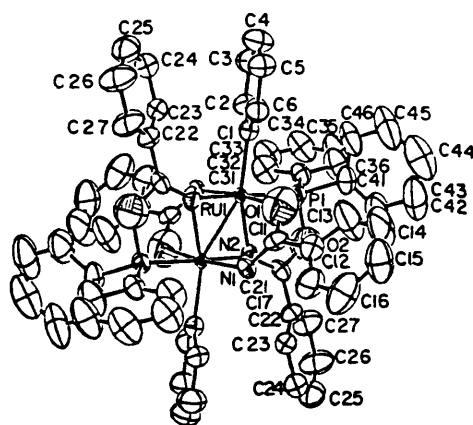
the number of reactions observed and the potentials at which they occurred were found to be dependent on the solvents employed in the measurement. For the compound $[\text{Ru}_2(\text{HNOCCF}_3)_4\text{Cl}]^{38}$ it was reported that in non-bonding or weakly bonding solvents (TBAP supporting electrolyte) two or three redox processes were observed (in THF and acetonitrile four processes were observed, the sum of the peak currents for the first three processes was equal to that of the fourth process), while in strongly bonding solvents eg DMSO only one process was observed.

In both of the electrochemical investigations^{38,40} the addition of chloride ions to the electrochemical cell affected the number of electron transfer reactions that were observed. For example, the addition of chloride ions to the electrochemical cell containing $[\text{Ru}_2(\text{HNOCCF}_3)_4\text{Cl}]^{38}$, in non-bonding or weakly bonding solvents, resulted in a decrease in the peak currents of the first two processes with a concomitant rise in the peak current of the third. In strongly bonding solvents the single process observed was shifted to a more cathodic potential. Both sets of authors concluded that the chains present in the solid state break down in solution and an equilibrium mixture exists between three differently axially ligated adducts, as illustrated in Scheme 2.1. The addition of chloride ions to the electrochemical cell^{38,40} alters the position of the equilibrium, pushing it towards the anionic bis-chloride adduct so that in the limiting case only the bis-chloride adduct is present. Conversely the addition of silver ions to the electrochemical cell³⁸ removes chloride ions from the solution and thus displaces the equilibrium towards the bis-solvato adduct. Series of electrochemical experiments involving the recording of voltammograms, with varying amounts of added chloride or silver ions in the electrochemical cell, allowed the assignments of the individual voltammetric waves to particular axially ligated adducts.

The electrochemical behaviour of two other compounds,

$[\text{Ru}_2(\text{HNOCC}_6\text{H}_5)_4\text{Cl}]^{99}$ and $[\text{Ru}_2(\text{HNOCC}_6\text{H}_5)_4\text{Cl}]^{98}$, has also been studied. In both cases two reductions were observed. For the compound $[\text{Ru}_2(\text{HNOCC}_6\text{H}_5)_4\text{Cl}]^{99}$ an oxidation was also observed. The addition of chloride ions to an electrochemical cell containing $[\text{Ru}_2(\text{HNOCC}_6\text{H}_5)_4\text{Cl}]^{98}$ caused a shift to a more cathodic potential of the first reduction process and the emergence of two new processes, a quasireversible oxidation and an irreversible reduction.

Further investigations into the compound $[\text{Ru}_2(\text{HNOCC}_6\text{H}_5)_4\text{Cl}]$, revealed that it reacts with triphenylphosphine in a DMSO/methanol solvent mixture. The reaction results in the oxidation of the $[\text{Ru}_2]^{+5}$ unit to $[\text{Ru}_2]^{+6}$ and the rearrangement of ligands to form the compound



(2.2)

$[\text{Ru}_2(\text{C}_6\text{H}_5)_2(\text{HNOCC}_6\text{H}_5)_2(\text{NC}(\text{C}_6\text{H}_5)\text{OP}(\text{C}_6\text{H}_5)_2)]^{98}$ (2.2). Crystallographic studies on this compound have shown it to possess a edge-sharing bioctahedral structure. The $[\text{NC}(\text{C}_6\text{H}_5)\text{OP}(\text{C}_6\text{H}_5)_2]$ ligands are co-ordinated to the diruthenium(III/III) unit in both bridging and chelating modes, with the nitrogen atom co-ordinated to both metal ions⁹⁸. The authors were unable to establish the oxidising agent involved in the reaction but, the lower than 50% yield led to the suggestion that a disproportionation reaction may have occurred. Similar reactions were subsequently reported with other variously substituted aryl amidates and aryl tertiary phosphines^{99,100}.

The electrochemical studies carried out to date indicate that the

substituent group attached to the amidate ligand plays an important role in determining the redox potential of the electron transfer reactions. For the compound $[\text{Ru}_2(\text{HNOCCF}_3)_4\text{Cl}]$, which contains an electron withdrawing substituent group (CF_3), only reductions are observed³⁸, while for the compound $[\text{Ru}_2(\text{HNOCC}(\text{CH}_3)_3)_4\text{Cl}]$, which contains an electron donating substituent group ($\text{C}(\text{CH}_3)_3$), oxidations are observed⁴⁰. This chapter will examine the effect of ligand substituent groups on the electrochemical behaviour of a range of chlorotetrakis(amidato)diruthenium(II/III) compounds.

2.2 Preparation and Characterisation.

Eleven chlorotetrakis(amidato)diruthenium(II/III) compounds have been prepared in good yield. The method of preparation was to stir $[\text{Ru}_2(\text{O}_2\text{CCH}_3)_4\text{Cl}]$, for extended periods, with an excess of the ligand HRNOCR' , at elevated temperature under a dinitrogen atmosphere. This method is strictly analogous to that reported previously for the synthesis of the compounds $[\text{Ru}_2(\text{HNOCCF}_3)_4\text{Cl}]$ ³⁸, $[\text{Ru}_2(\text{HNOCC}(\text{CH}_3)_3)_4\text{Cl}]$ ⁴⁰, and $[\text{Ru}_2(\text{HNOCC}_6\text{H}_4\text{R}')_4\text{Cl}]$ ($\text{R}'=\text{H}$ ⁴¹, Cl ⁴²). The excess ligand was removed by vacuum sublimation onto a water-cooled cold finger. The amidate ligands employed are illustrated in Figure 2.1. The compounds formed have been characterised using infrared spectroscopy and microanalytical measurements. Magnetic susceptibility measurements have also been made (see experimental section).

The microanalytical data obtained on the eleven compounds indicate that they are of the general formula $[\text{Ru}_2(\text{RNOCR}')_4\text{Cl}]$ ($\text{R}, \text{R}'=\text{H}, \text{CH}_3, \text{CF}_3, \text{C}_6\text{H}_5, \text{C}_6\text{H}_4\text{CH}_3, \text{C}_6\text{H}_4\text{CF}_3, \text{C}_6\text{H}_4\text{Cl}$ not all possible combinations). Comparison of the infrared

Scheme 2.1 A scheme illustrating the equilibrium existing between different axially ligated tetra-bridged diruthenium(II/III) compounds in solution.

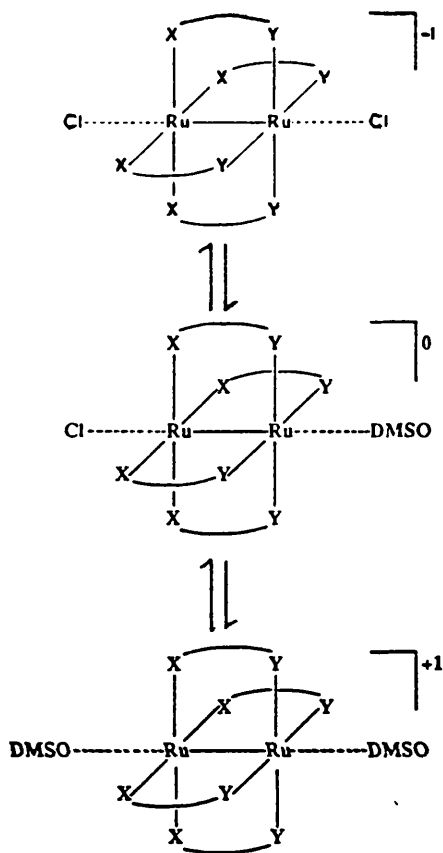
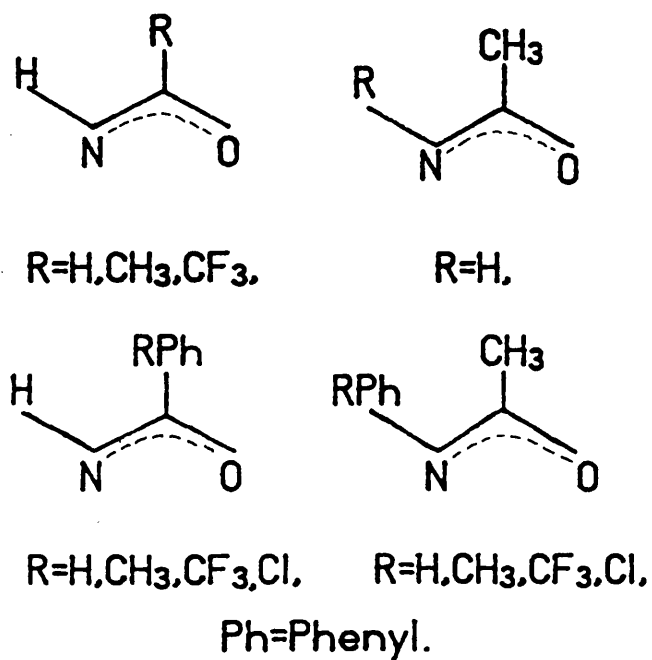


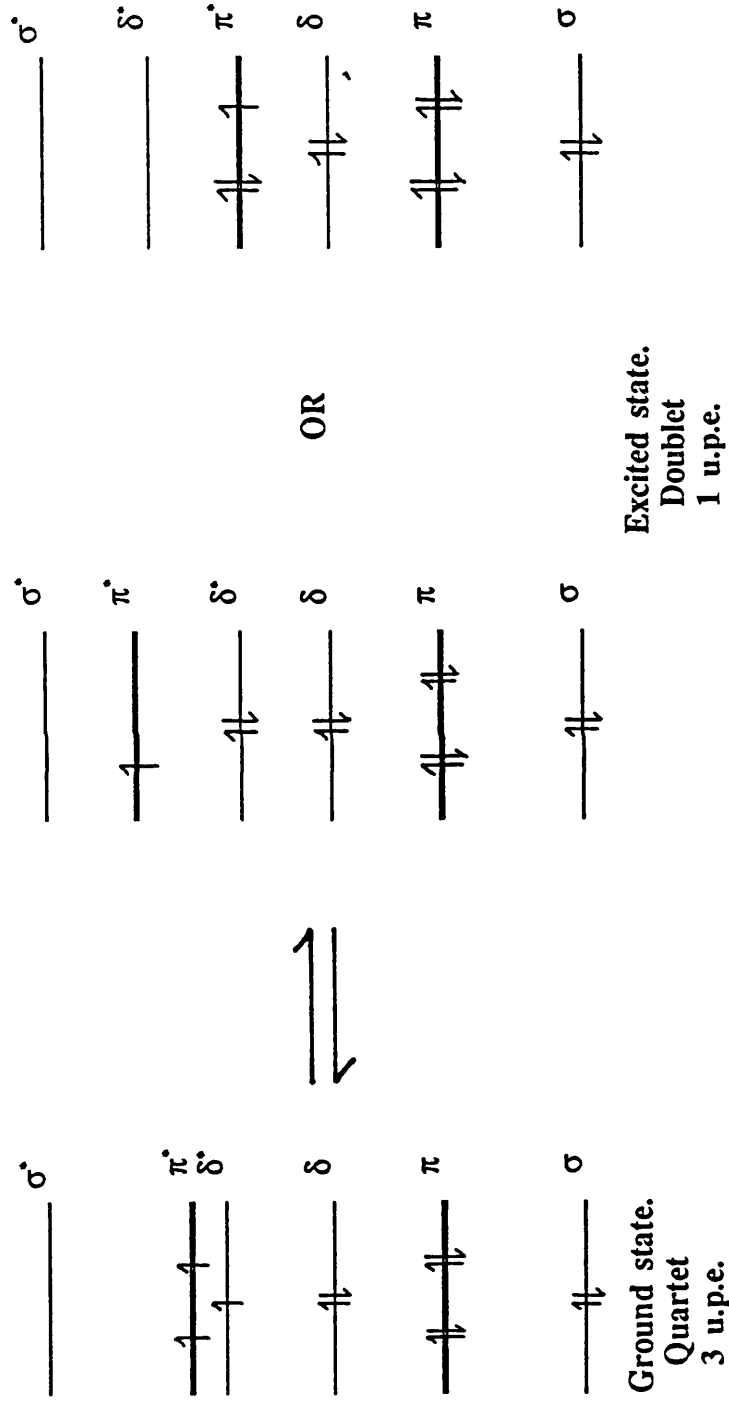
Figure 2.1 Diagrammatic representations of the amidate ligands used.



spectra ($4000\text{-}250\text{ cm}^{-1}$) of the products with that recorded for $[\text{Ru}_2(\text{O}_2\text{CCH}_3)_4\text{Cl}]$ reveals the absence of bands due to symmetric and asymmetric O-C-O stretches at 1470 cm^{-1} and 1560 cm^{-1} respectively. No detailed study of the infrared spectra of compounds of this type has appeared in the literature but it does not seem unreasonable to tentatively assign symmetric and asymmetric N-C-O stretches to bands in the region $1410\text{-}1430\text{ cm}^{-1}$ and $1510\text{-}1540\text{ cm}^{-1}$ respectively. Bands in the region $1130\text{-}1160\text{ cm}^{-1}$ in the spectra of $[\text{Ru}_2(\text{HNOCR}')_4\text{Cl}]$ ($\text{R}'=\text{CF}_3, \text{CF}_3\text{C}_6\text{H}_4$) and $[\text{Ru}_2(\text{CF}_3\text{C}_6\text{H}_4\text{NOCCH}_3)_4\text{Cl}]$ have been tentatively assigned to the C-F stretch. For the compounds $[\text{Ru}_2(\text{HNOCR}')_4\text{Cl}]$ bands in the region $3260\text{-}3370\text{ cm}^{-1}$ have been tentatively assigned to the N-H stretch.

Previous magnetic susceptibility measurements on chlorotetrakis (carboxylato)diruthenium(II/III) compounds^{15,24} have revealed the presence of three unpaired electrons per diruthenium unit (Section 1.4.1). Room temperature measurements made during this study have given results which indicate values of μ_{eff} between 2.26 BM and 5.54 BM per diruthenium unit (see Table 2.7). These results suggest an equilibrium may exist between a ground state electronic configuration, $\sigma^2\pi^4\delta^2\delta^*\pi^2$ where the π^* and the δ^* orbitals are essentially degenerate and an excited state $\sigma^2\pi^4\delta^2\delta^*\pi^*$ or $\sigma^2\pi^4\delta^2\pi^3$ configuration (Figure 2.2). A similar scheme has been postulated to explain the unusual magnetic properties of $[\text{Os}_2(\text{O}_2\text{CR})_4\text{Cl}_2]$ molecules¹⁰¹. As the new measurements have only been made at room temperature however, no firm conclusions can be made.

Figure 2.2 Qualitative molecular orbital schemes illustrating the proposed equilibrium between the ground state (quartet) and the excited state (doublet).



2.3 Electrochemical Investigations.

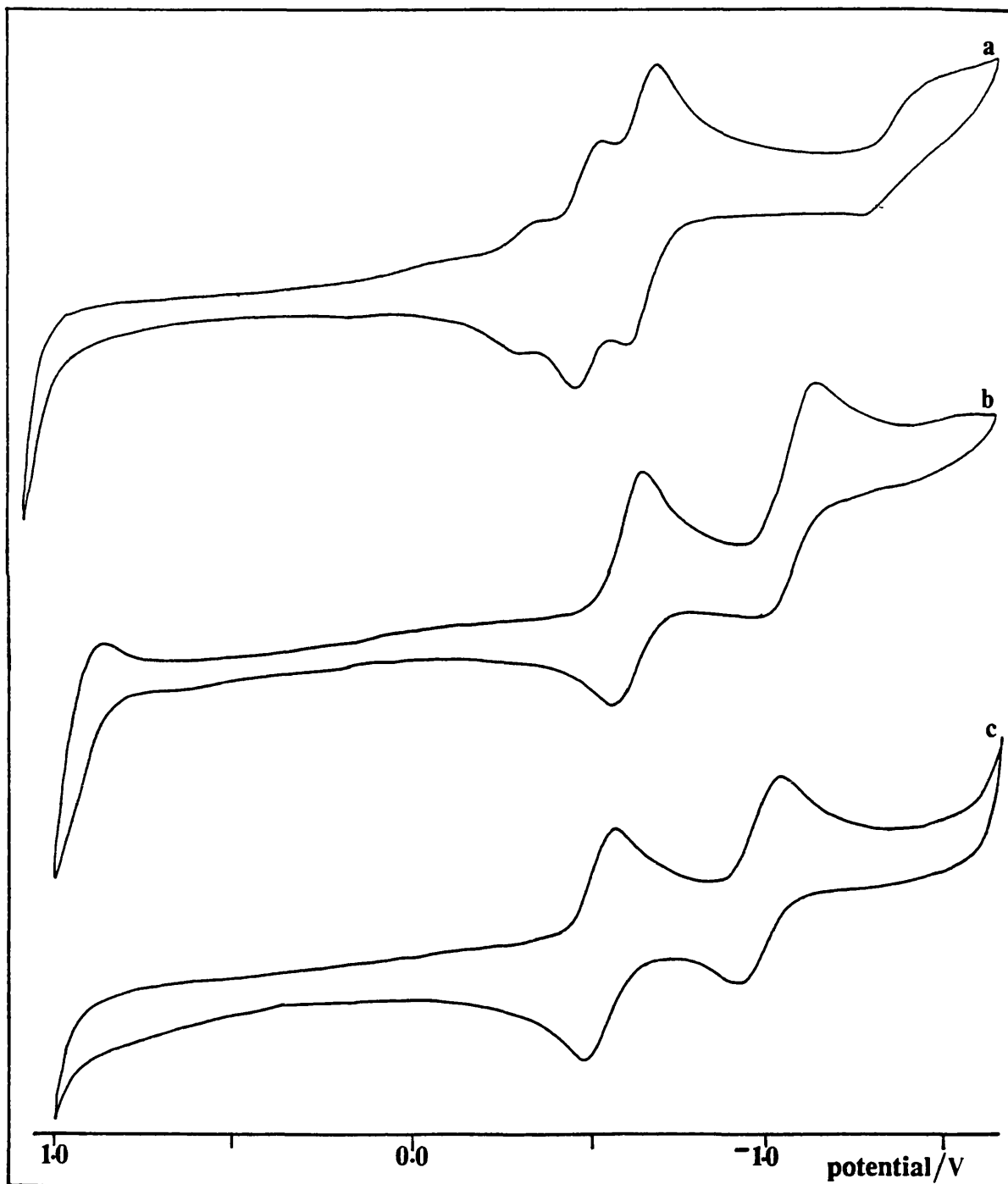
2.3.1 Results.

The electrochemical behaviour of each of the eleven compounds prepared has been studied in DMSO (0.1 M TBABF₄ supporting electrolyte) using cyclic and A.C. voltammetric techniques (Appendix 1). At least one and upto four reduction processes have been observed in the potential range -2.0 V to +1.0 V. for all compounds. An oxidation process has also been observed for three of the compounds studied.

For the compounds [Ru₂(RNOCC₆H₄)₄Cl] (R'=C₆H₅, CH₃C₆H₄, CF₃C₆H₄, ClC₆H₄) three evenly spaced quasireversible reductions are observed, the difference in potential between each process being approximately 100-150 mV. For one of these compounds [Ru₂(CH₃C₆H₄NOCC₆H₄)₄Cl] a fourth quasireversible reduction is also observed. The compounds [Ru₂(HNOCR')₄Cl] (R'=CH₃, C₆H₅, CF₃C₆H₄, ClC₆H₄) exhibit only two quasireversible reductions, while two quasireversible reductions and a quasireversible oxidation are observed for [Ru₂(HNOCR')₄Cl] (R'=H, CH₃C₆H₄). Finally the compounds [Ru₂(HNOCR')₄Cl] (R=CF₃, CH₃) exhibit only one quasireversible reduction within the solvent range (Figure 2.3). For the compounds [Ru₂(HNOCR')₄Cl] (R'=H, CH₃, C₆H₅, CH₃C₆H₄, CF₃C₆H₄, ClC₆H₄) the first reduction is broad and for one compound, [Ru₂(HNOCC₆H₄CH₃)₄Cl], a shoulder is observed on the cathodic side of this reduction wave.

The addition of chloride ions (in the form of [C₆H₅(^{CH₂}C₂H₅)₃N]Cl) and silver ions (in the form of Ag[BF₄]) to the electrochemical cell has resulted in changes in the number of observed reactions and their redox potentials. The addition of chloride ions to the electrochemical cell containing the compounds

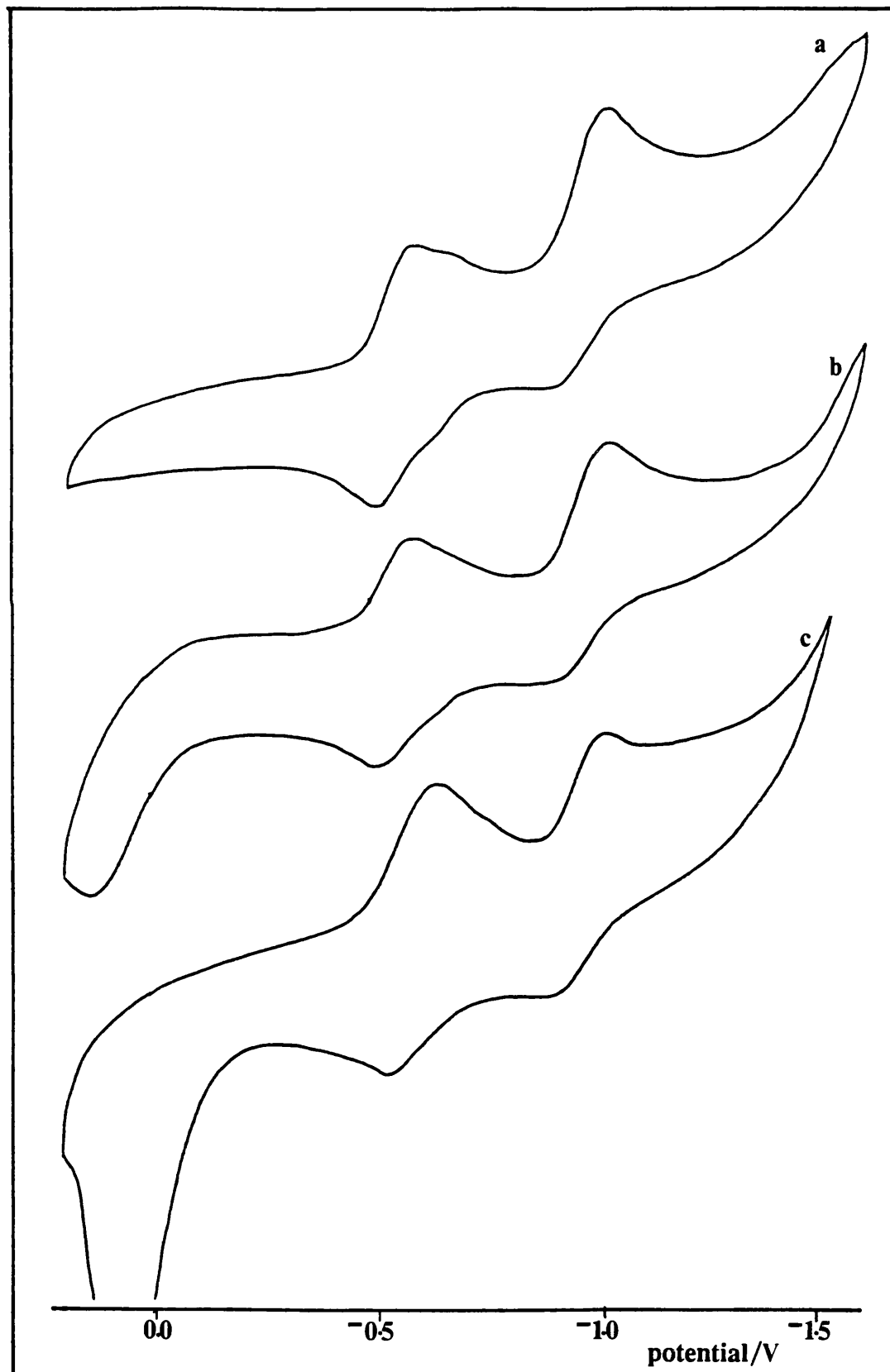
Figure 2.3 Cyclic voltammograms recorded in DMSO (0.1 M TBABF₄ supporting electrolyte) for a) [Ru₂(CH₃C₆H₄NOCCH₃)₄Cl], b) [Ru₂(HNOCC₆H₄CH₃)₄Cl], and c) [Ru₂(HNOCC₆H₄CF₃)₄Cl].



$[\text{Ru}_2(\text{HNOCR}')_4\text{Cl}]$ ($\text{R}'=\text{H}, \text{CH}_3, \text{CF}_3, \text{C}_6\text{H}_5, \text{CH}_3\text{C}_6\text{H}_4, \text{CF}_3\text{C}_6\text{H}_4, \text{ClC}_6\text{H}_4$) results in a sharpening of the peaks due to the first reduction, and a shift in the half-wave potential of this reduction process to a more cathodic, *ie.* more negative value (Figure 2.4). The shift observed is in the range 40-80 mV, with the single exception of $[\text{Ru}_2(\text{HNOCCF}_3)_4\text{Cl}]$, where the reduction moves to a half-wave potential 120 mV more cathodic. For the compounds where an oxidation is also observed ($\text{R}'=\text{H}, \text{CH}_3\text{C}_6\text{H}_4$) the addition of chloride ions causes a cathodic shift in the half-wave potential of the oxidation by an average value of 90 mV. For the compound $[\text{Ru}_2(\text{HNOCC}_6\text{H}_5)_4\text{Cl}]$ the addition of chloride ions to the electrochemical cell results in the appearance of a quasi-reversible oxidation close to the solvent limit. The addition of silver ions to solutions of these compounds also results in a sharpening of the first reduction wave for each compound, but the half wave potentials observed for these processes are not noticeably altered. The shoulder observed for the compound $[\text{Ru}_2(\text{HNOCC}_6\text{H}_4\text{CH}_3)_4\text{Cl}]$ collapses on the addition of silver ions to the electrochemical cell. Neither the addition of chloride ions or the addition of silver ions has any noticeable effect on the second reduction process observed for these compounds.

The addition of chloride ions to solutions of the compounds $[\text{Ru}_2(\text{RNOCCH}_3)_4\text{Cl}]$ ($\text{R}=\text{C}_6\text{H}_5, \text{CH}_3\text{C}_6\text{H}_4, \text{CF}_3\text{C}_6\text{H}_4, \text{ClC}_6\text{H}_4$) where three evenly spaced reduction processes are observed initially, results in a small decrease in the peak currents of the first and second reduction waves accompanied by a concomitant increase in the peak current for the third reduction wave. The addition of silver ions to solutions of these compounds has the opposite effect causing a small decrease in the peak currents of the second and third reduction waves with a corresponding rise in the peak current for the first reduction wave. The extent to which the peak currents observed are effected varies depending on the substituent

Figure 2.4 Cyclic voltammograms recorded for $[\text{Ru}_2(\text{HNOCC}_6\text{H}_4\text{Cl})_4\text{Cl}]$ in
a) DMSO b) DMSO + Ag^+ ions and c) DMSO + Cl^- ions
(0.1 M TBABF_4 supporting electrolyte).



attached to the nitrogen atom. For the compound $[\text{Ru}_2(\text{CH}_3\text{C}_6\text{H}_4\text{NOCCH}_3)_4\text{Cl}]$ the addition of less than one molar equivalent of silver ions causes the complete collapse of the third reduction wave accompanied by concomitant rises in the peak currents of the first two processes. The addition of a ten-fold excess of chloride ions cause an increase in the peak current of the third reduction wave and a corresponding decrease in the peak currents for the first two processes (Figure 2.5a). The effect of these additions is less pronounced for the compound $[\text{Ru}_2(\text{CF}_3\text{C}_6\text{H}_4\text{NOCCH}_3)_4\text{Cl}]$ and virtually no alteration is observed in the peak currents of the three processes (Figure 2.5b). Neither of these additions has any observable effect on the fourth reduction wave observed for the compound $[\text{Ru}_2(\text{CH}_3\text{C}_6\text{H}_4\text{NOCCH}_3)_4\text{Cl}]$.

2.3.2 Electrochemical Behaviour-A Rationalisation.

The hypothesis that diruthenium(II/III) compounds of this type exist as an equilibrium mixture of three adducts in solution is well documented^{38,40} (see Sections 1.6 and 2.1 and Scheme 2.1). The addition of chloride and silver ions to the electrochemical cell will effect the position of that equilibrium and the changes that this gives rise to in the cyclic voltammograms allows the assignment of the redox reactions to specific axially ligated adducts.

The compounds $[\text{Ru}_2(\text{RNOCCH}_3)_4\text{Cl}]$ ($\text{R}=\text{C}_6\text{H}_4, \text{CF}_3\text{C}_6\text{H}_4, \text{ClC}_6\text{H}_4$) exhibit three reduction waves while four reduction processes are observed for the compound $[\text{Ru}_2(\text{CH}_3\text{C}_6\text{H}_4\text{NOCCH}_3)_4\text{Cl}]$. The first three reduction processes are jointly responsible for the transfer of one electron per mole of $[\text{Ru}_2(\text{RNOCCH}_3)_4\text{Cl}]$ as determined by comparison of the limiting current of a stirred voltammogram with that of a known concentration of ferrocene. The reduction process is therefore

Figure 2.5a Cyclic voltammograms recorded for $[\text{Ru}_2(\text{CH}_3\text{C}_6\text{H}_4\text{NOCCH}_3)_4\text{Cl}]$ in

a) DMSO b) DMSO + Ag^+ ions and c) DMSO + Cl^- ions

(0.1 M TBABF_4 supporting electrolyte).

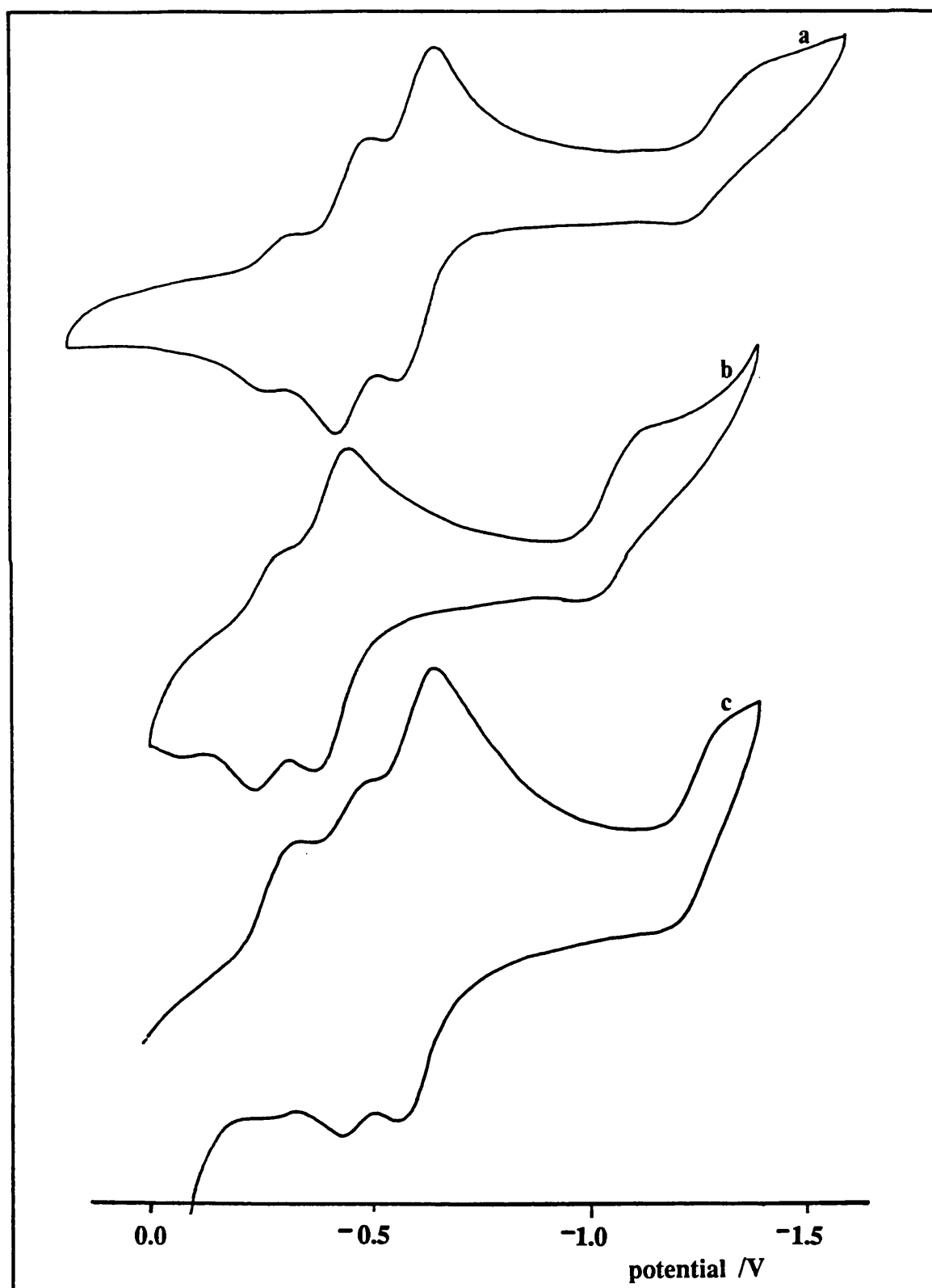
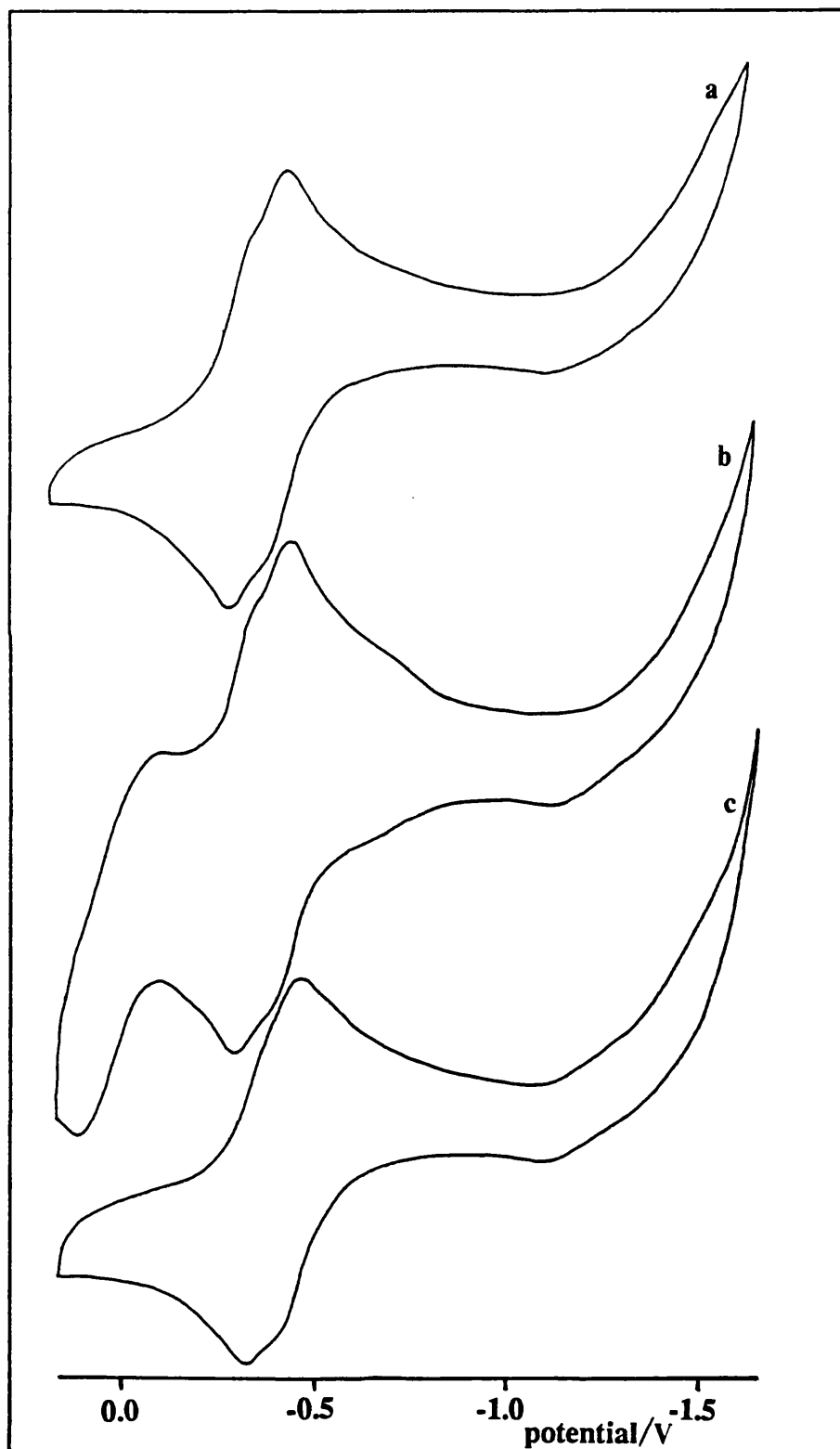


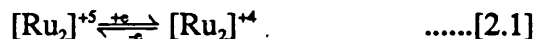
Figure 2.5b Cyclic voltammograms recorded for $[\text{Ru}_2(\text{CF}_3\text{C}_6\text{H}_4\text{NOCCH}_3)_4\text{Cl}]$ in

a) DMSO b) DMSO + Ag^+ ions and c) DMSO + Cl^- ions

(0.1 M TBABF_4 supporting electrolyte).



assigned as in Equation 2.1.



Comparison of the limiting current of a stirred voltammogram for the fourth reduction (observed for $[\text{Ru}_2(\text{CH}_3\text{C}_6\text{H}_4\text{NOCCH}_3)_4\text{Cl}]$), with that of a known concentration of ferrocene, indicates that the fourth reduction is also a one-electron process. The absence of a return wave indicates that the reduction is irreversible suggesting that the $[\text{Ru}_2]^{+3}$ unit formed initially is short lived and undergoes rapid decomposition. The current carried by this fourth reduction is be equal to the sum of the currents carried by the first three reductions (Figure 2.6). Together these two observations allow the assignment of this reduction to Equation 2.2.



Although the changes observed in the cyclic voltammograms on the addition of silver or chloride ions to the cell are small, these changes, coupled with the knowledge that the positively charged bis-solvato species should always be the easiest to reduce and the hardest to oxidise while the bis-chloro species which is negatively charged should be the hardest to reduce and the easiest to oxidise, allows the assignments of individual waves to be made. The changes in the cyclic voltammograms on the addition of silver ions to the electrochemical cell allows a reduction process to be assigned to the bis-solvato cations (Reduction 1), while the changes observed on the addition of chloride ions to the cell, leads to the assignment of the most cathodic reduction to the bis-chloro anions (Reduction 3). This leaves the reduction at intermediate potentials which must be attributed to the

Figure 2.6 Cyclic voltammogram and stirred voltammogram for $[\text{Ru}_2(\text{CH}_3\text{C}_6\text{H}_4\text{NOCCH}_3)_4\text{Cl}]$ in DMSO (0.1 M TBABF₄ supporting electrolyte.)



mono-chloro/mono-solvato adduct (Reduction 2). These assignments parallel those made in previous studies^{38,40}. The behaviour of the fourth reduction (Reduction 4) of the dinuclear unit observed for the compound $[\text{Ru}_2(\text{CH}_3\text{C}_6\text{H}_4\text{NOCCCH}_3)_4\text{Cl}]$ on the addition of silver or chloride ions suggests that after the first reduction (Equation 2.1) the kinetics of axial ligand exchange between the three adducts is too fast for the reduction of the individual adducts to be observed. The possibility that only one of the three adducts exists after the initial reduction has been considered, but is thought to be unlikely, since the addition either of silver or chloride ions to the cell has no observable effect on the redox potential for that fourth reduction process.

Diruthenium(II/III) compounds containing amidate ligands with the substituent group attached to the nitrogen atom have not been previously reported. The results obtained here are unusual in that reduction processes are observed for all three adducts. Previously^{38,40} only one reduction process has been observed for chlorotetrakis(amidato)diruthenium(II/III) compounds investigated in DMSO (this process usually being attributed to the bis-dimethylsulphoxide adduct). The presence of three processes suggests that the rate of exchange between different axially ligated adducts for these compounds must be slower than the electrochemical experiment. In addition it implies that despite an enormous excess of DMSO the equilibrium is not displaced to favour the formation of only the bis-solvato adduct.

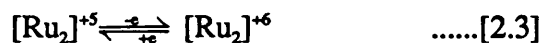
For the compounds $[\text{Ru}_2(\text{HNOCR}')_4\text{Cl}]$ ($\text{R}'=\text{H}, \text{CH}_3, \text{C}_6\text{H}_5, \text{CH}_3\text{C}_6\text{H}_4, \text{CF}_3\text{C}_6\text{H}_4, \text{ClC}_6\text{H}_4$) two reduction processes were observed. The first reduction has been found to be responsible for the transfer of one electron per mole of $[\text{Ru}_2(\text{RNOCR}')_4\text{Cl}]$ on a similar basis to that described above, and can be assigned to Equation 2.1. The peak current of the re-oxidation wave for the second reduction process decreases with decreasing scan rate indicating sluggish charge transfer kinetics. This suggests that the $[\text{Ru}_2]^{+3}$ unit is short lived and undergoes

decomposition at a rate comparable with the cyclic voltammetric experiment. This reduction is assigned to Equation 2.2.

On the addition of chloride ions to the electrochemical cell the potential of the first reduction process is shifted to a more negative value. This addition has no observable effect on the second reduction process. This observation mirrors that previously reported^{38,40} for $[\text{Ru}_2(\text{HNOCR})_4\text{Cl}]$ ($\text{R}=\text{CF}_3, \text{C}(\text{CH}_3)_3$). The presence of a single broad peak for the first reduction process suggests that the rate of exchange between the different axially ligated adducts is comparable with, or faster than, the timescale of the electrochemical experiment.

The reduction observed in the presence of excess chloride ion can be assigned to the bis-chloro adduct (Reduction 3). It is likely that the reduction observed in the absence of excess chloride ions is an average involving contributions from all three adducts (Reduction 1/2/3). The addition of less than one molar equivalent of silver ions to the electrochemical cell has the effect of sharpening the peaks due to the first reduction process but does not appear to cause any change in the half-wave potential of this process. This indicates that the addition of less than one molar equivalent of silver ions is insufficient to alter the position of the equilibrium to an extent detectable within the error of the electrochemical experiment. The second reduction process originally observed was unaffected by the addition of chloride or silver ions and therefore is assigned to an equilibrium mixture of all three adducts (Reduction 4), for the reasons stated previously.

A quasireversible oxidation wave is observed in the cyclic voltammograms of two of these compounds ($\text{R}'=\text{H}, \text{CH}_3\text{C}_6\text{H}_4$). It seems likely that this oxidation can be assigned to Equation 2.3 but the close proximity of the



solvent front makes the verification of this impossible. On the addition of excess chloride ion to the electrochemical cell this oxidation process is shifted to a more cathodic potential by approximately 120 mV, and for the compound $[\text{Ru}_2(\text{HNOCC}_6\text{H}_5)_4\text{Cl}]$, a quasireversible oxidation process is observed just inside the solvent limit which was not visible initially. The oxidation observed in the presence of excess chloride ions can be tentatively assigned to the bis-chloro adduct, but the proximity to the solvent front makes conclusive assignment of these waves impossible. The assignments discussed above are summarized in Table 2.3.

These results suggest that the solution behaviour of these two sets of compounds $[\text{Ru}_2(\text{RNOCCH}_3)_4\text{Cl}]$ and $[\text{Ru}_2(\text{HNOCR}')_4\text{Cl}]$ ($\text{R}, \text{R}' = \text{H}, \text{CH}_3, \text{CF}_3, \text{C}_6\text{H}_4\text{CF}_3, \text{C}_6\text{H}_5, \text{C}_6\text{H}_4\text{Cl}, \text{C}_6\text{H}_4\text{CH}_3,$) is not identical. Many factors will effect the difference in reduction potential between the bis-dimethylsulphoxide adducts and the bis-chloro adducts, and also, the effect that the addition of chloride or silver ions has on the position of the equilibrium between the different axially ligated species present in solution. These will include the electronic effect of the bridging ligand and its substituents on the orbitals involved in bonding the axial ligands, in particular their effects on the σ donor/acceptor and π donor/acceptor properties of the metal centres, and the steric effects of the substituent on co-ordination to the axial site of each ruthenium ion.

When the substituent group R' , is attached to the carbon atom of the bridging ligand (ie $[\text{Ru}_2(\text{HNOCR}')_4\text{Cl}]$) it is expected to have less affect on the redox centre and the orbitals involved in axial bonding than if it were attached to the nitrogen atom. As a consequence of this the difference in potential between the reduction of the bis-dimethylsulphoxide adduct and that of the bis-chloro adduct will be small and the identity of the substituent will play a relatively small part in determining the magnitude of this difference. The effect of a substituent on the

Table 2.3 Electrochemical Results for the compounds $[\text{Ru}_2(\text{RNOCR}')_4\text{Cl}]$ recorded in DMSO (0.1 M TBABF₄ supporting electrolyte.)

Compound	Red.1 ^b E_{1p}/V^a	Red.2 ^c E_{1p}/V^a	Red.1/2/3 ^d E_{1p}/V^a	Red.3 ^e E_{1p}/V^a	Red.4 ^f E_{1p}/V^a	Ox.1 ^g E_{1p}/V^a	Ox.1/2/3 ^d E_{1p}/V^a
$[\text{Ru}_2(\text{HNOCCF}_3)_4\text{Cl}]$	-	-	-0.03(150)	-0.15(140)	-	-	-
$[\text{Ru}_2(\text{CF}_3\text{C}_6\text{H}_4\text{NOCCH}_3)_4\text{Cl}]$	-0.22(60)	-0.33(60)	-	-0.44(60)	-	-	-
$[\text{Ru}_2(\text{ClC}_6\text{H}_4\text{NOCCH}_3)_4\text{Cl}]$	-0.26(60)	-0.41(70)	-	-0.52(60)	-	-	-
$[\text{Ru}_2(\text{HNOCC}_6\text{H}_4\text{CF}_3)_4\text{Cl}]$	-	-	-0.52(80)	-0.57(110)	-0.96(100)	-	-
$[\text{Ru}_2(\text{C}_6\text{H}_3\text{NOCCH}_3)_4\text{Cl}]$	-0.29(60)	-0.45(60)	-	-0.58(60)	-	-	-
$[\text{Ru}_2(\text{HNOCC}_6\text{H}_4\text{Cl})_4\text{Cl}]$	-	-	-0.58(80)	-0.63(90)	-0.99(130)	-	-
$[\text{Ru}_2(\text{HNOCC}_6\text{H}_3)_4\text{Cl}]$	-	-	-0.60(70)	-0.65(70)	-1.04(120)	+0.84(70)	-
$[\text{Ru}_2(\text{CH}_3\text{C}_6\text{H}_4\text{NOCCH}_3)_4\text{Cl}]$	-0.34(60)	-0.50(60)	-	-0.65(60)	-1.54 ^g	-	-
$[\text{Ru}_2(\text{HNOCH})_4\text{Cl}]$	-	-	-0.59(90)	-0.67(140)	-1.09(110)	+0.77(90)	+0.92(90)
$[\text{Ru}_2(\text{HNOCC}_6\text{H}_4\text{CH}_3)_4\text{Cl}]$	-	-	-0.64(80)	-0.68(80)	-1.09(140)	+0.80(90)	+0.89(90)
$[\text{Ru}_2(\text{HNOCCCH}_3)_4\text{Cl}]$	-	-	-0.87(120)	-0.93(140)	-	-	-

a) $\Delta E/mV$ given in parenthesis.

b) Reduction of the bis-solvato adduct.

c) Reduction of the mono-chloro/mono-solvato adduct.

d) Reduction/oxidation of an 'average' condition involving all three adducts.

e) Reduction/oxidation of the bis-chloro adduct (potentials shown in bold only visible with an excess of chloride ions.

f) Reduction of the bis-solvato \rightleftharpoons mono-chloro/mono-solvato \rightleftharpoons bis-chloro equilibrium mixture.

g) Value given E_{pc} (recorded at 100 mVs^{-1}).

carbon atom of the bridging ligand on the orbitals involved in bonding axial ligands is likely to be small and also they will not cause any significant steric hindrance at the axial sites. This will result in a fast rate of axial ligand exchange and hence the observation of a single averaged electrochemical response under standard conditions. The identity of the substituent will have little influence on the position of the equilibrium between different axially ligated species and hence the effects observed upon the addition of silver or chloride ions will be similar in magnitude regardless of the identity of that substituent.

When the substituent group is attached to the nitrogen atom of the bridging ligand, the effect of the different substituents on the redox centre will be greatly enhanced. This will result in larger differences between the redox potentials for the reduction of the bis-dimethylsulphoxide and bis-chloro adducts. These differences in potential are found to increase as the electron withdrawing ability of the substituent group attached to the nitrogen atom decreases. The increased electronic effect, of varying substituents, on the orbitals involved in bonding the axial ligand, and the steric hindrance at the axial site, will result in a slower rate of exchange of axial ligands and hence reduction processes for each of the three axial adducts will be observed under standard conditions. The effect of the addition of chloride or silver ions on the position of the equilibrium will be substantially determined by the identity of the substituent group on the nitrogen atom.

Pronounced changes are observed in the relative peak currents observed for the reduction of the compound $[\text{Ru}_2(\text{CH}_3\text{C}_2\text{H}_4\text{NOCCH}_3)_4\text{Cl}]$ on the addition of silver or chloride ions. The extent of these changes decrease as the electron withdrawing ability of the substituent group attached to the nitrogen atom of the bridging ligand increases such that for the compound $[\text{Ru}_2(\text{CF}_3\text{C}_2\text{H}_4\text{NOCCH}_3)_4\text{Cl}]$ the addition of silver or chloride ions to the electrochemical cell appears to have little or no effect

on the relative peak heights of the three components of the reduction process.

2.3.3 Ligand Substituent Effects.

An analysis of the electrochemical results for the eleven chlorotetrakis(amidato)diruthenium(II/III) compounds has revealed that the redox potentials for electron transfer reactions are dependent on both the identity and position of the substituent groups attached to the [N-C-O] bridging unit. The effects observed upon changing the identity and position of the substituent group will be dealt with separately. For the purposes of this discussion only the reduction behaviour of the bis-chloro adduct of each compound i.e. $[\text{Ru}_2(\text{RNOCR}')_4\text{Cl}_2]^-$ (Reduction 3) will be included.

a) Identity of the Substituent Group.

The electron donating or withdrawing ability of the substituent group has a considerable effect on the ease of reduction. A difference of 780 mV is observed between the reduction potentials of $[\text{Ru}_2(\text{HNOCCF}_3)_4\text{Cl}_2]^-$ and $[\text{Ru}_2(\text{HNOCCCH}_3)_4\text{Cl}_2]^-$ ($E_{1/2} = -0.15$ V and -0.93 V vs. Ag/AgCl respectively). The former contains four electron withdrawing $-\text{CF}_3$ substituents while the latter contains four electron donating $-\text{CH}_3$ substituents with respect to the Hammett scale of substituent parameters (Appendix 2). Thus as would be expected it is easier to reduce a compound co-ordinated by $[\text{HNOCCF}_3]^-$ ligands. The observations made during this study are in good agreement with the results obtained earlier by Bear, Kadish *et. al.*^{38,39}, who observed a difference in reduction potential between these two compounds $[\text{Ru}_2(\text{HNOCCF}_3)_4\text{Cl}]^{38}$ and $[\text{Ru}_2(\text{HNOCCCH}_3)_4\text{Cl}]^{39}$ of 750 mV.

These results can also be compared with work done on related dirhodium(II/II) compounds^{69,71,76,78}. There is a good correlation between the results of this study and the results obtained by Bear, Kadish *et.al.*⁶⁹ who studied a range of tetrakis(carboxylato)dirhodium(II/II) compounds. In that study a difference of 600 mV was observed between the reduction potentials of the compounds $[\text{Rh}_2(\text{O}_2\text{CCF}_3)_4]$ and $[\text{Rh}_2(\text{O}_2\text{CCH}_3)_4]$ in DMSO ($E_{1/2} = -1.07$ and -1.65 V vs. S.C.E. respectively). The results obtained here can also be compared with those obtained by Bear, Kadish and co-workers on the compounds $[\text{Rh}_2(\text{HNOCCH}_3)_4]$ ^{71,78} and $[\text{Rh}_2(\text{HNOCCF}_3)_4]$ ⁷⁶, although for these compounds oxidations are observed rather than reductions. A potential difference of 940mV is observed between the half-wave potentials for the oxidations of the two compounds ($E_{1/2} = 0.15$ and 1.09 V vs. S.C.E. respectively). The validity of this comparison is limited however since the solvent used by Bear and co-workers in their study (acetonitrile) differs from that used here (DMSO). These results do however suggest that, at least in a qualitative sense, for compounds containing amidate ligands, the electronic effect of the ligand substituent on the diruthenium unit is less pronounced than on the dirhodium unit. This is not unreasonable given that the molecular orbitals involved in both studies are unlikely to be of a similar energy and/or symmetry.

b) Position of the Substituent Group.

The use of the amidato ligand allows the variation of substituents on both the nitrogen atom and the carbon atom of the bridging ligand. The results which have been obtained indicate that moving a substituent group from one of these atoms to the other will result in a change in the reduction potentials. On moving the substituent (C_6H_5 , $\text{CH}_3\text{C}_6\text{H}_4$, ClC_6H_4 , $\text{CF}_3\text{C}_6\text{H}_4$) from the nitrogen atom to the

carbon atom a cathodic shift in the reduction potential is observed. For example, the reduction potential observed for the compound $[\text{Ru}_2(\text{HNOCC}_6\text{H}_4\text{CF}_3)_4\text{Cl}_2]^-$ (-0.57 V) is 150 mV more negative than that observed for the compound $[\text{Ru}_2(\text{CF}_3\text{C}_6\text{H}_4\text{NOCCH}_3)_4\text{Cl}_2]^-$ (-0.42 V). The magnitude of the change decreases as the electron withdrawing ability of the substituent group decreases and so for the compounds $[\text{Ru}_2(\text{HNOCC}_6\text{H}_4\text{CH}_3)_4\text{Cl}_2]^-$ and $[\text{Ru}_2(\text{CH}_3\text{C}_6\text{H}_4\text{NOCCH}_3)_4\text{Cl}_2]^-$ the difference in the reduction potential is only 30 mV (-0.68 V and -0.65 V respectively). This trend is illustrated in Table 2.4. In moving a substituent group from the nitrogen atom to the carbon atom it is being displaced further from the diruthenium centre. The change observed in the reduction potential indicates that the influence of the electron withdrawing ability of the substituent on the redox centre is decreased as the substituents are moved away from the diruthenium unit, re-enforcing the view that the reductions are metal based.

The shifts in redox potential over a range of substituents (C_6H_5 , $\text{CH}_3\text{C}_6\text{H}_4$, ClC_6H_4 , $\text{CF}_3\text{C}_6\text{H}_4$) clearly demonstrates that variation of the substituent group on the carbon atom has a smaller effect on the redox potential than does changing the substituent group on the nitrogen atom. For the compounds $[\text{Ru}_2(\text{HNO}\overset{\text{C}}{\underset{\lambda}{\text{C}}}_6\text{H}_4\text{CH}_3)_4\text{Cl}_2]^-$ and $[\text{Ru}_2(\text{HNOCC}_6\text{H}_4\text{CF}_3)_4\text{Cl}_2]^-$ the difference observed in half-wave potential is 110 mV, which can be compared with a value of 230 mV for the compounds $[\text{Ru}_2(\text{CH}_3\text{C}_6\text{H}_4\text{NOCCH}_3)_4\text{Cl}_2]^-$ and $[\text{Ru}_2(\text{CF}_3\text{C}_6\text{H}_4\text{NOCCH}_3)_4\text{Cl}_2]^-$. On the other hand the half-wave potentials for the reduction of the compounds $[\text{Ru}_2(\text{HNOCH})_4\text{Cl}_2]^-$ and $[\text{Ru}_2(\text{HNOCC}_6\text{H}_4\text{Cl})_4\text{Cl}_2]^-$ differ by only 40 mV compared with a difference of 410 mV for the compounds $[\text{Ru}_2(\text{HNOCC}_6\text{H}_4\text{CH}_3)_4\text{Cl}_2]^-$ and $[\text{Ru}_2(\text{ClC}_6\text{H}_4\text{NOCCH}_3)_4\text{Cl}_2]^-$. The variation in half-wave potential observed over the complete range of substituents when attached to the carbon atom is 100 mV, while a change in half-wave potential of 510 mV is observed when the substituents are

attached to the nitrogen atom. This effect can be illustrated graphically using a plot of half-wave potentials against the sum of the appropriate *p*-Hammett parameters (Appendix 2) for each of the two sets of data. A linear relationship is observed for each set of data and an increased gradient is observed when the substituent is attached to the nitrogen atom (Figure 2.7). These observations support the simple hypothesis that the effect of the electron withdrawing or donating ability of the substituent will be reduced as the substituent is moved away from the metal centre and hence that the redox reactions are metal rather than ligand based.

A subset of the compounds studied has allowed the effect of distance of a substituent group from the metal centres to be examined in detail. Table 2.5 presents the half-wave potentials for the reduction of the bis-chloro adducts of the compounds $[\text{Ru}_2(\text{HNOCR})_4\text{Cl}]$, $[\text{Ru}_2(\text{HNOCC}_6\text{H}_4\text{R})_4\text{Cl}]$, and $[\text{Ru}_2(\text{RC}_6\text{H}_4\text{NOCCH}_3)_4\text{Cl}]$ ($\text{R}=\text{H}, \text{CH}_3, \text{CF}_3$). For completeness the compounds $[\text{Ru}_2(\text{RNOCH})_4\text{Cl}_2]^-$ and $[\text{Ru}_2(\text{RC}_6\text{H}_4\text{NOCH})_4\text{Cl}_2]^-$ should also be studied, but these compounds are not available. It is argued that $[\text{Ru}_2(\text{RC}_6\text{H}_4\text{NOCCH}_3)_4\text{Cl}_2]^-$ is sufficiently similar to $[\text{Ru}_2(\text{RC}_6\text{H}_4\text{NOCH})_4\text{Cl}_2]^-$ for its use in this context to be valid. Two specific examples will be discussed, that of the electron withdrawing substituent $-\text{CF}_3$ and the electron donating substituent $-\text{CH}_3$. The ion $[\text{Ru}_2(\text{HNOCCF}_3)_4\text{Cl}_2]^-$ is reduced at a half-wave potential of -0.15 V, if a $[\text{C}_6\text{H}_4]^-$ group is placed between the $-\text{CF}_3$ substituent and the carbon atom, ie $[\text{Ru}_2(\text{HNOCC}_6\text{H}_4\text{CF}_3)_4\text{Cl}_2]^-$, then the reduction moves to a half-wave potential of -0.57 V. For the compound $[\text{Ru}_2(\text{CF}_3\text{C}_6\text{H}_4\text{NOCCH}_3)_4\text{Cl}_2]^-$ the $-\text{CF}_3$ substituent has been moved to the nitrogen atom, although with a $[\text{C}_6\text{H}_4]^-$ group between the substituent and the nitrogen, and a half-wave potential of -0.42 V is observed. Turning to the substituent group $-\text{CH}_3$, the ion $[\text{Ru}_2(\text{HNOCCCH}_3)_4\text{Cl}_2]^-$ is reduced at a half-wave potential of -0.78 V. In the ion $[\text{Ru}_2(\text{HNOCC}_6\text{H}_4\text{CH}_3)_4\text{Cl}_2]^-$, an electron withdrawing group, $[\text{C}_6\text{H}_4]^-$, has been

Table 2.4 Electrochemical data for $[\text{Ru}_2(\text{RNOCR}')_4\text{Cl}_2]^-$ in DMSO
(0.1 M TBABF₄ supporting electrolyte).


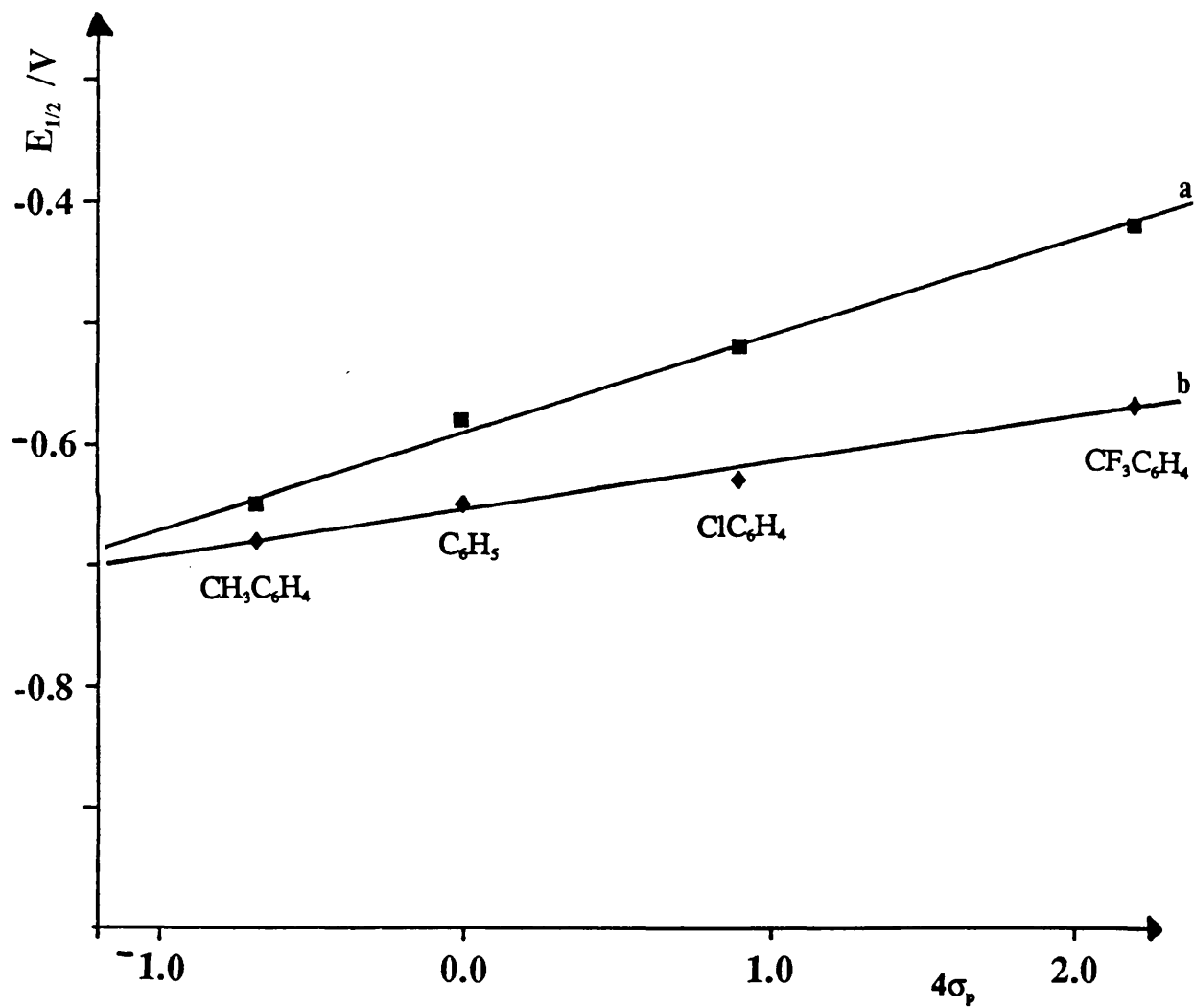
	Substituent, R.			
	CH ₃ C ₆ H ₄	C ₆ H ₅	ClC ₆ H ₄	CF ₃ C ₆ H ₄
$[\text{Ru}_2(\text{RNOCCCH}_3)_4\text{Cl}_2]^-$ $E_{1/2}/\text{V}$ (1)	-0.65	-0.58	-0.52	-0.42
$[\text{Ru}_2(\text{HNOCR})_4\text{Cl}_2]^-$ $E_{1/2}/\text{V}$ (2)	-0.68	-0.65	-0.63	-0.57
Shift in Potential (2)-(1)/mV	-30	-60	-110	-130
Electron withdrawing ability.				

Table 2.5 Electrochemical data for $[\text{Ru}_2(\text{RNOCR}')_4\text{Cl}_2]^-$ in DMSO
(0.1 M TBABF₄ supporting electrolyte).

R	$[\text{Ru}_2(\text{HNOCR})_4\text{Cl}_2]^-$ $E_{1/2} / \text{V}$	$[\text{Ru}_2(\text{HNOCC}_6\text{H}_4\text{R})_4\text{Cl}_2]^-$ $E_{1/2} / \text{V}$	$[\text{Ru}_2(\text{RC}_6\text{H}_4\text{NOCCH}_3)_4\text{Cl}_2]^-$ $E_{1/2} / \text{V}$
H	-0.76	-0.65	-0.59
CH ₃	-0.78	-0.68	-0.65
CF ₃	-0.13	-0.57	-0.43

Figure 2.7 Graphs of $E_{1/2}$ /V against the sum of the appropriate p -Hammett parameters for a) $[\text{Ru}_2(\text{RNOCCCH}_3)_4\text{Cl}_2]^-$ and b) $[\text{Ru}_2(\text{HNOCR}')_4\text{Cl}_2]^-$



introduced between the carbon atom of the bridge and the electron donating substituent $-\text{CH}_3$. This has the effect of making the substituent ($-\text{C}_6\text{H}_4\text{CH}_3$) effectively electron withdrawing in nature and leads to the reduction becoming easier ($E_{1/2} = -0.68 \text{ V}$). For the ion $[\text{Ru}_2(\text{CH}_3\text{C}_6\text{H}_4\text{NOCCH}_3)_4\text{Cl}_2]^+$ a half-wave potential of -0.65 V is observed reflecting the fact that the substituent has been moved closer to the redox centre. The changes in redox potential as each of these substituent groups are moved away from the diruthenium unit parallels the trends already discussed above, with the effect of the electron withdrawing or donating ability of the substituent group on the electrochemical behaviour of the compound, decreasing as the substituent is moved away from the diruthenium unit.

2.4 Conclusions.

Eleven chlorotetrakis(amidato)diruthenium(II/III) have been prepared and characterised. Magnetic susceptibility measurements carried out suggest that at ambient temperature the electronic configuration of the metal-metal bond is an equilibrium between the configurations $\sigma^2\pi^4\delta^2\delta^*\pi^2$ (ie quartet state) and $\sigma^2\pi^4\delta^2\delta^*\pi^*$ or $\sigma^2\pi^4\delta^2\pi^{*3}$ (ie doublet states).

The electrochemical behaviour of the compounds has been studied in DMSO (0.1 M TBABF₄ supporting electrolyte) and between one and four reduction processes have been observed for each compound. For three compounds an oxidation has also been observed. The results obtained suggest that the solution redox chemistry of these compounds is highly dependent upon the substituent groups bound to the carbon and nitrogen atoms. The results obtained in this study closely parallel those reported previously for related diruthenium (II/III) compounds ie

$[\text{Ru}_2(\text{HNOCR}')_4\text{Cl}]$ ($\text{R}' = \text{CF}_3$ ³⁸, CH_3 ³⁹, $\text{C}(\text{CH}_3)_3$ ⁴⁰).

Diruthenium(II/III) compounds containing amidate ligands of the type $[\text{RNOCCH}_3]^-$ have not been reported previously. This study shows that the rate of exchange between the different axially ligated species for these compounds is considerably slower than observed for compounds containing ligands of the type $[\text{HNOCR}']^-$ thereby allowing the identification of redox reactions for each of the three different adducts to be made.

The effect of the identity, and position of the substituent group, on the ease of reduction of the bis-chloro adduct has also been investigated. The observations made here indicate that the electron withdrawing/donating ability of the substituent has a considerable effect on the ease of reduction, with electron withdrawing substituent groups giving rise to the easiest reductions. This leads to the conclusion that electron withdrawing substituents attached to the bridging ligands causes a lowering of the lowest unoccupied molecular orbital (LUMO), to which the electron will be added. The magnitude of this effect decreases on moving the substituent group further from the Ru-Ru bond, supporting the view that the reduction is substantially metal based.

2.5 Experimental.

2.5.1 Materials and Instrumentation.

Ruthenium trichloride was received on loan from Johnson Matthey plc, all other chemicals were obtained from commercial sources. DMSO was stored over activated molecular sieve. Dichloromethane was allowed to stand for at least 24 hours over potassium hydroxide and then distilled from phosphorous pentoxide before use. THF was distilled from sodium before use. All other chemicals and solvents were used without further purification.

Infrared spectra have been recorded using a Perkin-Elmer PE983 Infrared Spectrophotometer. Samples have been prepared as potassium bromide disks. Magnetic susceptibility measurements have been made using a Johnson Matthey Magnetic Susceptibility Balance. Analytical data were obtained from the analytical section of the Chemistry Department of University College London.

Voltammetric studies were carried out using a Metrohm E506 potentiostat interfaced with a Metrohm E505 cell stand utilizing a three electrode geometry. The working electrode was a platinum wire electrode (Metrohm EA285). The reference electrode was a non-aqueous Ag/AgCl/Cl⁻, CH₂Cl₂ electrode separated from the bulk solution by a glass frit (Metrohm EA441/5). The auxiliary electrode was a platinum wire. Cyclic voltammetric measurements also used a Metrohm E612 VA scanner in conjunction with a Hewitt Packard 7035B XY recorder.

Before all experiments the cell was degassed with solvent saturated nitrogen, and nitrogen was passed through the cell during the experiment. The supporting electrolyte used was tetrabutylammonium tetrafluoroborate (TBABF₄). Chloride ions were added to the electrochemical cell in the form of

Benzyltriethylammonium chloride and silver ions in the form of silver tetrafluoroborate. Measurements were made at scan rates of 0.02 to 0.50 Vs⁻¹. All potentials are reported against an Ag/AgCl electrode against which ferrocene is oxidised at +0.60 V.

2.5.2 Synthesis of [Ru₂(O₂CCH₃)₄Cl].

The compound [Ru₂(O₂CCH₃)₄Cl] was prepared by the method previously reported by Wilkinson *et. al.*¹⁰².

2.5.3 Synthesis of [Ru₂(HNOCH)₄Cl].

[Ru₂(O₂CCH₃)₄Cl] (0.1046 g; 0.20 mMol) was stirred with H₂NOCH (1.0 g; excess) at 70 °C for 20 hours, under a dinitrogen atmosphere. The excess ligand was removed under reduced pressure at 70°C. The procedure was repeated to ensure complete ligand exchange.

2.5.4 Synthesis of [Ru₂(HNOCCCH₃)₄Cl].

[Ru₂(O₂CCH₃)₄Cl] (0.1535 g; 0.30 mMol) was stirred with H₂NOCCH₃ (1.0 g; excess) at 120 °C for 10 hours, under a dinitrogen atmosphere. The excess ligand was removed by vacuum sublimation onto a water-cooled cold finger at 120 °C. The procedure was repeated to ensure complete ligand exchange.

2.5.5 Synthesis of other $[\text{Ru}_2(\text{RNOCR}')_4\text{Cl}]$ compounds.

The compounds $[\text{Ru}_2(\text{RNOCR}')_4\text{Cl}]$ ($\text{R}=\text{H}$, $\text{R}'=\text{CF}_3, \text{C}_6\text{H}_5, \text{C}_6\text{H}_4\text{CH}_3, \text{C}_6\text{H}_4\text{CF}_3, \text{C}_6\text{H}_4\text{Cl}$; $\text{R}'=\text{CH}_3$, $\text{R}=\text{C}_6\text{H}_5, \text{C}_6\text{H}_4\text{CH}_3, \text{C}_6\text{H}_4\text{CF}_3, \text{C}_6\text{H}_4\text{Cl}$) were prepared using an analogous method to that describe above. Specific details of experimental temperatures, times and yields for each compound are summarized in Table 2.6, Analytical data, magnetic susceptibility and infrared spectroscopic results are given in Tables 2.7, and 2.8.

Table 2.6 Experimental details for the synthesis of the compounds
 $[\text{Ru}_2(\text{RNOCR}')_4\text{Cl}]$

Compound.	Time/hours ^a	Temp./°C	yield/%
$[\text{Ru}_2(\text{HNOCH})_4\text{Cl}]$	20	70	92
$[\text{Ru}_2(\text{HNOCCCH}_3)_4\text{Cl}]^{\text{b}(38)}$	10	120	93
$[\text{Ru}_2(\text{HNOCC}_6\text{H}_5)_4\text{Cl}]^{\text{b}(40)}$	15	130	81
$[\text{Ru}_2(\text{HNOCCF}_3)_4\text{Cl}]^{\text{b}(37)}$	25	130	87
$[\text{Ru}_2(\text{HNOCC}_6\text{H}_4\text{CH}_3)_4\text{Cl}]$	20	160	58
$[\text{Ru}_2(\text{HNOCC}_6\text{H}_4\text{CF}_3)_4\text{Cl}]$	8	190	94
$[\text{Ru}_2(\text{HNOCC}_6\text{H}_4\text{Cl})_4\text{Cl}]^{\text{b}(41)}$	8	180	84
$[\text{Ru}_2(\text{C}_6\text{H}_5\text{NOCCH}_3)_4\text{Cl}]$	15	120	69
$[\text{Ru}_2(\text{CH}_3\text{C}_6\text{H}_4\text{NOCCH}_3)_4\text{Cl}]$	10	120	74
$[\text{Ru}_2(\text{CF}_3\text{C}_6\text{H}_4\text{NOCCH}_3)_4\text{Cl}]$	15	160	64
$[\text{Ru}_2(\text{ClC}_6\text{H}_4\text{NOCCH}_3)_4\text{Cl}]$	8	180	89

- a) Total time exposed to molten ligand.
 b) previously reported (reference given in parenthesis).

Table 2.7 Microanalytical Data for the compounds $[\text{Ru}_2(\text{RNOCR}')_4\text{Cl}]$.

Compound.	Microanalytical data								μ_{eff} /BM.
	%C		%H		%N		calc. ^a		
	found.	calc. ^a	found	calc. ^a	found	calc. ^a	found	calc. ^a	
$[\text{Ru}_2(\text{HNOCH})_4\text{Cl}]$	12.6	11.6	2.2	2.0	13.5	13.5	13.5	13.5	^b
$[\text{Ru}_2(\text{HNOCCH}_3)_4\text{Cl}]$	20.4	20.5	3.3	3.4	10.6	10.6	10.6	11.6	4.48
$[\text{Ru}_2(\text{HNOCC}_6\text{H}_5)_4\text{Cl}]$	45.6	46.8	3.3	3.4	7.4	7.4	7.4	7.8	5.54
$[\text{Ru}_2(\text{HNOCCF}_3)_4\text{Cl}]$	14.2	14.0	1.8	0.6	10.4	10.4	10.4	8.2	2.26
$[\text{Ru}_2(\text{HNOCC}_6\text{H}_4\text{CH}_3)_4\text{Cl}]$	51.5	49.6	4.4	4.1	7.4	7.4	7.4	7.2	3.57
$[\text{Ru}_2(\text{HNOCC}_6\text{H}_4\text{CF}_3)_4\text{Cl}]$	43.4	44.1	2.1	2.3	5.2	5.2	5.2	6.4	3.22
$[\text{Ru}_2(\text{HNOCC}_6\text{H}_4\text{Cl})_4\text{Cl}]$	38.8	39.2	2.7	2.3	7.3	7.3	7.3	6.6	3.18
$[\text{Ru}_2(\text{C}_6\text{H}_5\text{NOCCH}_3)_4\text{Cl}]$	50.0	49.6	4.5	4.1	6.8	6.8	6.8	7.2	^b
$[\text{Ru}_2(\text{CH}_3\text{C}_6\text{H}_4\text{NOCCH}_3)_4\text{Cl}]$	53.9	52.0	5.1	4.9	6.8	6.8	6.8	6.8	3.53
$[\text{Ru}_2(\text{CF}_3\text{C}_6\text{H}_4\text{NOCCH}_3)_4\text{Cl}]$	42.3	41.3	3.1	2.7	5.3	5.3	5.3	5.4	3.08
$[\text{Ru}_2(\text{ClC}_6\text{H}_4\text{NOCCH}_3)_4\text{Cl}]$	40.8	42.1	3.0	3.1	6.1	6.1	6.1	6.1	3.26

a) Calculated for the given formula.

b) Insufficient sample for accurate measurement.

**Table 2.8 Infrared spectroscopic data for the compounds [Ru₂(RNOCR')₄Cl]
(recorded in the form of KBr disks).**

Compound.	wavenumbers /cm ⁻¹
[Ru ₂ (HNOCH) ₄ Cl]	3273s ^a ,1684m,1535s ^b ,1412s ^c ,1309s,1166s,762m,697m, 513w,448s,403m.
[Ru ₂ (HNOCC ₂ H ₅) ₄ Cl]	3311s ^a ,1653w,1512s ^b ,1462s,1408s ^c ,1210s,1179s,1037w, 936w,743m,686s,601s,391s,345m.
[Ru ₂ (HNOCC ₆ H ₅) ₄ Cl]	3342m ^a ,1596w,1512s ^b ,1481m,1447s,1424m ^c ,1213m,1114m 1028w,837w,789w,689s,651m,525m,391w.
[Ru ₂ (HNOCCF ₃) ₄ Cl]	3265m ^a ,1726m,1676s,1584m ^b ,1428m ^c ,1259m,1194s,1152s ^d , 1076w,854m,793m,724s,521w.
[Ru ₂ (HNOCC ₆ H ₄ CH ₃) ₄ Cl]	3372m ^a ,3357m ^a ,1661w,1607m,1519m ^b ,1485s,1439s ^c , 1393m,1217m,1198m,1183m,1106m,1015w,846w,823w, 777w,731m,659m,628m,494m,475m.
[Ru ₂ (HNOCC ₆ H ₄ CF ₃) ₄ Cl]	3326m ^a ,1653w,1615w,1592w,1527m ^b ,1496m,1443m ^c , 1324s,1221w,1171s ^d ,1122s,1064s,1015m,854m,766w, 693w,674w,559m.
[Ru ₂ (HNOCC ₆ H ₄ Cl) ₄ Cl]	3349m ^a ,1669m,1657m,1592s,1577m,1512s ^b ,1479s,1443s ^c , 1397s,1277w,1221m,1118m,1087s,1011s,839s,739m, 724m,655w,578s, 483w.
[Ru ₂ (C ₆ H ₅ NOCCH ₃) ₄ Cl]	1680m,1626s,1592s,1542s ^b ,1489s,1435s ^c ,1408s,1374m, 1355m,1313m,1229s,1026m,961w,970w,850m,754s,693s, 644m,506w,441w,376m.

Table 2.8 Cont'd.

Compound.	wavenumbers /cm ⁻¹ .
[Ru ₂ (CH ₃ C ₆ H ₄ NOCCH ₃) ₄ Cl]	1680m,1634s,1600s,1538s ^b ,1504s,1424s ^c ,1401s,1351m, 1324m,1233s,1102w,1018m,961m,862m,812m,712m,693w 636m,601w,510m,422w,380w,334w.
[Ru ₂ (CF ₃ C ₆ H ₄ NOCCH ₃) ₄ Cl]	1638m,1607m,1512m ^b ,1489m,1408s ^c ,1320s,1240m,1164s ^d , 1122s,1102s,1064s,1015m,961w,873m,842w,823w,680w, 644w,601w,372w.
[Ru ₂ (ClC ₆ H ₄ NOCCH ₃) ₄ Cl]	1642m,1592m,1523m ^b ,1508m,1489s,1431s ^c ,1401s,1236m, 1118w,1087s,1011s,961w,865w,839w,819w,743w,697w, 640w,502w,399w.

- a) Assigned to N-H stretch.
 b) Tentatively assigned to N-C-O asymmetric stretch.
 c) Tentatively assigned to N-C-O symmetric stretch.
 d) Assigned to C-F stretch.

Chapter Three.

**A synthetic, structural, and electrochemical investigation
into the compound**

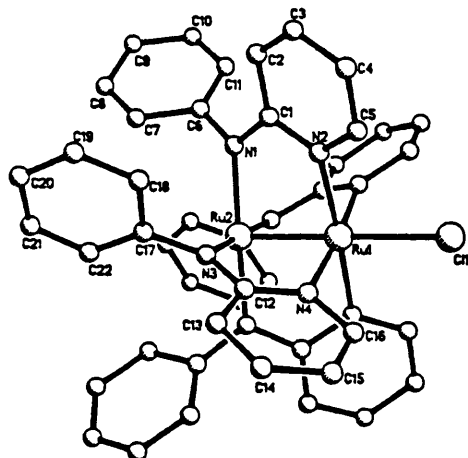


3.1	Introduction.	100
3.2	Preparation and characterisation.	102
3.3	The crystal structure of $[\text{Ru}_2(\text{O}_2\text{CCH}_3)(\text{CH}_3\text{C}_5\text{H}_3\text{NNH})_3\text{Cl}].$	102
3.4	The electrochemical behaviour of $[\text{Ru}_2(\text{O}_2\text{CCH}_3)(\text{CH}_3\text{C}_5\text{H}_3\text{NNH})_3\text{Cl}].$	108
	3.4.1 Behaviour in dimethylsulphoxide	110
	3.4.2 Behaviour in acetonitrile.	116
	3.4.3 Electrochemical behaviour - A rationalisation.	120
3.5	Conclusions.	122
3.6	Experimental.	124
	3.6.1 Materials and Instrumentation.	124
	3.6.2 Synthesis of $[\text{Ru}_2(\text{O}_2\text{CCH}_3)(\text{CH}_3\text{C}_5\text{H}_3\text{NNH})_3\text{Cl}].$	124
	3.6.3 The crystal structure determination of $[\text{Ru}_2(\text{O}_2\text{CCH}_3)(\text{CH}_3\text{C}_5\text{H}_3\text{NNH})_3\text{Cl}].$	125

3.1 Introduction.

Several diruthenium(II/III) compounds have been prepared using variously substituted aminopyridine ligands providing examples of compounds containing [N-C-N] bridging units. The compounds $[\text{Ru}_2(\text{C}_5\text{H}_4\text{NNC}_6\text{H}_5)_4\text{Cl}]^{45}$, $[\text{Ru}_2(\text{C}_5\text{H}_4\text{NNCH}_3)_4\text{Cl}]^{46}$, and $[\text{Ru}_2(\text{C}_5\text{H}_4\text{NNCH}_2\text{C}_6\text{H}_5)_4\text{Cl}]^{46}$ were prepared by stirring chlorotetrakis(acetato)diruthenium(II/III) with an excess of the appropriate aminopyridine ligand at elevated temperatures. This procedure was strictly analogous to that used to prepare the chlorotetrakis(amidato)diruthenium(II/III) compounds discussed in Chapter 2. The compound $[\text{Ru}_2(\text{C}_5\text{H}_4\text{NNC}_6\text{H}_5)_4\text{C}\equiv\text{CC}_6\text{H}_5]^{48}$ was prepared by the reaction of $\text{Li}[\text{C}\equiv\text{CC}_6\text{H}_5]$ with $[\text{Ru}_2(\text{C}_5\text{H}_4\text{NNC}_6\text{H}_5)_4\text{Cl}]$ in a toluene/THF mixture.

Crystallographic studies on the compounds $[\text{Ru}_2(\text{C}_5\text{H}_4\text{NNC}_6\text{H}_5)_4\text{Cl}]^{45}$ (3.1) and $[\text{Ru}_2(\text{C}_5\text{H}_4\text{NNC}_6\text{H}_5)_4\text{C}\equiv\text{CC}_6\text{H}_5]^{48}$ indicate that both these compounds exist as

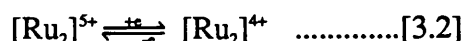
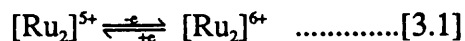


(3.1)

discrete molecules, with all four bridging ligands orientated in the same direction, effectively blocking one of the axial sites. The axial ligand in both cases is attached to the ruthenium ion co-ordinated by the four pyridyl nitrogen atoms.

There is considerable twisting about the Ru-Ru bond with torsion angles observed of 22^{045} and 19.5^{048} .

The electrochemical behaviour of three of the compounds prepared has been studied and the results summarized in Table 1.4. A reversible or near-reversible oxidation and a quasireversible or reversible reduction are observed for each compound, and have been assigned to metal based processes (Equations 3.1 and 3.2).



A second, quasireversible reduction is observed for the compound $[\text{Ru}_2(\text{C}_5\text{H}_4\text{NNCH}_3)_4\text{Cl}]^{46}$ at a more cathodic potential. The addition of excess chloride ions to the electrochemical cell results in the replacement of these two processes with a single reduction. For the compound $[\text{Ru}_2(\text{C}_5\text{H}_4\text{NNC}_6\text{H}_5)_4\text{Cl}]^{49}$ an irreversible reduction ($E_{pc} = -1.57$ V) and a quasireversible oxidation ($E_{1/2} = +1.45$ V) are also observed, while for the compound $[\text{Ru}_2(\text{C}_5\text{H}_4\text{NNC}_6\text{H}_5)_4(\text{C}\equiv\text{CC}_6\text{H}_5)]^{48}$ an irreversible oxidation was observed ($E_{pa} = +1.05$ V). The assignment of these reactions was not discussed in either case.

Attempts have been made to prepare another example of a diruthenium(II/III) compound containing [N-C-N] bridging units using 2-amino-6-picoline ligands. The results obtained are presented in this chapter.

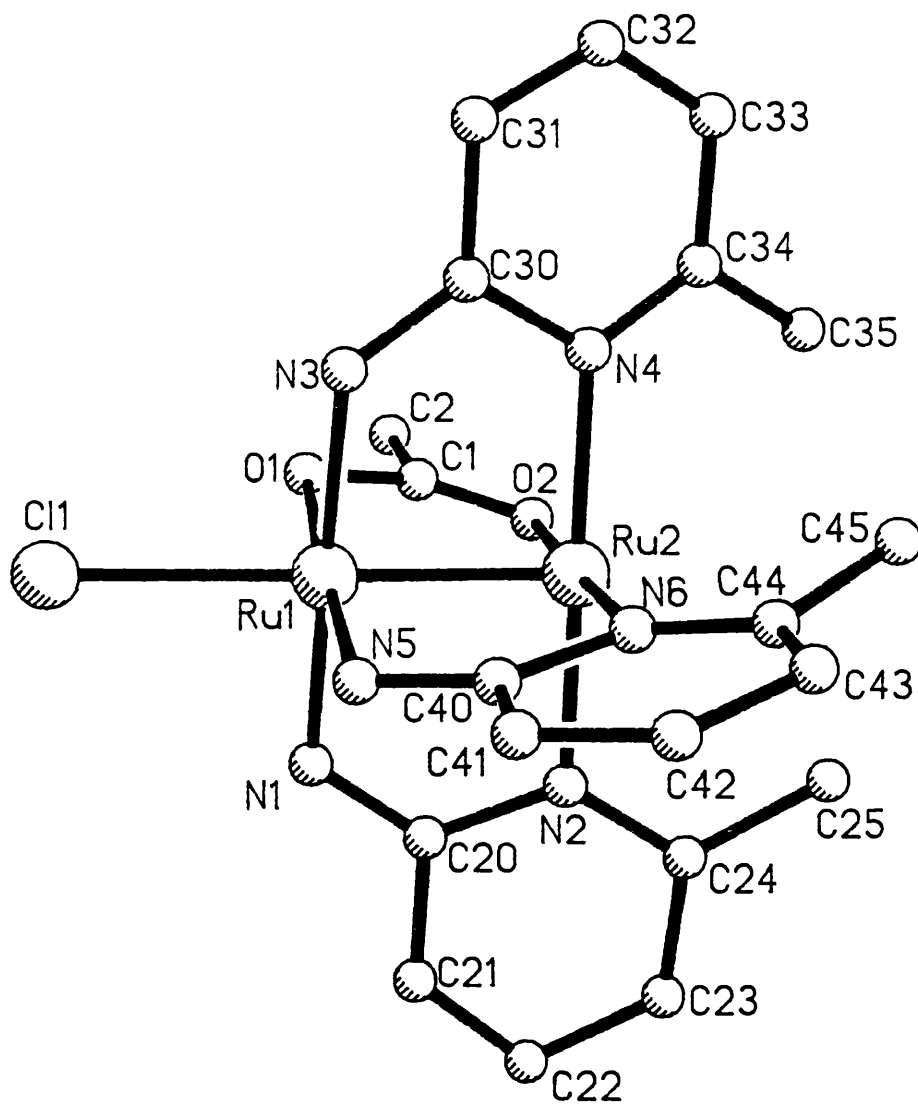
3.2 Preparation and characterisation.

Several attempts to prepare the compound $[\text{Ru}_2(\text{CH}_3\text{C}_5\text{H}_3\text{NNH})_4\text{Cl}]$ have been made by the reaction of $[\text{Ru}_2(\text{O}_2\text{CCH}_3)_4\text{Cl}]$ with an excess of 2-amino-6-picoline at elevated temperature. The method used was strictly analogous to that described in Chapter 2 for the preparation of chlorotetrakis(amidato) diruthenium(II/III) compounds. Analytical data obtained on the product of each reaction indicate that only three carboxylate ligands are replaced by the 2-amino-6-picoline ligands, giving the compound $[\text{Ru}_2(\text{O}_2\text{CCH}_3)(\text{CH}_3\text{C}_5\text{H}_3\text{NNH})_3\text{Cl}]$. Infrared spectroscopic results also indicate the presence of acetato and picolinamidate ligands. Symmetric and asymmetric O-C-O stretches have been tentatively assigned to bands at 1470 and 1560 cm^{-1} respectively, while the skeletal vibrations of the pyridyl rings of the picolinamidate ligands have been assigned to the band at 1607 cm^{-1} . A mass spectrum has been obtained for the compound using electron impact methods. The highest mass peak observed occurs at 583 m/e which can be attributed to $[\text{Ru}_2(\text{O}_2\text{CCH}_3)(\text{CH}_3\text{C}_5\text{H}_3\text{NNH})_3]^+$ (based on ^{101}Ru).

3.3 The crystal structure of $[\text{Ru}_2(\text{O}_2\text{CCH}_3)(\text{CH}_3\text{C}_5\text{H}_3\text{NNH})_3\text{Cl}]$.

Crystals of the title compound, suitable for x-ray diffraction studies, have been obtained by slow evaporation of a solution of $[\text{Ru}_2(\text{O}_2\text{CCH}_3)(\text{CH}_3\text{C}_5\text{H}_3\text{NNH})_3\text{Cl}]$ in dichloromethane mixed with n-hexane. The structure obtained is illustrated in Figure 3.1. Full experimental details are given in Section 3.5.

Figure 3.1 Ball and stick diagram illustrating the structure of $[\text{Ru}_2(\text{O}_2\text{CCH}_3)(\text{CH}_3\text{C}_2\text{H}_3\text{NNH})_3\text{Cl}]$.



Three 2-amino-6-picolinate ligands bridge the $[\text{Ru}_2]^{45}$ unit with all three methyl groups blocking one axial site. A chloride ion fills the vacant axial site of the ruthenium ion co-ordinated by the amide nitrogen atoms, with a Ru-Cl bond length of 2.473(4) Å. The Ru-Ru bond length is 2.287(2) Å.

A related compound has been studied crystallographically by Cotton *et. al.*¹⁰³. The structure of the compound $[\text{Ru}_2(\text{O}_2\text{CCH}_3)(\text{ClC}_5\text{H}_3\text{NO})_3\text{Cl}]$ is illustrated in Figure 3.2. This compound adopts a similar arrangement of bridging ligands as the compound reported here. The Ru-Ru and Ru-Cl bond lengths, 2.282(4) Å and 2.474(9) Å respectively, are essentially the same as those observed here. For the compound $[\text{Ru}_2(\text{O}_2\text{CCH}_3)(\text{ClC}_5\text{H}_3\text{NO})_3\text{Cl}]$ the average torsion angle observed about the Ru-Ru bond is 1°. This compares with an average value of 13° observed in the compound $[\text{Ru}_2(\text{O}_2\text{CCH}_3)(\text{CH}_3\text{C}_5\text{H}_3\text{NNH})_3\text{Cl}]$ (Figure 3.3).

The structure of the compound $[\text{Ru}_2(\text{ClC}_5\text{H}_3\text{NO})_4\text{Cl}]$ has also been reported⁴³ with all four bridging ligands orientated in the same direction. In this compound the bridging ligands are twisted about the Ru-Ru bond axis giving an average torsion angle of 19°. This implies that four pendant chlorides at one end of the molecule causes considerable steric hindrance. This observation coupled with the difference in the torsion angles observed for the two compounds $[\text{Ru}_2(\text{O}_2\text{CCH}_3)(\text{ClC}_5\text{H}_3\text{NO})_3\text{Cl}]$ and $[\text{Ru}_2(\text{O}_2\text{CCH}_3)(\text{CH}_3\text{C}_5\text{H}_3\text{NNH})_3\text{Cl}]$ strongly suggests that the existence of a compound, $[\text{Ru}_2(\text{CH}_3\text{C}_5\text{H}_3\text{NNH})_4\text{Cl}]$, with the four bridging ligands in a polar arrangement is extremely unlikely.

The compound $[\text{Ru}_2(\text{O}_2\text{CCH}_3)(\text{ClC}_5\text{H}_3\text{NO})_3\text{Cl}]$ ¹⁰³ was prepared by refluxing chlorotetrakis(acetato)diruthenium(II/III) with an excess of ligand in methanol. In order to prepare the compound $[\text{Ru}_2(\text{ClC}_5\text{H}_3\text{NO})_4\text{Cl}]$ ⁴³ it was necessary to use considerably harsher conditions, stirring $[\text{Ru}_2(\text{O}_2\text{CCH}_3)_4\text{Cl}]$ with an excess of the molten ligand. These extreme conditions are also necessary to prepare

Figure 3.2 Ball and stick diagram illustrating the structure of $[\text{Ru}_2(\text{O}_2\text{CCH}_3)(\text{ClC}_6\text{H}_4\text{NO})_3\text{Cl}]$.

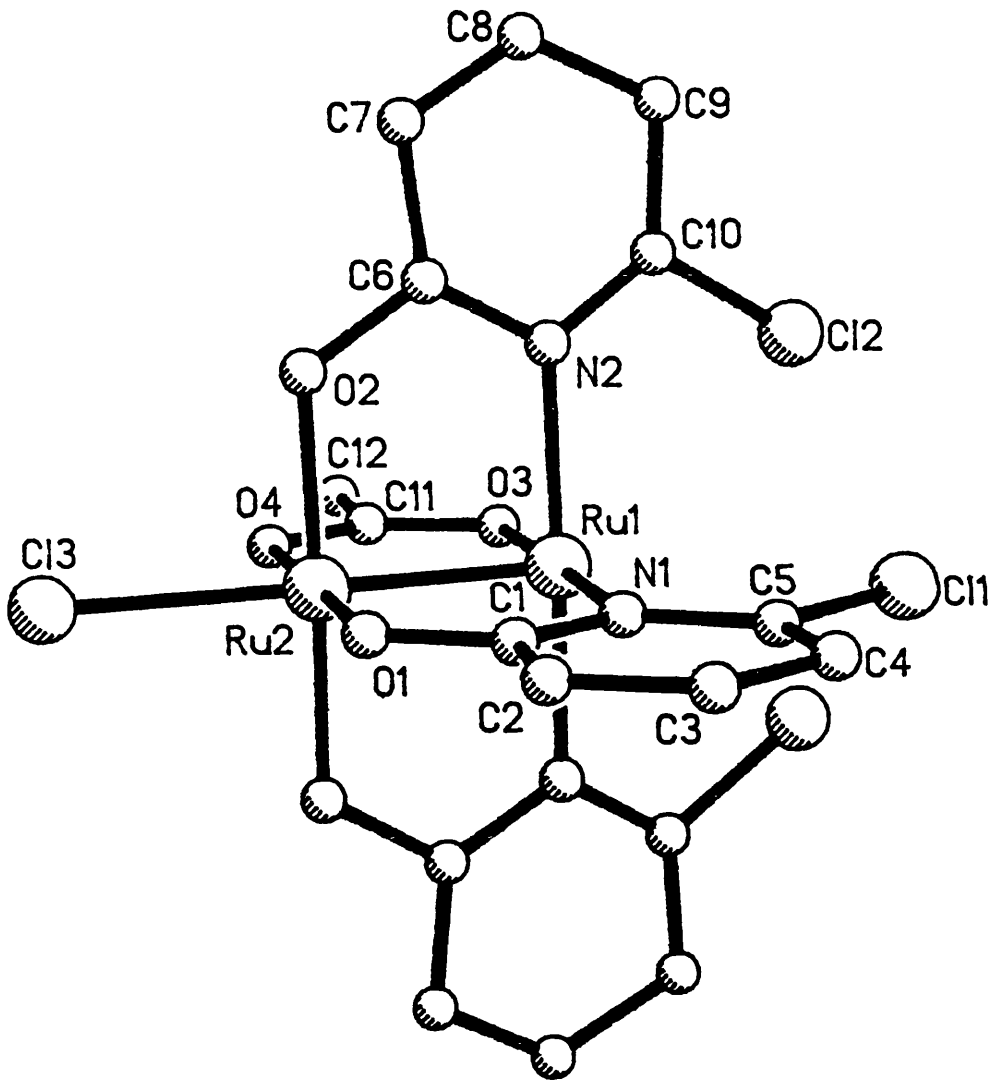
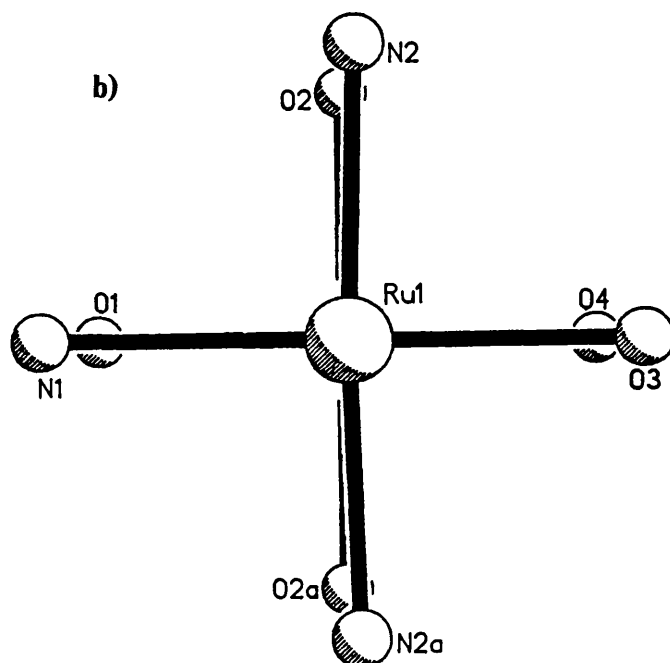
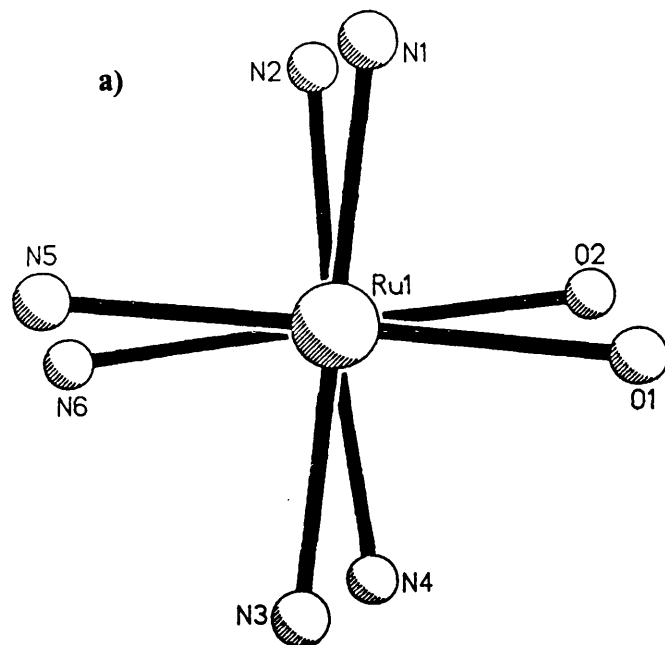
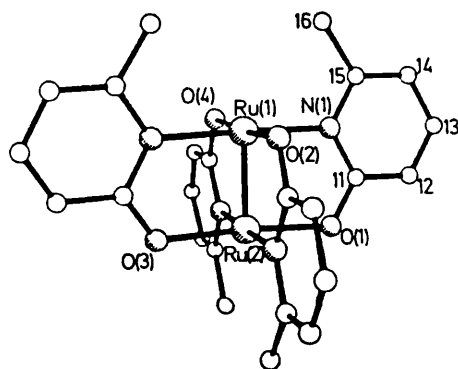


Figure 3.3 Ball and stick diagrams illustrating the immediate co-ordination sphere the ruthenium ions for a) $[\text{Ru}_2(\text{O}_2\text{CCH}_3)(\text{CH}_3\text{C}_5\text{H}_3\text{NNH})_3\text{Cl}]$ and b) $[\text{Ru}_2(\text{O}_2\text{CCH}_3)(\text{ClC}_5\text{H}_3\text{NO})_3\text{Cl}]$.



$[\text{Ru}_2(\text{O}_2\text{CCH}_3)(\text{CH}_3\text{C}_5\text{H}_3\text{NNH})_3\text{Cl}]$. Attempts to prepare $[\text{Ru}_2(\text{CH}_3\text{C}_5\text{H}_3\text{NNH})_4\text{Cl}]$ and $[\text{Ru}_2(\text{CH}_3\text{C}_5\text{H}_3\text{NO})_4\text{Cl}]$ ¹⁰³ using this method have proved unsuccessful, once again suggesting that the steric hindrance caused by the pendant methyl groups, would be too great for these compounds to be stable with all four ligands orientated in the same direction. The existence of a $[\text{Ru}_2]^{5+}$ compound containing these ligands in an arrangement other than a polar one is also unlikely since this would prevent the formation of a strong Ru-Cl bond at either end of the molecule.

The compound $[\text{Ru}_2(\text{CH}_3\text{C}_5\text{H}_3\text{NO})_4]$ (3.2) has been prepared and its



(3.2)

crystal structure reported^{104,105}. This compound was prepared in small yield (8%) from the reaction of $[\text{Ru}_2(\text{O}_2\text{CCH}_3)\text{Cl}]$ and $\text{Na}[\text{CH}_3\text{C}_5\text{H}_3\text{NOH}]$ in methanol at room temperature, and has been found to contain a $[\text{Ru}_2]^{4+}$ unit indicating that the starting material has undergone a reduction. The absence of the necessity for a chloride ion to bind to one ruthenium ion has enabled the complexation of four $[\text{CH}_3\text{C}_5\text{H}_3\text{NO}]^-$ ligands in a 2:2 transoid configuration. The fact that this compound has been prepared under relatively mild conditions provides further evidence for the hypothesis that the preparation of the compound $[\text{Ru}_2(\text{CH}_3\text{C}_5\text{H}_3\text{NO})_4\text{Cl}]$ or for that matter the compound $[\text{Ru}_2(\text{CH}_3\text{C}_5\text{H}_3\text{NNH})_4\text{Cl}]$ is extremely unlikely due to unfavourable steric interactions.

A considerable range of diruthenium(II/III) compounds containing hydroxypyridine and aminopyridine ligands have been studied crystallographically and have been found to exist as discrete molecules, with the bridging ligands arranged to allow a strong Ru-Cl bond at one end of the molecule. The Ru-Ru and Ru-Cl bond lengths for these compounds are presented in Table 3.1. The table also includes examples of diruthenium(II/III) compounds which exist as linear chain polymers. When available the torsion angles about the Ru-Ru bond are quoted to indicate the extent to which the bridging ligands are twisted about the Ru-Ru bond. The Ru-Ru bond length is relatively unaffected by the nature of the bridging ligands involved but a considerable variation is observed for the Ru-Cl bond length. Discrete molecules with one chloride ion axial, and the other axial site vacant, exhibit the shortest Ru-Cl bond lengths. The presence of a linear chain structure, or the occupation of the vacant site by a neutral ligand, causes an increase in the Ru-Cl bond length by *ca.* 0.1 Å. The compound being discussed here exhibits Ru-Ru and Ru-Cl bond lengths which are comparable with those found in similar compounds. It is interesting to note that the variation in the Ru-Ru bond lengths over a wide range of bridging ligands is small, in contrast to the variation observed in the metal-metal bond distances observed for compounds containing dirhodium units (Tables 1.5 and 1.7)

3.4 The electrochemical behaviour of $[\text{Ru}_2(\text{O}_2\text{CCH}_3)(\text{CH}_3\text{C}_2\text{H}_3\text{NNH})_3\text{Cl}]$.

The electrochemical behaviour of the compound

$[\text{Ru}_2(\text{O}_2\text{CCH}_3)(\text{CH}_3\text{C}_2\text{H}_3\text{NNH})_3\text{Cl}]$ has been studied in two solvents, DMSO and

Table 3.1 Structural data for the compounds $[\text{Ru}_2(\text{ligand})_4\text{Cl}]$.

Compound.	Ru-Ru /Å	Ru-Cl /Å	av. Torsion ^a
$[\text{Ru}_2(\text{O}_2\text{CCH}_3)_4\text{Cl}]$	2.287(2)	2.577(1)	-
$[\text{Ru}_2(\text{HNOCC}_6\text{H}_5)_4\text{Cl}]$	2.293[1]	2.593[2]	-
$[\text{Ru}_2(\text{HNOCC}_6\text{H}_4\text{Cl})_4\text{Cl}]$	2.296[1]	2.583[2]	1.2°
$[\text{Ru}_2(\text{C}_5\text{H}_4\text{NO})_4\text{Cl}(\text{C}_5\text{H}_4\text{NOH})]$	2.286(1)	2.558(2)	2.2°
$[\text{Ru}_2(\text{ClC}_5\text{H}_3\text{NO})_4\text{Cl}]$	2.281(1)	2.443(2)	18.8°
$[\text{Ru}_2(\text{FC}_5\text{H}_3\text{NO})_4\text{Cl}]$	2.284(1)	2.427(3)	0.0 ^{ob}
$[\text{Ru}_2(\text{O}_2\text{CCH}_3)_2(\text{CH}_3\text{C}_5\text{H}_3\text{NO})_2\text{Cl}]$	2.278(2)	2.419(5)	1.3°
$[\text{Ru}_2(\text{O}_2\text{CCH}_3)(\text{ClC}_5\text{H}_3\text{NO})_3\text{Cl}]$	2.282(1)	2.474(9)	0.9°
$[\text{Ru}_2(\text{C}_5\text{H}_4\text{NNC}_6\text{H}_5)_4\text{Cl}]$	2.275(3)	2.437(7)	22.7°
$[\text{Ru}_2(\text{O}_2\text{CCH}_3)_2(\text{C}_5\text{H}_4\text{NNC}_6\text{H}_5)_2$ $(\text{C}_5\text{H}_4\text{NNC}_6\text{H}_5)]$	2.308(1)	2.560(2)	2.8°
$[\text{Ru}_2(\text{O}_2\text{CCH}_3)(\text{CH}_3\text{C}_5\text{H}_3\text{NNH})\text{Cl}]$	2.287(2)	2.473(4)	13.1°

a) average torsion angle X-Ru1-Ru2-X' (X,X' = O,N).

b) Due to crystal symmetry.

acetonitrile. The results obtained in the two solvents vary considerably and are discussed separately.

3.4.1 Behaviour in dimethylsulphoxide¹⁰⁶.

Three well defined responses have been observed in the potential range +1.0 V to -1.6 V as illustrated in Figure 3.4a. The electron transfer reactions at approximately -0.5 V and -1.3 V have been assigned to reductions of the dinuclear molecule, while the reaction at +0.55 V is due to its oxidation. The one-electron nature of the two reductions has been confirmed by comparison of the limiting current of a stirred voltammogram with that of a known quantity of ferrocene in a separate experiment.

The first reduction process can be assigned to equation 3.3.



This process has two components at $E_{pc} = -0.41$ and -0.64 V, an observation which can be rationalised by invoking the existence of an equilibrium mixture of different axially ligated adducts as previously discussed in Chapter 2. The observation of two waves rather than three suggests that two of the adducts are in rapid equilibrium.

Only a single re-oxidation wave is observed for this process at $E_{pa} = -0.27$ V suggesting that the three mono-reduced species are in rapid equilibrium.

A cyclic voltammogram recorded from +0.16 V to -0.49 V shows a distinct decrease in the peak current for the wave at $E_{pa} = -0.27$ V, suggesting that this wave includes contributions from the adduct reduced at $E_{pc} = -0.64$ V as well as that reduced at $E_{pc} = -0.41$ V (Figure 3.5a). A cyclic voltammogram recorded from

Figure 3.4 Cyclic voltammograms of $[\text{Ru}_2(\text{O}_2\text{CCH}_3)(\text{CH}_3\text{C}_2\text{H}_3\text{NNH})_3\text{Cl}]$ in DMSO (0.1 M TBABF_4 supporting electrolyte) a) no added ions, b) one molar equiv. Cl^- , c) 10 fold molar excess Cl^- , d) less than one molar equiv. Ag^+ .

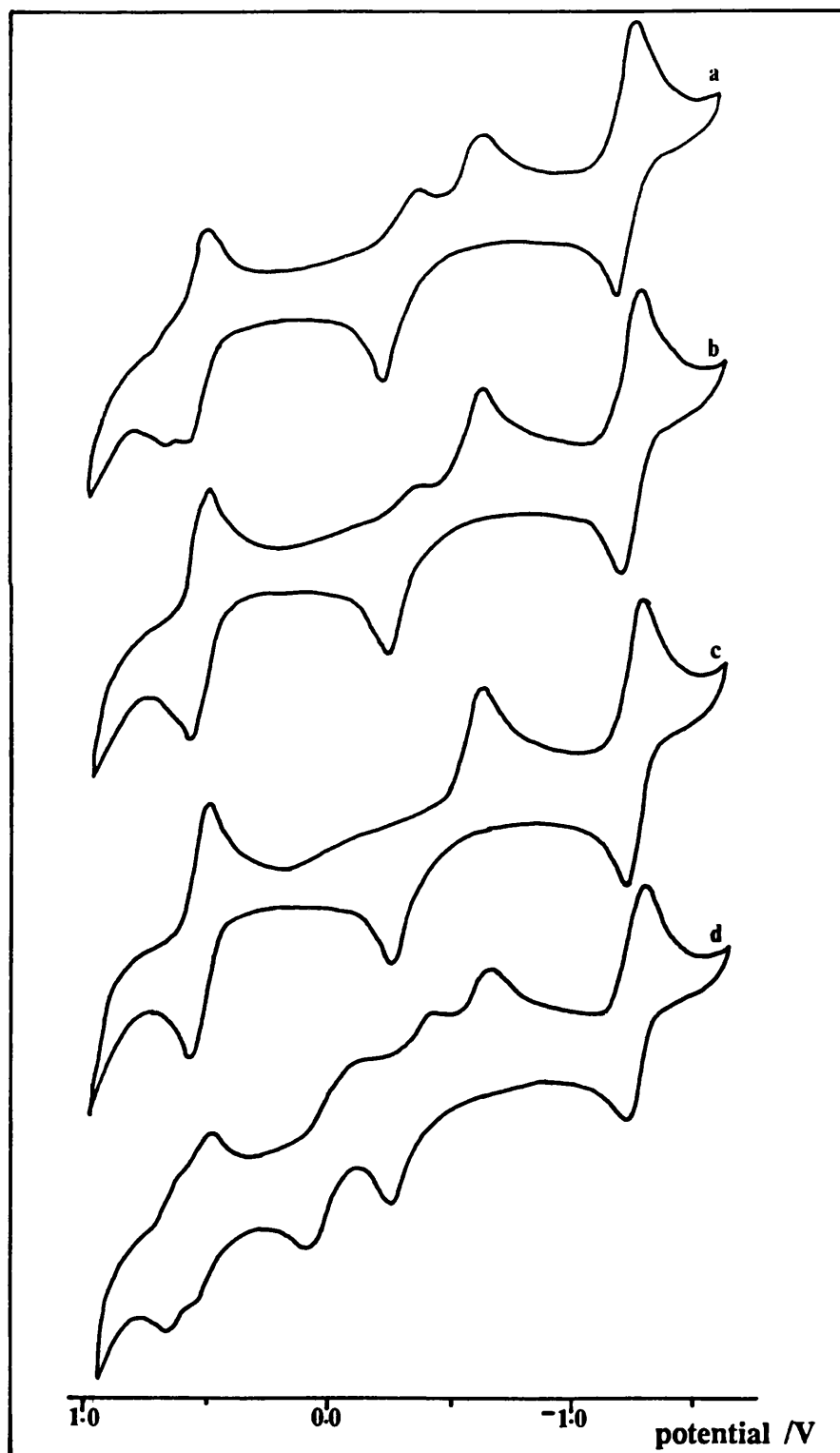
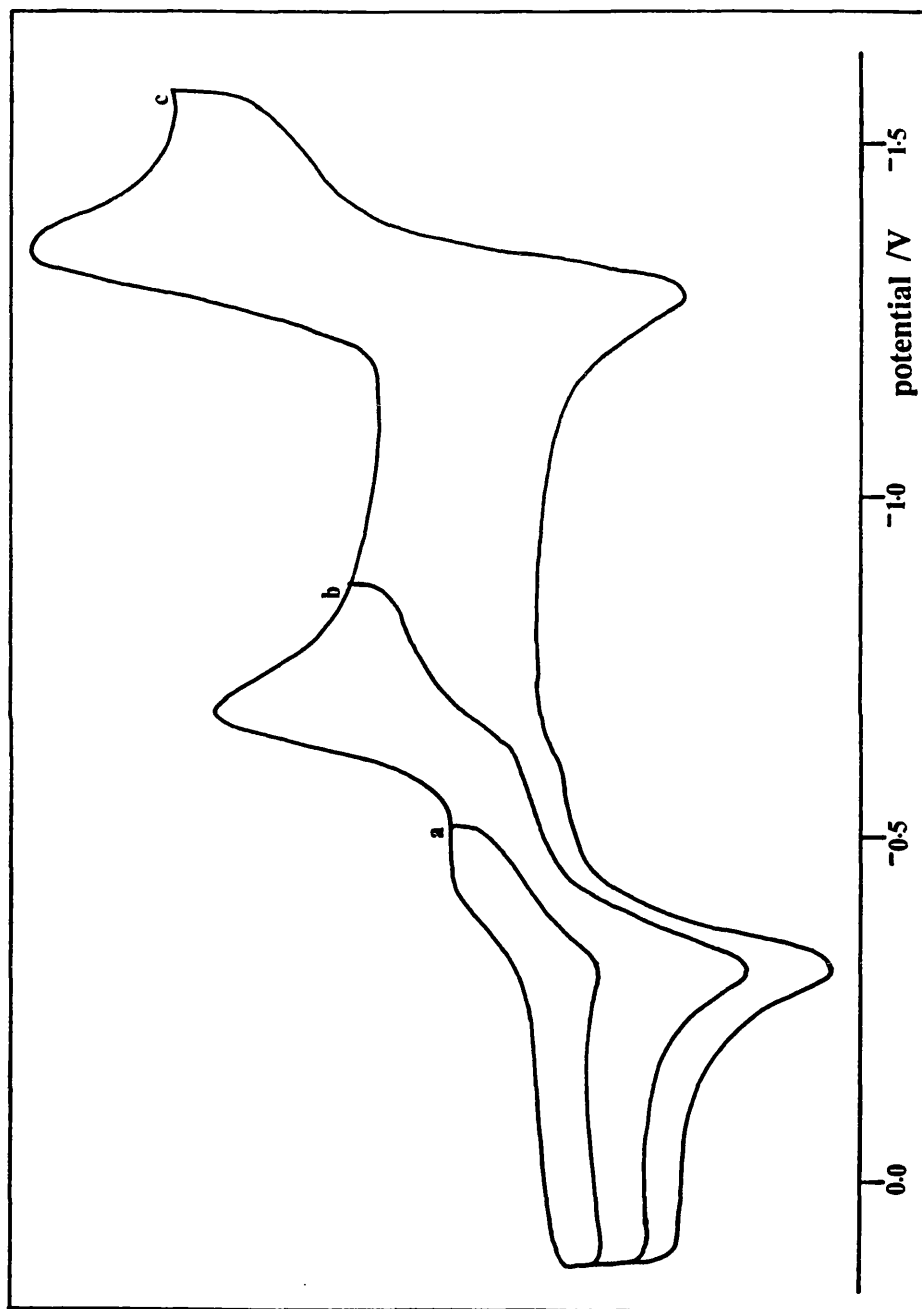


Figure 3.5 Cyclic voltammograms of $[\text{Ru}_2(\text{O}_2\text{CCH}_3)(\text{CH}_3\text{C}_6\text{H}_4\text{NNH})_3\text{Cl}]$ in DMSO (0.1 M TBABF₄ supporting electrolyte)

a) +0.16 to -0.41 V, b) +0.16 to -0.84 V, c) +0.16 to -1.54 V.



+0.16 V to -0.84 V reveals a small ill-defined wave at $E_{pa} = -0.53$ V which has been assigned to the re-oxidation of a small quantity of the adduct reduced at $E_{pc} = -0.64$ V (Figure 3.5b).

The second reversible reduction occurs at $E_{1/2} = -1.27$ V, and the current carried by this wave is equal to that of its precursors. The observation of a single wave confirms that the various mono-reduced species are in rapid equilibrium. The reversible nature of this reduction is unprecedented. Previously, a second reduction wave, when observed, has been irreversible⁴⁹, quasireversible³⁹, or assigned to the reduction of co-ordinated ligands⁹⁸. The addition of free ligand to the electrochemical cell has had no effect on the position or reversibility of this process and argues for the process being metal based. Thus it is assigned to Equation 3.4



The $[\text{Ru}_2]^{3+}$ centre is unique in having a formal bond order of only 1.5 between the ruthenium ions.

A single oxidation process is observed at $E_{pa} = +0.56$ V with an ill-defined shoulder at approximately $E_{pa} = +0.64$ V. Comparison of the limiting current of a stirred voltammogram with that observed for the two reduction processes already discussed indicates that this process is also a one-electron one, and is assigned to Equation 3.5



The presence of a single re-reduction wave at $E_{pc} = +0.48$ V indicates that the

mono-oxidised species, like the mono-reduced ones, are also in rapid equilibrium.

In order to assign peaks to specific axially ligated adducts additions of chloride ions and silver ions have been made to the electrochemical cell. The addition of a ten-fold molar excess of chloride ions to the cell results in a sharpening of the voltammetric peaks and the loss of the reduction wave at $E_{pc} = -0.41$ V and shoulder at $E_{pa} = +0.64$ V (Figure 3.5b,c). The three waves observed each carry identical currents and are assigned to the reduction or oxidation of the bis-chloro adduct $[\text{ClRu}(\text{O}_2\text{CCH}_3)(\text{CH}_3\text{C}_5\text{H}_3\text{NNH})_3\text{RuCl}]$. This addition has no observable effect on the potential of the reduction at $E_{1/2} = -1.27$ V or the re-oxidation wave at $E_{pa} = -0.27$ V, suggesting that the addition does not significantly alter the position of the equilibrium between the mono-reduced species.

The addition of less than one molar equivalent of silver ions to the electrochemical cell displaces the equilibrium between the different axially ligated adducts in the direction of the bis-dimethylsulphoxide adducts. In the cyclic voltammogram a new reduction wave is observed at $E_{pc} = -0.15$ V, with a corresponding re-oxidation wave at $E_{pa} = +0.10$ V. A new, but poorly defined, oxidation is observed at *ca.* $+0.75$ V, and a shoulder at $E_{pc} = +0.60$ V is observed on the re-reduction wave at $E_{pc} = +0.49$ V (Figure 3.4d). The oxidation observed at $E_{pa} = +0.75$ V and the reduction process at $E_{pc} = -0.15$ V are assigned to the bis-dimethylsulphoxide adduct, $[(\text{DMSO})\text{Ru}(\text{O}_2\text{CCH}_3)(\text{CH}_3\text{C}_5\text{H}_3\text{NNH})_3\text{Ru}(\text{DMSO})]^+$. The oxidation at $E_{pa} = +0.65$ V and the reduction at $E_{pc} = -0.41$ V are assigned to the mono-chloro/mono-dimethylsulphoxide adduct, $[\text{ClRu}(\text{O}_2\text{CCH}_3)(\text{CH}_3\text{C}_5\text{H}_3\text{NNH})_3\text{Ru}(\text{DMSO})]^\circ$. These assignments are summarised in Table 3.2.

Table 3.2 Electrochemical results for $[\text{Ru}_2(\text{O}_2\text{CCH}_3)(\text{CH}_3\text{C}_6\text{H}_3\text{NNH})_3\text{Cl}]$ in DMSO (0.1 M TBABF₄ supporting electrolyte).

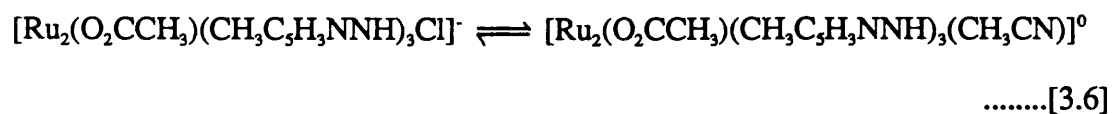
	DMSO		DMSO + Cl ⁻		DMSO + Ag ⁺	
	E _{pc} ^a	E _{pa} ^a	E _{pc} ^a	E _{pa} ^a	E _{pc} ^a	E _{pa} ^a
Reduction 1 ^c	-	-	-	-	-0.15	+0.10
Reduction 2 ^d	-0.41	-0.27	-	-0.28	-0.42	-0.25
Reduction 3 ^e	-0.64	-0.53 ^b	-0.63	-	-0.65	-
Reduction 4 ^f	-1.30	-1.23	-1.31	-1.24	-1.30	-1.22
Oxidation 1 ^c	+0.48	+0.56	+0.48	+0.55	+0.49	+0.55
Oxidation 2 ^d	-	+0.64	-	-	+0.60	+0.66
Oxidation 3 ^e	-	-	-	-	-	+0.75

- a) Potentials quoted in V vs. Ag/AgCl reference.
 b) Only visible on scan from +0.16 V to -0.84 V.
 c) Reduction/oxidation of the bis-acetonitrile adduct.
 d) Reduction/oxidation of the mono-chloro/mono-acetonitrile adduct.
 e) Reduction/oxidation of the bis-chloro adduct.
 f) Reduction/oxidation of the equilibrium mixture
 bis-acetonitrile \rightleftharpoons mono-chloro/mono-acetonitrile \rightleftharpoons bis-chloro.

3.4.2 Behaviour in acetonitrile.

Four well-defined redox processes have been observed in the potential range -1.70 V to +1.90 V. Two processes have been assigned to reductions, one at $E_{pc} = -0.61$ V is quasireversible, while the second at $E_{pc} = -1.30$ V is irreversible. The two remaining processes are assigned to oxidations, one at $E_{pa} = +0.64$ V is quasireversible while the second at $E_{pa} = +1.52$ V is irreversible. The two irreversible processes will not be discussed further. The quasireversible processes carry identical currents and comparison of the limiting current of a stirred voltammogram with that of a known concentration of ferrocene measured in a separate experiment confirms these processes to be one-electron in nature, and thus they can be assigned to Equations 3.3 and 3.5.

The reduction at $E_{pc} = -0.61$ V has two closely spaced re-oxidation waves associated with it at $E_{pa} = -0.40$ and -0.49 V. This behaviour indicates that following the reduction of $[\text{Ru}_2(\text{O}_2\text{CCH}_3)(\text{CH}_3\text{C}_5\text{H}_3\text{NNH})_3\text{Cl}]$, the reduced species is an equilibrium mixture of two components. (Equation 3.6)



such that on the reverse scan the re-oxidation of

$[\text{Ru}_2(\text{O}_2\text{CCH}_3)(\text{CH}_3\text{C}_5\text{H}_3\text{NNH})_3\text{Cl}]^-$ is observed at $E_{pa} = -0.49$ V while the species

$[\text{Ru}_2(\text{O}_2\text{CCH}_3)(\text{CH}_3\text{C}_5\text{H}_3\text{NNH})_3(\text{CH}_3\text{CN})]^0$ is re-oxidised at $E_{pa} = -0.40$ V. The

quasireversible oxidation is uncomplicated suggesting that the

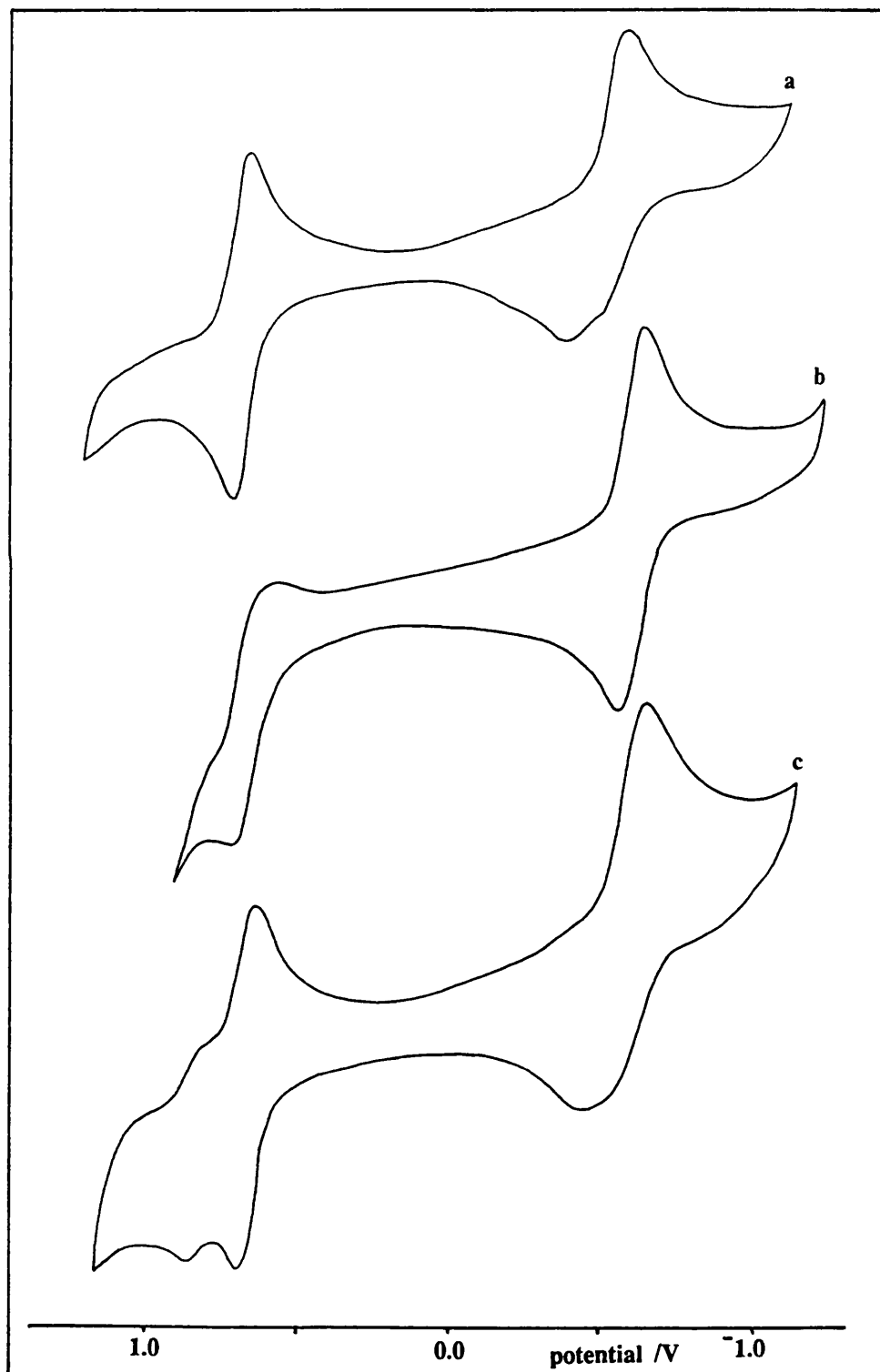
$[\text{Ru}_2(\text{O}_2\text{CCH}_3)(\text{CH}_3\text{C}_5\text{H}_3\text{NNH})_3\text{Cl}]^+$ unit remains intact (Figure 3.6a).

The addition of an excess of chloride ions to the electrochemical cell

Figure 3.6 Cyclic voltammograms of $[\text{Ru}_2(\text{O}_2\text{CCH}_3)(\text{CH}_3\text{C}_6\text{H}_3\text{NNH})_3\text{Cl}]$ in acetonitrile (0.1 M TBABF_4 supporting electrolyte)

a) no added ions, b) 10 fold molar excess Cl^- ,

c) less than one molar equiv. Ag^+ .



causes a shift in the potential of the reduction process at $E_{pc} = -0.61$ V to $E_{pc} = -0.64$ V. The associated re-oxidation waves at $E_{pa} = -0.40$ and -0.49 V, are replaced by a single wave at $E_{pa} = -0.55$ V. This process is quasireversible and may arise from the reduction of $[\text{ClRu}(\text{O}_2\text{CCH}_3)(\text{CH}_3\text{C}_5\text{H}_3\text{NNH})_3\text{RuCl}]^-$. The change observed in the oxidation at wave $E_{pa} = +0.64$ V is not well defined due a reduction of the solvent range caused by the addition of chloride ions to the cell. A considerable increase in the peak separation, from 70 mV before the addition of chloride ions to 140 mV, with excess chloride ions present in the cell is observed (Figure 3.6b). Once again it is assumed that this process is associated with the bis-chloro adduct. Unfortunately the close proximity of the solvent front has prevented detailed investigations into this electron transfer process.

The addition of less than one equivalent of silver ions to the electrochemical cell does not alter the potential of the cathodic wave due to the reduction of $[\text{Ru}_2(\text{O}_2\text{CCH}_3)(\text{CH}_3\text{C}_5\text{H}_3\text{NNH})_3\text{Cl}]^0$ but the replacement of the two anodic waves observed previously with a broad wave at $E_{pa} = -0.43$ V indicates that the addition of silver ions to the electrochemical cell has caused a shift in the position of equilibrium towards the solvated species. For the oxidation the addition of silver ions results in the appearance of an additional set of peaks at $E_{pa} = +0.80$ V and $E_{pc} = +0.73$ V (Figure 3.6c)^{which} is consistent with the establishment of an equilibrium mixture (Equation 3.7). The assignments discussed are summarised in Table 3.3.

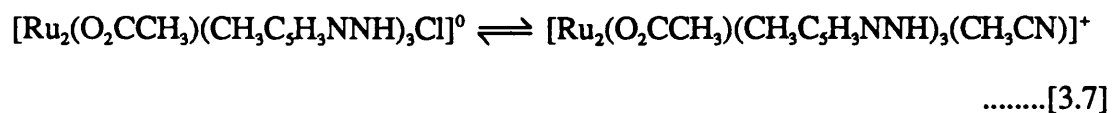


Table 3.3 Electrochemical results for $[\text{Ru}_2(\text{O}_2\text{CCH}_3)(\text{CH}_3\text{C}_5\text{H}_3\text{NNH})_3\text{Cl}]$ in Acetonitrile (0.1 M TBABF₄ supporting electrolyte).

	CH ₃ CN		CH ₃ CN + Cl ⁻		CH ₃ CN + Ag ⁺	
	E _{pc} ^a	E _{pa} ^a	E _{pc} ^a	E _{pa} ^a	E _{pc} ^a	E _{pa} ^a
Reduction 1 ^c	-	-0.40	-	-	-	-
Reduction 1/2 ^d	-	-	-	-	-0.61	-0.43 ^b
Reduction 2 ^e	-0.61	-0.49	-	-	-	-
Reduction 3 ^f	-	-	-0.64	-0.55	-	-
Reduction 4 ^g	-1.30	-	-	-	-	-
Oxidation 1 ^f	-	-	+0.52 ^b	+0.66	-	-
Oxidation 2 ^e	+0.57	+0.64	-	-	+0.57	+0.63
Oxidation 3 ^c	-	-	-	-	0.73	+0.80
Oxidation 4 ^g	-	+1.52	-	-	-	-

- a) Potentials quoted in V vs. Ag/AgCl reference.
 b) Peak observed is broad.
 c) Reduction/oxidation of the bis-acetonitrile adduct.
 d) Reduction of the equilibrium mixture
 bis-acetonitrile \rightleftharpoons mono-chloro/mono-acetonitrile.
 e) Reduction/oxidation of the mono-chloro/mono-acetonitrile adduct.
 f) Reduction/oxidation of the bis-chloro adduct.
 g) Reduction/oxidation of the equilibrium mixture
 bis-acetonitrile \rightleftharpoons mono-chloro/mono-acetonitrile \rightleftharpoons bis-chloro.

3.4.3 Electrochemical behaviour - A rationalisation.

The electrochemical behaviour of several related diruthenium(II/III) compounds has been reported previously^{44,46-49}. The polar arrangement of bridging ligands in these compounds results in the formation of strong axial Ru-Cl bonds. This results in greater stability of this bond in solution in contrast to the behaviour of the chlorotetrakis(amidato)diruthenium(II/III) compounds^{38,40}, where equilibrium mixtures of different axially ligated species are often observed in solution.

The compounds $[\text{Ru}_2(\text{O}_2\text{CCH}_3)_2(\text{CH}_3\text{C}_5\text{H}_3\text{NO})_2\text{Cl}]^{47}$ and $[\text{Ru}_2(\text{ClC}_5\text{H}_3\text{NO})_4\text{Cl}]^{49}$ have both been studied electrochemically in acetonitrile and two closely spaced reduction processes are observed. These processes are attributed to the reduction of an equilibrium mixture of dissociated and undissociated species. Similar electrochemical behaviour is observed in acetonitrile for the compound $[\text{Ru}_2(\text{O}_2\text{CCH}_3)(\text{CH}_3\text{C}_5\text{H}_3\text{NNH})_3\text{Cl}]$.

The electrochemistry of only one closely related diruthenium(II/III) compound has been studied in DMSO, namely $[\text{Ru}_2(\text{C}_3\text{H}_4\text{NNCH}_3)_4\text{Cl}]^{46}$. Two reductions ($E_{1/2} = -0.78$ and -1.11 V) and one oxidation ($E_{1/2} = +0.24$ V) were observed. On the addition of chloride ions to the cell the two reduction waves collapsed and a new reduction process was observed at $E_{1/2} = -0.84$ V indicating the presence of a rapid equilibrium between associated and dissociated species. In Chapter 2 it has been noted that where there is no steric hindrance at the axial sites fast exchange between dimethylsulphoxide molecules and chloride ions occurs and only an 'average' environment is observed. When there is steric hindrance at one or both axial sites the rate of exchange between dimethylsulphoxide molecules and chloride ions is slowed sufficiently for processes due to individual species to be observed. This comparison can be made between the compounds

$[\text{Ru}_2(\text{C}_5\text{H}_4\text{NNCH}_3)_4\text{Cl}]^{46}$ and $[\text{Ru}_2(\text{O}_2\text{CCH}_3)(\text{CH}_3\text{C}_5\text{H}_3\text{NNH})_3\text{Cl}]$, and satisfactorily explains the differences in the solution behaviour of these compounds.

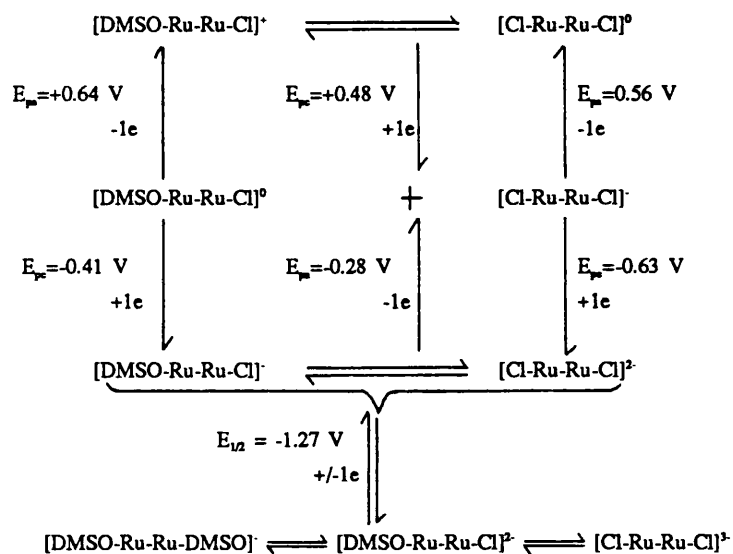
The differences in behaviour observed in the two solvents employed here are the result of several factors. Firstly, the solvent molecules will co-ordinate to the diruthenium unit through different donor atoms. Acetonitrile will bond through a nitrogen atom, while DMSO can bind through an oxygen atom or a sulphur atom. Nitrogen is a relatively 'hard' donor atom and hence will stabilise ruthenium in a high oxidation state. Sulphur being a 'soft' donor atom is more likely to bind to ruthenium in a low oxidation state while oxygen being a 'hard' donor atom will prefer ruthenium in a high oxidation state. Constant exchange may occur between solvent molecules and chloride ions while in solution and as a consequence of this it is not inconceivable that the mode of co-ordination of the DMSO molecule will alter depending on the oxidation state of the metal ions. (During the study of substituent group effect on the electrochemistry of tetrakis(carboxylato)dirhodium(II/II) compounds⁶⁷ it was noted that, the reaction mechanism appeared to be unaffected by whether the DMSO was sulphur, or oxygen bound). The donor ability of the solvents will also influence the electrochemical behaviour observed. DMSO is a stronger donor solvent than acetonitrile (as measured by Gutmann's donor numbers) and is therefore more likely to labilise the Ru-Cl bond resulting in the establishment of an equilibrium mixture of different axially ligated species. The results obtained suggest that the donor ability of acetonitrile does not cause sufficient labilisation of the Ru-Cl bond in the compound $[\text{Ru}_2(\text{O}_2\text{CCH}_3)(\text{CH}_3\text{C}_5\text{H}_3\text{NNH})_3\text{Cl}]$ for the equilibrium mixture to be established under normal cell conditions.

3.5 Conclusions.

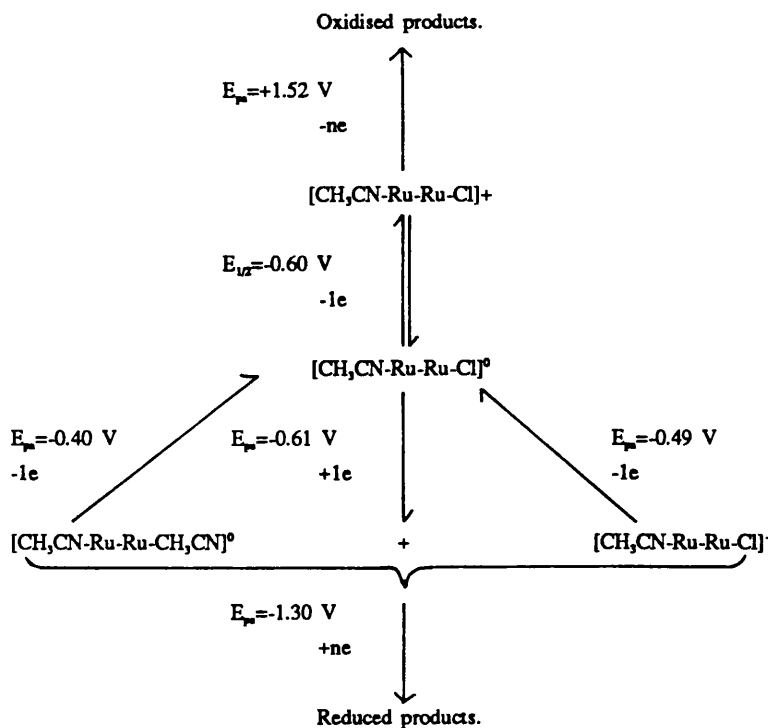
The compound $[\text{Ru}_2(\text{O}_2\text{CCH}_3)(\text{CH}_3\text{C}_5\text{H}_3\text{NNH})_3\text{Cl}]$ has been prepared and characterised using microanalysis, infrared spectroscopy, and mass spectrometry. X-ray crystallographic measurements have confirmed that the compound exists as discrete molecules in the crystal lattice with the diruthenium unit bridged by three 2-amino-6-picolinate ligands and one acetate ligand. The 2-amino-6-picolinate ligands are arranged such that the three pendant methyl groups are blocking the axial site of one of the ruthenium ions while the axial site of the other ruthenium ion is co-ordinated by a chloride ion. Ru-Ru and Ru-Cl bond distances are consistent with those obtained for related diruthenium compounds.

The electrochemical behaviour of this compound has been studied in two solvents, DMSO and acetonitrile. The results obtained in each solvent are markedly different and are summarised in Schemes 3.1 and 3.2. The behaviour in acetonitrile has mirrored that observed previously for related compounds, but, the behaviour observed in DMSO is more in line with that observed previously for chlorotetrakis(amidato)diruthenium(II/III) compounds. In addition, in DMSO it has been possible to oxidise the $[\text{Ru}_2]^{5+}$ unit to $[\text{Ru}_2]^{6+}$ and reduce it in two reversible one electron steps to $[\text{Ru}_2]^{3+}$ in which a formal Ru-Ru bond order of 1.5 must be invoked.

Scheme 3.1 The electrochemical behaviour of $[\text{Ru}_2(\text{O}_2\text{CCH}_3)(\text{CH}_3\text{C}_5\text{H}_3\text{NNH})_3\text{Cl}]$ in DMSO (0.1 M TBABF₄ supporting electrolyte).



Scheme 3.2 The electrochemical behaviour of $[\text{Ru}_2(\text{O}_2\text{CCH}_3)(\text{CH}_3\text{C}_5\text{H}_3\text{NNH})_3\text{Cl}]$ in acetonitrile (0.1 M TBABF₄ supporting electrolyte).



3.5 Experimental.

3.5.1 Materials and instrumentation.

With the exception of 2-amino-6-picoline which was purified by vacuum sublimation, all chemicals were used as previously described in Section 2.5.1 and 2.5.2

Crystallographic studies were carried out using a Nicolet R3m/V diffractometer. Computations were carried out on a Microvax II computer using the SHELXTL Plus program system¹⁰⁷. Mass spectra were recorded by the ULIRS Mass Spectrometry Service at the London School of Pharmacy. All other techniques are as described previously in Section 2.5.1.

3.5.2 Synthesis of $[\text{Ru}_2(\text{O}_2\text{CCH}_3)(\text{CH}_3\text{C}_5\text{H}_3\text{NNH})_3\text{Cl}]$.

$[\text{Ru}_2(\text{O}_2\text{CCH}_3)_4\text{Cl}]$ (0.1053 g, 0.21 mMol) was stirred with an excess of $[\text{CH}_3\text{C}_5\text{H}_3\text{NNH}_2]$ (1.0 g, excess) at 50 °C under a dinitrogen atmosphere for six hours. The excess ligand was removed by vacuum sublimation onto a water-cooled cold finger at 50 °C. The whole procedure was repeated using a fresh batch of ligand to ensure complete exchange (Yield = 70 %).

Microanalytical data found C 39.4, H 4.1, N 13.7 %

Calculated for $\text{C}_{20}\text{H}_{24}\text{N}_6\text{O}_2\text{ClRu}_2$ C 38.9, H 3.9, N 13.6 %.

Infrared spectrum (KBr disk)

3357m,3328m,1607s,1560m,1542m,1519m,1470s,1428s,1386m,1233m,1160m,1091w,
1034w,1003w,774s,751m,728w,689w,628w,330s.

3.5.3 The crystal structure determination of $[\text{Ru}_2(\text{O}_2\text{CCH}_3)(\text{CH}_3\text{C}_5\text{H}_3\text{NNH})_3\text{Cl}]$.

A dark green crystal of approximate size 0.6 x 0.1 x 0.1 mm was mounted on a glass fibre. All geometric and intensity data were taken from this crystal by using an automated four-circle diffractometer (Nicolet R3m/V) equipped with graphite monochromated Mo-K α radiation. Important crystallographic parameters are given in Table 3.4.

The lattice vectors were identified by application of the automatic indexing routine of the diffractometer to the positions of 15 reflections taken from a rotation photograph and centred by the diffractometer. Axial photographs were used to verify the Laue class and cell dimensions, and precise cell dimensions were obtained by least-squares fit to the goniometer positions of 15 accurately located reflections in the range $6^\circ \leq 2\theta \leq 29^\circ$. The ω - 2θ technique was used to measure 2751 unique data in the range $5^\circ \leq 2\theta \leq 50^\circ$. Three standard reflections were remeasured every 97 scans, these showed no significant loss in intensity during the data collection. The data were corrected for Lorentz and polarization effects. There were 1661 unique reflections with $F_o^2 > 3\sigma(F_o^2)$. From the systematically absent data the space group was uniquely defined as $\text{Pna}2_1$.

The positions of the heavy atoms were determined using a Patterson map and the remaining non-hydrogen atoms were found by iterative application of least-squares refinement and difference-fourier synthesis. No attempt was made to locate the hydrogen atoms and all non-hydrogen atoms were refined anisotropically.

The final cycle of refinement included 279 parameters for 1661 variables. This final cycle gave $R=0.069$ and $R'=0.049$ and did not shift any parameter by more than 0.067 times its standard deviation. the final difference fourier map was featureless with the highest peak being 1.1 e/ \AA^3 .

Table 3.4 Crystallographic data for $\text{Ru}_2(\text{O}_2\text{CCH}_3)(\text{CH}_3\text{C}_5\text{H}_3\text{NNH})_3\text{Cl}$.

Formula	$\text{C}_{20}\text{H}_{24}\text{N}_6\text{O}_2\text{ClRu}_2$
fw	618.09
Space group	$\text{Pna}2_1$
a, Å	16.528(8)
b, Å	14.391(7)
c, Å	9.430(4)
α , deg	90.0
β , deg	90.0
γ , deg	90.0
V, Å ³	2242.8
Z	4
F(000)	1228
d_{calc} , g/cm ³	1.83
Cryst. size	0.6 x 0.1 x 0.1
$\mu(\text{Mo-K}\alpha)$, cm ⁻¹	14.35
Data collection instrument.	Nicolet R3m/V
Radiation	$\text{Mo}(\lambda=0.71073 \text{ \AA})$
Orientation reflections:	
no.; range (2θ)	15, $6 < 2\theta < 29$
Temp., °C	18
No. of unique data;	2751
Total with $F_o^2 \geq 3\sigma(F_o^2)$	1661
No. of parameters	279
R ^a	0.069
R ^b	0.049
Weighting scheme	$w=1/(\sigma^2(F)+0.00007F^2)$
Largest shift/esd, final cycle	0.067
Largest peak, e/Å ³	1.1

$$\text{a) } R = \frac{\sum[|F_o| - |F_c|]}{\sum|F_o|}$$

$$\text{b) } R' = \frac{\sum[(|F_o| - |F_c|) \cdot \sqrt{w}]}{\sum[|F_o| \cdot \sqrt{w}]}$$

Table 3.5 Atomic co-ordinates ($\times 10^4$) and equivalent isotropic displacement parameters ($\text{\AA}^2 \times 10^3$) for $[\text{Ru}_2(\text{O}_2\text{CCH}_3)(\text{CH}_3\text{C}_5\text{H}_3\text{NNH})_3\text{Cl}]$.

Atom	x	y	z	U(eq) ^a
Ru1	998(1)	1247(1)	0	36(1)
Ru2	1804(1)	2538(1)	54(5)	33(1)
Cl1	123(3)	-147(3)	-18(12)	69(2)
O1	19(7)	2122(8)	-521(13)	43(4)
O2	891(8)	3292(8)	-917(14)	43(5)
N1	1215(12)	1075(13)	-2050(21)	56(7)
N2	2221(8)	2226(12)	-1964(15)	46(6)
N3	779(10)	1440(10)	2135(16)	33(5)
N4	1320(9)	2933(10)	1994(17)	41(5)
N5	1955(8)	458(9)	540(15)	38(5)
N6	2734(8)	1800(11)	1113(17)	41(6)
C1	235(12)	2949(15)	-932(17)	39(7)
C2	-477(10)	3504(13)	-1551(24)	50(7)
C20	1786(15)	1539(15)	-2691(21)	54(8)
C21	2044(15)	1327(18)	-4134(20)	77(10)
C22	2608(15)	1815(16)	-4947(43)	82(10)
C23	2986(13)	2550(22)	-4135(25)	85(11)
C24	2790(13)	2759(18)	-2648(23)	65(9)
C25	3148(20)	3548(20)	-1765(38)	88(13)
C30	900(10)	2261(12)	2796(18)	34(6)
C31	653(11)	2435(16)	4216(19)	52(6)
C32	768(12)	3309(12)	4694(19)	46(7)
C33	1129(13)	3983(14)	3865(23)	57(8)
C34	1361(12)	3807(14)	2496(21)	45(6)
C35	1685(12)	4541(13)	1597(25)	57(8)
C40	2616(12)	826(15)	1103(21)	48(7)
C41	3215(13)	235(13)	1753(22)	51(7)
C42	3881(14)	641(22)	2294(25)	80(11)
C43	3964(14)	1653(17)	2341(23)	60(9)
C44	3385(11)	2147(16)	1740(24)	51(8)
C45	3395(14)	3211(19)	1912(30)	53(9)

a) Equivalent isotropic U defined as 1/3 of the trace of the orthogonalized U_{ij} tensor.

Table 3.6 Bond lengths (Å) for [Ru₂(O₂CCH₃)(CH₃C₅H₃NNH)₃Cl].

Ru1-Ru2	2.287(2)	Ru1-Cl1	2.473(4)
Ru1-O1	2.108(11)	Ru1-N1	1.981(20)
Ru1-N1	2.064(15)	Ru1-N5	2.014(12)
Ru2-O2	2.072(12)	Ru2-N2	2.073(14)
Ru2-N4	2.076(16)	Ru2-N6	2.119(14)
O1-C1	1.301(21)	O2-C1	1.191(22)
N1-C20	1.304(27)	N2-C20	1.401(26)
N2-C24	1.374(23)	N3-C30	1.350(21)
N4-C30	1.411(21)	N4-C34	1.346(22)
N5-C40	1.335(24)	N6-C40	1.415(23)
N6-C44	1.325(23)	C1-C2	1.539(23)
C20-C21	1.459(27)	C21-C22	1.397(36)
C22-C23	1.447(38)	C23-C24	1.470(31)
C24-C25	1.527(37)	C30-C31	1.422(23)
C31-C32	1.349(25)	C32-C33	1.381(26)
C33-C34	1.370(26)	C34-C35	1.457(27)
C40-C41	1.442(27)	C41-C42	1.347(31)
C42-C43	1.463(33)	C43-C44	1.320(28)
C44-C45	1.540(35)		

Table 3.7 Bond angles (°) for $[\text{Ru}_2(\text{O}_2\text{CCH}_3)(\text{CH}_3\text{C}_3\text{H}_3\text{NNH})_3\text{Cl}]$.

Cl1-Ru1-Ru2	179.1(3)	O1-Ru1-Ru2	88.1(3)
O1-Ru1-Cl1	92.0(3)	N1-Ru1-Ru2	91.0(6)
N1-Ru1-Cl1	89.9(6)	N1-Ru1-O1	89.2(6)
N3-Ru1-Ru2	88.4(4)	N3-Ru1-Cl1	90.8(5)
N3-Ru1-O1	90.8(5)	N3-Ru1-N1	179.4(7)
N5-Ru1-Ru2	89.6(4)	N5-Ru1-Cl1	90.2(4)
N5-Ru1-O1	177.5(5)	N5-Ru1-N1	91.9(7)
N5-Ru1-N3	88.1(6)	O2-Ru2-Ru1	89.5(4)
N2-Ru2-Ru1	89.9(5)	N2-Ru2-O2	87.1(5)
N4-Ru2-Ru1	91.0(4)	N4-Ru2-O2	88.0(6)
N4-Ru2-N2	175.1(6)	N6-Ru2-Ru1	91.5(4)
N6-Ru2-O2	177.9(6)	N6-Ru2-N2	94.8(6)
N6-Ru2-N4	90.1(6)	C1-O1-Ru1	113.9(11)
C1-O2-Ru2	116.8(12)	C20-N1-Ru1	121.3(16)
C20-N2-Ru2	115.5(13)	C24-N2-Ru2	122.5(15)
C24-N2-C20	121.0(18)	C30-N3-Ru1	122.8(11)
C30-N4-Ru2	118.3(11)	C34-N4-Ru2	123.1(13)
C34-N4-C30	118.5(16)	C40-N5-Ru1	121.6(12)
C40-N6-Ru2	113.2(12)	C44-N6-Ru2	127.6(14)
C44-N6-C40	119.3(18)	O2-C1-O1	128.7(18)
C2-C1-O1	112.2(17)	C2-C1-O2	119.1(18)
N2-C20-N1	120.4(19)	C21-C20-N1	122.4(24)
C21-C20-N2	117.0(24)	C22-C21-C20	127.0(29)
C23-C22-C21	111.5(32)	C24-C23-C22	124.0(26)
C23-C24-N2	119.0(23)	C25-C24-N2	115.1(21)

Table 3.7 continued;

C25-C24-C23	126.0(24)	N4-C30-N3	115.2(15)
C31-C30-N3	123.2(17)	C31-C30-N4	121.6(17)
C32-C31-C30	116.1(19)	C33-C32-C31	121.8(17)
C34-C33-C32	121.6(19)	C33-C34-N4	119.4(19)
C35-C34-N4	119.4(17)	C35-C34-C33	121.1(19)
N6-C40-N5	120.8(17)	C41-C40-N5	120.0(18)
C41-C40-N6	119.1(19)	C42-C41-C40	117.8(20)
C43-C42-C41	121.3(21)	C44-C43-C42	117.1(22)
C43-C44-N6	125.2(22)	C45-C44-N6	115.5(19)
C45-C44-C43	118.9(21)		

Chapter Four.

**The electrochemical behaviour of
Dirhodium(II/II) compounds containing both carboxylate
and amidate ligands.**

4.1	Introduction.	132
4.2	Preparation and characterisation.	135
4.3	Electrochemical investigation.	136
	4.3.1 Results.	136
	4.3.1 Electrochemical behaviour - A rationalisation.	141
4.4	Conclusion.	146
4.5	Experimental	149
	4.5.1 Materials and Instrumentation.	149
	4.5.2 Synthesis of $[\text{Rh}_2(\text{O}_2\text{CCH}_3)_4(\text{CH}_3\text{OH})_2]$.	149
	4.5.3 Synthesis of $[\text{Rh}_2(\text{O}_2\text{CC}(\text{CH}_3)_3)_4]$.	149
	4.5.4 Synthesis of $[\text{Rh}_2(\text{O}_2\text{CCH}_3)_n(\text{HNOCC}_2\text{H}_5)_{4-n}]$.	149
	4.5.5 Synthesis of $[\text{Rh}_2(\text{O}_2\text{CCH}_3)_n(\text{HNOCC}_3\text{H}_7)_{4-n}]$.	150
	4.5.6 Synthesis of $[\text{Rh}_2(\text{O}_2\text{CCH}_3)_n(\text{HNOCC}(\text{CH}_3)_3)_{4-n}]$.	150
	4.5.7 Synthesis of $[\text{Rh}_2(\text{O}_2\text{CC}(\text{CH}_3)_3)_n(\text{HNOCC}(\text{CH}_3)_3)_{4-n}]$.	150
	4.5.8 Synthesis of bispyridine adducts.	151

4.1 Introduction.

The stepwise reaction of tetrakis(carboxylato)dirhodium(II/II) complexes with amidate ligands can result in the formation of up to four compounds $[\text{Rh}_2(\text{O}_2\text{CCH}_3)_n(\text{R}'\text{NOCR}'')_{4-n}\text{L}_2]$ ($n=0,1,2,3$) with a total of twelve possible isomers, as illustrated in Figure 1.14 and discussed in Section 1.7.2. The reactions of tetrakis(acetato)dirhodium(II/II) with four different amidate ligands have been reported. Reactions involving the amidate ligands trifluoroacetamide^{69,73} or benzamide⁷⁰ have resulted in a single product $[\text{Rh}_2(\text{HNOCR}'')_4]$ ($\text{R}''=\text{CH}_3, \text{C}_6\text{H}_5$) being isolated. The electrochemical behaviour of $[\text{Rh}_2(\text{HNOCCF}_3)_4]$ has been studied in nine different non-aqueous solvents⁷⁶. A reversible one-electron oxidation was observed between +0.91 and +1.08 V(vs S.C.E.) in seven of the solvents. In pyridine or pyridine/acetonitrile mixtures a rapid chemical reaction was found to follow the oxidation.

The reactions involving the ligands acetamide^{71,75,78} or acetanilide^{72,74,77} have resulted in the formation of mixtures containing a number of different species, namely $[\text{Rh}_2(\text{O}_2\text{CCH}_3)_n(\text{HNOCCCH}_3)_{4-n}]$ and $[\text{Rh}_2(\text{O}_2\text{CCH}_3)_n(\text{C}_6\text{H}_5\text{NOCCH}_3)_{4-n}]$ ($n=0,1,2,3,4$). Separation of the differently substituted complexes has been achieved by the use of HPLC techniques. For the compounds containing acetamide ligands, individual isomers of the same stoichiometry were not separated. When the HPLC was run at a slow rate the band assigned to $[\text{Rh}_2(\text{O}_2\text{CCH}_3)_2(\text{HNOCCCH}_3)_2]$ was observed to split into three components⁷⁵. No splitting was observed for the other bands suggesting that only one isomer of each of the other species was present. This was further confirmed when the crystal structure determinations of two of these species, $[\text{Rh}_2(\text{HNOCCCH}_3)_4]$ and $[\text{Rh}_2(\text{O}_2\text{CCH}_3)(\text{HNOCCCH}_3)_3]$ were obtained, and both were found to be crystallographically well behaved. ¹H n.m.r. spectroscopic data

also indicated the presence of only one isomer for each of these two samples⁷⁵. For the compounds containing acetanilide ligands two of the possible isomers for each of $n=0$, $n=1$ and $n=2$ were separated^{74,77}, and the two isomers obtained for $n=0$ studied crystallographically⁷⁴. The electrochemical behaviour of these two series of compounds has also been reported^{74,78} and the results obtained are illustrated in Tables 4.1 and 4.2. One or two oxidations were observed for each species and a stepwise cathodic shift in the half-wave potential of these reactions was observed on changing from $[\text{Rh}_2(\text{O}_2\text{CCH}_3)_4\text{S}_2]$ through to $[\text{Rh}_2(\text{R}'\text{NOCR}'')_4\text{S}_2]$ ($\text{R}'=\text{H}$; $\text{R}''=\text{CH}_3, \text{C}_6\text{H}_5$; $\text{S}=\text{solvent}$). Each series of compounds was studied in several solvents and the results indicated that the shift in oxidation potential observed on changing the bridging ligands was dependent on the solvent in which the compound was studied and hence the axial ligation. In particular, both reports^{74,78} reached the conclusion that the π -acceptor properties of the axial ligand effects the shift in potential observed, with the largest shifts being observed in acetonitrile and pyridine which both have poor π -acceptor properties. The differences observed in redox potential for different isomers of the same species were very small. For $[\text{Rh}_2(\text{O}_2\text{CCH}_3)_n(\text{C}_6\text{H}_5\text{NOCCH}_3)_{4-n}]$ the half-wave potentials for two isomers of the same empirical formula differ by no more than 50 mV. For the compound $[\text{Rh}_2(\text{O}_2\text{CCH}_3)_2(\text{HNOCCCH}_3)_2]$, where three isomers were studied together, only a slight broadening of the cyclic voltammetric waves was observed⁷⁷.

Concerted efforts have been made to prepare a new example of a tetrakis(amidato)dirhodium(II/II) complex in order to study the effect of solvent on the electrochemical behaviour of this type of compound. Initially work centred on the ligand trimethylacetamide in order that a comparison could be made with the electrochemical behaviour of the compound $[\text{Rh}_2(\text{HNOCCF}_3)_4]$ ⁷⁶. The latter

Table 4.1 Electrochemical results for $[\text{Rh}_2(\text{O}_2\text{CCH}_3)_n(\text{HNOCCCH}_3)_{4-n}]$ in several solvents (0.1 M TBAP supporting electrolyte).

Solvent.	$E_{1/2} / \text{V}$ (vs S.C.E.)				
	n=0	n=1	n=2	n=3	n=4
CH_3CN	0.15	0.37	0.62	0.91	1.17
$\text{C}_5\text{H}_5\text{N}$	0.08	0.26	0.52	-	-
DMSO	0.31	0.52	0.72	0.88	1.00
CH_2Cl_2^a	0.25	0.35	0.44	-	0.64

a) Contains 0.1 M $\text{P}(\text{C}_6\text{H}_5)_3$.

Table 4.2 Electrochemical results for $[\text{Rh}_2(\text{O}_2\text{CCH}_3)_n(\text{HNOCCCH}_3)_{4-n}]$ in several solvents (0.1 M TBAP supporting electrolyte).

Solvent.	$E_{1/2} / \text{V}$ (vs S.C.E.)				
	n=0	n=1	n=2	n=3	n=4
DMSO	0.41	0.55	0.73	0.88	1.0
	0.40	0.51	0.76	-	-
CH_2Cl_2	0.60	0.76	0.97	1.13	1.3
	0.55	0.76	0.95	-	-

compound containing the electron withdrawing group (CF_3) while the former, $[\text{Rh}_2(\text{HNOCC}(\text{CH}_3)_3)_4]$, contains an electron donating group ($\text{C}(\text{CH}_3)_3$). Attempts to prepare $[\text{Rh}_2(\text{HNOCC}(\text{CH}_3)_3)_4]$ by stirring $[\text{Rh}_2(\text{O}_2\text{CCH}_3)_4(\text{CH}_3\text{OH})_2]$ with an excess of ligand at elevated temperature proved unsuccessful. The temperature of the reaction mixture and the length of time the mixture was stirred were both varied but all attempts resulted in the preparation of a mixture of compounds, $[\text{Rh}_2(\text{O}_2\text{CCH}_3)_n(\text{HNOCC}(\text{CH}_3)_3)_{4-n}\text{L}_2]$. Changing the starting material from $[\text{Rh}_2(\text{O}_2\text{CCH}_3)_4(\text{CH}_3\text{OH})_2]$ to $[\text{Rh}_2(\text{O}_2\text{CC}(\text{CH}_3)_3)_4]$ also resulted in a related mixture of compounds. Fresh attempts were made to prepare new compounds using the ligands butyramide and propanamide, under various conditions. These were also unsuccessful, once again resulting in mixtures of several closely related species.

Unfortunately the use of HPLC techniques to separate the mixtures obtained was not possible. Given the results described above it was decided to study the electrochemical behaviour of these compounds *in situ*, and the results of that study are presented here.

4.2 Preparation and Characterisation.

Each of the four series of compounds to be discussed here have been prepared by stirring $[\text{Rh}_2(\text{O}_2\text{CCH}_3)_4(\text{CH}_3\text{OH})_2]$ (or in one case $[\text{Rh}_2(\text{O}_2\text{CC}(\text{CH}_3)_3)_4]$) with an excess of the appropriate ligand at elevated temperature under a dinitrogen atmosphere. The excess ligand is removed by vacuum sublimation onto a water cooled cold finger. Characterisation of these mixtures of compounds using microanalytical data is difficult because the percentage of each species present cannot be determined accurately. The use of ^1H n.m.r. spectroscopy is further

complicated by the presence of more than one isomer for many of the compounds.

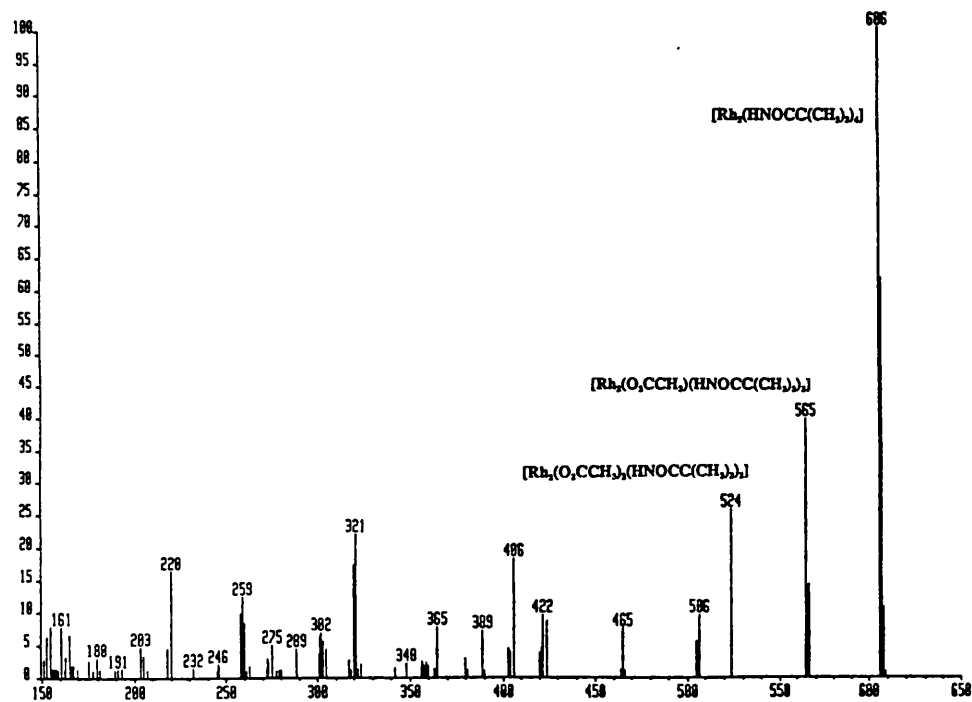
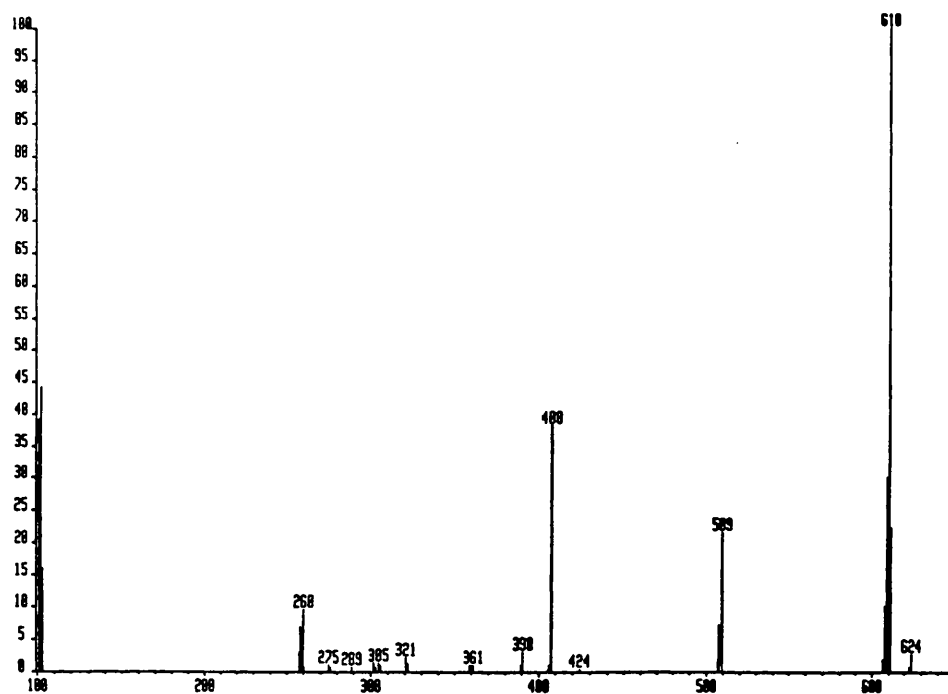
Electron impact mass spectroscopy has proved a useful technique for characterising one of the series obtained, namely $[\text{Rh}_2(\text{O}_2\text{CCH}_3)_n(\text{HNOCC}(\text{CH}_3)_3)_{4-n}]$, where mass peaks are observed which can be assigned to the species where $n=0,1,2$ (Figure 4.1). For the compound $[\text{Rh}_2(\text{O}_2\text{CC}(\text{CH}_3)_3)_n(\text{HNOCC}(\text{CH}_3)_3)_{4-n}]$ the five possible species have masses of 607, 608, 609, 610, and 611 m/e. The mass spectrum obtained for this mixture shows a set of peaks in the region 607-611 m/e which can with reasonable certainty be assigned to the five species present in the mixture (Figure 4.2). This technique was unsuccessful for the mixtures containing butyramide and propanamide ligands.

Initial electrochemical studies of these series of compounds gave inconsistent results. It was decided that these were probably due to variations in the axial ligation and in order to overcome this problem the bispyridine adduct of each series was prepared by stirring the crude product in a methanol/pyridine mixture.

4.3 Electrochemical Investigation.

4.3.1 Results.

The electrochemical behaviour of four mixtures with the general formula $[\text{Rh}_2(\text{O}_2\text{CR})_n(\text{HNOCR}'')_{4-n}(\text{C}_5\text{H}_5\text{N})_2]$ ($\text{R}=\text{CH}_3, \text{C}(\text{CH}_3)_3$; $\text{R}''=\text{C}_2\text{H}_5, \text{C}_3\text{H}_7, \text{C}(\text{CH}_3)_3$, $n=0,1,2,3,4$) have been studied in acetonitrile (0.1 M TBABF₄ supporting electrolyte) using cyclic and a.c. voltammetric techniques. Between three and five oxidation processes are observed for each sample in the potential range +1.8 V to -1.8 V. For the mixtures where $\text{R}=\text{CH}_3$ and $\text{R}''=\text{C}_2\text{H}_5$ or $\text{C}(\text{CH}_3)_3$ four

Figure 4.1 Mass spectrum of $[\text{Rh}_2(\text{O}_2\text{CCH}_3)_n(\text{HNOCC}(\text{CH}_3)_3)_{4-n}]$.Figure 4.2 Mass spectrum of $[\text{Rh}_2(\text{O}_2\text{CC}(\text{CH}_3)_3)_n(\text{HNOCC}(\text{CH}_3)_3)_{4-n}]$.

evenly spaced quasireversible oxidations are observed, while for $R=CH_3$, $R''=C_3H_7$, three quasireversible processes are observed. For the mixture where $R=R''=C(CH_3)_3$, five quasireversible oxidation processes can be identified (Figure 4.3). The difference in half-wave potential for each pair of peaks is approximately 250 mV for the compounds prepared from $[Rh_2(O_2CCH_3)_4(CH_3OH)_2]$ and 200 mV for the compound prepared from $[Rh_2(O_2CC(CH_3)_3)_4]$.

The addition of $[Rh_2(O_2CCH_3)_4(C_5H_5N)_2]$ to the electrochemical cell for the mixtures where $R=CH_3$ results in the appearance of an additional oxidation process at a half-wave potential of +1.16 V. The addition of $[Rh_2(O_2C(CH_3)_3)_4(C_5H_5N)_2]$ to the electrochemical cell containing the mixture $[Rh_2(O_2CC(CH_3)_3)_n(HNOCC(CH_3)_3)_{4-n}(C_5H_5N)_2]$ causes an increase in the peak current of the oxidation process at $E_{1/2}=1.04$ V. Previous work has shown that for compounds with the general formula $[Rh_2(O_2CR)_n(HNOCR'')_{4-n}L_2]$, the half-wave potential for the oxidation of the compound becomes less positive as n decreases^{74,77,78}. This observation coupled with the results given above allows the assignment of oxidation processes to individual species, these assignments are presented in Table 4.3. A total cathodic shift of between 880 mV and 940 mV is observed in the half-wave potential on changing from four bridging acetate ligands to four bridging amidate ligands. On changing from four pivalate bridging ligands to four bridging trimethylacetamidate ligands a shift of 800 mV is observed. This last value probably gives the best indication of the effect of replacing four carboxylate ligands with four amidate ligands since there is no change in the substituent group attached to the carbon atom of the ligand bridge. The species $[Rh_2(HNOCC(CH_3)_3)_4(C_5H_5N)_2]$ has been prepared by two different routes and slightly different half-wave potentials for the oxidation of this species have been observed (0.22 and 0.24 V). This difference is probable due to slight differences in the

Figure 4.3 A.C. voltammograms for the oxidation of
 $[\text{Rh}_2(\text{O}_2\text{CR})_n(\text{R}'\text{NOCR}'')_{4-n}(\text{C}_5\text{H}_5\text{N})_2]$ in acetonitrile
 (0.1 M TBABF₄ supporting electrolyte)

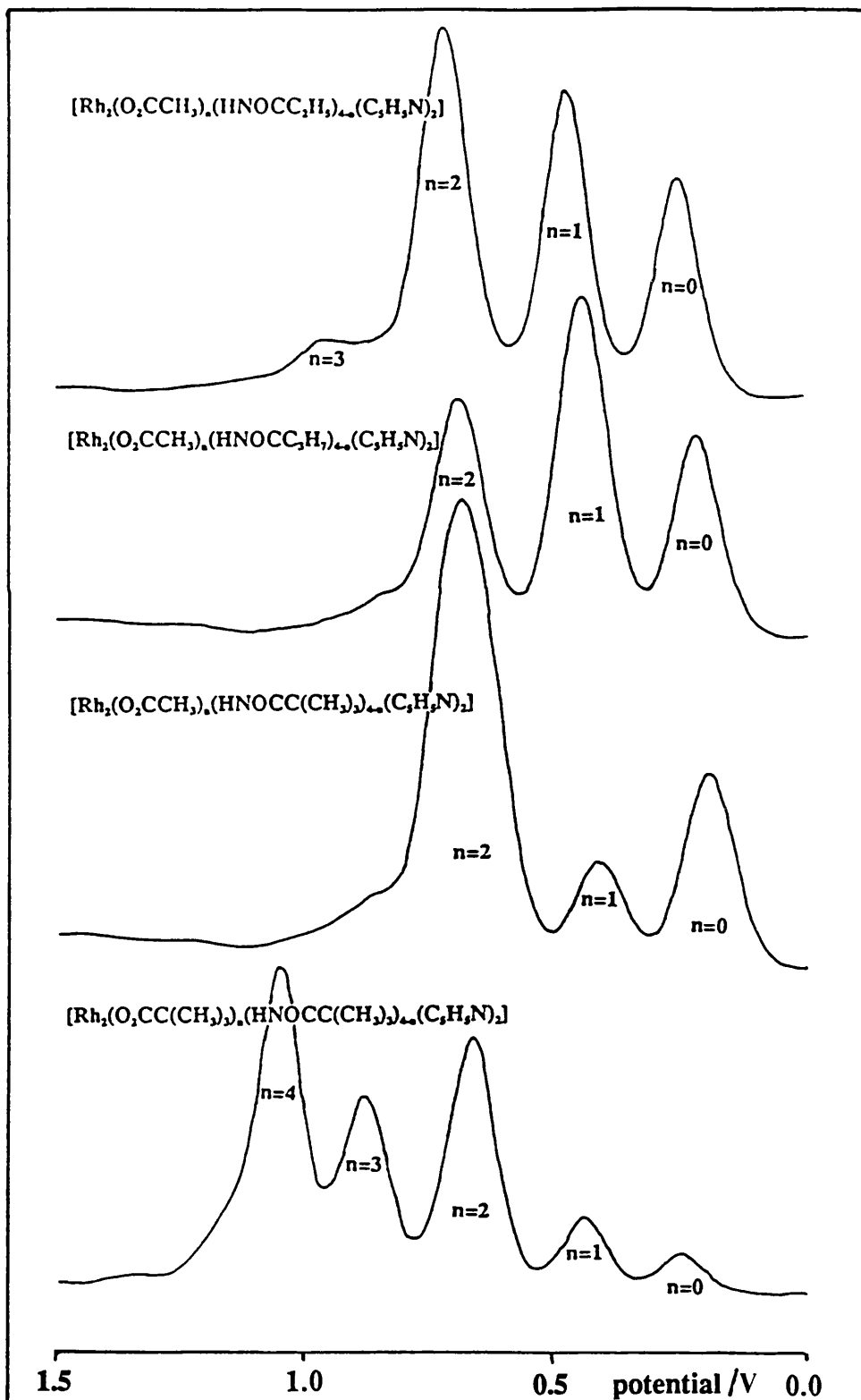


Table 4.3 Electrochemical results for the compounds $[\text{Rh}_2(\text{O}_2\text{CR})_n(\text{R}'\text{NOCR}'')_{4-n}(\text{C}_3\text{H}_5\text{N})_2]$ recorded in acetonitrile (0.1 M TBABF₄ supporting electrolyte) and the appropriate Taft parameters given in parenthesis.

Compound.	n=0		n=1		n=2		n=3		n=4	
	$E_{1/2}^a$	($4\sigma^{*b}$)	$E_{1/2}^a$	($4\sigma^{*b}$)	$E_{1/2}^a$	($4\sigma^{*b}$)	$E_{1/2}^a$	($4\sigma^{*b}$)	$E_{1/2}^a$	($4\sigma^{*b}$)
$[\text{Rh}_2(\text{O}_2\text{CCH}_2)_n(\text{HNOCC}_2\text{H}_5)_{4-n}(\text{C}_3\text{H}_5\text{N})_2]$	0.28	(-0.40)	0.50	(-0.30)	0.74	(-0.20)	0.98	(-0.10)	1.16	(0.00)
$[\text{Rh}_2(\text{O}_2\text{CCH}_2)_n(\text{HNOCC}_3\text{H}_7)_{4-n}(\text{C}_3\text{H}_5\text{N})_2]$	0.26	(-0.46)	0.48	(-0.345)	0.73	(-0.23)	-	(-0.115)	1.16	(0.00)
$[\text{Rh}_2(\text{O}_2\text{CCH}_2)_n(\text{HNOCC}(\text{CH}_3)_3)_{4-n}(\text{C}_3\text{H}_5\text{N})_2]$	0.22	(-1.20)	0.44	(-0.90)	0.72	(-0.60)	0.96	(-0.30)	1.16	(0.00)
$[\text{Rh}_2(\text{O}_2\text{CC}(\text{CH}_3)_3)_n(\text{HNOCC}(\text{CH}_3)_3)_{4-n}(\text{C}_3\text{H}_5\text{N})_2]$	0.24	(-1.20)	0.43	(-1.20)	0.67	(-1.20)	0.86	(-1.20)	1.04	(-1.20)

a) Half-wave potentials given in V vs Ag/AgCl.

b) $4\sigma^*$ is equal to the sum of the appropriate Taft parameters.

electrochemical cell conditions, but the possibility of different isomers or isomer mixtures being present cannot be ruled out.

It is not possible to say unequivocally that these reactions are one-electron in nature because the exact composition of the mixtures is not known. Previous results suggest that this is likely however, and that the reactions can probably be assigned to Equation 4.1



4.3.3 Electrochemical behaviour - A rationalisation.

The results obtained here indicate that on changing the four bridging ligands co-ordinated to the dirhodium(II/II) unit from a ligand containing two oxygen donor atoms to a ligand containing one oxygen and one nitrogen donor atom, a shift to more negative potential of approximately 900 mV is observed in the half-wave potential for the oxidation of the compound. The trend in oxidation potential suggests an increase in the ease of oxidation and points to an increase in the energy of the orbital from which the electron is removed, the HOMO (this will be the π^* or the δ^* anti-bonding orbital depending on which is higher in energy), upon the substitution of carboxylate ligands by amidate ligands. This observation is in agreement with previous results for tetrakis(amidato)dirhodium(II/II) compounds^{70,74,76-78}.

This study, like the two previously reported^{74,77,78}, has examined series of compounds with the general formula $[\text{Rh}_2(\text{O}_2\text{CR})_n(\text{R}'\text{NOCR}'')_{4-n}\text{L}_2]$. For each of the four series of compounds studied a linear relationship is observed between

the half-wave potential and the value of n . This is illustrated in Figure 4.4. A variation in the gradient of these graphs on changing the solvent used for the electrochemical experiment has been reported^{74,77,78}, leading to the suggestion that the relationship between the half-wave potential of the oxidation process and the number of acetate/amidate ligands is dependent on the solvent used, as discussed in Section 4.1. The results obtained here indicate that the relationship between the half-wave potential and the number of acetate/amidate ligands are present is also dependent on the identity of the substituent groups R, R' and R''. It is found that when R=CH₃, the gradient becomes more positive as the electron donating ability of the substituent group increases. The variation in gradient is small but, suggests that the effect of the electron donating/withdrawing ability on the ease of oxidation, should be investigated further.

Taft parameters are used as a measure of the electron donating/withdrawing ability of a substituent group (see Appendix 2). Graphs of half-wave potential against the sum of the appropriate Taft parameters (Table A2.1) for three of the four compounds studied are presented in Figure 4.5. A linear relationship is observed for each compound suggesting a direct relationship between the half-wave potential of the oxidation and the electron donating ability of the substituent group attached to the carbon atom of the bridging ligands. A direct comparison of the results obtained here with those reported previously is complicated by the use of different reference systems and electrolytes and by the use of different axial ligands and solvents. The results obtained by Bear, Kadish *et al.*⁷⁴ for the compound $[\text{Rh}_2(\text{O}_2\text{CCH}_3)_n(\text{C}_6\text{H}_5\text{NOCCH}_3)_{4-n}]$ in dichloromethane and DMSO have been plotted against the appropriate Taft parameters. The graphs obtained are illustrated in Figure 4.6. As in this study approximately linear correlations are observed.

Figure 4.4 Plot of $E_{1/2}$ /V (vs Ag/AgCl) vs. n for the oxidation of the compounds $[\text{Rh}_2(\text{O}_2\text{CR})_n(\text{R}'\text{NOCR}'')_{4-n}(\text{C}_5\text{H}_5\text{N})_2]$ in acetonitrile (0.1 M TBABF₄ supporting electrolyte) a) R=CH₃,R''=C₂H₅; b) R=CH₃,R''=C₃H₇; c) R=CH₃,R''=C(CH₃)₃ and d) R=R''=C(CH₃)₃.

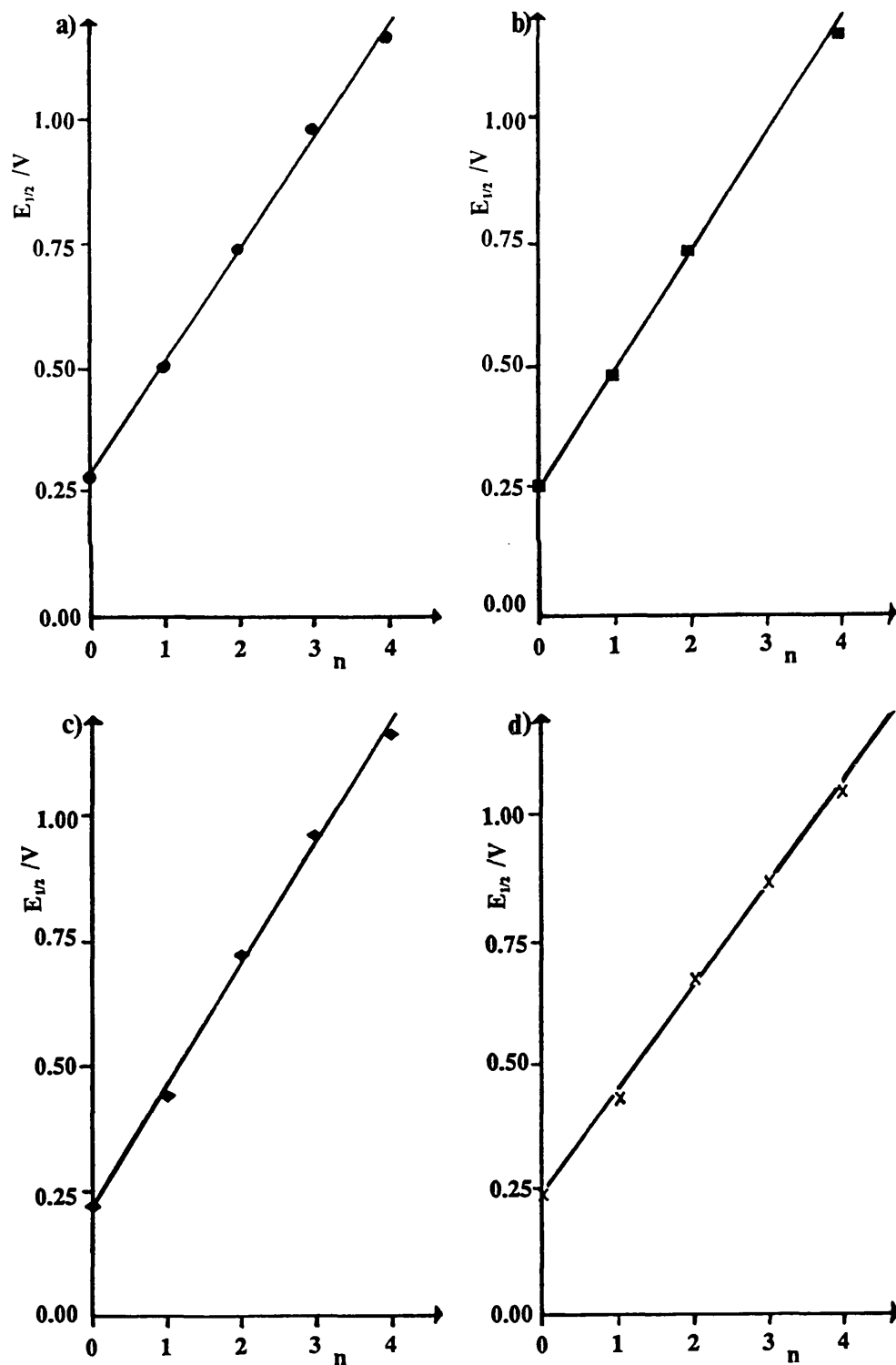


Figure 4.5 Plot of $E_{1/2}$ /V (vs Ag/AgCl) vs. $4\sigma^*$ for the oxidation of the compounds $[\text{Rh}_2(\text{O}_2\text{CR})_n(\text{R}'\text{NOCR}'')_{4-n}(\text{C}_5\text{H}_5\text{N})_2]$ in acetonitrile (0.1 M TBABF₄ supporting electrolyte) a) $\text{R}=\text{CH}_3, \text{R}''=\text{C}_2\text{H}_5$ (●); b) $\text{R}=\text{CH}_3, \text{R}''=\text{C}_3\text{H}_7$ (■); and c) $\text{R}=\text{CH}_3, \text{R}''=\text{C}(\text{CH}_3)_3$ (◆).

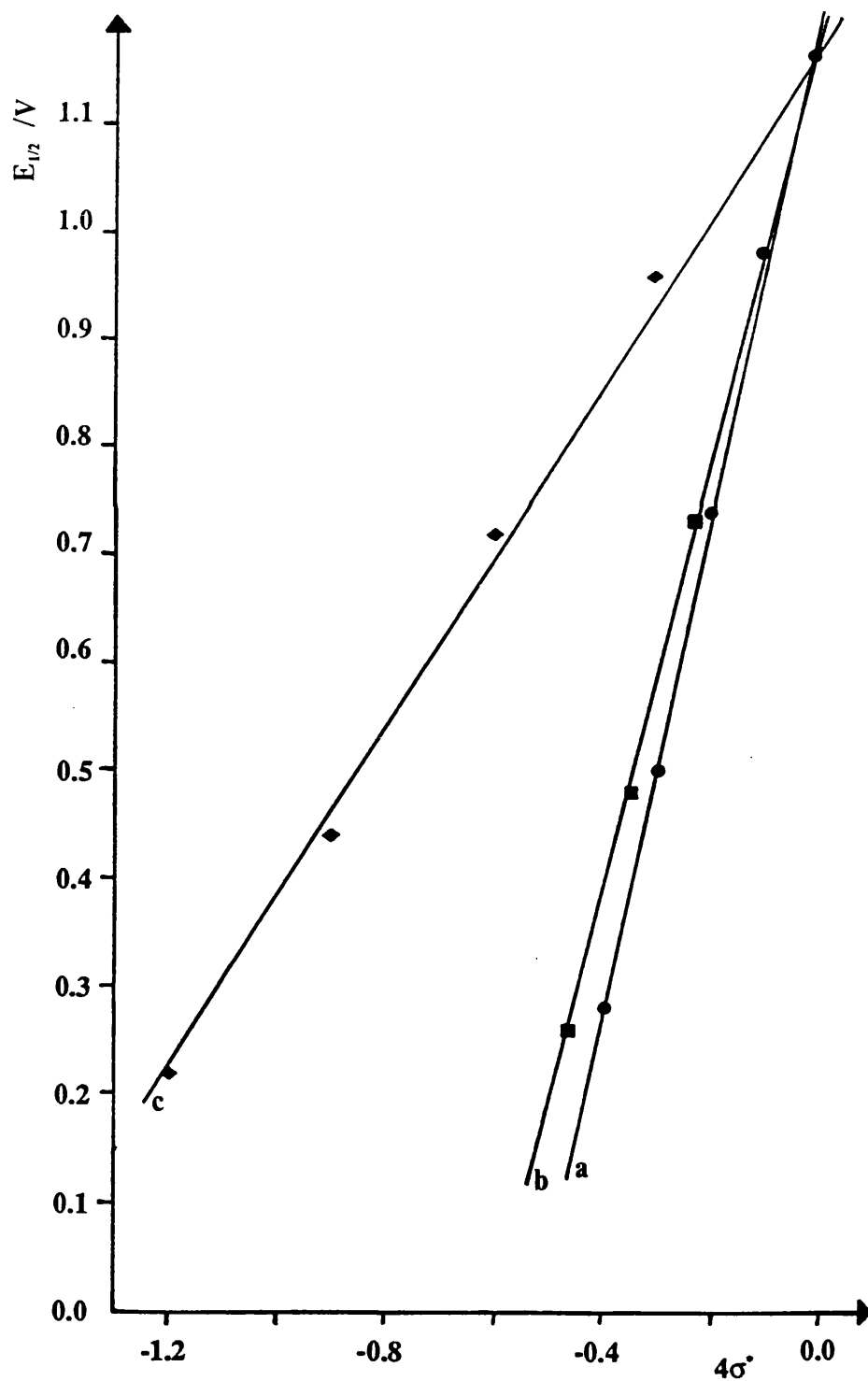
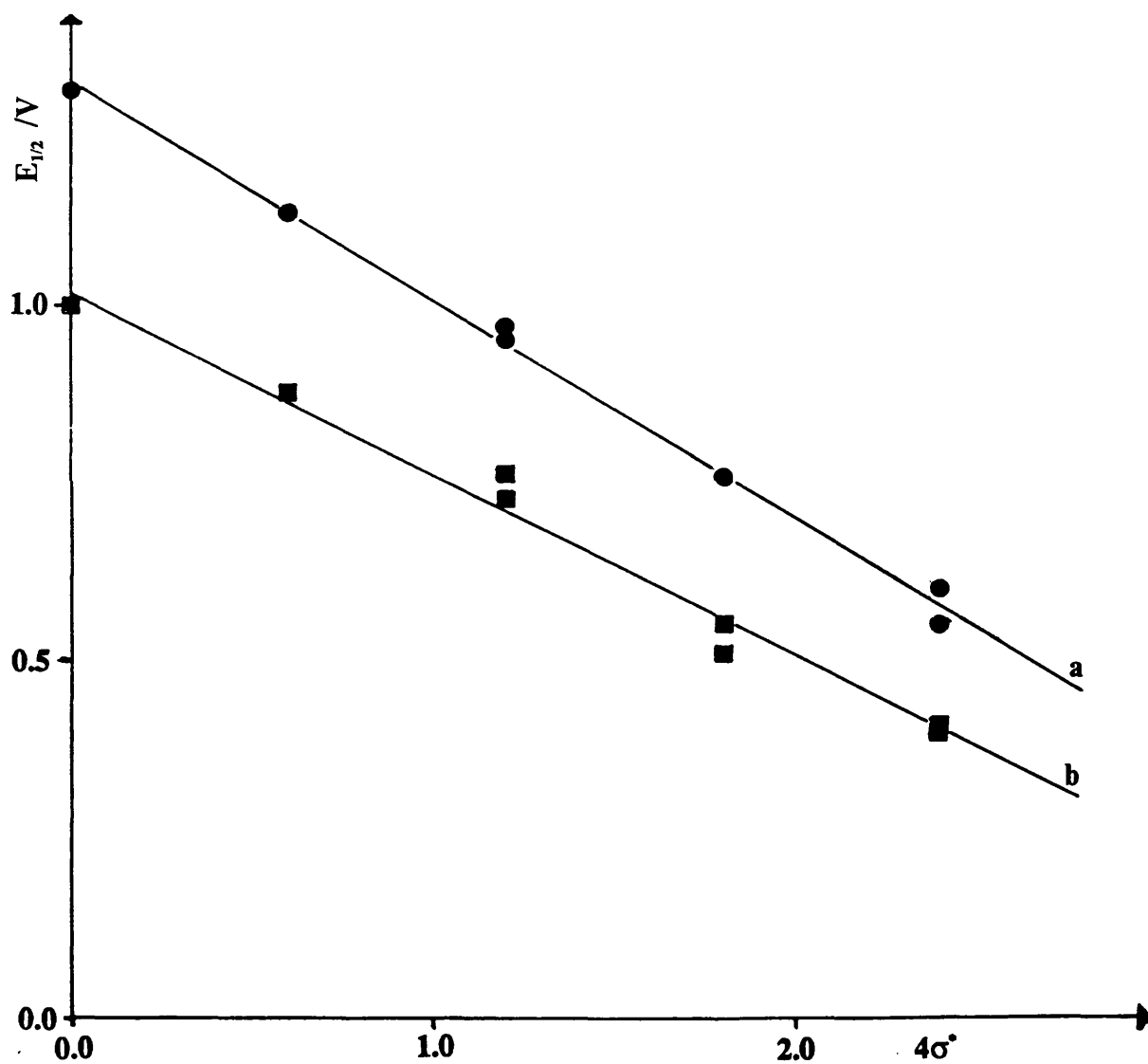


Figure 4.6 Plot of $E_{1/2}$ /V (vs S.C.E.) vs. $4\sigma'$ for the oxidation of the compounds $[\text{Rh}_2(\text{O}_2\text{CCH}_3)_n(\text{C}_6\text{H}_5\text{NOCCH}_3)_{4-n}]$ in a) CH_2Cl_2 (●) and b) DMSO (■) (0.1 M TBAP supporting electrolyte).



A more interesting use of these results is to examine the behaviour of each species (eg $n=2$) across a range of different amidate ligands. Using the graph discussed above a linear relationship is observed between the half-wave potential of the oxidation for each different metal amidate complex and the sum of the appropriate Taft parameters. This linear relationship is observed for each value of n . To a reasonable approximation a straight line with the same gradient can be drawn through each set of data as illustrated in Figure 4.7 (although for $n=3,4$ there is insufficient data for accurate results to be obtained and these two examples can only be considered in the broadest qualitative sense). These graphs indicate that the effect of the substituent groups on the ease of oxidation is very similar for each value of n . This strongly suggests that the extent to which the electron donating/withdrawing ability of a substituent group effects oxidation potential of this type of tetrabridged dirhodium(II/II) compound is approximately the same whether the substituent is attached to the carbon atom of a carboxylate bridging ligand, or the carbon atom of an amidate bridging ligand.

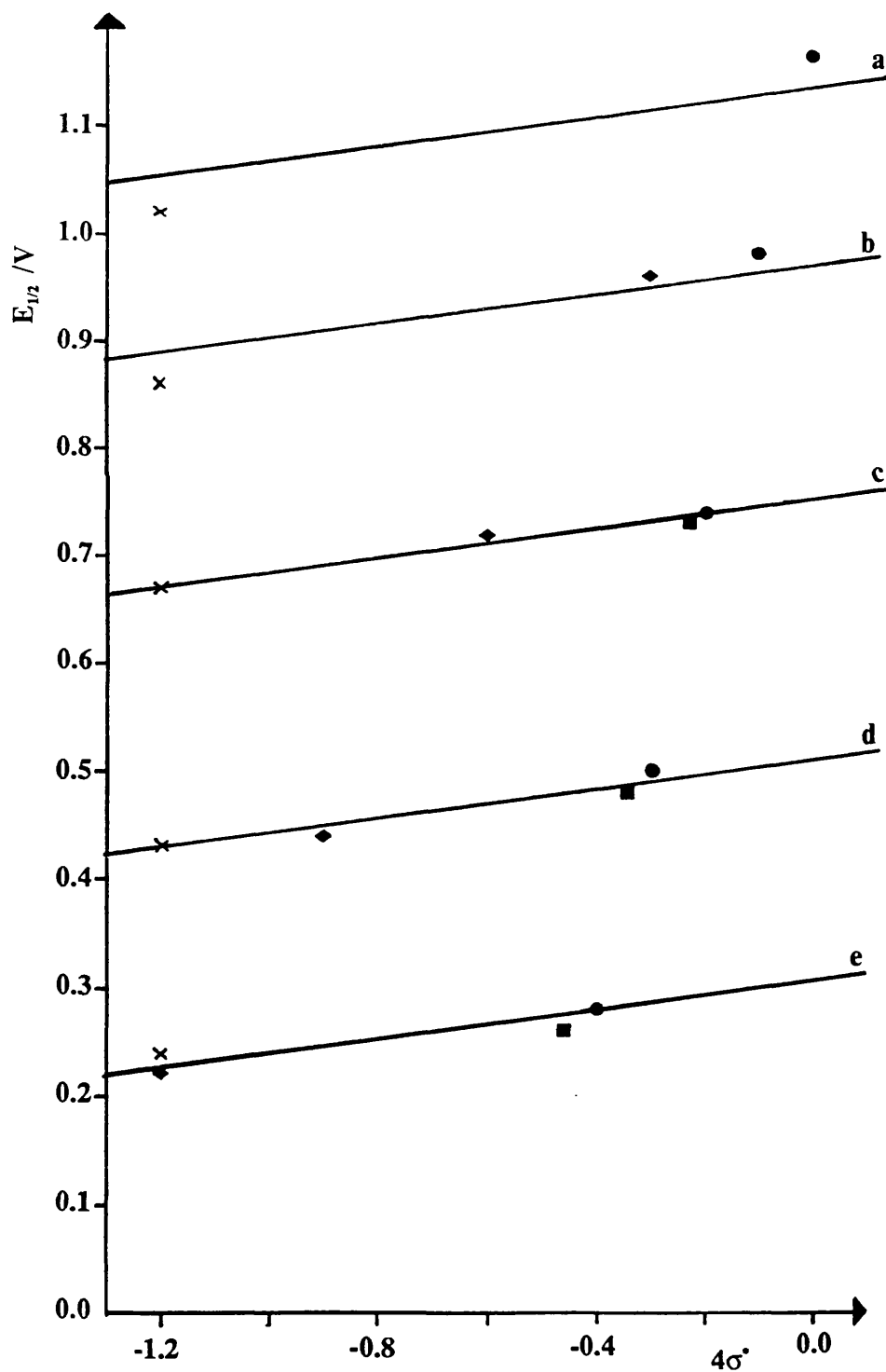
The above results, coupled with the shift in the oxidation potential of approximately 800 mV on changing the bridging ligands from four carboxylate to four amidate ligands, are consistent with the electronic effect of the substituent group attached to the carbon atom of the bridging ligand being small in comparison with changes in the donor atoms themselves.

4.4 Conclusions.

The stepwise exchange of carboxylate ligands for amidate ligands in compounds of the type $[\text{Rh}_2(\text{O}_2\text{CR})_n(\text{R}'\text{NOCR}'')_{4-n}]$ causes a stepwise cathodic shift

Figure 4.7 Plot of $E_{1/2}$ /V (vs Ag/AgCl) vs. $4\sigma^*$ for the oxidation of the compounds $[\text{Rh}_2(\text{O}_2\text{CR})_n(\text{R}'\text{NOCR}'')_{4-n}(\text{C}_5\text{H}_5\text{N})_2]$ $\text{R}=\text{CH}_3, \text{R}''=\text{C}_2\text{H}_5$ (●); $\text{R}=\text{CH}_3, \text{R}''=\text{C}_3\text{H}_7$ (■); $\text{R}=\text{CH}_3, \text{R}''=\text{C}(\text{CH}_3)_3$ (◆) and $\text{R}=\text{R}''=\text{C}(\text{CH}_3)_3$ (×) in acetonitrile (0.1 M TBABF₄ supporting electrolyte)

a) $n=4$; b) $n=3$; c) $n=2$; d) $n=1$; e) $n=0$.



in the half-wave potential observed for the oxidation of the dirhodium unit. This shift in the redox potential has been found to be dependent on the electron donating/withdrawing ability of the substituent groups R and R''. It has been observed that the substituent groups R and R'' effect the half-wave potential observed to a similar extent and that this effect is small compared to the effect of changing the donor atoms on each bridging ligand from two oxygen atoms to one of an oxygen atom and a nitrogen atom.

4.5 Experimental.

4.5.1 Materials and Instrumentation.

Materials and instrumentation used are as described in Section 2.5.1.

Rhodium trichloride was received on loan from Johnson Matthey plc.

4.5.2 Synthesis of $[\text{Rh}_2(\text{O}_2\text{CCH}_3)_4(\text{CH}_3\text{OH})_2]$.

The compound $[\text{Rh}_2(\text{O}_2\text{CCH}_3)_4(\text{CH}_3\text{OH})_2]$ was prepared by the method previously reported by Wilkinson et. al.¹⁰⁸.

4.5.3 Synthesis of $[\text{Rh}_2(\text{O}_2\text{CC}(\text{CH}_3)_3)_4]$.

$[\text{Rh}_2(\text{O}_2\text{CCH}_3)_4(\text{CH}_3\text{OH})_2]$ (0.2764 g; 0.55 mMol) was refluxed in trimethylacetic acid (3 cm³) for 4 hours under a dinitrogen atmosphere. The trimethylacetic acid was removed under reduced pressure at 70 °C to yield the final pale green product.

4.5.4 Synthesis of $[\text{Rh}_2(\text{O}_2\text{CCH}_3)_4(\text{HNOCC}_2\text{H}_5)_4]$.[§]

$[\text{Rh}_2(\text{O}_2\text{CCH}_3)_4(\text{CH}_3\text{OH})_2]$ (0.1500 g; 0.30 mMol) was stirred with $\text{H}_2\text{NOCC}_2\text{H}_5$ (1.0 g; excess) at 100 °C for 16 hours under a dinitrogen atmosphere.

§ Due to ambiguities in the exact proportions of each component in the product mixtures yields and microanalytical data are not quoted. The general procedure described normally results in near quantitative yields. There is no reason why this should not be true in this study.

The excess ligand was removed by vacuum sublimation at 100 °C onto a water cooled cold finger.

4.5.5 Synthesis of $[\text{Rh}_2(\text{O}_2\text{CCH}_3)_4(\text{HNOCC}_3\text{H}_7)_4]^\text{s}$

$[\text{Rh}_2(\text{O}_2\text{CCH}_3)_4(\text{CH}_3\text{OH})_2]$ (0.3448 g; 0.68 mMol) was stirred with $\text{H}_2\text{NOCC}_3\text{H}_7$ (2.0 g; excess) at 125 °C for 20 hours under a dinitrogen atmosphere. The excess ligand was removed by vacuum sublimation at 125 °C onto a water cooled cold finger. The product was dissolved in dichloromethane (10 cm³) and a solid residue (product A; $[\text{Rh}_2(\text{O}_2\text{CCH}_3)_4(\text{HNOCC}_3\text{H}_7)_2]$) was filtered off and air dried for two hours. The volume of dichloromethane was reduced to 5 cm³ under reduced pressure and diethyl ether (10 cm³) was added to precipitate product B which was filtered off and air dried for 2 hours.

4.5.6 Synthesis of $[\text{Rh}_2(\text{O}_2\text{CCH}_3)_4(\text{HNOCC}(\text{CH}_3)_3)_4]^\text{s}$

$[\text{Rh}_2(\text{O}_2\text{CCH}_3)_4(\text{CH}_3\text{OH})_2]$ (0.2135 g; 0.42 mMol) was stirred with $\text{H}_2\text{NOCC}(\text{CH}_3)_3$ (1.0 g; excess) at 160 °C for 25 hours under a dinitrogen atmosphere. The excess ligand was removed by vacuum sublimation at 160 °C onto a water cooled cold finger. The procedure was repeated using fresh ligand.

4.5.7 Synthesis of $[\text{Rh}_2(\text{O}_2\text{CCH}_3)_4(\text{HNOCC}(\text{CH}_3)_3)_4]^\text{s}$

$[\text{Rh}_2(\text{O}_2\text{CCH}_3)_4(\text{CH}_3\text{OH})_2]$ (0.1430 g; 0.23 mMol) was stirred with $\text{H}_2\text{NOCC}(\text{CH}_3)_3$ (1.0 g; excess) at 160 °C for 15 hours under a dinitrogen atmosphere. The excess ligand was removed by vacuum sublimation at 160 °C

onto a water-cooled cold finger. The procedure was repeated using fresh ligand. The product was dissolved in diethyl ether (10 cm³) and a solid residue (excess ligand) was filtered off. The diethyl ether was then removed under reduced pressure.

4.5.8 Synthesis of bispyridine adducts.

To ensure that the electrochemical results were not affected by variations in axial ligation the bispyridine adducts of each series of compounds were prepared using the following method. $[\text{Rh}_2(\text{O}_2\text{CR})_n(\text{HNOCR}'')_{4-n}]$ (0.05 g approximate) was stirred in methanol containing pyridine (0.01ml; excess) for one hour. The methanol and excess pyridine were removed under reduced pressure to yield the final product.

Chapter Five.

**A Synthetic and Structural Investigation
into the Compounds**



5.1	Introduction.	154
5.2	Preparation and characterisation.	155
5.3	Structural investigations of $[\text{Rh}_2(\text{O}_2\text{CR})_2(\text{CF}_3\text{COCHCOCF}_3)_2(\text{C}_5\text{H}_5\text{N})_2]$.	163
5.4	Investigation of the <i>cis</i> and <i>trans</i> isomers of $[\text{Rh}_2(\text{O}_2\text{CR})_2(\text{CF}_3\text{COCHCOCH}_3)_2(\text{C}_5\text{H}_5\text{N})_2]$.	168
5.4.1	Separation and characterisation of the <i>cis</i> and <i>trans</i> isomers of the compound $[\text{Rh}_2(\text{O}_2\text{CCH}_3)_2(\text{CF}_3\text{COCHCOCH}_3)_2(\text{C}_5\text{H}_5\text{N})_2]$.	170
5.4.2	Structural investigation of the <i>cis</i> and <i>trans</i> isomers of the compound $[\text{Rh}_2(\text{O}_2\text{CCH}_3)_2(\text{CF}_3\text{COCHCOCH}_3)_2(\text{C}_5\text{H}_5\text{N})_2]$.	176
5.4.3	A rationalisation of the ^1H n.m.r. spectroscopic results and the solid state structures of the <i>cis</i> and <i>trans</i> isomers of $[\text{Rh}_2(\text{O}_2\text{CCH}_3)_2(\text{CF}_3\text{COCHCOCH}_3)_2(\text{C}_5\text{H}_5\text{N})_2]$.	183
5.5	Conclusions.	184
5.6	Experimental.	185
5.6.1	Materials and instrumentation.	185
5.6.2	Synthesis of $[\text{Rh}_2(\text{O}_2\text{CC}_2\text{H}_5)_4]$.	185
5.6.3	Synthesis of $[\text{Rh}_2(\text{O}_2\text{CCH}_3)_2(\text{CH}_3\text{COCHCOCH}_3)_2(\text{C}_5\text{H}_5\text{N})_2]$.	185
5.6.4	Synthesis of $[\text{Rh}_2(\text{O}_2\text{CCH}_3)_2(\text{CF}_3\text{COCHCOCH}_3)_2(\text{C}_5\text{H}_5\text{N})_2]$.	186

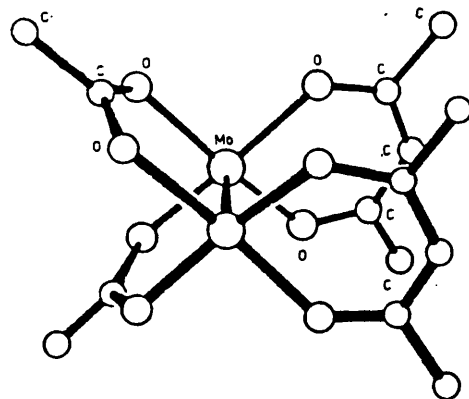
5.6.5	Separation of the <i>cis</i> and <i>trans</i> isomers of the compound [Rh ₂ (O ₂ CCH ₃) ₂ (CF ₃ COCHCOCH ₃) ₂ (C ₅ H ₅ N) ₂].	187
5.6.6	Synthesis of [Rh ₂ (O ₂ CCH ₃) ₂ (CF ₃ COCHCOCF ₃) ₂ (C ₅ H ₅ N) ₂].	189
5.6.7	Synthesis of [Rh ₂ (O ₂ CC ₂ H ₅) ₂ (CF ₃ COCHCOCH ₃) ₂ (C ₅ H ₅ N) ₂].	189
5.6.8	Synthesis of [Rh ₂ (O ₂ CC ₂ H ₅) ₂ (CF ₃ COCHCOCF ₃) ₂ (C ₅ H ₅ N) ₂].	191
5.6.9	Synthesis of [Rh ₂ (O ₂ CC(CH ₃) ₃) ₂ (CF ₃ COCHCOCH ₃) ₂ (C ₅ H ₅ N) ₂].	191
5.6.10	Synthesis of [Rh ₂ (O ₂ CC(CH ₃) ₃) ₂ (CF ₃ COCHCOCF ₃) ₂ (C ₅ H ₅ N) ₂].	192
5.6.11	The crystal structure determination of [Rh ₂ (O ₂ CCH ₃) ₂ (CF ₃ COCHCOCF ₃) ₂ (C ₅ H ₅ N) ₂].	193
5.6.12	The crystal structure determination of [Rh ₂ (O ₂ CC(CH ₃) ₃) ₂ (CF ₃ COCHCOCF ₃) ₂ (C ₅ H ₅ N) ₂].	194
5.6.13	The crystal structure determination of [<i>trans</i> -Rh ₂ (O ₂ CCH ₃) ₂ (CF ₃ COCHCOCH ₃) ₂ (C ₅ H ₅ N)].	194
5.6.14	The crystal structure determination of [<i>cis</i> -Rh ₂ (O ₂ CCH ₃) ₂ (CF ₃ COCHCOCH ₃) ₂ (C ₅ H ₅ N)0.5C ₅ H ₅ N].	195

5.1 Introduction.

The majority of the chemistry of dirhodium(II/II) compounds studied to date has concentrated on compounds containing four identical bridging ligands⁵⁸⁻⁸⁶. Interest has also been shown in compounds containing two different bridging ligands⁸⁷⁻⁹⁷ (Chapter 4) and compounds containing a combination of bridging and chelating ligands¹⁰⁹⁻¹¹³.

Dirhodium(II/II) compounds containing carboxylate and β -diketonate ligands were first reported in 1967¹⁰⁹. The compounds, $[\text{Rh}_2(\text{O}_2\text{CCH}_3)_2(\text{RCOCHCOR}')_2(\text{H}_2\text{O})_2]$ ($\text{R}, \text{R}' = \text{CH}_3, \text{CF}_3$), were each prepared as the aquo-adducts by refluxing $[\text{Rh}_2(\text{O}_2\text{CCH}_3)_4(\text{CH}_3\text{OH})_2]$ with an excess of the ligand or its sodium salt in water. The products were insoluble in water. The pyridine and substituted pyridine adducts were prepared by stirring the compounds in the appropriate ligand. Characterisation of these products by I.R., ^1H n.m.r., and ^{19}F n.m.r. spectroscopy indicated the presence of both carboxylate and β -diketonate ligands. Close examination of the ^1H n.m.r. spectroscopic results reveal that compounds containing the β -diketonate ligand $[\text{CH}_3\text{COCHCOCF}_3]^-$ existed as a mixture of *cis* and *trans* isomers. Several possible structures were discussed and it was suggested that the most likely structure was that containing a cisoid arrangement of carboxylate ligands with a chelating β -diketonate ligand co-ordinated to each rhodium ion and the axial rhodium sites occupied by neutral ligands.

The structure of an analogous dimolybdenum compound $[\text{Mo}_2(\text{O}_2\text{CCH}_3)_2(\text{CH}_3\text{COCHCOCH}_3)_2]$ (5.1) has been reported¹¹⁰ and is consistent with that suggested by Cenini *et. al.*¹⁰⁹. Four dirhodium compounds containing combinations of bridging and chelating ligands have previously been studied crystallographically, $[\text{Rh}_2(\text{O}_2\text{CCH}_3)_2(\text{DMG})_2(\text{P}(\text{C}_6\text{H}_5)_3)_2]$ ¹¹¹, $[\text{Rh}_2(\text{O}_2\text{CH})_2(\text{chel})_2\text{Cl}_2]$ ¹¹²



(5.1)

(chel = 1,10 phenanthroline) and $[\text{Rh}_2(\text{O}_2\text{CCH}_3)_2(\text{chel})_2(\text{L})_2](\text{ClO}_4)_2$ ¹¹³ (chel=3,4,7,8-tetramethylphenanthroline, 1,10-phenanthroline, 4,7-dimethylphenanthroline;

L=N-methylimidazole). These compounds have the same basic geometry, with the carboxylate groups in a cisoid arrangement and one chelating ligand co-ordinated to each metal ion.

This chapter will re-examine the work of Cenini *et. al.*¹⁰⁹. The original work has been repeated and extended to include a range of carboxylate ligands. The structures of several of these compounds will be discussed and the separation and characterisation of the *cis* and *trans* isomers of the compound $[\text{Rh}_2(\text{O}_2\text{CCH}_3)_2(\text{CH}_3\text{COCHCOCF}_3)_2(\text{C}_5\text{H}_5\text{N})_2]$ is reported.

5.2 Preparation and Characterisation.

Seven compounds have been prepared with the general composition $[\text{Rh}_2(\text{O}_2\text{CR})_2(\text{R}'\text{COCHCOCR}'')_2(\text{L})_2]$ (R=CH₃, C₂H₅, C(CH₃)₃; R', R''=CH₃, CF₃; L=C₅H₅N, H₂O not all possible combinations). The method of preparation employed involved refluxing the tetrakis(carboxylato)dirhodium(II/II) compound with an excess of the

β -diketone ($[\text{CH}_3\text{COCH}_2\text{COCF}_3]$, $[\text{CF}_3\text{COCH}_2\text{COCF}_3]$) or its sodium salt, $\text{Na}[\text{CH}_3\text{COCHCOCH}_3]$, in water or a water/ethanol mixture (1:1). The pyridine adducts were prepared by stirring the reaction residue in methanol with an excess of pyridine. The final product was precipitated from dichloromethane using n-hexane. Attempts to prepare the compounds $[\text{Rh}_2(\text{O}_2\text{CR})_2(\text{CH}_3\text{COCHCOCH}_3)_2(\text{C}_5\text{H}_5\text{N})_2]$ ($\text{R}=\text{C}_2\text{H}_5, \text{C}(\text{CH}_3)_3$) using the method described above proved unsuccessful.

Alternative solvents (acetone, methanol) were examined but in each case the starting materials were retrieved unchanged. The reactions of $[\text{Rh}_2(\text{O}_2\text{CC}(\text{CH}_3)_3)_4]$ with the ligands $\text{CF}_3\text{COCH}_2\text{COCH}_3$ and $\text{CF}_3\text{COCH}_2\text{COCF}_3$ resulted in the formation of two products. The first was isolated and found to be $[\text{Rh}_2(\text{O}_2\text{CC}(\text{CH}_3)_3)_4(\text{C}_5\text{H}_5\text{N})_2]$, the second product was found to have the desired composition.

Micro-analytical data (Table 5.4) indicate that the composition of each product is $[\text{Rh}_2(\text{O}_2\text{CR})_2(\text{R}'\text{COCHCOCR}'')_2(\text{C}_5\text{H}_5\text{N})_2]$ with two exceptions. Figures obtained for the compound where $\text{R}=\text{R}'=\text{R}''=\text{CH}_3$ show that this compound contains only one axial pyridine per dirhodium unit, while figures for the compound with $\text{R}=\text{C}_2\text{H}_5, \text{R}'=\text{CH}_3, \text{R}''=\text{CF}_3$ indicate the presence of one molecule of propanoic acid per binuclear molecule. These observations have been confirmed by ^1H n.m.r. spectroscopy.

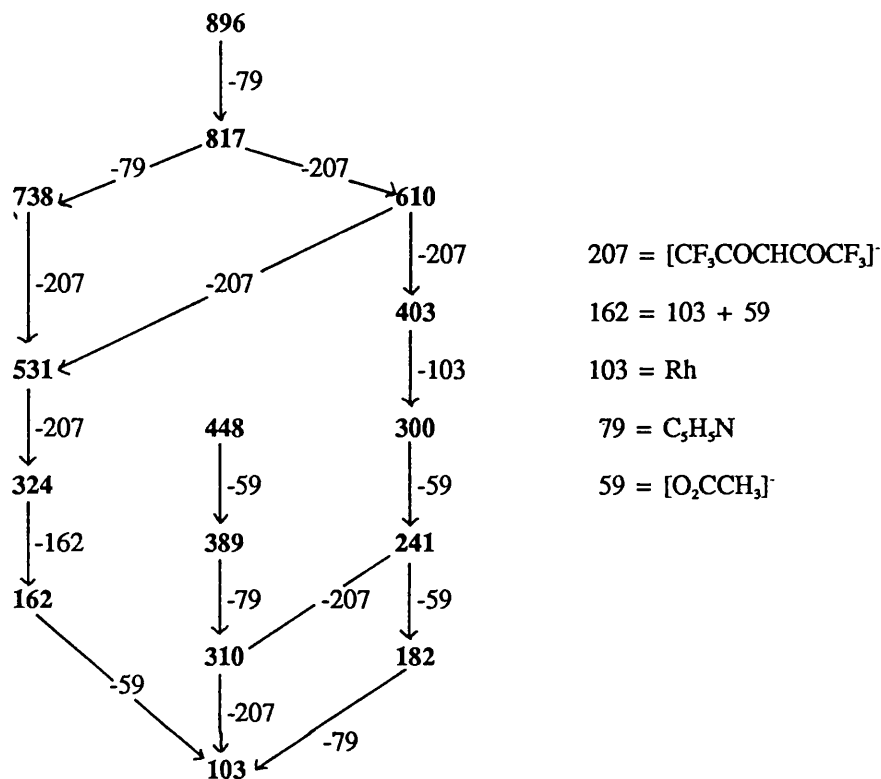
Infrared spectroscopic measurements made for each compound have confirmed the presence of both carboxylate and β -diketonate ligands. Tentative assignments of peaks due to the symmetric and asymmetric O-C-O stretches, the $\text{O}=\text{C}$ stretch in the β -diketonate ligand, the C-F stretch and the Rh-O stretch have been made with reference to assignments reported previously¹¹⁴⁻¹¹⁷ (Table 5.5).

Mass spectrometry results have been obtained using electron impact methods for all but one of the seven compounds prepared. The electron impact and

the fast atom bombardment methods were both found to be unsuccessful for the compound $[\text{Rh}_2(\text{O}_2\text{CCH}_3)_2(\text{CH}_3\text{COCHCOCH}_3)_2(\text{C}_5\text{H}_5\text{N})]$. The decay patterns observed for each compound reveal that the loss of one of the carboxylate bridges causes a considerable reduction in stability of the $[\text{Rh}_2]^{4+}$ unit resulting in the cleavage of the Rh-Rh bond and giving rise to peaks due to $[\text{Rh}(\text{R}'\text{COCHCOR}'')(\text{O}_2\text{CR})(\text{C}_5\text{H}_5\text{N})]^+$, $[\text{Rh}(\text{R}'\text{COCHCOCR}'')(\text{O}_2\text{CR})]^+$, and $[\text{Rh}(\text{O}_2\text{CR})(\text{C}_5\text{H}_5\text{N})]^+$ etc. The pyridine molecules are easily displaced and are often the first ligand to be lost. A selection of the mass spectra obtained indicating in detail some of the decay patterns observed are illustrated in Figure 5.1.

The ^1H n.m.r. spectrum recorded for each compound have confirmed the presence of both carboxylate and β -diketonate ligands in a 1:1 ratio. For example figure 5.2 illustrates the ^1H n.m.r. spectra obtained for the compound $[\text{Rh}_2(\text{O}_2\text{CCH}_3)_2(\text{CF}_3\text{COCHCOCF}_3)_2(\text{C}_5\text{H}_5\text{N})_2]$, the peak at 2.11 ppm is due to the six methyl protons of the acetate groups $[\text{O}_2\text{CCH}_3]^-$, the peak at 5.78 ppm is due to two γ -carbon protons of the β -diketonate ligands $[\text{CF}_3\text{COCHCOCF}_3]^-$. The triplets centred at 7.56 ppm [*meta* H] and 7.96 ppm [*para* H] and the doublet centred at 8.75 ppm [*ortho* H] are due to the pyridine protons. Integration is consistent with a ratio of 1:1:1 for the ligands. These measurements also highlight the existence of *cis* and *trans* isomers in compounds prepared using the $[\text{CF}_3\text{COCH}_2\text{COCH}_3]^-$ ligand (these will be discussed fully in section 5.4). The ^1H n.m.r. spectrum obtained for the compound $[\text{Rh}_2(\text{O}_2\text{CC}_2\text{H}_5)_2(\text{CF}_3\text{COCH}_2\text{COCH}_3)_2(\text{C}_5\text{H}_5\text{N})_2\cdot\text{C}_2\text{H}_5\text{CO}_2\text{H}]$ is illustrated in Figure 5.3. For the *cis* isomer two quartets (centred at 2.31 and 2.40 ppm) and two triplets (centred at 1.04 and 1.09 ppm) are observed which can be attributed to the propionate protons $[\text{C}_2\text{H}_5\text{CO}_2]^-$ while the singlets at 1.89 ppm and 5.45 ppm can be assigned to the protons of the β -diketonate ligands $[\text{CH}_3\text{COCHCOCF}_3]^-$ and $[\text{CH}_3\text{COCHCOCF}_3]^-$ respectively. For the *trans* isomer the quartet at 2.36 ppm, the

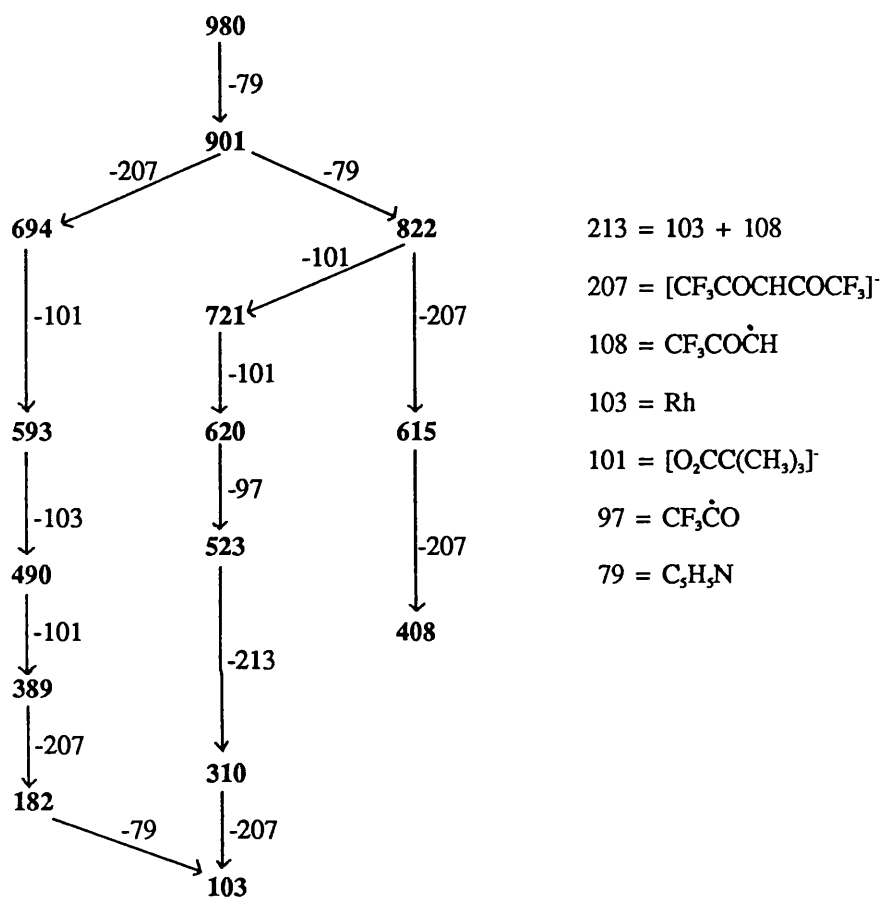
Figure 5.1a Some decay pathways observed in the mass spectrum of



$[\text{Rh}_2(\text{O}_2\text{CCH}_3)_2(\text{CF}_3\text{COCHCOCF}_3)_2(\text{C}_5\text{H}_5\text{N})_2]^+$	896 ^b
$[\text{Rh}_2(\text{O}_2\text{CCH}_3)_2(\text{CF}_3\text{COCHCOCF}_3)_2(\text{C}_5\text{H}_5\text{N})]^+$	817
$[\text{Rh}_2(\text{O}_2\text{CCH}_3)_2(\text{CF}_3\text{COCHCOCF}_3)_2]^+$	738
$[\text{Rh}(\text{O}_2\text{CCH}_3)(\text{CF}_3\text{COCHCOCF}_3)(\text{C}_5\text{H}_5\text{N})]^+$	448
$[\text{Rh}(\text{CF}_3\text{COCHCOCF}_3)(\text{C}_5\text{H}_5\text{N})]^+$	389
$[\text{Rh}(\text{CF}_3\text{COCHCOCF}_3)]^+$	310
$[\text{Rh}(\text{O}_2\text{CCH}_3)(\text{C}_5\text{H}_5\text{N})]^+$	241
$[\text{Rh}(\text{O}_2\text{CCH}_3)_2]^+$	221
$[\text{Rh}(\text{C}_5\text{H}_5\text{N})]^+$	182
$[\text{Rh}(\text{O}_2\text{CCH}_3)]^+$	162

- a) Mass spectrum illustrated on page 160.
 b) Not observed.

Figure 5.1b Some decay pathways observed in the mass spectrum of



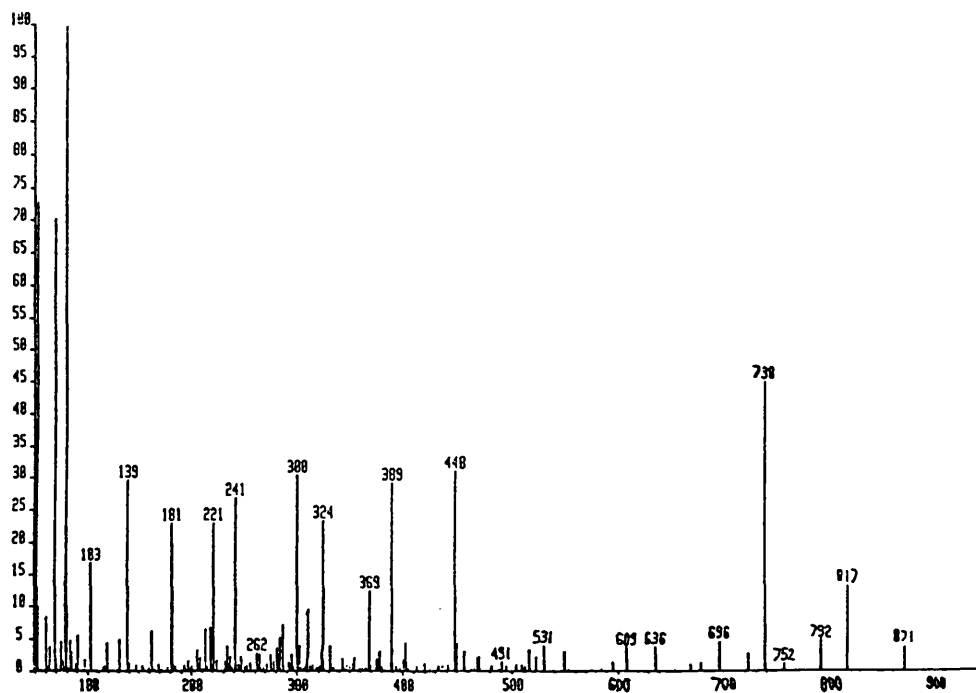
$[\text{Rh}_2(\text{O}_2\text{CC}(\text{CH}_3)_3)_2(\text{CF}_3\text{COCHCOCF}_3)_2(\text{C}_5\text{H}_5\text{N})_2]^+$	980
$[\text{Rh}_2(\text{O}_2\text{CC}(\text{CH}_3)_3)_2(\text{CF}_3\text{COCHCOCF}_3)_2(\text{C}_5\text{H}_5\text{N})]^+$	901
$[\text{Rh}_2(\text{O}_2\text{CC}(\text{CH}_3)_3)_2(\text{CF}_3\text{COCHCOCF}_3)_2]^+$	822
$[\text{Rh}(\text{O}_2\text{CC}(\text{CH}_3)_3)(\text{CF}_3\text{COCHCOCF}_3)(\text{C}_5\text{H}_5\text{N})]^+$	490
$[\text{Rh}(\text{CF}_3\text{COCHCOCF}_3)(\text{C}_5\text{H}_5\text{N})]^+$	389
$[\text{Rh}(\text{CF}_3\text{COCHCOCF}_3)]^+$	310
$[\text{Rh}(\text{C}_5\text{H}_5\text{N})]^+$	182

a) Mass spectrum illustrated on page 160.

Figure 5.1c Mass spectra of

a) $[\text{Rh}_2(\text{O}_2\text{CCH}_3)_2(\text{CF}_3\text{COCHCOCF}_3)_2(\text{C}_5\text{H}_5\text{N})_2]$ andb) $[\text{Rh}_2(\text{O}_2\text{CC}(\text{CH}_3)_3)_2(\text{CF}_3\text{COCHCOCF}_3)_2(\text{C}_5\text{H}_5\text{N})_2]$.

a)



b)

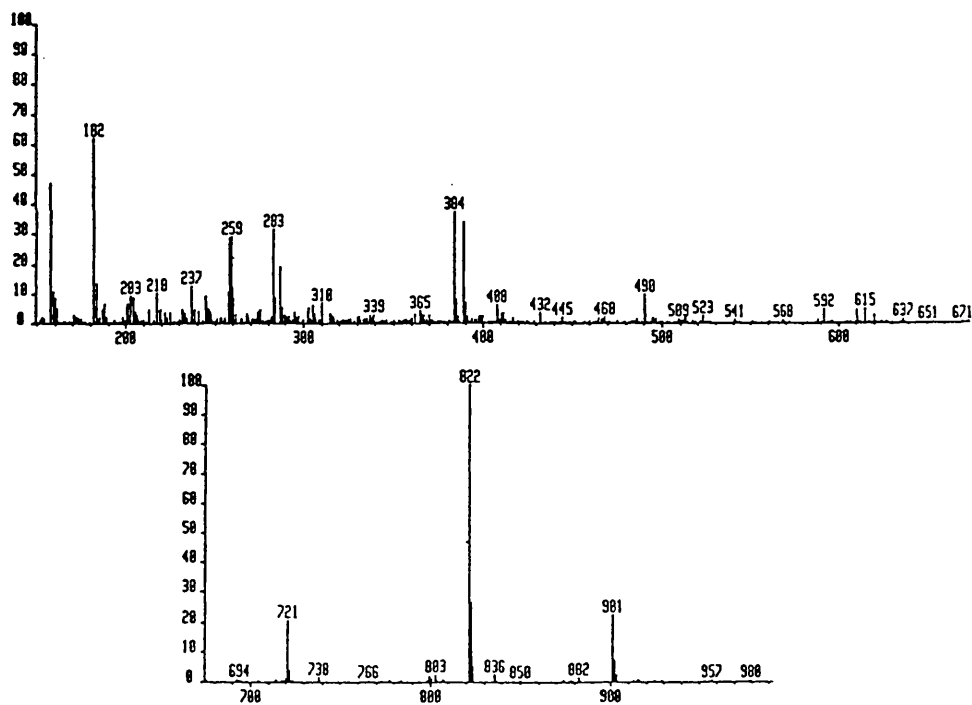


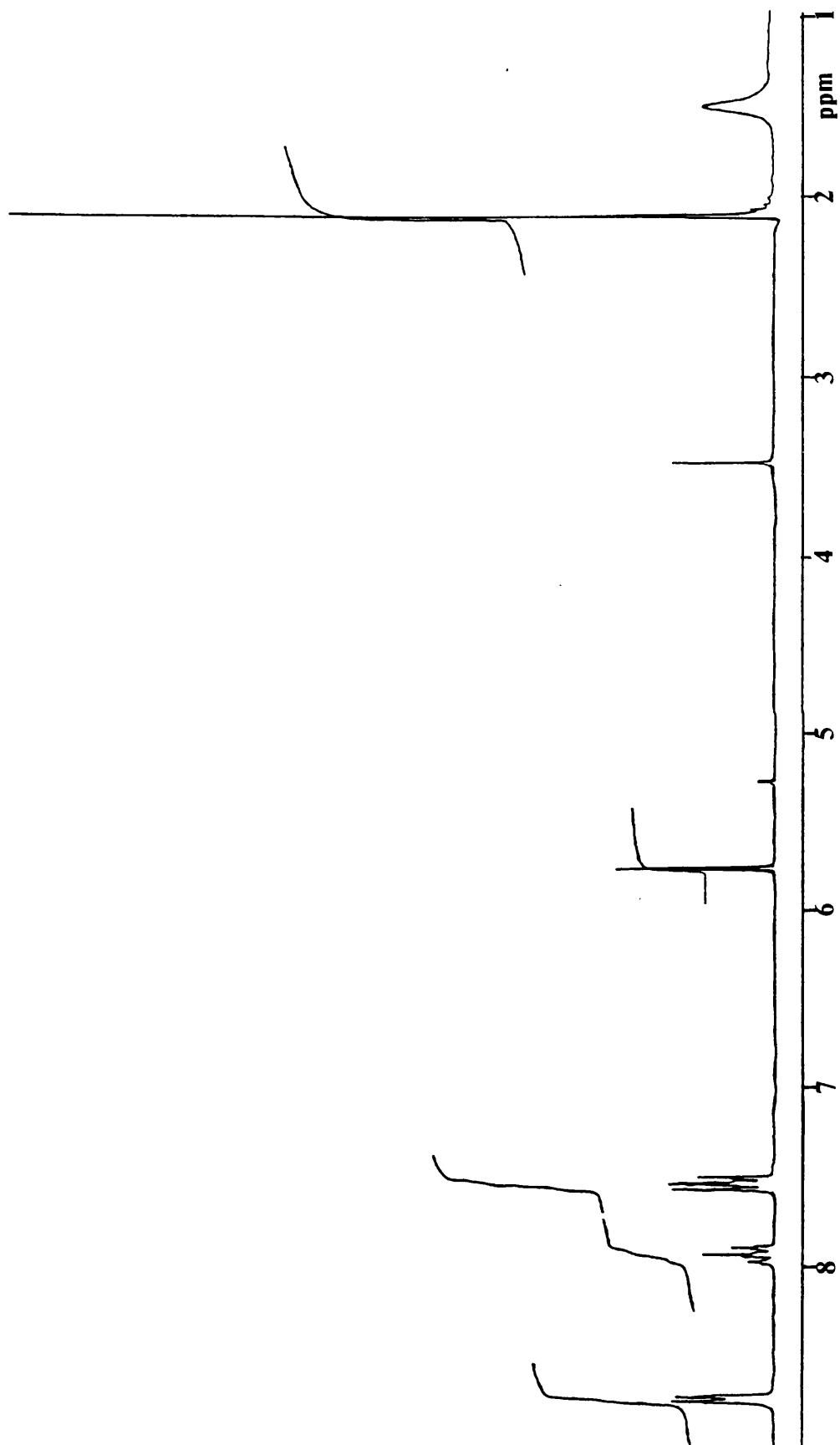
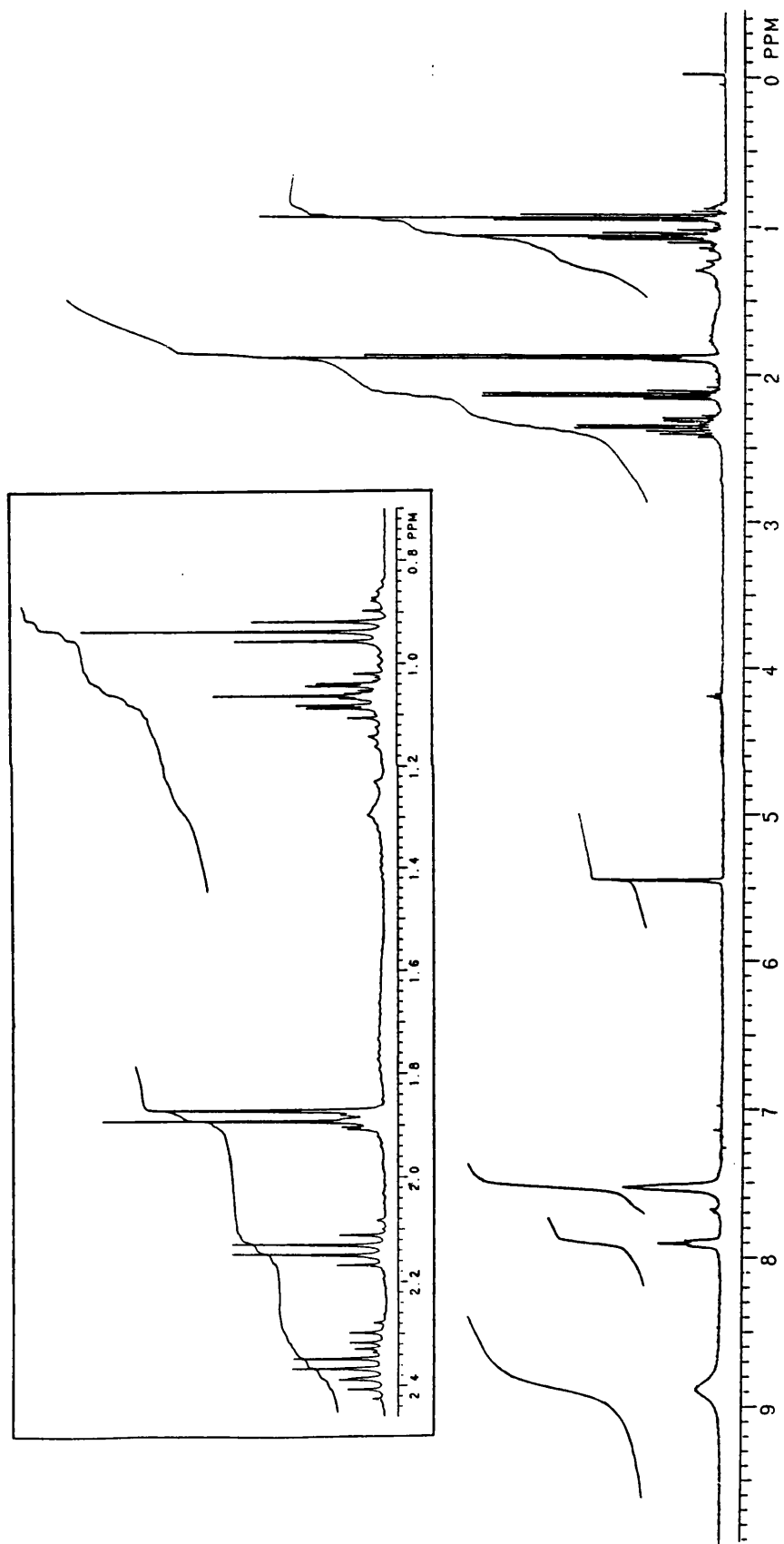
Figure 5.2 ^1H n.m.r. spectrum of $[\text{Rh}_2(\text{O}_2\text{CCH}_3)_2(\text{CF}_3\text{COCHCOCCF}_3)_2(\text{C}_5\text{H}_5\text{N})_2]$ 

Figure 5.3 ^1H n.m.r. spectrum of $[\text{Rh}_2(\text{O}_2\text{CC}_2\text{H}_5)_2(\text{CH}_3\text{COCHCOCCF}_3)_2(\text{C}_2\text{H}_5\text{N})_2]$.

triplet centred at 1.06 ppm and the singlets at 1.87 and 5.44 ppm can all be assigned on the same basis. The quartet at 2.14 ppm and the triplet at 0.94 ppm are due to the propanoic acid. Thus the propanoic acid is a solvent of crystallisation, rather than bound in any way to the dirhodium unit, which would have resulted in two sets of signals, one for each isomer.

^{19}F n.m.r. spectra were recorded where appropriate and a single peak was observed at approximately -75 ppm for compounds containing $[\text{CF}_3\text{COCHCOCF}_3]^-$ ligands. Two peaks are observed in a similar position, one for each isomer, for compounds containing $[\text{CF}_3\text{COCHCOCH}_3]^-$ ligands. Full spectroscopic results are given in section 5.6.

5.3 Structural Investigations of $[\text{Rh}_2(\text{O}_2\text{CR})_2(\text{CF}_3\text{COCHCOCF}_3)_2(\text{C}_5\text{H}_5\text{N})_2]$ ($\text{R}=\text{CH}_3, \text{C}(\text{CH}_3)_3$).

Crystals of $[\text{Rh}_2(\text{O}_2\text{CR})_2(\text{CF}_3\text{COCHCOCF}_3)_2(\text{C}_5\text{H}_5\text{N})_2]$

($\text{R}=\text{CH}_3$,¹¹⁸ $\text{C}(\text{CH}_3)_3$)[§] were obtained by slow evaporation of solutions of these compounds in 1:1 dichloromethane/n-hexane mixtures. Both crystals were red in colour and found to be suitable for x-ray crystallographic study. The two structures are essentially the same containing a $[\text{Rh}_2]^{4+}$ unit bridged by two carboxylate ligands in a cisoid arrangement. A chelating β -diketonate ligand is co-ordinated to each rhodium ion while the sites *trans* to the Rh-Rh bond are occupied by pyridine molecules. These results confirm the structure suggested by Cenini *et. al.* (Figures

§ The structure of $[\text{Rh}_2(\text{O}_2\text{CCH}_3)_2(\text{CF}_3\text{COCHCOCF}_3)_2(\text{C}_5\text{H}_5\text{N})_2]$ will be referred to as structure 5.1.

The structure of $[\text{Rh}_2(\text{O}_2\text{CC}(\text{CH}_3)_3)_2(\text{CF}_3\text{COCHCOCF}_3)_2(\text{C}_5\text{H}_5\text{N})_2]$ will be referred to as structure 5.2.

5.4a and 5.5a). Important bond lengths and angles for these two structures are presented in Table 5.1.

The Rh-Rh bond length observed for structure 5.1 (2.523(2) Å) is significantly longer than that observed in structure 5.2 (2.492(1) Å). These bond lengths are consistent with results reported previously for the compounds $[\text{Rh}_2(\text{O}_2\text{CCH}_3)_4(\text{H}_2\text{O})_2]^{20}$ and $[\text{Rh}_2(\text{O}_2\text{CC}(\text{CH}_3)_3)_4(\text{H}_2\text{O})_2]^{56}$ (2.3855(5) Å and 2.371(1) Å respectively). The source of these differences is most probable electronic in nature.

A comparison of the torsion angles observed about the Rh-Rh bond for structure 5.1 and 5.2 reveals that the β -diketonate ligands of structure 5.2 (O4-Rh1-Rh2-O8 24.3°; O1-Rh1-Rh2-O5 24.1°) are shifted from an eclipsed configuration by 10° more than those in structure 5.1 (O4-Rh1-Rh2-O8 14.2°; O1-Rh1-Rh2-O5 14.9°). This suggests greater steric interactions between the chelating ligands in the former case. The carboxylate groups are twisted by approximately 12° in structure 5.1 and 20° in structure 5.2 (Figures 5.4b and 5.5b).

The dihedral angle observed between the least squares planes defined by atoms Rh1-O1-C5-C6-C7-O4 and Rh2-O5-C10-C11-C12-O8 are 23.9° and 23.3° for structures 5.1 and 5.2 respectively such that the separation is greatest in the region of the $-\text{CF}_3$ substituent groups. These angles also imply considerable unfavourable steric interaction between the $-\text{CF}_3$ substituent groups on the two β -diketonate ligands. A bending of the N1-Rh1-Rh2-N2 axis, giving average Rh-Rh-N angles of 170.4[4]° for structure 5.1 and 174.5[2]° for structure 5.2, is observed with pyridine rings pushed towards the carboxylate ligands indicating that there are also repulsive forces between the β -diketonate ligands and the pyridine molecules (Figures 5.4c and 5.5c). Similar non-linearity is also observed other dirhodium(II/II) compounds containing bridging and chelating ligands, and compounds containing four bridging ligands. For example Rh-Rh-N interbond angles of 165.30(8)° and

Table 5.1 Structural data for $[\text{Rh}_2(\text{O}_2\text{CCH}_3)_2(\text{CF}_3\text{COCHCOCF}_3)_2(\text{C}_5\text{H}_5\text{N})_2]$ (5.1) and $[\text{Rh}_2(\text{O}_2\text{CC}(\text{CH}_3)_2)_2(\text{CF}_3\text{COCHCOCF}_3)_2(\text{C}_5\text{H}_5\text{N})_2]$ (5.2).

	Structure 5.1	structure 5.2
Rh-Rh	2.523(2) Å	2.492(1) Å
Rh-N	2.242[15] Å	2.233[7] Å
Rh-O carboxy. (av.)	2.022[16] Å	2.027[8] Å
Rh-O β-diket. (av.)	2.010[17] Å	2.008[8] Å
Rh1-Rh2-N1	170.6(3)°	174.5(1)°
Rh2-Rh1-N2	169.3(3)°	174.4(2)°
O-Rh-O carboxy. (av.)	91.1[6]°	92.4[3]°
O-Rh-O β-diket. (av.)	94.6[5]°	94.6[3]°
Av. torsion angle (β-diket.) ^a	14.6°	24.2°
Av. torsion angle (carboxy.) ^b	12.0°	20.0°
Dihedral angle ^c	23.9°	23.3°

a) Angles O1-Rh1-Rh2-O5 and O4-Rh1-Rh2-O8.

b) Angles O3-Rh1-Rh2-O7 and O2-Rh1-Rh2-O6.

c) Angle between the planes defined by the atoms Rh1-O1-C5-C6-C7-O4 and Rh2-O5-C10-C11-C12-O8.

Figure 5.4 Ball and stick diagrams illustrating the crystal structure of $[\text{Rh}_2(\text{O}_2\text{CCH}_3)_2(\text{CF}_3\text{COCHCOCF}_3)_2(\text{C}_5\text{H}_5\text{N})_2]$.

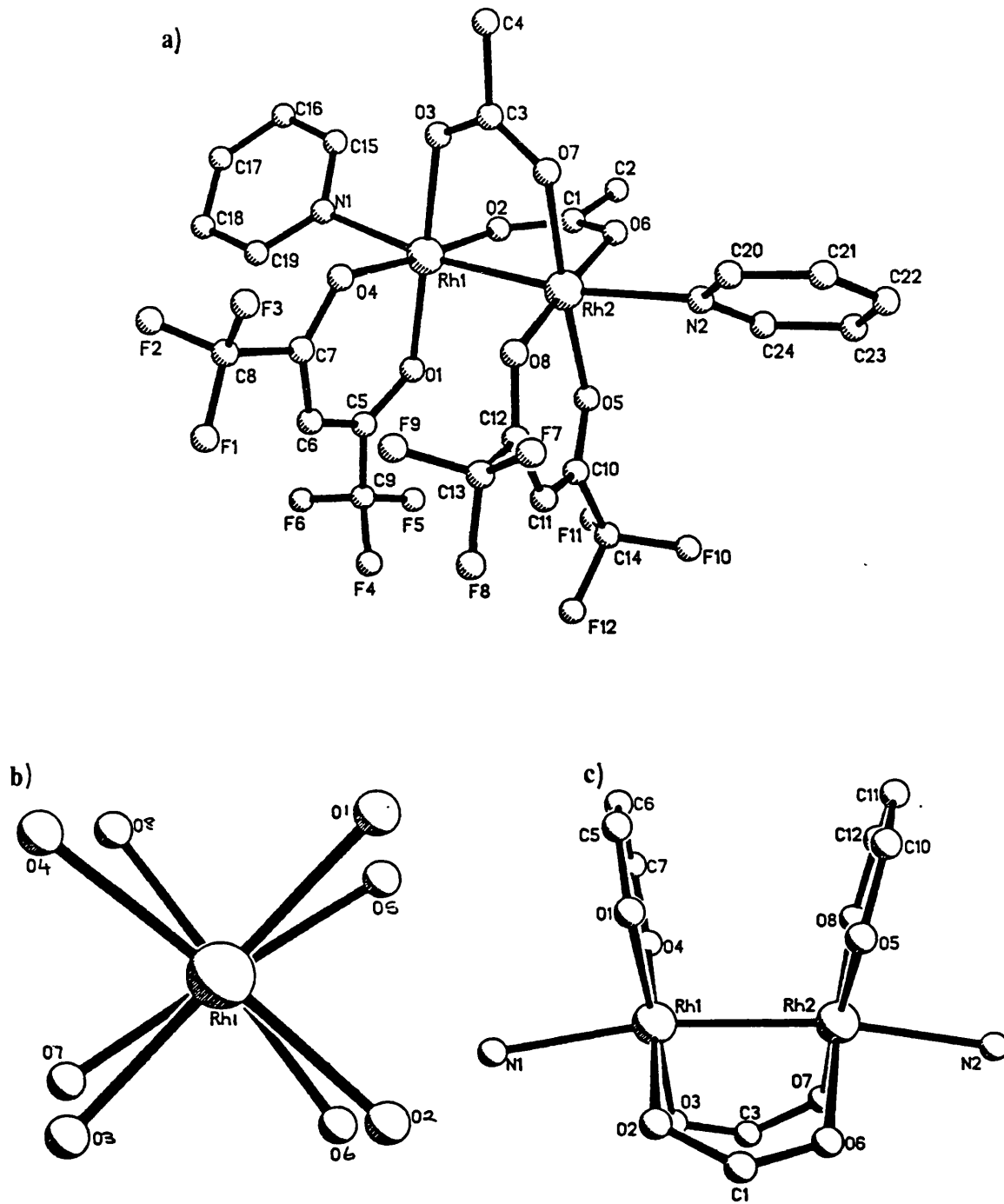
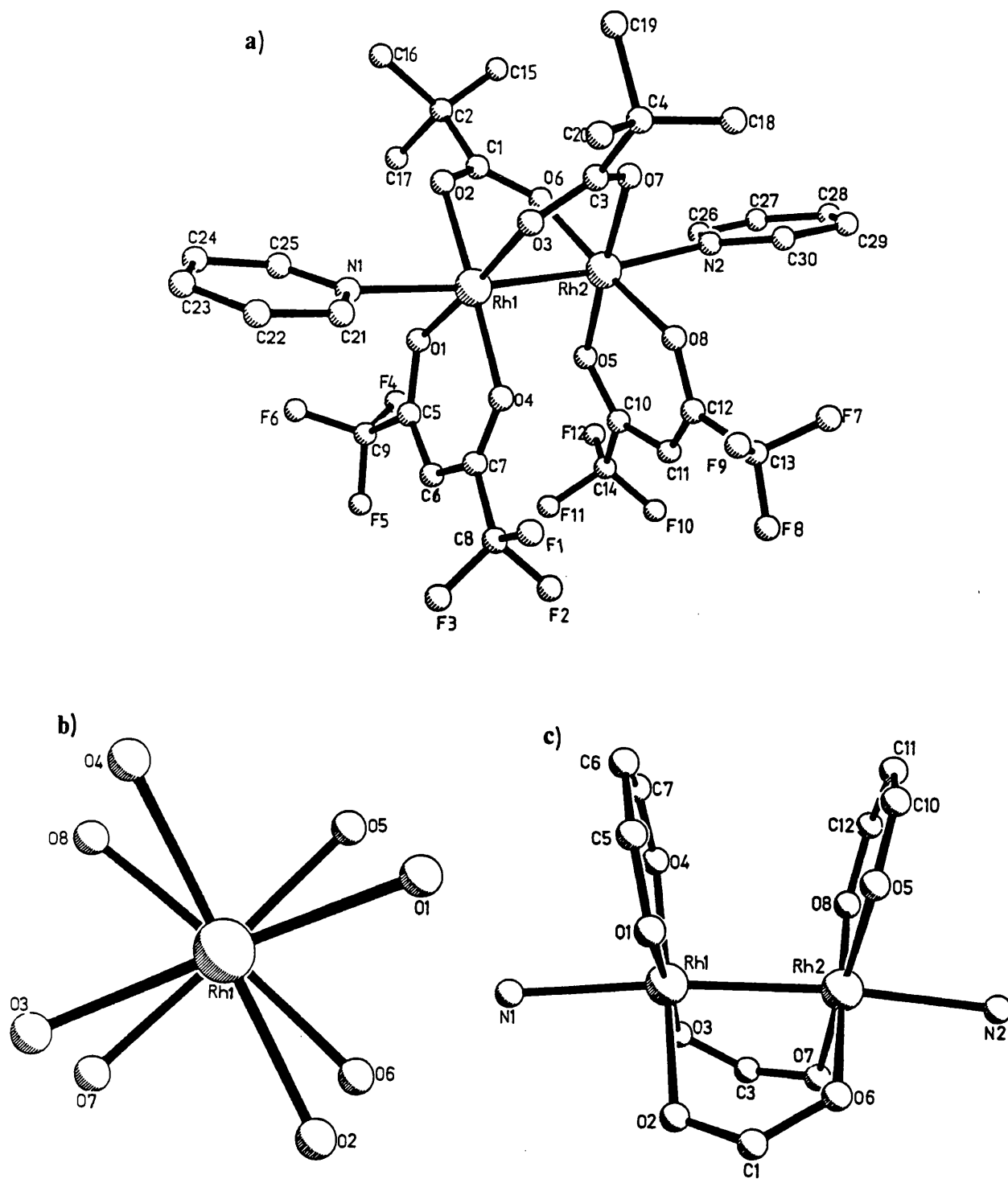


Figure 5.5 Ball and stick diagrams illustrating the crystal structure of $[\text{Rh}_2(\text{O}_2\text{CC}(\text{CH}_3)_2)_2(\text{CF}_3\text{COCHCOCF}_3)_2(\text{C}_5\text{H}_5\text{N})_2]$.



167.02(7)° are observed for the compound $[\text{Rh}_2(\text{O}_2\text{CCH}_3)_2(\text{chel})_2(\text{L})_2][\text{ClO}_4]_2$ ¹¹³ (chel=1,10-phenanthroline, L=N-methylimidazole), while a Rh-Rh-S angle of 176.42(4)° and, a Rh-Rh-N angle of 174.71(9)° are observed for the compounds $[\text{Rh}_2(\text{O}_2\text{CCH}_3)_4(\text{DMSO})_2]$ ⁵² and $[\text{Rh}_2(\text{O}_2\text{CC}_2\text{H}_5)_4(\text{C}_{12}\text{H}_8\text{N}_2)_2]$ ⁵³ respectively.

Structural data for some related compounds are presented in Table 5.2.

The Rh-Rh bond lengths observed for structures 5.1 and 5.2 are considerable shorter than those observed previously for dirhodium(II/II) compounds containing a combination of bridging and chelating ligands¹¹¹⁻¹¹³. The degree of twisting of the chelating ligands from an eclipsed configuration, in compounds reported previously, of between 16 and 20°, is closely similar to those observed for structures 5.1 and 5.2. The dihedral angles between the least squares planes of the chelating ligands are considerably smaller (9-15°) than those observed here. All the Rh-Rh bond lengths observed for dirhodium(II/II) compounds containing a combination of bridging and chelating ligands fall between 2.3693(2) Å for $[\text{Rh}_2(\text{O}_2\text{CCH}_3)_4(\text{C}_5\text{H}_5\text{N})_2]$ ⁵⁴ (four bridging ligands) and 2.934(2) Å for $[\text{Rh}_2(\text{DMG})_4(\text{P}(\text{C}_6\text{H}_5)_3)_2]$ ²⁷ (four chelating ligands). The stepwise increase in Rh-Rh bond length on changing from four bridging ligands to a combination of two bridging and two chelating ligands and finally to four chelating ligands suggests that the bite angle of the bridging ligands has considerable influence on the Rh-Rh bond lengths observed.

5.4 Investigations into the *Cis* and *Trans* Isomers of the Compounds



Reactions carried out using the β-diketonate ligand $\text{CF}_3\text{COCH}_2\text{COCH}_3$,

Table 5.2 Structural data for $[\text{Rh}_2(\text{O}_2\text{CR})_2(\text{chel})_2(\text{L})_2]$, $[\text{Rh}_2(\text{O}_2\text{CR})_4(\text{L})_2]$ and $[\text{Rh}_2(\text{chel})_4(\text{L})_2]$.

Compound	Rh-Rh (Å)	Rh-axial (Å)	Ref.
$[\text{Rh}_2(\text{O}_2\text{CCH}_3)_4(\text{C}_5\text{H}_5\text{N})_2]$	2.3964(2)	2.227[3]	54
$[\text{Rh}_2(\text{O}_2\text{CCH}_3)_2(\text{C}_{12}\text{H}_8\text{N}_2)_2(\text{C}_4\text{H}_5\text{N}_2)_2](\text{ClO}_4)_2$	2.5557(4)	2.198[4]	113
$[\text{Rh}_2(\text{O}_2\text{CCH}_3)_2(\text{C}_{14}\text{H}_{12}\text{N}_2)_2(\text{C}_4\text{H}_5\text{N}_2)_2](\text{ClO}_4)_2$	2.565(1)	2.231[6]	113
$[\text{Rh}_2(\text{O}_2\text{CCH}_3)_2(\text{C}_{16}\text{H}_{16}\text{N}_2)_2(\text{C}_4\text{H}_5\text{N}_2)_2](\text{ClO}_4)_2$	2.564(1)	2.21[1]	113
$[\text{Rh}_2(\text{O}_2\text{CH})_2(\text{C}_{12}\text{H}_8\text{N}_2)_2\text{Cl}_2]^b$	2.576	2.504	112
$[\text{Rh}_2(\text{O}_2\text{CCH}_3)_2(\text{dmg})_2(\text{P}(\text{C}_6\text{H}_5)_3)_2]^a$	2.618(5)	2.485[13]	111
$[\text{Rh}_2(\text{dmg})_4(\text{P}(\text{C}_6\text{H}_5)_3)_2]^a$	2.934(2)	2.439[7]	27

a) dmg is the monoanion of dimethylglyoxime.

b) No e.s.d. values quoted.

have resulted in the formation of products containing a mixture of *cis* and *trans* isomers (Figure 5.6). ^1H n.m.r. spectroscopy can be used to detect these two isomers. Figure 5.7 illustrates the ^1H n.m.r. spectrum obtained for the compound $[\text{Rh}_2(\text{O}_2\text{CC}(\text{CH}_3)_3)_2(\text{CF}_3\text{COCHCOCH}_3)_2(\text{C}_5\text{H}_5\text{N})_2]$. In the *cis* isomer the two carboxylate ligands are in different chemical environments and the methyl protons of these ligands ($(\text{CH}_3)_3\text{CCO}_2$) give two resonances at 1.06 and 1.11 ppm. The two β -diketonate ligands are equivalent and give rise to one set of peaks at 1.90 ppm ($\text{CF}_3\text{COCHCOCH}_3$) and 5.49 ppm ($\text{CF}_3\text{COCHCOCH}_3$). In the *trans* isomer the carboxylate ligands are equivalent giving one peak at 1.09 ppm. The β -diketonate ligands are also equivalent and also give just one set of peaks at 1.88 ppm and 5.48 ppm. The peaks due to the pyridine protons are not sufficiently well resolved to assign them to individual isomers. ^{19}F n.m.r. spectroscopic measurements reveal one resonance for each isomer.

5.4.1 Separation and characterisation of the *cis* and *trans* isomers of the compound $[\text{Rh}_2(\text{O}_2\text{CCH}_3)_2(\text{CF}_3\text{COCHCOCH}_3)_2(\text{C}_5\text{H}_5\text{N})_2]$

The *cis* and *trans* isomers of the title compound have been separated using column chromatography. The isomeric mixture of compounds which are red in colour initially become green as they are eluted down a silica gel column. The integration of the ^1H n.m.r. spectra obtained of the individual isomers reveals that one of the axial pyridine molecules had been displaced from each isomer. The change of colour as the compound is eluted is most likely due to this loss of pyridine, the dependence of colour on the axial ligation of dirhodium(II/II) compounds being well documented⁶⁶. Examination of the ^1H n.m.r. spectrum obtained before separation and the ^1H n.m.r. spectra obtained of the individual

Figure 5.6 Diagrammatic representations of the *cis* and *trans* isomers of $[\text{Rh}_2(\text{O}_2\text{CCH}_3)_2(\text{CH}_3\text{COCHCOCF}_3)_2(\text{C}_5\text{H}_5\text{N})_2]$.

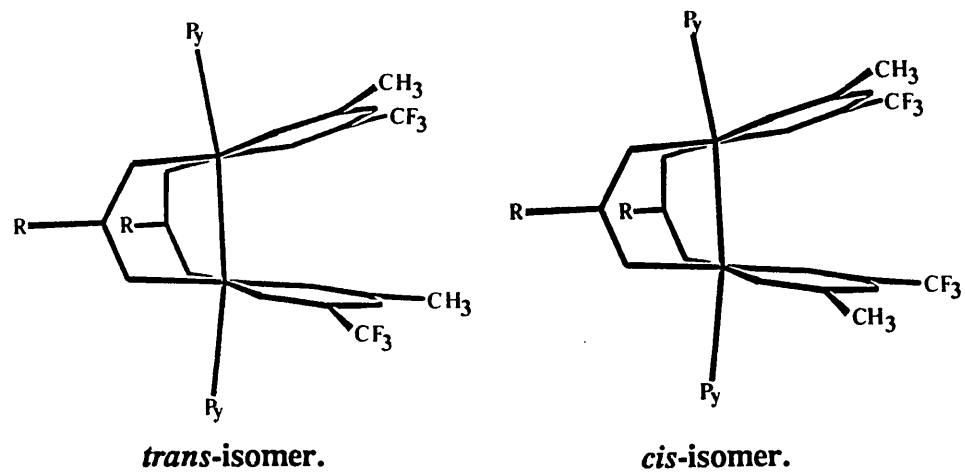
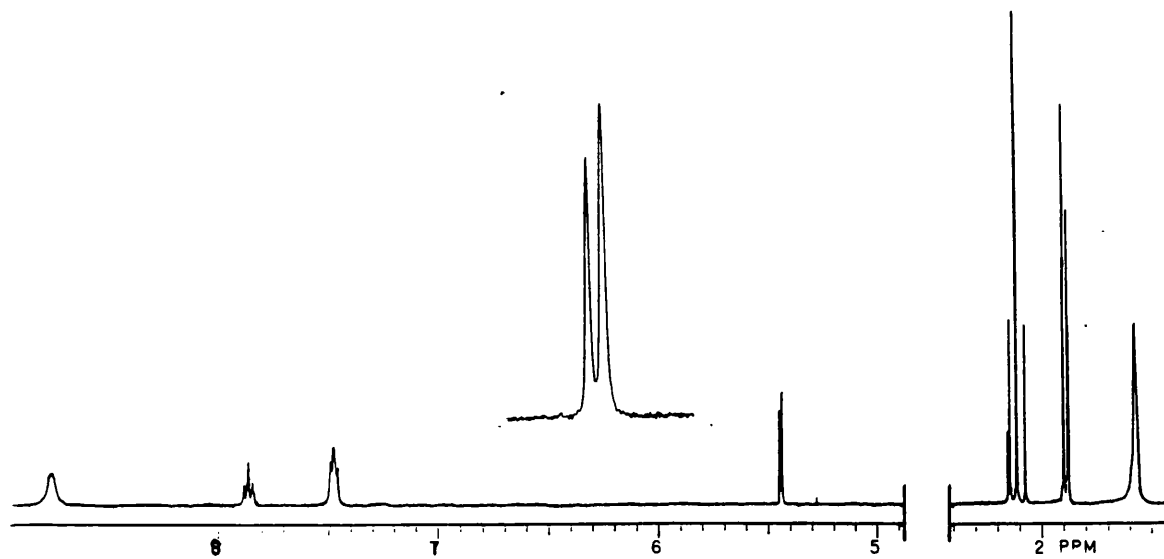


Figure 5.7 ^1H n.m.r. spectrum of the compound $[\text{Rh}_2(\text{O}_2\text{CCH}_3)_2(\text{CH}_3\text{COCHCOCF}_3)_2(\text{C}_5\text{H}_5\text{N})_2]$.



isomers reveals that the peak due to the proton attached to the γ -carbon of each of the two β -diketonate ligand has shifted down field by *ca.* 0.1 ppm while the doublet due to the *ortho*-hydrogens of the pyridine ligands has been shifted upfield by *ca.* 0.2 ppm.

Variable temperature ^1H n.m.r. spectra have been recorded for each isomer over a range of 20 to -80 $^\circ\text{C}$, these are illustrated in Figures 5.8 and 5.9. For both isomers a broadening and then splitting of the peaks, due to the β -diketonate protons, is observed as the temperature is lowered. For the *trans* isomer the peak due to the acetate protons is also split on reducing the temperature. The two singlets observed ^{at} room temperature for the carboxylate methyl protons in the *cis* isomer do not split further on lowering the temperature. The peaks due to the pyridine protons appear to be remain unaltered. The peak due to the proton attached to the γ -carbon of the β -diketonate ligand is the first peak to broaden and split with two peaks becoming apparent between -10 and -20 $^\circ\text{C}$. The peaks due to the β -diketonate methyl protons and, in the case of the *trans* isomer, the carboxylate methyl protons split at a slightly lower temperature, two peaks becoming apparent between -20 and -30 $^\circ\text{C}$. As the temperature is lowered further the separation between these pairs of peaks increases and at -80 $^\circ\text{C}$ the separation between the two peaks due to the proton of the γ -carbon is *ca.* 0.19 ppm for both isomers. This is considerably greater than the separation observed between peaks due to the methyl protons of the β -diketonate ligands (*cis*-isomer 0.005 ppm and *trans*-isomer 0.033 ppm) and the carboxylate ligands (*cis*-isomer 0.051 ppm and *trans*-isomer 0.049 ppm).

The ^{19}F n.m.r. spectra recorded for each isomer, along with that recorded for the isomeric mixture $[\text{Rh}_2(\text{O}_2\text{CCH}_3)_2(\text{CF}_3\text{COCHCOCH}_3)_2(\text{C}_5\text{H}_5\text{N})_2]$, are illustrated in Figure 5.10. In the initial reaction product (isomeric mixture) two

Figure 5.8 Variable temperature ^1H n.m.r. for
 $[\text{cis-Rh}_2(\text{O}_2\text{CCH}_3)_2(\text{CH}_3\text{COCHCOCF}_3)_2(\text{C}_5\text{H}_5\text{N})]$.

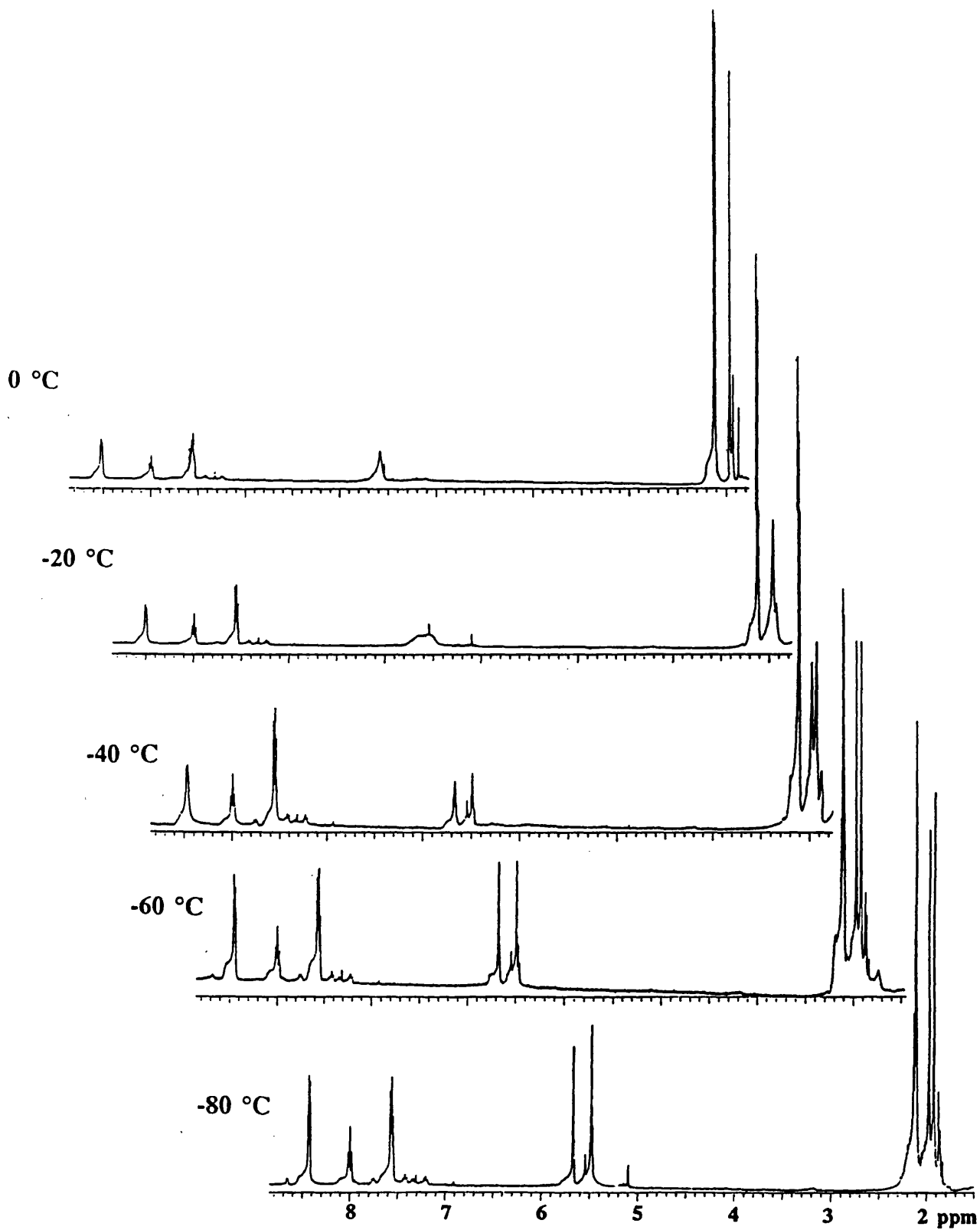


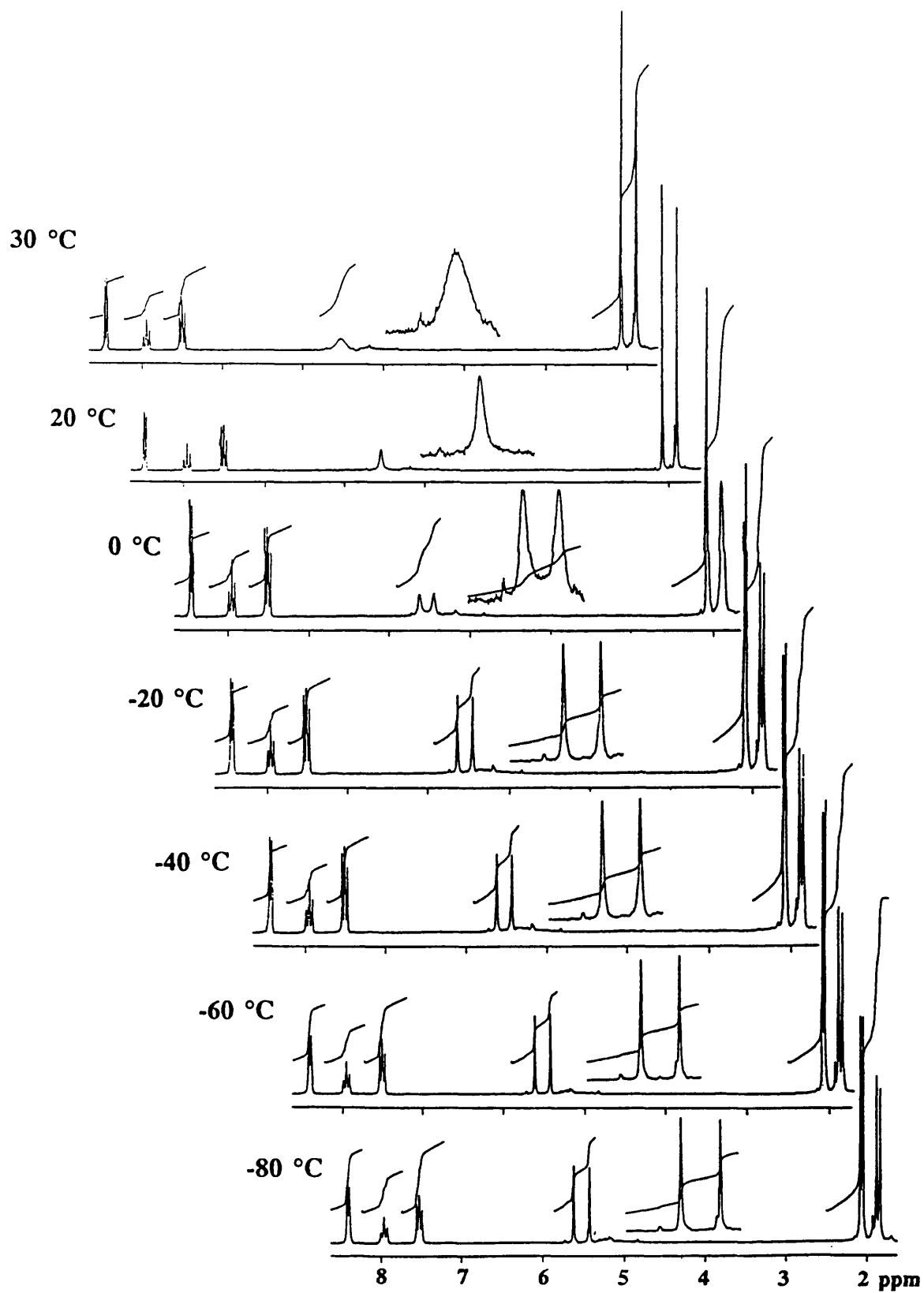
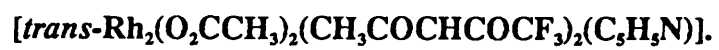
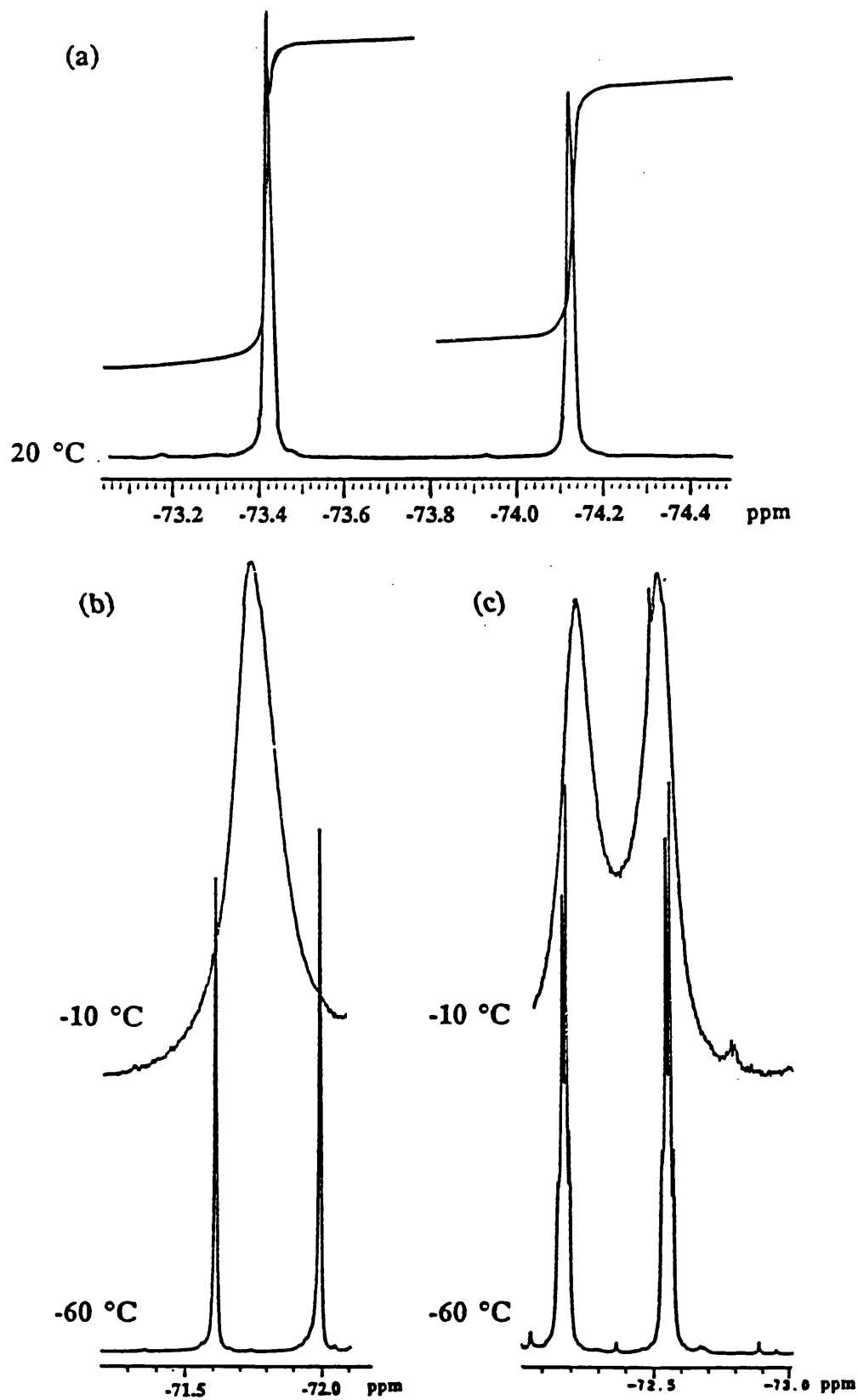
Figure 5.9 Variable temperature ^1H n.m.r. for

Figure 5.10 ^{19}F n.m.r. spectra of a) $[\text{Rh}_2(\text{O}_2\text{CCH}_3)_2(\text{CH}_3\text{COCHCOCF}_3)_2(\text{C}_5\text{H}_5\text{N})_2]$
 b) [*trans*- $\text{Rh}_2(\text{O}_2\text{CCH}_3)_2(\text{CH}_3\text{COCHCOCF}_3)_2(\text{C}_5\text{H}_5\text{N})$] and
 c) [*cis*- $\text{Rh}_2(\text{O}_2\text{CCH}_3)_2(\text{CH}_3\text{COCHCOCF}_3)_2(\text{C}_5\text{H}_5\text{N})$].



singlets are observed at room temperature. Spectra of the separated isomers have been recorded at -10 °C and -60 °C. At -10 °C two broad peaks are observed for the *cis*-isomer while only one broad peak is apparent for the *trans* isomer. Spectra recorded at -60 °C indicate that the two peaks observed for the *cis*-isomer are resolved into two quartets and the peak observed for the *trans*-isomer has resolved into a pair of singlets. The quartets observed for the *cis*-isomer suggest that "through space" coupling may be occurring between the two CF₃ groups resulting in a quartet for each CF₃ resonance. The absence of this behaviour for the *trans* isomer is not unexpected given the considerably greater distance between the CF₃ groups in the *trans* isomer. Work is continuing^{to} confirm this hypothesis.

Comparison of the integral heights for the two peaks observed at room temperature for the isomeric mixture suggests that the isomers are present in a ratio of 45%(*cis*):55%(*trans*). Approximately the same ratio of products is observed for each of the isomeric mixtures prepared.

5.4.2 Structural investigation into the *cis* and *trans* isomers of the compound [Rh₂(O₂CCH₃)₂(CF₃COCHCOCH₃)₂(C₅H₅N)].

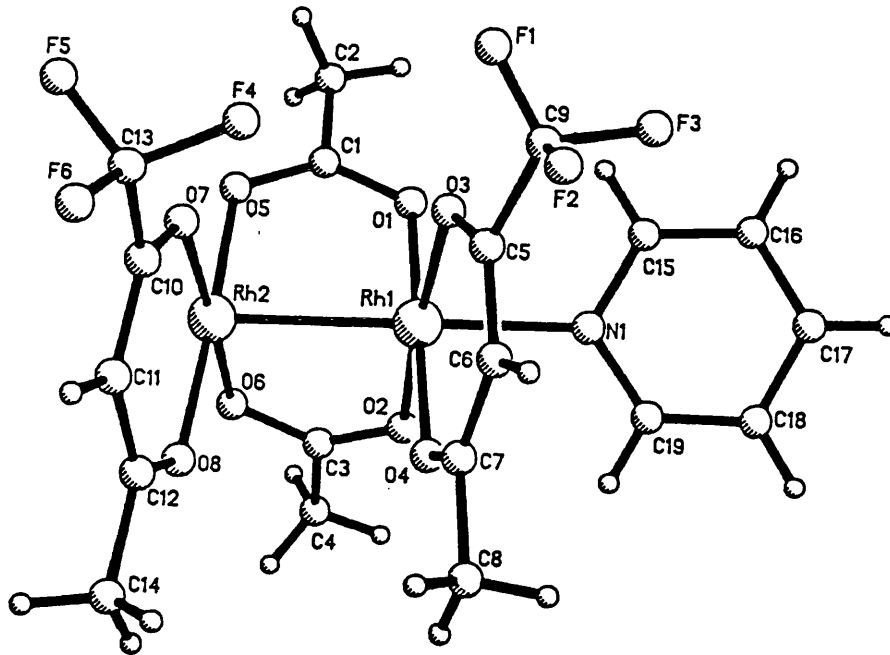
Crystals of both the *cis* and *trans* isomers of the title compound have been obtained by slow evaporation of dichloromethane solutions of each isomer. Both crystals were green in colour and found to be suitable for x-ray crystallographic study. The crystal structures^{§§} obtained of each are illustrated in Figures 5.11a and 5.12a. The structures are similar to those already discussed in

§§The structure of [*cis*-Rh₂(O₂CCH₃)₂(CF₃COCHCOCH₃)₂(C₅H₅N)] will be referred to as structure 5.3*cis*.

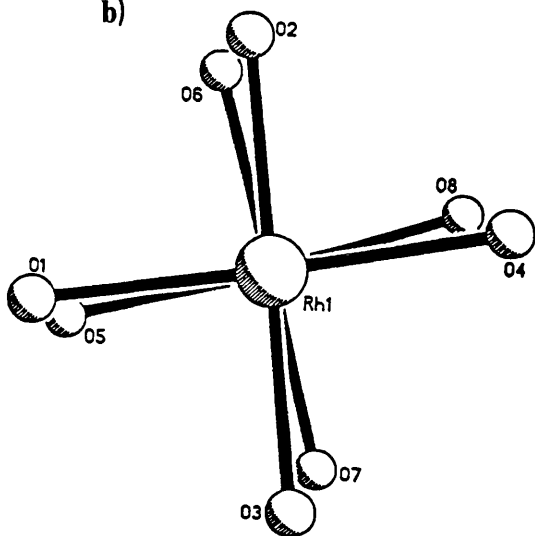
The structure of [*trans*-Rh₂(O₂CCH₃)₂(CF₃COCHCOCH₃)₂(C₅H₅N)] will be referred to as structure 5.3*trans*.

Figure 5.11 Ball and stick diagrams illustrating the crystal structure of $[cis-Rh_2(O_2CCH_3)_2(CH_3COCHCOCF_3)_2(C_5H_5N).0.5C_5H_5N]$.

a)



b)



c)

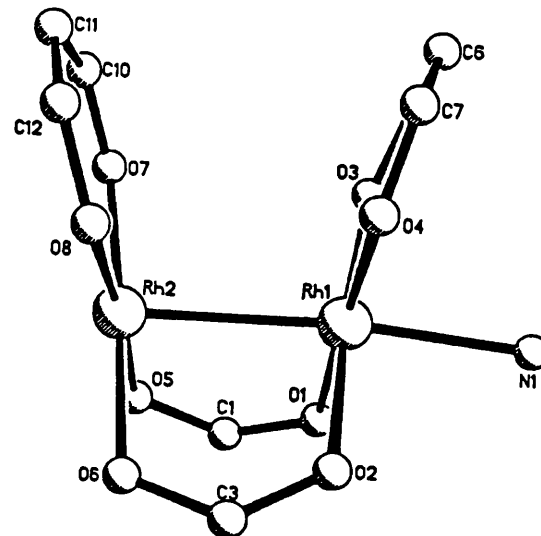
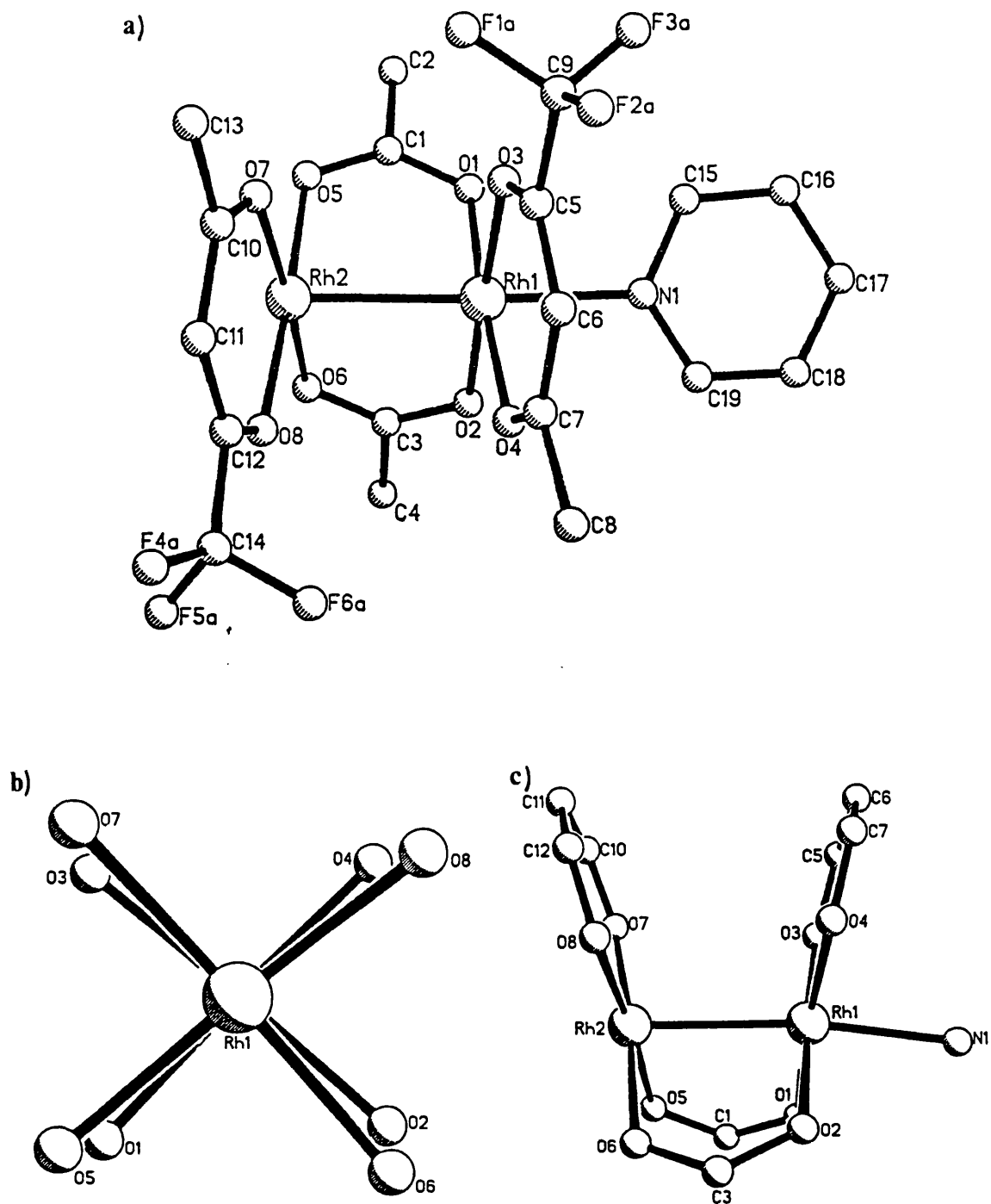


Figure 5.12 Ball and stick diagrams illustrating the crystal structure of
 $[trans-Rh_2(O_2CCH_3)_2(CH_3COCHCOCF_3)_2(C_5H_5N)]$.



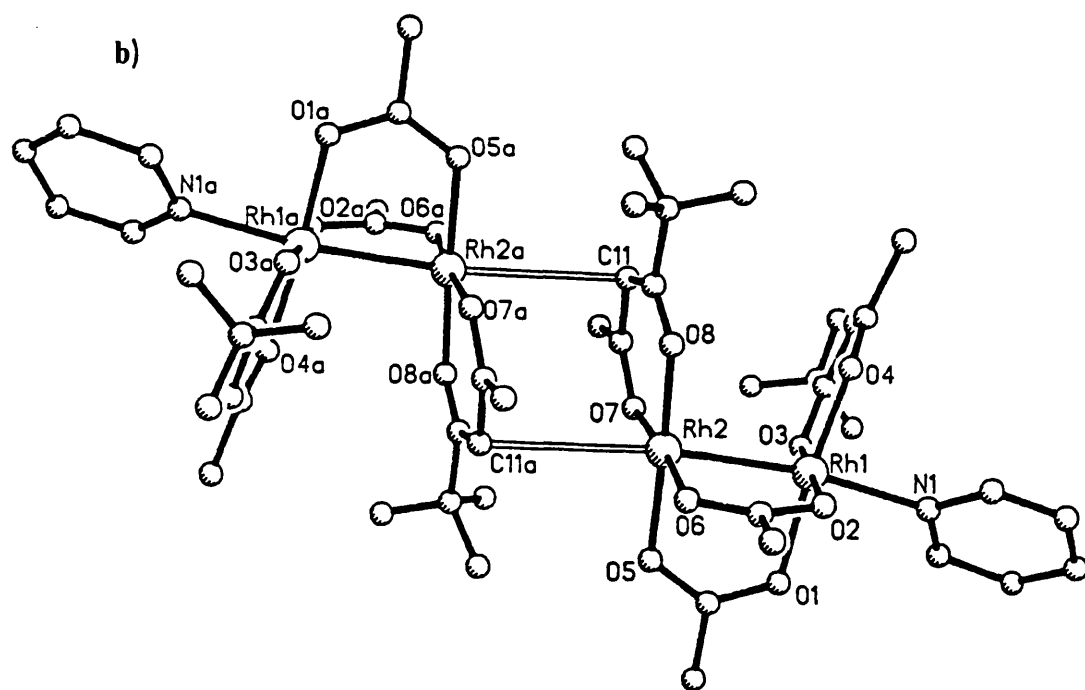
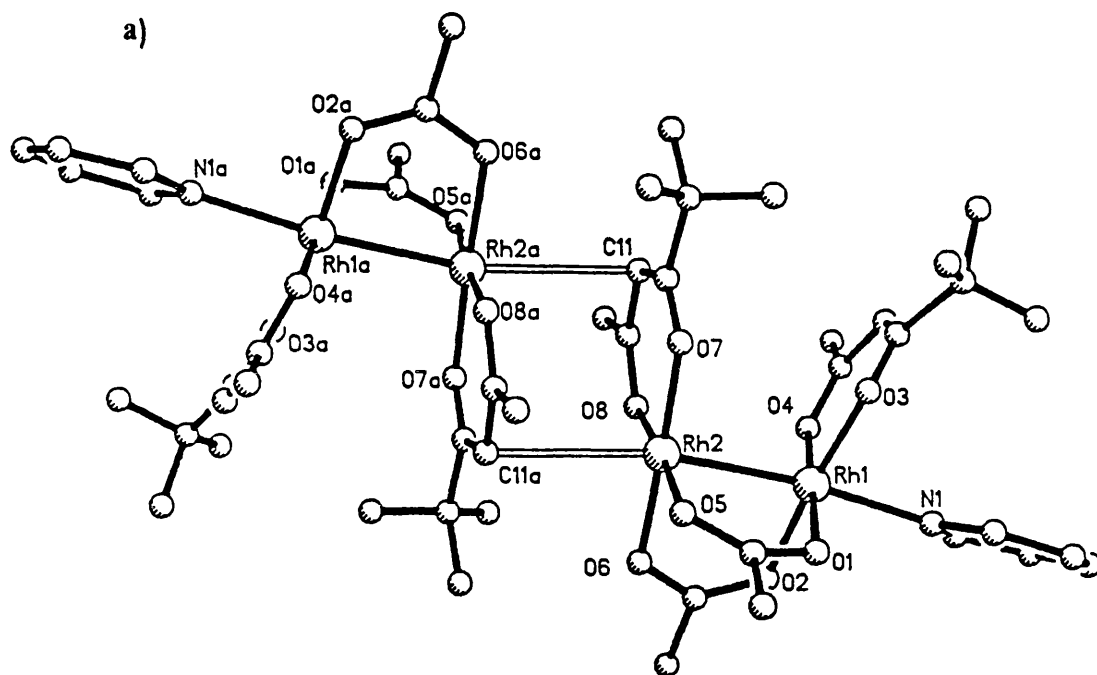
Section 5.3, containing a $[\text{Rh}_2]^{4+}$ unit bridged by two acetate ligands in a cisoid arrangement. Each rhodium ion is co-ordinated by a chelating $[\text{CF}_3\text{COCHCOCH}_3]^-$ group. The axial site of one rhodium ion is occupied by a pyridine molecule while the axial site of the second rhodium ion appears to be vacant.

Structures 5.3*cis* and 5.3*trans*¹¹⁹ are in most respects closely similar, however the Rh-Rh bond distances observed are statistically different, 2.522(2) Å for structure 5.3*cis* and 2.534(1) Å for structure 5.3*trans*. The Rh-N bond lengths observed for both isomers are essentially the same 2.133(10) Å (*trans*) and 2.134(10) Å (*cis*) and are considerably shorter than previously observed for structures 5.1 (2.242[15] Å) and 5.2 (2.233[7] Å), suggesting that the pyridine molecules in structures 5.3*cis* and 5.3*trans* are more strongly bound to the rhodium ion than in either structure 5.1 or 5.2.

The axial site of the second rhodium ion was at first thought to be vacant, but examination of the crystal packing arrangement for these two structures has revealed that they actually exist, in the solid state, as dimers. Pairs of molecules are linked via the "vacant" axial site of the rhodium ion on one molecule, and the γ -carbon of a β -diketonate ligand on the adjacent molecule in the lattice (Figure 5.13). The Rh-C distances observed, 2.861 Å for structure 5.3*cis* and 3.106 Å for structure 5.3*trans* are too long to be considered 'formal' bonds but do suggested strong Van Der Waals interactions between the rhodium ion and the γ -carbon of the β -diketonate ligand on the adjacent molecule. This type of interaction is not unprecedented and examples of iron(II) and mercury(II) compounds containing metal- γ -carbon interactions have been reported^{120,121}.

In both isomers the β -diketonate ligands are shifted from an eclipsed configuration giving average torsion angles about the Rh-Rh bond of 8.0° and 7.1° for structures 5.3*cis* and 5.3*trans* respectively (Figures 5.11b and 5.12b). These

Figure 5.13 Ball and stick diagrams of

a) $[cis-Rh_2(O_2CCH_3)_2(CH_3COCHCOCF_3)_2(C_5H_5N) \cdot 0.5C_5H_5N]_2$ andb) $[trans-Rh_2(O_2CCH_3)_2(CH_3COCHCOCF_3)_2(C_5H_5N)]_2$ 

angles are considerably smaller than observed for structures 5.1 (14°) and 5.2 (24°). The dihedral angle (30.5° for 5.3*cis* and 29.3° for 5.3*trans*) observed between the planes of the β -diketonate ligands (defined by the atoms Rh1-O3-C5-C6-C7-O4 and Rh2-O7-C10-C11-C12-O8) and the Rh-Rh-N angles of 173.9° (5.3*cis*) and 171.8° (5.3*trans*) indicates greater bending about the Rh-Rh-N axis than observed for structures 5.1 and 5.2 (Figures 5.11c and 5.12c). Bond lengths and angles are presented in Table 5.3.

In structures 5.1 and 5.2 a pyridine molecule fills the axial site on each rhodium ion. As a consequence the size of the dihedral angle between the planes of the β -diketonate ligands will be the result of two opposing, unfavourable interactions, between the β -diketonate ligands and the pyridine molecules and, between the CF_3 groups on the two β -diketonate ligands. The size of the dihedral angle will affect the extent to which the bridging and chelating ligands are twisted about the Rh-Rh bond in order to overcome the repulsive forces between the $-\text{CF}_3$ substituent groups on the two β -diketonate ligands. In structures 5.3*cis* and 5.3*trans* the axial site of one rhodium ion is co-ordinated by a pyridine molecule and can be expected to behave in a similar way to that observed for structures 5.1 or 5.2. The axial site of the second rhodium ion is linked via a Rh-C interaction to the adjacent molecule in lattice. This will be a favourable interaction and pull the γ -carbon atom towards the rhodium ion of the adjacent molecule causing an increase in the dihedral angle between the planes of the β -diketonate ligands. This will result a greater separation between the $-\text{CF}_3$ substituent groups on the two β -diketonate ligands therefore the extent to which the ligands will be twisted about the Rh-Rh bond will be smaller than observed for structures 5.1 or 5.2.

Table 5.3 Structural data for

[*cis*-Rh₂(O₂CCH₃)₂(CF₃COCHCOCH₃)₂(C₅H₅N).0.5C₅H₅N] (*5.3cis*)and [*trans*-Rh₂(O₂CCH₃)₂(CF₃COCHCOCH₃)₂(C₅H₅N)] (*5.3trans*).

	Structure <i>5.3cis</i>	structure <i>5.3trans</i>
Rh-Rh	2.522(2) Å	2.534(1) Å
Rh-N	2.134(10) Å	2.133(10) Å
Rh-O acetate (av.)	2.023[20] Å	2.029[17] Å
Rh-O β-diket. (av.)	2.003[20] Å	2.000[18] Å
N1-Rh1-Rh2	173.9(3)°	171.8(3)°
O-Rh-O acetate (av.)	90.5[6]°	90.9[6]°
O-Rh-O β-diket. (av.)	93.5[6]°	94.4[4]°
Av. torsion angle (β-diket.) ^a	8.0°	7.1°
Av. torsion angle (acetate) ^b	7.2°	6.8°
Dihedral angle ^c	30.5°	29.3°

a) angles O3-Rh1-Rh2-O7 and O4-Rh1-Rh2-O8.

b) angles O1-Rh1-Rh2-O5 and O2-Rh1-Rh2-O6.

c) angle between the planes defined by the atoms Rh1-O3-C5-C6-C7-O4 and Rh2-O7-C10-C11-C12-O8.

5.4.3 A Rationalisation of the ^1H n.m.r. Spectroscopic Results and the Solid State Structures of the *Cis* and *Trans* Isomers of $[\text{Rh}_2(\text{O}_2\text{CCH}_3)_2(\text{CF}_3\text{COCHCOCH}_3)_2(\text{C}_5\text{H}_5\text{N})]$.

The results obtained from the structural analysis of the title compounds (structure 5.3*cis* and 5.3*trans*) can be used to explain the solution behaviour observed during variable temperature ^1H n.m.r. spectroscopic measurements of these compounds. The changes observed in the ^1H n.m.r. spectra as the temperature is lowered suggests that at room temperature an average structure is observed, with the pyridine ligands exchanging with the solvent at a rapid rate while the Rh-C interaction is cleaving and recombining at a much slower rate, and hence a broad signal is observed for the proton of the γ -carbon atom. As the temperature is lowered, the rates of exchange decrease to a point where the dimeric form of the compound observed in the solid state is "frozen out". This is supported by the fact that the chemical shift differences between the two peaks due to the proton of the γ -carbon at -80°C is considerably larger than the differences observed for the methyl protons of the β -diketonate ligands, or the methyl protons of the carboxylate ligands, consistent with the argument that the environments of the two γ -carbon protons are most markedly different.

The reaction of $[\text{Rh}_2(\text{O}_2\text{CCH}_3)_4(\text{CH}_3\text{OH})_2]$ with $[\text{CH}_3\text{COCH}_2\text{COCH}_3]$ resulted in the formation of a green compound for which both microanalytical data and ^1H n.m.r. spectroscopic data indicate the presence of only one molecule of pyridine per dirhodium unit. This suggests that the compound $[\text{Rh}_2(\text{O}_2\text{CCH}_3)_2(\text{CH}_3\text{COCHCOCH}_3)_2(\text{C}_5\text{H}_5\text{N})]$ has been formed and has the same gross structure as the *cis* and *trans* isomers of $[\text{Rh}_2(\text{O}_2\text{CCH}_3)_2(\text{CF}_3\text{COCHCOCH}_3)_2(\text{C}_5\text{H}_5\text{N})]$. The addition of pyridine to samples of either of the two isomers results in the

solution returning to its original red colour, but the addition of pyridine to the compound $[\text{Rh}_2(\text{O}_2\text{CCH}_3)_2(\text{CH}_3\text{COCHCOCH}_3)_2(\text{C}_5\text{H}_5\text{N})]$ has no visible effect, suggesting a much stronger Rh-C interaction may exist in this case. Unfortunately the latter compound is poorly soluble in all solvents and crystals suitable for X-ray crystallographic investigation have not been obtained.

5.5 Conclusions.

Seven compounds have been isolated and characterised during this study. These compounds have been found to exist as either a single species or a mixture of two isomers. The *cis* and *trans* isomers of one compound, $[\text{Rh}_2(\text{O}_2\text{CCH}_3)_2(\text{CF}_3\text{COCHCOCH}_3)_2(\text{C}_5\text{H}_5\text{N})]$, have been separated and characterised. Crystal structures of two species $[\text{Rh}_2(\text{O}_2\text{CR})_2(\text{CF}_3\text{COCHCOCF}_3)_2(\text{C}_5\text{H}_5\text{N})_2]$ ($\text{R}=\text{CH}_3^{118}, \text{C}(\text{CH}_3)_3$) and of the *cis* and *trans*¹¹⁹ isomers of $[\text{Rh}_2(\text{O}_2\text{CCH}_3)_2(\text{CF}_3\text{COCHCOCH}_3)_2(\text{C}_5\text{H}_5\text{N})]$ have been determined. These structures have confirmed the geometry suggested by Cenini et. al.¹⁰⁹ and have revealed the existence of an unusual Rh-C interaction between adjacent molecules, in the structures of the *cis* and *trans* isomers of the compound $[\text{Rh}_2(\text{O}_2\text{CCH}_3)_2(\text{CF}_3\text{COCHCOCH}_3)_2(\text{C}_5\text{H}_5\text{N})]$. It is suggested that this Rh-C interaction is also present in $[\text{Rh}_2(\text{O}_2\text{CCH}_3)_2(\text{CH}_3\text{COCHCOCH}_3)_2(\text{C}_5\text{H}_5\text{N})]$. The behaviour of this compound on the addition of pyridine suggests that the Rh-C interaction is strongest in this case.

Work in this area is continuing with a view to answering the questions raised here. Attempts to prepare compounds of the type $[\text{Rh}_2(\text{OSCR})_2(\text{R}'\text{COCHCOR}'')_2\text{L}_2]^{122}$ have proved unsuccessful, but attempts to prepare the related compounds $[\text{Rh}_2(\text{HNOCR})_2(\text{R}'\text{COCHCOR}'')_2\text{L}_2]^{123}$ are in progress.

5.6 Experimental.

5.6.1 Materials and Instrumentation.

^1H n.m.r. spectra were recorded on Varian XL 200 MHz and Varian VXR 400 MHz n.m.r. spectrometers. ^{19}F n.m.r. spectra were recorded using a Varian VXR 400 MHz Spectrometer. With the exception of the variable temperature ^1H n.m.r. spectra and the low temperature ^{19}F n.m.r. spectra which were recorded in CD_2Cl_2 (referenced to CH_2Cl_2 and CFCl_3 , respectively) all ^1H n.m.r. and ^{19}F n.m.r. spectra were recorded in CDCl_3 (referenced to CHCl_3 and CFCl_3 , respectively).

All chemicals and other instrumentation used are as detailed in Section 2.5.1. Crystallographic procedures closely paralleled those described in Sections 3.6.1 and 3.6.3.

5.6.2 Synthesis of $[\text{Rh}_2(\text{O}_2\text{CC}_2\text{H}_5)_4]$.

$[\text{Rh}_2(\text{O}_2\text{CCH}_3)_4(\text{CH}_3\text{OH})_2]$ (0.1710 g; 0.30 mMol) was refluxed in propanoic acid (3 cm^3) for 4 hours. The propanoic acid was removed under reduced pressure to yield the final product.

5.6.3 Synthesis of $[\text{Rh}_2(\text{O}_2\text{CCH}_3)_2(\text{CH}_3\text{COCHCOCH}_3)_2(\text{C}_5\text{H}_5\text{N})]$.

$[\text{Rh}_2(\text{O}_2\text{CCH}_3)_4(\text{CH}_3\text{OH})_2]$ (0.117 g; 0.23 mMol) was refluxed in water (20 cm^3) with $\text{Na}[\text{CH}_3\text{COCHCOCH}_3]$ (0.200 g; 1.64 mMol) for 30 minutes. The mixture was allowed to cool overnight and a brown precipitate was filtered off and

air dried. The precipitate was redissolved in methanol (10 cm³) to which C₅H₅N (0.05 cm³; 0.62 mMol) had been added. The solution was stirred for one hour during which time the solution became green in colour. The methanol was removed under reduced pressure, and the residue redissolved in dichloromethane (5 cm³), from which the product was precipitated with n-hexane (25 cm³). The product (0.0682 g; 0.11 mMol) was filtered off and air dried for 2 hours. (Yield = 48%).

Infrared Spectrum (KBr disk).

3433b,1573s,1546s,1516s,1443s,1389s,1351w,1267w,1213w,1068w,1015w,934w,770m, 701m,644w,464w,353w,315w cm⁻¹.

¹H n.m.r. spectrum (CDCl₃)

δ=1.88(s,12H,CH₃COCHCOCH₃), 2.14(s,6H,CH₃CO₂), 5.16(s,2H,CH₃COCHCOCH₃), 7.45(t,2H,*m*-H,C₅H₅N), 7.85(t,1H,*p*-H,C₅H₅N), 8.55(d,2H,*o*-H,C₅H₅N) ppm.

5.6.4 Synthesis of [Rh₂(O₂CCH₃)₂(CF₃COCHCOCH₃)₂(C₅H₅N)₂].

[Rh₂(O₂CCH₃)₄(CH₃OH)₂] (0.156 g; 0.31 mMol) was refluxed with [CF₃COCH₂COCH₃] (0.5 cm³; 4.12mMol) in water (20 cm³) for a total of 12 hours, with a second addition of [CF₃COCH₂COCH₃] (0.5 cm³; 4.12mMol) being made after the first 6 hours. The mixture was allowed to cool and a green precipitate filtered off and air dried for 2 hours. The precipitate was redissolved in methanol (10 cm³) to which C₅H₅N (0.05 cm³; 0.62 mMol) had been added. The solution was stirred for 1 hour during which time it became red in colour. The methanol was removed under reduced pressure and the residue redissolved in dichloromethane (5 cm³), from which the product was precipitated using n-hexane (20 cm³). The product (0.1670 g; 0.21 mMol) was filtered off and air dried. (Yield = 69%).

Infrared Spectrum (KBr disk)

3449b,1607m,1542s,1481m,1443s,1420w,1340m,1267s,1210s,1198s,1152s,1137s,
1095m,1064w,1003w,946w,819w,789w,754w,697s,624w,598w,530w,350w cm⁻¹.

¹H n.m.r. spectrum (CDCl₃)

cis-isomer δ= 1.91(s,6H,CH₃COCHCOCF₃), 2.07(s,3H,CH₃CO₂), 2.14(s,3H,CH₃CO₂),
5.46(s,2H,CH₃COCHCOCH₃), 7.49(t,4H,*m*-H,C₅H₅N), 7.87(t,2H,*p*-H,C₅H₅N),
8.76(d,4H,*o*-H,C₅H₅N) ppm.

trans-isomer δ= 1.88(s,6H,CH₃COCHCOCF₃), 2.11(s,3H,CH₃CO₂),
5.45(s,2H,CH₃COCHCOCH₃), 7.49(t,4H,*m*-H,C₅H₅N), 7.87(t,2H,*p*-H,C₅H₅N),
8.76(d,4H,*o*-H,C₅H₅N) ppm.

¹⁹F n.m.r. spectrum (CDCl₃).

cis-isomer δ= -74.13 (s,6F,CH₃COCHCOCF₃) ppm.

trans-isomer δ= -73.42 (s,6F,CH₃COCHCOCF₃) ppm.

5.6.5 Separation of the *cis* and *trans* isomers of the compound

A sample of the title compound was passed down a column (diameter 1.5 cm and length 40 cm) of silica gel (60-120 mesh) eluted with a mixture of dichloromethane (80%) ether (8%) and n-hexane (12%). Fractions (2 cm³) were collected and the solvent allowed to evaporate at room temperature overnight. The composition of each fraction was verified using ¹H n.m.r. spectroscopic measurements and fractions of the same composition combined and redissolved in dichloromethane (2 cm³). Slow evaporation of these solutions yielded green crystals of the two isomers of the mono-adduct [Rh₂(O₂CCH₃)₂(CF₃COCHCOCH₃)₂(C₅H₅N)].

cis-isomer**¹H n.m.r. spectrum (CD₂Cl₂).**

20 °C δ = 1.97(s,6H,CH₃COCHCOCF₃), 2.11(s,3H,CH₃CO₂), 2.13(s,3H,CH₃CO₂),

5.87(s,2H,CH₃COCHCOCH₃), 7.55(t,4H,*m*-H,C₅H₅N),

7.99(t,2H,*p*-H,C₅H₅N), 8.55(d,4H,*o*-H,C₅H₅N) ppm.

-80 °C δ = 1.92(s,3H,CH₃COCHCOCF₃), 1.97(s,3H,CH₃COCHCOCF₃),

2.10(s,3H,CH₃CO₂), 2.11(s,3H,CH₃CO₂), 5.48(s,1H,CH₃COCHCOCH₃),

5.67(s,1H,CH₃COCHCOCH₃), 7.56(t,4H,*m*-H,C₅H₅N), 8.00(t,2H,*p*-H,C₅H₅N),

8.43(d,4H,*o*-H,C₅H₅N) ppm.

¹⁹F n.m.r. spectrum (CD₂Cl₂).

-10 °C δ =-72.29(s,3F,CF₃COCHCOCH₃), -72.56(s,3F,CF₃COCHCOCH₃) ppm.

-60 °C δ =-72.17(q,3F,CF₃COCHCOCH₃, \bar{J} =5.2 Hz),

-72.55(q,3F,CF₃COCHCOCH₃, \bar{J} =5.3 Hz) ppm.

trans-isomer**¹H n.m.r. spectrum (CD₂Cl₂).**

20 °C δ = 1.90(s,6H,CH₃COCHCOCF₃), 2.09(s,6H,CH₃CO₂),

5.55(s,2H,CH₃COCHCOCH₃), 7.52(t,4H,*m*-H,C₅H₅N), 7.96(t,2H,*p*-H,C₅H₅N),

8.48(d,4H,*o*-H,C₅H₅N) ppm.

-80 °C δ = 1.85(s,3H,CH₃COCHCOCF₃), 1.89(s,3H,CH₃COCHCOCF₃),

2.06(s,3H,CH₃CO₂), 2.10(s,3H,CH₃CO₂), 5.44(s,1H,CH₃COCHCOCH₃),

5.63(s,1H,CH₃COCHCOCH₃), 7.53(t,4H,*m*-H,C₅H₅N), 7.97(t,2H,*p*-H,C₅H₅N),

8.41(d,4H,*o*-H,C₅H₅N) ppm.

¹⁹F n.m.r. spectrum (CD₂Cl₂).

-10 °C δ =-71.89(s,6F,CF₃COCHCOCH₃) ppm.

-60 °C δ = -71.61(s,3F,CF₃COCHCOCH₃), -71.99(s,3F,CF₃COCHCOCH₃) ppm.

5.6.6 Synthesis of [Rh₂(O₂CCH₃)₂(CF₃COCHCOCF₃)₂(C₅H₅N)₂].

The title compound was prepared using the procedure described in Section 5.6.4. Quantity of [Rh₂(O₂CCH₃)₄(CH₃OH)₂] used 0.242 g; 0.48 mMol. mass of product 0.2738 g; 0.31 mMol. (Yield = 66%).

Infrared Spectrum (KBr disk)

3449b,1600s,1558s,1512m,1477m,1443s,1363w,1301s,1225m,1210m,1187s,1137s, 1064w,1030w,1003w,865w,754w,701s,651w,621w,440w,360w,326w cm⁻¹.

¹H n.m.r. spectrum (CDCl₃)

δ = 2.11(s,6H,CH₃CO₂), 5.78(s,2H,CH₃COCHCOCH₃), 7.56(t,4H,*m*-H,C₅H₅N), 7.96(t,2H,*p*-H,C₅H₅N), 8.75(d,4H,*o*-H,C₅H₅N) ppm.

¹⁹F n.m.r. spectrum (CDCl₃).

δ = -75.09 (s,12F,CF₃COCHCOCF₃) ppm.

5.6.7 Synthesis of [Rh₂(O₂CC₂H₅)₂(CF₃COCHCOCH₃)₂(C₅H₅N)₂].

Rh₂(O₂CC₂H₅)₄ (0.107 g; 0.21 mMol) was refluxed in a 1:1 mixture of water and ethanol (20 cm³) with [CF₃COCH₂COCH₃] (0.5 cm³; 4.12 mMol) for 12 hours with a second addition of [CF₃COCH₂COCH₃] (0.5 cm³; 4.12 mMol) made after the first 6 hours. The mixture was reduced in volume to 5 cm³ under reduced pressure. The precipitate formed was filtered and air dried. The precipitate was

then redissolved in methanol (10 cm³) containing C₅H₅N (0.05 cm³; 0.62 mMol). The mixture was stirred for 1 hour during which time it became red in colour. The methanol was removed under reduced pressure and the residue redissolved in dichloromethane (5 cm³). The product (0.1154 g; 0.14 mMol) was precipitated by the addition of n-hexane (25 cm³), filtered off and air dried for 2 hours (Yield = 54%).

Infrared Spectrum (KBr disk)

3433b,1700w,1642w,1600s,1550s,1512w,1458m,1443s,1416s,1363w,1298s,1213m, 1187s,1137s,1064w,1030w,1003w,865w,760w,735w,697m,655w,621w,601w,422w cm⁻¹.

¹H n.m.r. spectrum (CDCl₃)

cis-isomer δ= 0.94(t,6H,CH₃CH₂CO₂H, J=7.6 Hz), 2.14(q,4H, CH₃CH₂CO₂H, J=7.6 Hz), 1.04(t,3H,CH₃CH₂CO₂, J=7.6 Hz), 1.09(t,3H,CH₃CH₂CO₂, J=7.5 Hz), 2.31(q,2H,CH₃CH₂CO₂, J=7.6 Hz), 2.40(q,2H,CH₃CH₂CO₂, J=7.5 Hz), 1.89(s,6H,CH₃COCHCOCF₃), 5.45(s,2H,CH₃COCHCOCH₃), 7.53(t,4H,*m*-H,C₅H₅N), 7.90(t,2H,*p*-H,C₅H₅N), 8.9(b,4H,*o*-H,C₅H₅N) ppm.

trans-isomer δ= 0.94(t,6H,CH₃CH₂CO₂H, J=7.6 Hz), 2.14(q,4H,CH₃CH₂CO₂H, J=7.6 Hz), 1.06(t,6H,CH₃CH₂CO₂, J=7.6 Hz), 2.36(q,4H,CH₃CH₂CO₂, J=7.6 Hz), 1.87(s,6H,CH₃COCHCOCF₃), 5.44(s,2H,CH₃COCHCOCH₃), 7.53(t,4H,*m*-H,C₅H₅N), 7.90(t,2H,*p*-H,C₅H₅N), 8.9(b,4H,*o*-H,C₅H₅N) ppm.

¹⁹F n.m.r. spectrum (CDCl₃).

cis-isomer δ= -74.15 (s,6F,CH₃COCHCOCF₃) ppm.

trans-isomer δ= -73.49 (s,6F,CH₃COCHCOCF₃) ppm.

5.6.8 Synthesis of $[\text{Rh}_2(\text{O}_2\text{CC}_2\text{H}_5)_2(\text{CF}_3\text{COCHCOCF}_3)_2(\text{C}_5\text{H}_5\text{N})_2]$.

The title compound was prepared using the method described in Section 5.6.7 for the compound $[\text{Rh}_2(\text{O}_2\text{CC}_2\text{H}_5)_2(\text{CF}_3\text{COCHCOCF}_3)_2(\text{C}_5\text{H}_5\text{N})_2]$.

Quantity of $[\text{Rh}_2(\text{O}_2\text{CC}_2\text{H}_5)_4]$ used 0.142 g; 0.28 mMol. Mass of product 0.1798 g; 0.19 mMol. (Yield = 68%).

Infrared Spectrum (KBr disk).

3449b,1634w,1600m,1542s,1470m,1443m,1424m,1342m,1301w,1263s,1213s,1145s, 1099m,1070w,1034w,1003w,946w,896w,819w,789m,751m,697s,621w,598w,536w, 420w,349w cm^{-1} .

^1H n.m.r. spectrum (CDCl_3)

$\delta = 2.07(\text{t}, 6\text{H}, \text{CH}_3\text{CH}_2\text{CO}_2, \text{J}=7.6 \text{ Hz})$, $2.35(\text{q}, 4\text{H}, \text{CH}_3\text{CH}_2\text{CO}_2, \text{J}=7.6 \text{ Hz})$,
 $5.79(\text{s}, 2\text{H}, \text{CH}_3\text{COCHCOCH}_3)$, $7.57(\text{t}, 4\text{H}, m\text{-H}, \text{C}_5\text{H}_5\text{N})$, $7.98(\text{t}, 2\text{H}, p\text{-H}, \text{C}_5\text{H}_5\text{N})$,
 $8.75(\text{d}, 4\text{H}, o\text{-H}, \text{C}_5\text{H}_5\text{N})$ ppm.

^{19}F n.m.r. spectrum (CDCl_3).

$\delta = -75.14$ (s, 12F, $\text{CF}_3\text{COCHCOCF}_3$) ppm.

5.6.9 Synthesis of $[\text{Rh}_2(\text{O}_2\text{CC}(\text{CH}_3)_3)_2(\text{CF}_3\text{COCHCOCH}_3)_2(\text{C}_5\text{H}_5\text{N})_2]$.

$[\text{Rh}_2(\text{O}_2\text{CC}(\text{CH}_3)_3)_4]$ (0.143 g; 0.23 mMol) was refluxed in ethanol (20 cm^3) with $[\text{CF}_3\text{COCH}_2\text{COCH}_3]$ (0.5 cm^3 ; 4.12 mMol) for a total of 16 hours, a second addition of $[\text{CF}_3\text{COCH}_2\text{COCH}_3]$ (0.5 cm^3 ; 4.12 mMol) being made after the first 8 hours. The ethanol was removed under reduced pressure and replaced with methanol (10 cm^3) to which $\text{C}_5\text{H}_5\text{N}$ (0.05 cm^3 ; 0.62 mMol) had been added. The

mixture was stirred for 1 hour during which time the solution became red and a pink precipitate formed. The precipitate was filtered off and air dried for 2 hours. The red filtrate was evaporated to dryness under reduced pressure. The residue was redissolved in dichloromethane (5 cm³) and a red product (0.0636 g; 0.07 mMol) precipitated by the addition of n-hexane (30 cm³). (Yield = 23% red product).

Infrared Spectrum (KBr disk)

3456b,1600s,1542s,1519s,1479s,1443s,1416s,1374w,1359m,1305s,1225s,1213s,1187s, 1137s,1068w,1034w,1007w,900w,869w,777m,758m,735w,697m,651w,636w,621m, 601w, 456w cm⁻¹.

¹H n.m.r. spectrum (CDCl₃)

cis-isomer δ= 1.09(s,9H,(CH₃)₃CCO₂), 1.11(s,9H,(CH₃)₃CCO₂), 1.90(s,6H,CH₃COCHCOCF₃), 5.49(s,2H,CH₃COCHCOCH₃), 7.43(t,4H,*m*-H,C₅H₅N), 7.83(t,2H,*p*-H,C₅H₅N), 8.64(d,4H,*o*-H,C₅H₅N) ppm.

trans-isomer δ= 1.09(s,18H,(CH₃)₃CCO₂), 1.88(s,6H,CH₃COCHCOCF₃), 5.48(s,2H,CH₃COCHCOCH₃), 7.43(t,4H,*m*-H,C₅H₅N), 7.83(t,2H,*p*-H,C₅H₅N), 8.64(d,4H,*o*-H,C₅H₅N) ppm.

¹⁹F n.m.r. spectrum (CDCl₃).

cis-isomer δ= -74.19 (s,6F,CH₃COCHCOCF₃) ppm.

trans-isomer δ= -73.71 (s,6F,CH₃COCHCOCF₃) ppm.

5.6.10 Synthesis of [Rh₂(O₂CC(CH₃)₃)₂(CF₃COCHCOCF₃)₂(C₅H₅N)₂].

The title compound was prepared using the method described in Section 5.6.9 for the compound [Rh₂(O₂CC(CH₃)₃)₂(CF₃COCHCOCH₃)₂(C₅H₅N)₂].

Quantity of $[\text{Rh}_2(\text{O}_2\text{CC}(\text{CH}_3)_3)_4]$ used 0.1377 g; 0.22 mMol. Mass of product 0.0985 g; 0.10 mMol (Yield = 45% red product).

Infrared Spectrum (KBr disk)

3478b,1634w,1607m,1542s,1519s,1481s,1447w,1420s,1378w,1363w,1343w,1263s, 1213s,1152s,1137s,1102m,1068w,1034w,1007w,946w,904w,789m,751w,697m,636w, 601w,533w,464w cm^{-1} .

^1H n.m.r. spectrum (CDCl_3)

δ = 1.06(s,6H, $(\text{CH}_3)_3\text{CCO}_2$), 5.76(s,2H, $\text{CH}_3\text{COCHCOCH}_3$), 7.54(t,4H,*m*-H, $\text{C}_5\text{H}_5\text{N}$), 7.93(t,2H,*p*-H, $\text{C}_5\text{H}_5\text{N}$), 8.77(d,4H,*o*-H, $\text{C}_5\text{H}_5\text{N}$) ppm.

^{19}F n.m.r. spectrum (CDCl_3).

δ = -75.18 (s,12F, $\text{CF}_3\text{COCHCOCF}_3$) ppm.

5.6.11 The crystal structure determination of

$[\text{Rh}_2(\text{O}_2\text{CCH}_3)_2(\text{CF}_3\text{COCHCOCF}_3)_2(\text{C}_5\text{H}_5\text{N})_2]$ (Structure 5.1).

A red crystal of the title compound suitable for x-ray crystallographic study was obtained by slow evaporation of a solution of $[\text{Rh}_2(\text{O}_2\text{CCH}_3)_2(\text{CF}_3\text{COCHCOCF}_3)_2(\text{C}_5\text{H}_5\text{N})_2]$ in a dichloromethane:n-hexane mixture (1:1). Measurements of the unit cell constants and the collection of data were performed as described in Section 3.6.3. Crystallographic parameters are presented in Table 5.6a. The positions of the rhodium atoms were derived from a three dimensional Patterson map. The positions of all other non-hydrogen atoms were determined by iterative application of least squares refinement and difference Fourier analysis. All non-hydrogen atoms were refined anisotropically and no attempt was

made to locate the hydrogen atoms. Tables 5.6b, 5.6c, and 5.6d present atomic coordinates, bond lengths and interbond angles respectively.

5.6.12 The crystal structure determination of



Crystallographic measurements were carried out as previously described on a red crystal of the title compound obtained by the slow evaporation of a solution of $[\text{Rh}_2(\text{O}_2\text{CC}(\text{CH}_3)_3)_2(\text{CF}_3\text{COCHCOCF}_3)_2(\text{C}_5\text{H}_5\text{N})_2]$ in a dichloromethane:n-hexane mixture (1:1). Crystallographic data are presented in Table 5.7a. The positions of the rhodium atoms were determined by direct methods and all other non-hydrogen atoms were located as described in Section 5.6.10. No attempt was made to locate the hydrogen atoms and all non-hydrogen atoms were refined anisotropically. Atomic co-ordinates, bond lengths and interbond angles are presented in Tables 5.7b, 5.7c and 5.7d.

5.6.13 The crystal structure determination of



Green crystals of the title compound were obtained by slow evaporation of a solution of $[\textit{trans}\text{-Rh}_2(\text{O}_2\text{CCH}_3)_2(\text{CF}_3\text{COCHCOCH}_3)_2(\text{C}_5\text{H}_5\text{N})]$ in dichloromethane, and were found to be suitable for x-ray crystallographic measurements. The structure of this compound was determined as described previously (Section 3.6.3). Crystallographic parameters are presented in Table 5.8a. The positions of the rhodium atoms was determined using direct methods. All other

non-hydrogen atoms were located as previously described (Section 5.6.10). The fluorine atoms were disordered over two sites. A satisfactory model for the disorder was found by assuming a 75% occupancy of one site (F1a-F6a attached to C9 and C14) and a 25% occupancy of the alternative site (F1b-F6b attached to C8 and C13). No attempt was made to locate the hydrogen atoms and with the exception of F3b all non-hydrogen atoms were refined anisotropically. Atomic co-ordinates, bond lengths and interbond angles are given in Tables 5.8b, 5.8c, and 5.8d.

5.6.14 The crystal structure determination of



(Structure 5.3*cis*).

X-ray crystallographic measurements were carried out on a green crystal of the title compound obtained by slow evaporation of a solution of $[cis-Rh_2(O_2CCH_3)_2(CF_3COCHCOCH_3)_2(C_5H_5N)]$ in dichloromethane. The positions of the rhodium atoms were located using direct methods and all other non-hydrogen atoms were located as previously described (Section 5.6.10). Crystallographic parameters are given in Table 5.9a. The hydrogen atoms were placed in idealised positions and assigned common isotropic temperature factors ($U = 0.08 \text{ \AA}^2$). All non-hydrogen atoms were refined anisotropically. A severely disordered molecule (most probable of solvent) was also observed in the lattice. Several attempts were made to identify this molecule, only one half of which is crystallographically unique. The most reasonable solution was that it was a pyridine molecule, however attempts to refine a chemically reasonable model did not lead to a satisfactory convergent refinement. Therefore, since this molecule did not show any short contacts with the

compound of interest, the atoms were allowed to refine freely, with an occupancy of one half (determined by previous least-squares refinement) to a chemically imperfect result, so that the more important part of the structure would not be lost. Atomic co-ordinates, bond lengths, and interbond angles are given in Tables 5.9b, 5.9c, and 5.9d.

Table 5.4 Microanalytical data for the compounds $[\text{Rh}_2(\text{O}_2\text{CR})_2(\text{R}'\text{COCHCOR}'')]_2(\text{C}_3\text{H}_5\text{N})_n$ ($n=1,2$).

Compound	Microanalytical data					
	%C		%H		%N	
	found	calc. ^a	found	calc. ^a	found	calc. ^a
$[\text{Rh}_2(\text{O}_2\text{CCH}_3)_2(\text{CH}_3\text{COCHCOCH}_3)_2(\text{C}_3\text{H}_5\text{N})]$	37.7	37.9	4.3	4.2	2.6	2.3
$[\text{Rh}_2(\text{O}_2\text{CCH}_3)_2(\text{CF}_3\text{COCHCOCH}_3)_2(\text{C}_3\text{H}_5\text{N})_2]$	36.3	36.5	3.0	3.1	3.1	3.6
$[\text{cis-Rh}_2(\text{O}_2\text{CCH}_3)_2(\text{CF}_3\text{COCHCOCH}_3)_2(\text{C}_3\text{H}_5\text{N}) \cdot 0.5\text{C}_3\text{H}_5\text{N}]$	34.3	34.5	2.9	2.9	1.8	2.8
$[\text{trans-Rh}_2(\text{O}_2\text{CCH}_3)_2(\text{CF}_3\text{COCHCOCH}_3)_2(\text{C}_3\text{H}_5\text{N})]$	32.6	32.2	2.4	2.7	1.8	2.0
$[\text{Rh}_2(\text{O}_2\text{CCH}_3)_2(\text{CF}_3\text{COCHCOCF}_3)_2(\text{C}_3\text{H}_5\text{N})_2]$	32.8	32.1	2.2	2.0	3.1	3.1
$[\text{Rh}_2(\text{O}_2\text{CC}_2\text{H}_5)_2(\text{CF}_3\text{COCHCOCH}_3)_2(\text{C}_3\text{H}_5\text{N})_2 \cdot \text{C}_2\text{H}_5\text{CO}_2\text{H}]$	39.1	39.1	3.8	3.9	3.3	3.2
$[\text{Rh}_2(\text{O}_2\text{CC}_2\text{H}_5)_2(\text{CF}_3\text{COCHCOCF}_3)_2(\text{C}_3\text{H}_5\text{N})_2]$	33.7	33.8	2.5	2.4	2.8	3.0
$[\text{Rh}_2(\text{O}_2\text{CC}(\text{CH}_3)_2)_2(\text{CF}_3\text{COCHCOCH}_3)_2(\text{C}_3\text{H}_5\text{N})_2]$	41.1	41.3	4.1	4.2	3.2	3.2
$[\text{Rh}_2(\text{O}_2\text{CC}(\text{CH}_3)_2)_2(\text{CF}_3\text{COCHCOCF}_3)_2(\text{C}_3\text{H}_5\text{N})_2]$	37.4	36.7	3.7	3.1	2.6	2.9

a) Calculated for the given formula.

Table 5.5 Tentative infrared band assignments for $[\text{Rh}_2(\text{O}_2\text{CR})_2(\text{R}'\text{COCHCOR}'')_2(\text{C}_5\text{H}_5\text{N})_2]$

Compound.	Carboxylate		β -diketonate		M-O stretch cm^{-1}
	O-C-O asym. cm^{-1}	O-C-O sym. cm^{-1}	C=O stretch cm^{-1}	C-F stretch cm^{-1}	
$[\text{Rh}_2(\text{O}_2\text{CCH}_3)_2(\text{CH}_3\text{COCHCOCH}_3)_2(\text{C}_5\text{H}_5\text{N})]$	1546	1443	1573	-	465
$[\text{Rh}_2(\text{O}_2\text{CCH}_3)_2(\text{CF}_3\text{COCHCOCH}_3)_2(\text{C}_5\text{H}_5\text{N})_2]$	1542	1443	1607	1152	a
$[\text{Rh}_2(\text{O}_2\text{CCH}_3)_2(\text{CF}_3\text{COCHCOCF}_3)_2(\text{C}_5\text{H}_5\text{N})_2]$	1558	1443	1600	1130	440
$[\text{Rh}_2(\text{O}_2\text{CC}_2\text{H}_5)_2(\text{CF}_3\text{COCHCOCH}_3)_2(\text{C}_5\text{H}_5\text{N})_2, \text{C}_2\text{H}_5\text{CO}_2\text{H}]$	1550	1416	1600	1140	420
$[\text{Rh}_2(\text{O}_2\text{CC}_2\text{H}_5)_2(\text{CF}_3\text{COCHCOCF}_3)_2(\text{C}_5\text{H}_5\text{N})_2]$	1542	1424	1600	1145	420
$[\text{Rh}_2(\text{O}_2\text{CC}(\text{CH}_3)_3)_2(\text{CF}_3\text{COCHCOCH}_3)_2(\text{C}_5\text{H}_5\text{N})_2]$	1542	1479	1600	1137	456
$[\text{Rh}_2(\text{O}_2\text{CC}(\text{CH}_3)_3)_2(\text{CF}_3\text{COCHCOCF}_3)_2(\text{C}_5\text{H}_5\text{N})_2]$	1542	1481	1607	1152/1137	465

a) not observed.

Table 5.6a Crystallographic data for the compound



Formula	$\text{C}_{24}\text{H}_{18}\text{N}_2\text{O}_8\text{F}_{12}\text{Rh}_2$
fw	872
Space group	$\text{P}\bar{1}$
a, Å	10.397(5)
b, Å	12.620(7)
c, Å	12.764(8)
α , deg	88.63(5)
β , deg	70.61(4)
γ , deg	74.20(4)
V, Å ³	1515(1)
Z	2
F(000)	876
d_{calc} , g/cm ³	1.96
Cryst. size; mm	0.3 x 0.2 x 0.03
$\mu(\text{Mo-K}\alpha)$, cm ⁻¹	11.5
Data collection instrument.	Nicolet R3m/V
Radiation.	Mo ($\lambda = 0.71073$)
Orientation reflections:	
no.; range (2θ)	19 ; $7.8 \leq 2\theta \leq 26.6$
Temp., °C	20
No. of unique data;	5690
Total with $F_o^2 \geq 1.5\sigma(F_o^2)$	3447
No. of parameters	433
R ^a	0.0812
R ^b	0.0707
Weighting scheme	$w = 1.0000/(\sigma^2F + 0.000151F^2)$
Largest shift/esd, final cycle	0.012
Largest peak, e/Å ³	1.08

$$\text{a) } R = \Sigma[|F_o| - |F_c|] / \Sigma|F_o|$$

$$\text{b) } R' = \Sigma[(|F_o| - |F_c|) \cdot w^{1/2}] / \Sigma[|F_o| \cdot w^{1/2}]$$

Table 5.6b Atomic coordinates ($\times 10^4$) and equivalent isotropic displacement parameters ($\text{\AA}^2 \times 10^3$) for the compound
 $[\text{Rh}_2(\text{O}_2\text{CCH}_3)_2(\text{CF}_3\text{COCHCOCF}_3)_2(\text{C}_5\text{H}_5\text{N})_2]$.

Atom	x	y	z	U(eq) ^a
Rh1	293(1)	2098(1)	3329(1)	38(1)
Rh2	2956(1)	1653(1)	2441(1)	37(1)
N1	-2012(11)	2287(9)	4372(9)	41(5)
N2	5302(11)	1043(9)	1851(9)	41(5)
O1	-26(9)	3719(7)	3597(8)	45(4)
O2	669(10)	1870(7)	4785(7)	44(4)
O3	582(10)	452(7)	3092(8)	45(4)
O4	-155(9)	2244(7)	1893(7)	43(4)
O5	3149(10)	3080(8)	2933(8)	53(4)
O6	2989(10)	1176(7)	3950(8)	46(4)
O7	2843(10)	164(7)	2001(8)	51(4)
O8	3032(10)	2095(8)	903(8)	52(4)
F1	-870(13)	3961(9)	-77(8)	94(6)
F2	-2354(11)	3163(10)	853(9)	99(6)
F3	-283(12)	2216(8)	-96(8)	92(6)
F4	-72(24)	6118(11)	2594(12)	204(14)
F5	-249(26)	5728(10)	4101(15)	188(14)
F6	-1893(16)	6080(12)	3712(27)	291(20)
F7	4440(18)	2365(15)	-1275(10)	180(10)
F8	3516(23)	4011(14)	-1007(12)	183(13)

Table 5.6b cont'd

F9	2315(18)	3006(18)	-850(11)	179(12)
F10	4988(12)	4530(9)	2666(11)	108(7)
F11	2931(15)	5023(10)	3783(13)	122(8)
F12	3406(16)	5674(9)	2210(13)	131(9)
C1	1889(15)	1430(10)	4792(11)	39(6)
C2	2069(17)	1139(13)	5922(12)	62(7)
C3	1727(14)	-145(10)	2439(12)	42(6)
C4	1785(16)	-1317(11)	2134(13)	60(7)
C5	-395(14)	4405(10)	2944(11)	42(6)
C6	-641(15)	4198(11)	1965(12)	52(6)
C7	-519(14)	3156(11)	1532(10)	44(5)
C8	-998(18)	3108(13)	526(12)	58(7)
C9	-619(20)	5570(13)	3324(17)	69(9)
C10	3363(15)	3822(12)	2243(16)	61(7)
C11	3443(17)	3847(14)	1123(15)	67(8)
C12	3283(15)	2991(13)	560(13)	58(7)
C13	3422(21)	3075(21)	-635(16)	90(10)
C14	3649(23)	4757(15)	2776(22)	86(11)
C15	-2301(15)	1546(11)	5135(12)	50(6)
C16	-3654(16)	1615(14)	5840(13)	68(8)
C17	-4729(16)	2479(13)	5802(13)	62(7)
C18	-4504(18)	3262(15)	5049(17)	77(9)
C19	-3119(17)	3137(12)	4358(14)	60(7)
C20	6073(16)	363(14)	914(12)	63(7)

Table 5.6b cont'd

C21	7520(17)	-76(15)	592(14)	72(8)
C22	8211(17)	167(13)	1266(14)	61(8)
C23	7474(15)	860(12)	2203(11)	47(6)
C24	6018(14)	1276(12)	2487(11)	48(6)

a) Equivalent isotropic U defined as 1/3 of the trace of the orthogonalized U_{ij} tensor.

Table 5.6c Bond lengths (Å) for the compound



Rh1-Rh2	2.523(3)	Rh1-N1	2.271(11)
Rh1-O1	1.999(8)	Rh1-O2	2.022(8)
Rh1-O3	2.032(8)	Rh1-O4	2.028(8)
Rh2-N2	2.212(10)	Rh2-O5	2.003(9)
Rh2-O6	2.013(8)	Rh2-O7	2.019(9)
Rh2-O8	2.009(9)	N1-C15	1.352(16)
N1-C19	1.348(17)	N2-C20	1.360(17)
N2-C24	1.354(16)	O1-C5	1.261(15)
O2-C1	1.241(15)	O3-C3	1.250(15)
O4-C7	1.239(15)	O5-C10	1.282(17)
O6-C1	1.251(15)	O7-C3	1.271(15)
O8-C12	1.264(16)	F1-C8	1.318(16)
F2-C8	1.314(18)	F3-C8	1.284(17)
F4-C9	1.225(20)	F5-C9	1.216(20)
F6-C9	1.237(21)	F8-C13	1.279(24)
F7-C13	1.239(24)	F10-C14	1.302(21)
F9-C13	1.293(22)	F12-C14	1.359(22)
F11-C14	1.252(24)	C1-C2	1.538(18)
C3-C4	1.518(17)	C5-C6	1.400(18)
C5-C9	1.491(19)	C6-C7	1.395(19)
C7-C8	1.531(18)	C11-C10	1.404(22)
C10-C14	1.519(24)	C12-C11	1.388(22)
C12-C13	1.487(23)	C15-C16	1.375(20)

Table 5.6 c cont'd

C16-C17	1.346(20)	C17-C18	1.374(23)
C18-C19	1.384(22)	C20-C21	1.373(21)
C21-C22	1.375(21)	C22-C23	1.364(20)
C23-C24	1.382(18)		

Table 5.6d Bond angles (°) for the compound



N1-Rh1-Rh2	169.3(3)	O1-Rh1-Rh2	95.5(3)
O1-Rh1-N1	89.6(4)	O1-Rh1-O2	88.7(4)
O1-Rh1-O3	178.6(4)	O2-Rh1-Rh2	85.4(3)
O2-Rh1-N1	85.3(4)	O3-Rh1-Rh2	85.8(3)
O3-Rh1-N1	89.2(4)	O3-Rh1-O2	90.5(4)
O4-Rh1-Rh2	96.7(3)	O4-Rh1-N1	92.3(4)
O4-Rh1-O1	94.4(3)	O4-Rh1-O2	176.0(4)
O4-Rh1-O3	86.3(4)	N2-Rh2-Rh1	170.6(3)
O5-Rh2-Rh1	96.9(3)	O5-Rh2-N2	87.4(4)
O5-Rh2-O6	85.4(4)	O5-Rh2-O7	176.3(4)
O5-Rh2-O8	94.7(4)	O6-Rh2-Rh1	84.8(3)
O6-Rh2-N2	87.2(4)	O7-Rh2-Rh1	85.0(3)
O7-Rh2-N2	90.3(4)	O7-Rh2-O6	91.6(4)
O8-Rh2-Rh1	98.1(3)	O8-Rh2-N2	89.8(4)
O8-Rh2-O6	177.1(4)	O8-Rh2-O7	88.2(4)
C15-N1-Rh1	118.2(8)	C19-N1-Rh1	124.9(9)
C19-N1-C15	116.6(12)	C20-N2-Rh2	123.2(9)
C24-N2-Rh2	119.4(9)	C24-N2-C20	117.2(11)
C5-O1-Rh1	122.0(8)	C1-O2-Rh1	120.5(8)
C3-O3-Rh1	120.4(8)	C7-O4-Rh1	121.6(8)
C10-O5-Rh2	120.4(10)	C1-O6-Rh2	121.3(8)
C3-O7-Rh2	121.4(9)	C12-O8-Rh2	121.7(10)
O6-C1-O2	125.4(12)	C2-C1-O2	117.7(12)

Table 5.6d cont'd

C2-C1-O6	116.9(12)	O7-C3-O3	124.6(11)
C4-C3-O3	117.8(12)	C4-C3-O7	117.6(12)
C6-C5-O1	128.1(12)	C9-C5-O1	113.0(12)
C9-C5-C6	118.9(13)	C7-C6-C5	125.1(12)
C6-C7-O4	128.7(12)	C8-C7-O4	113.7(12)
C8-C7-C6	117.3(12)	F2-C8-F1	105.3(12)
F3-C8-F1	109.0(14)	F3-C8-F2	109.0(15)
C7-C8-F1	111.7(13)	C7-C8-F2	110.6(13)
C7-C8-F3	111.1(12)	F5-C9-F4	104.9(20)
F6-C9-F4	106.2(20)	F6-C9-F5	99.6(21)
C5-C9-F4	114.4(16)	C5-C9-F5	117.9(15)
C5-C9-F6	112.3(16)	C11-C10-O5	130.5(14)
C14-C10-O5	110.2(16)	C14-C10-C11	119.3(16)
C13-C12-O8	111.3(17)	C11-C12-O8	129.8(14)
C10-C11-C12	122.5(14)	C13-C12-C11	118.9(15)
F8-C13-F7	106.7(17)	F9-C13-F7	105.8(24)
F9-C13-F8	100.2(20)	C12-C13-F7	114.2(18)
C12-C13-F8	114.8(22)	C12-C13-F9	113.9(14)
F11-C14-F10	108.3(21)	F12-C14-F10	104.5(16)
F12-C14-F11	107.4(18)	C10-C14-F10	110.6(16)
C10-C14-F11	116.1(17)	C10-C14-F12	109.3(18)
C16-C15-N1	122.7(13)	C17-C16-C15	118.8(14)
C18-C17-C16	121.2(15)	C19-C18-C17	116.9(15)

Table 5.6d cont'd

C18-C19-N1	123.7(15)	C21-C20-N2	123.0(14)
C22-C21-C20	118.2(16)	C23-C22-C21	120.3(15)
C24-C23-C22	118.9(13)	C23-C24-N2	122.3(12)

Table 5.7a Crystallographic data for the compound



Formula	$\text{C}_{30}\text{H}_{30}\text{N}_2\text{O}_8\text{F}_{12}\text{Rh}_2$
fw	980
Space group	$P2_1/c$
a, Å	11.298(3)
b, Å	18.226(3)
c, Å	20.665(3)
α , deg	90
β , deg	105.2(2)
γ , deg	90
V, Å ³	4108(1)
Z	4
F(000)	1944
d_{calc} , g/cm ³	1.59
Cryst. size; mm	0.3 X 0.3 X 0.4
$\mu(\text{Mo-K}\alpha)$, cm ⁻¹	8.54
Data collection instrument.	Nicolet R3m/V
Radiation.	Mo ($\lambda = 0.71073$)
Orientation reflections:	
no.; range (2θ)	29 ; $10.8 \leq 2\theta \leq 30.0$
Temp., °C	20
No. of unique data;	10260
Total with $F_o^2 \geq 3\sigma(F_o^2)$	6340
No. of parameters	487
R ^a	0.0593
R ^b	0.0605
Weighting scheme	$w = 1.0000/(\sigma^2F + 0.000386F^2)$
Largest shift/esd, final cycle	0.021
Largest peak, e/Å ³	1.01

$$\text{a) } R = \Sigma[|F_o| - |F_c|] / \Sigma|F_o|$$

$$\text{b) } R' = \Sigma[(|F_o| - |F_c|) \cdot w^{1/2}] / \Sigma[|F_o| \cdot w^{1/2}]$$

Table 5.7b Atomic coordinates ($\times 10^4$) and equivalent isotropic displacement parameters ($\text{\AA}^2 \times 10^3$) for the compound
 $[\text{Rh}_2(\text{O}_2\text{CC}(\text{CH}_3)_3)_2(\text{CF}_3\text{COCHCOCF}_3)_2(\text{C}_5\text{H}_5\text{N})_2]$.

Atom	x	y	z	U(eq) ^a
Rh1	2026(1)	3259(1)	2443(1)	44(1)
Rh2	1396(1)	4491(1)	1950(1)	41(1)
O1	2324(4)	2822(2)	1610(2)	49(2)
O2	255(4)	2979(2)	2037(2)	54(2)
O3	1642(4)	3672(3)	3276(2)	55(2)
O4	3802(4)	3504(3)	2855(2)	53(2)
O5	2273(4)	4439(2)	1219(2)	47(2)
O6	-37(4)	3948(2)	1346(2)	50(2)
O7	535(4)	4591(2)	2696(2)	52(2)
O8	2737(4)	5047(2)	2587(2)	50(2)
N1	2425(5)	2157(3)	2920(3)	58(2)
N2	645(5)	5562(3)	1497(3)	49(2)
C1	-353(6)	3324(4)	1538(3)	50(2)
C2	-1535(7)	2990(5)	1110(4)	71(3)
C3	961(6)	4226(4)	3226(3)	51(2)
C4	638(9)	4490(4)	3864(4)	72(3)
C5	3389(7)	2762(3)	1534(3)	52(2)
C6	4508(7)	2973(4)	1954(4)	66(3)
C7	4602(6)	3317(4)	2566(4)	57(3)
C8	5862(8)	3480(6)	2961(5)	105(5)

Table 5.7b cont'd

C9	3384(7)	2373(4)	873(3)	76(3)
C10	3271(7)	4766(4)	1281(3)	54(2)
C11	3988(7)	5163(4)	1821(4)	65(3)
C12	3675(7)	5263(4)	2415(4)	59(3)
C13	4519(8)	5720(5)	2957(4)	85(4)
C14	3723(7)	4737(4)	664(4)	74(3)
C15	-2430(14)	3534(9)	845(13)	279(13)
C16	-2009(11)	2391(7)	1511(6)	131(6)
C17	-1151(17)	2589(13)	560(7)	226(12)
C18	609(26)	5266(7)	3883(8)	254(16)
C19	-715(17)	4277(17)	3756(10)	285(17)
C20	1311(21)	4084(10)	4458(5)	212(11)
C21	3122(7)	2111(4)	3557(4)	67(3)
C22	3361(9)	1440(5)	3883(4)	84(4)
C23	2821(9)	811(5)	3556(5)	80(4)
C24	2088(8)	850(4)	2914(5)	79(4)
C25	1927(6)	1544(4)	2606(4)	69(3)
C26	56(7)	5584(4)	842(3)	56(3)
C27	-422(7)	6227(4)	519(4)	69(3)
C28	-282(8)	6869(4)	896(5)	77(4)
C29	310(8)	6861(4)	1567(5)	72(3)
C30	766(7)	6188(4)	1860(4)	61(3)
F1	5981(7)	3724(10)	3540(5)	301(9)

Table 5.7b cont'd

F2	6414(10)	3983(8)	2709(7)	261(8)
F3	6678(7)	3005(6)	2994(6)	219(6)
F4	2600(6)	2670(3)	367(2)	118(3)
F5	4459(5)	2348(4)	745(3)	132(3)
F6	3061(8)	1688(3)	896(3)	135(4)
F7	4035(7)	6337(4)	3033(5)	190(5)
F8	5561(6)	5859(6)	2870(4)	195(5)
F9	4704(9)	5436(5)	3541(3)	186(5)
F10	4364(9)	5236(5)	553(4)	194(5)
F11	4373(13)	4192(7)	637(5)	275(8)
F12	2907(7)	4697(6)	109(3)	164(5)

a) Equivalent isotropic U defined as 1/3 of the trace of the orthogonalized U_{ij} tensor.

Table 5.7c Bond lengths (Å) for the compound



Rh1-Rh2	2.492(1)	Rh1-O1	2.004(4)
Rh1-O2	2.023(4)	Rh1-O3	2.027(4)
Rh1-O4	2.013(4)	Rh1-N1	2.232(5)
Rh2-O5	2.014(4)	Rh2-O6	2.025(4)
Rh2-O7	2.035(4)	Rh2-O8	2.003(4)
Rh2-N2	2.233(5)	O1-C5	1.258(8)
O2-C1	1.247(7)	O3-C3	1.256(8)
O4-C7	1.253(8)	O5-C10	1.252(8)
O8-C12	1.265(8)	O7-C3	1.264(8)
O6-C1	1.285(7)	N1-C21	1.347(9)
N1-C25	1.338(9)	N2-C26	1.342(8)
N2-C30	1.353(8)	C3-C4	1.535(10)
C2-C16	1.548(12)	C4-C20	1.465(14)
C2-C17	1.508(17)	C1-C2	1.522(9)
C4-C18	1.415(14)	C2-C15	1.420(17)
C4-C19	1.536(19)	C5-C6	1.387(10)
C5-C9	1.538(9)	C6-C7	1.392(10)
C7-C8	1.473(11)	C8-F1	1.249(8)
C8-F2	1.294(8)	C9-F4	1.297(7)
C8-F3	1.254(8)	C9-F6	1.304(7)
C9-F5	1.310(7)	C10-C11	1.397(10)
C10-C14	1.494(9)	C11-C12	1.377(10)
C12-C13	1.515(10)	C13-F9	1.277(7)

Table 5.7c cont'd

C13-F7	1.279(7)	C14-F11	1.246(7)
C13-F8	1.262(7)	C14-F12	1.271(7)
C14-F10	1.258(7)	C21-C22	1.388(11)
C22-C23	1.388(13)	C23-C24	1.370(12)
C24-C25	1.407(11)	C26-C27	1.387(100)
C27-C28	1.392(12)	C28-C29	1.372(12)
C29-C30	1.405(10)		

Table 5.7d Bond angles (°) for the compound



O1-Rh1-Rh2	95.8(1)	O2-Rh1-Rh2	84.9(1)
O2-Rh1-O1	85.0(2)	O3-Rh1-Rh2	84.9(1)
O3-Rh1-O1	177.0(2)	O3-Rh1-O2	92.1(2)
O4-Rh1-Rh2	96.9(1)	O4-Rh1-O1	94.5(2)
O4-Rh1-O2	178.2(2)	O4-Rh1-O3	88.3(2)
N1-Rh1-Rh2	174.4(2)	N1-Rh1-O1	87.8(2)
N1-Rh1-O2	91.1(2)	N1-Rh1-O3	91.3(2)
N1-Rh1-O4	87.1(2)	O5-Rh2-Rh1	96.9(1)
O6-Rh2-O5	89.2(2)	O6-Rh2-Rh1	176.1(2)
O6-Rh2-O7	92.7(2)	O6-Rh2-O8	174.5(1)
O8-Rh2-Rh1	95.8(1)	O7-Rh2-O5	177.5(2)
O7-Rh2-Rh1	85.0(1)	O8-Rh2-O5	94.6(2)
O7-Rh2-O8	83.5(2)	N2-Rh2-Rh1	174.5(1)
N2-Rh2-O5	86.3(2)	N2-Rh2-O6	90.8(2)
N2-Rh2-O7	92.0(2)	N2-Rh2-O8	88.4(2)
C5-O1-Rh1	121.5(4)	C1-O2-Rh1	119.1(4)
C3-O3-Rh1	119.5(4)	C7-O4-Rh1	120.1(4)
C10-O5-Rh2	120.5(4)	C1-O6-Rh2	118.9(4)
C3-O7-Rh2	117.4(4)	C12-O8-Rh2	121.2(4)
C21-N1-Rh1	119.1(5)	C25-N1-Rh1	121.7(5)
C25-N1-C21	119.1(6)	C26-N2-Rh2	118.8(4)
C30-N2-Rh2	122.1(4)	C30-N2-C26	119.0(6)
C2-C1-O2	119.1(6)	O6-C1-O2	124.4(6)

Table 5.7d cont'd.

C16-C2-C1	110.2(7)	C2-C1-O6	116.5(6)
C15-C2-C16	112.8(12)	C15-C2-C1	111.9(9)
C17-C2-C16	105.6(11)	C17-C2-C1	104.5(8)
O7-C3-O3	125.4(6)	C17-C2-C15	111.4(14)
C4-C3-O7	117.2(6)	C4-C3-O3	117.4(6)
C20-C4-C3	111.9(8)	C18-C4-C3	110.5(8)
C19-C4-C3	104.3(9)	C20-C4-C18	119.5(13)
C19-C4-C20	105.8(15)	C19-C4-C18	103.2(16)
C6-C5-O1	129.9(6)	C9-C5-O1	111.7(6)
C9-C5-C6	118.3(6)	C7-C6-C5	122.3(7)
C6-C7-O4	131.5(7)	C8-C7-O4	113.2(7)
C8-C7-C6	115.3(7)	F3-C8-C7	118.7(8)
F1-C8-C7	116.6(8)	F1-C8-F3	107.5(11)
F2-C8-C7	114.7(9)	F2-C8-F3	94.9(10)
F2-C8-F1	101.0(12)	F4-C9-C5	111.4(6)
F5-C9-C5	114.1(6)	F5-C9-F4	108.9(7)
F6-C9-C5	110.1(6)	F6-C9-F4	106.9(7)
F6-C9-F5	105.0(7)	C11-C10-O5	130.3(6)
C14-C10-O5	113.3(6)	C14-C10-C11	116.3(6)
C12-C11-C10	123.4(7)	C11-C12-O8	129.7(7)
C13-C12-O8	112.0(6)	C13-C12-C11	118.2(7)
F7-C13-C12	111.5(7)	F9-C13-C12	113.0(7)
F9-C13-F7	102.1(9)	F8-C13-C12	115.8(7)
F8-C13-F7	106.6(9)	F8-C13-F9	106.7(9)

Table 5.7d cont'd

F12-C14-C10	116.3(7)	F10-C14-C10	118.1(7)
F10-C14-F12	101.3(8)	F11-C14-C10	113.8(7)
F11-C14-F12	102.1(9)	F11-C14-F10	103.0(10)
C22-C21-N1	121.2(8)	C23-C22-C21	119.2(8)
C24-C23-C22	120.3(8)	C25-C24-C23	117.3(8)
C24-C25-N1	122.9(8)	C27-C26-N2	122.6(7)
C28-C27-C26	117.9(7)	C29-C28-C27	120.7(7)
C30-C29-C28	118.1(7)	C29-C30-N2	121.7(7)

Table 5.8a Crystallographic data for the compound



Formula	$\text{C}_{19}\text{H}_{19}\text{NO}_8\text{F}_6\text{Rh}_2$
fw	709
Space group	$\text{P2}_1/\text{n}$
a, Å	9.660(2)
b, Å	19.976(3)
c, Å	13.202(2)
α , deg	90
β , deg	106.54(2)
γ , deg	90
V, Å ³	2442(1)
Z	4
F(000)	1392
d_{calc} , g/cm ³	1.93
Cryst. size; mm	0.14 x 0.30 x 0.30
$\mu(\text{Mo-K}\alpha)$, cm ⁻¹	13.83
Data collection instrument.	Nicolet R3m/V
Radiation.	Mo ($\lambda = 0.71073\text{Å}$)
Orientation reflections:	
no.; range (2θ)	50 ; $19.8 \leq 2\theta \leq 33.1$
Temp., °C	20
No. of unique data;	4322
Total with $F_o^2 \geq 1.5\sigma(F_o^2)$	2951
No. of parameters	374
R ^a	0.0776
R ^b	0.0604
Weighting scheme	$w = 1.0000/(\sigma^2F + 0.00088F^2)$
Largest shift/esd, final cycle	0.026
Largest peak, e/Å ³	1.006

$$\text{a) } R = \Sigma[|F_o| - |F_c|] / \Sigma|F_o|$$

$$\text{b) } R' = \Sigma[(|F_o| - |F_c|) \cdot w^{1/2}] / \Sigma[|F_o| \cdot w^{1/2}]$$

Table 5.8b Atomic coordinates ($\times 10^4$) and equivalent isotropic displacement parameters ($\text{\AA}^2 \times 10^3$) for the compound
 $[\textit{trans}\text{-Rh}_2(\text{O}_2\text{CCH}_3)_2(\text{CF}_3\text{COCHCOCH}_3)_2(\text{C}_5\text{H}_5\text{N})]$.

Atom	x	y	z	U(eq) ^a
Rh1	2640(1)	9074(1)	3275(1)	35(1)
Rh2	634(1)	9569(1)	1789(1)	41(1)
O1	1104(10)	8470(4)	3547(7)	46(4)
O2	2192(10)	9803(4)	4198(6)	43(3)
O3	3097(11)	8322(4)	2412(7)	48(4)
O4	4246(10)	9666(4)	3141(7)	43(3)
O5	-608(10)	8828(5)	2139(7)	54(4)
O6	257(10)	10153(4)	2944(7)	47(4)
O7	849(10)	9014(4)	581(7)	48(4)
O8	1737(10)	10337(4)	1446(7)	47(4)
N1	4096(12)	8634(5)	4639(8)	42(4)
C1	-178(16)	8452(7)	2934(11)	49(6)
C2	-1161(16)	7929(8)	3165(14)	72(7)
C3	1098(17)	10178(7)	3857(11)	47(6)
C4	814(18)	10728(7)	4581(12)	64(7)
C5	4216(20)	8359(7)	2097(11)	56(7)
C6	5246(17)	8863(8)	2196(12)	59(6)
C7	5173(16)	9482(7)	2697(10)	48(5)
C8	6407(20)	9971(9)	2754(16)	74(8)
C9	4471(15)	7730(8)	1489(11)	78(8)

Table 5.8b cont'd

C10	1400(17)	9222(7)	-101(11)	55(6)
C11	2064(16)	9848(7)	-142(10)	53(6)
C12	2179(14)	10336(7)	654(11)	45(5)
C13	1419(22)	8725(8)	-955(13)	67(7)
C14	3025(16)	10945(8)	566(10)	93(9)
C15	3986(18)	7959(6)	4776(12)	61(6)
C16	4878(19)	7637(8)	5683(12)	71(7)
C17	5842(17)	8019(7)	6463(12)	59(6)
C18	5953(16)	8712(7)	6280(10)	53(6)
C19	5044(14)	8994(6)	5375(10)	41(5)
F1a	3379(15)	7624(7)	668(10)	99(7)
F2a	5596(16)	7751(8)	1129(14)	139(9)
F3a	4587(22)	7216(7)	2089(12)	140(10)
F4a	3270(24)	11067(10)	-316(11)	171(11)
F5a	2395(21)	11496(8)	676(20)	175(14)
F6a	4214(14)	11018(8)	1324(11)	129(7)
F1b	7432(34)	9659(16)	2505(32)	85(18)
F2b	6589(56)	10326(24)	3597(30)	139(29)
F3b	5792(60)	10355(25)	1957(32)	158(21)
F4b	2152(75)	8204(22)	-515(28)	188(44)
F5b	174(33)	8440(25)	-1334(36)	141(30)
F6b	2006(50)	8917(19)	-1676(30)	112(25)

a) Equivalent isotropic U defined as 1/3 of the trace of the orthogonalized U_{ij} tensor.

Table 5.8c Bond lengths (Å) for the compound

[*trans*-Rh₂(O₂CCH₃)₂(CF₃COCHCOCH₃)₂(C₅H₅N)].

Rh1-Rh2	2.534(1)	Rh1-O1	2.022(8)
Rh1-O2	2.023(8)	Rh1-O3	2.008(9)
Rh1-O4	1.998(8)	Rh1-N1	2.133(10)
Rh2-O5	2.039(9)	Rh2-O6	2.033(9)
Rh2-O7	2.001(9)	Rh2-O8	1.993(9)
O1-C1	1.272(15)	O2-C3	1.268(16)
O3-C5	1.266(18)	O4-C7	1.258(15)
O5-C1	1.262(15)	O6-C3	1.249(15)
O7-C10	1.241(16)	O8-C12	1.238(15)
N1-C15	1.368(15)	N1-C19	1.339(14)
C1-C2	1.500(19)	C3-C4	1.532(18)
C5-C6	1.395(21)	C5-C9	1.547(19)
C6-C7	1.414(19)	C7-C8	1.527(21)
C8-F1b	1.290(10)	C8-F2b	1.288(10)
C8-F3b	1.301(10)	C9-F1a	1.297(9)
C9-F2a	1.305(9)	C9-F3a	1.283(9)
C10-C11	1.413(19)	C10-C13	1.505(19)
C11-C12	1.415(18)	C12-C14	1.487(18)
C13-F4b	1.300(10)	C13-F5b	1.296(10)
C13-F6b	1.297(10)	C14-F4a	1.277(9)
C14-F5a	1.286(9)	C14-F6a	1.299(9)
C15-C16	1.416(19)	C16-C17	1.401(19)
C17-C18	1.413(18)	C18-C19	1.385(17)

Table 5.8d Bond angles (°) for the compound

[*trans*-Rh₂(O₂CCH₃)₂(CF₃COCHCOCH₃)₂(C₅H₅N)].

O1-Rh1-Rh2	86.1(2)	O2-Rh1-Rh2	86.4(3)
O2-Rh1-O1	91.7(4)	O3-Rh1-Rh2	95.5(2)
O3-Rh1-O1	86.9(4)	O3-Rh1-O2	177.5(4)
O4-Rh1-Rh2	98.2(2)	O4-Rh1-O1	175.0(4)
O4-Rh1-O2	86.1(4)	O4-Rh1-O3	95.2(4)
N1-Rh1-Rh2	171.8(3)	N1-Rh1-O1	86.9(4)
N1-Rh1-O2	89.5(4)	N1-Rh1-O3	88.4(4)
N1-Rh1-O4	88.7(4)	O5-Rh2-Rh1	84.9(3)
O6-Rh2-Rh1	84.5(3)	O6-Rh2-O5	90.2(4)
O7-Rh2-Rh1	99.8(2)	O7-Rh2-O5	88.8(4)
O7-Rh2-O6	175.5(4)	O8-Rh2-Rh1	97.8(2)
O8-Rh2-O5	176.0(4)	O8-Rh2-O6	87.1(4)
O8-Rh2-O7	93.6(4)	C1-O1-Rh1	122.4(8)
C3-O2-Rh1	120.7(8)	C5-O3-Rh1	119.3(9)
C7-O4-Rh1	122.8(9)	C1-O5-Rh2	123.1(9)
C3-O6-Rh2	122.7(9)	C10-O7-Rh2	123.8(9)
C12-O8-Rh2	121.7(9)	C15-N1-Rh1	117.4(9)
C19-N1-Rh1	122.8(8)	C19-N1-C15	119.8(11)
O5-C1-O1	122.8(13)	C2-C1-O1	116.6(12)
C2-C1-O5	120.5(13)	O6-C3-O2	124.5(13)
C4-C3-O2	118.7(13)	C4-C3-O6	116.6(14)
C6-C5-O3	131.6(14)	C9-C5-O3	113.6(14)
C9-C5-C6	114.8(15)	C7-C6-C5	123.1(14)

Table 5.8d cont'd

C6-C7-O4	127.7(14)	C8-C7-O4	116.0(14)
C8-C7-C6	116.2(14)	F1b-C8-C7	108.8(22)
F2b-C8-C7	108.0(22)	F2b-C8-F1b	124.1(37)
F3b-C8-C7	99.6(31)	F3b-C8-F1b	106.5(36)
F3b-C8-F2b	107.1(41)	F1a-C9-C5	110.8(12)
F2a-C9-C5	115.8(14)	F2a-C9-F1a	105.3(14)
F3a-C9-C5	109.2(13)	F3a-C9-F1a	107.0(15)
F3a-C9-F2a	108.4(17)	C11-C10-O7	128.1(13)
C13-C10-O7	115.0(15)	C13-C10-C11	116.8(15)
C12-C11-C10	121.5(13)	C11-C12-O8	131.0(13)
C14-C12-O8	113.2(12)	C14-C12-C11	115.8(13)
F4b-C13-C10	108.3(22)	F5b-C13-C10	111.8(23)
F5b-C13-F4b	98.4(42)	F6b-C13-C10	117.1(24)
F6b-C13-F4b	105.6(38)	F6b-C13-F5b	113.5(33)
F4a-C14-C12	118.4(14)	F5a-C14-C12	113.7(14)
F5a-C14-F4a	99.0(17)	F6a-C14-C12	114.7(12)
F6a-C14-F4a	109.2(16)	F6a-C14-F5a	99.2(17)
C16-C15-N1	120.5(13)	C17-C16-C15	119.4(13)
C18-C17-C16	118.3(13)	C19-C18-C17	119.1(13)
C18-C19-N1	122.8(12)		

Table 5.9a Crystallographic data for the compound



Formula	$C_{21.5}H_{21.5}N_{1.5}O_8F_6Rh_2$
fw	749
Space group	C2/c
a, Å	20.967(7)
b, Å	13.160(3)
c, Å	20.726(7)
α , deg	90
β , deg	114.6(3)
γ , deg	90
V, Å ³	5197(1)
Z	8
F(000)	2944
d_{calc} , g/cm ³	1.91
Cryst. size; mm	0.06 x 0.12 x 0.30
$\mu(Mo-K\alpha)$, cm ⁻¹	13.38
Data collection instrument.	Nicolet R3m/V
Radiation.	Mo ($\lambda = 0.71073$ Å)
Orientation reflections:	
no.; range (2θ)	28 ; $6.7 \leq 2\theta \leq 22.6$
Temp., °C	20
No. of unique data;	4509
Total with $F_o^2 \geq 3\sigma(F_o^2)$	2651
No. of parameters	339
R ^a	0.0634
R ^b	0.0624
Weighting scheme	$w = 1.0000/(\sigma^2F + 0.000543F^2)$
Largest shift/esd, final cycle	0.019
Largest peak, e/Å ³	1.02

$$a) R = \Sigma[|F_o| - |F_c|] / \Sigma|F_o|$$

$$b) R' = \Sigma[(|F_o| - |F_c|) \cdot w^{1/2}] / \Sigma[|F_o| \cdot w^{1/2}]$$

Table 5.9b Atomic co-ordinates ($\times 10^4$) and equivalent isotropic displacement parameters ($\text{\AA}^2 \times 10^3$) for the compound

[*cis*-Rh₂(O₂CCH₃)₂(CF₃COCHCOCH₃)₂(C₅H₅N).0.5C₅H₅N].

Atom	x	y	z	U(eq) ^a
Rh1	2732(1)	4458(1)	1080(1)	39(1)
Rh2	2977(1)	6185(1)	705(1)	43(1)
O1	3461(5)	4816(7)	2055(4)	52(4)
O2	3472(5)	3948(7)	770(5)	50(4)
O3	1994(6)	4843(7)	1419(5)	55(5)
O4	2032(5)	4068(7)	113(5)	53(4)
O5	3601(5)	6390(7)	1749(5)	63(5)
O6	3792(5)	5502(8)	595(6)	65(5)
O7	2192(5)	6923(7)	818(5)	51(4)
O8	2430(5)	6011(7)	-342(4)	51(4)
N1	2641(5)	2974(7)	1448(5)	42(5)
C1	3734(7)	5686(12)	2193(7)	53(6)
C2	4243(9)	5891(12)	29392(8)	76(8)
C3	3839(7)	4538(11)	608(7)	49(6)
C4	4395(9)	4128(14)	399(10)	86(10)
C5	1351(8)	4574(11)	1027(9)	58(7)
C6	1055(9)	4194(11)	351(9)	66(8)
C7	1397(9)	4003(11)	-78(8)	60(7)
C8	974(8)	3646(13)	-827(7)	75(7)
C9	917(10)	4628(17)	1463(10)	81(10)

Table 5.9b cont'd.

C10	1648(8)	7158(11)	308(8)	54(7)
C11	1451(7)	6988(11)	-414(8)	59(7)
C12	1836(8)	6398(10)	-709(7)	51(6)
C13	11105(12)	7655(16)	497(12)	90(12)
C14	1552(10)	6221(12)	-1489(7)	85(9)
C15	2672(7)	2847(11)	2112(8)	54(7)
C16	2597(8)	1913(11)	2370(8)	62(7)
C17	2431(10)	1097(12)	1926(9)	75(9)
C18	2381(8)	1204(12)	1249(9)	66(8)
C19	2498(7)	2150(10)	1045(7)	50(6)
F1	1055(8)	5333(10)	1884(8)	144(9)
F2	217(7)	4617(14)	1045(7)	153(9)
F3	1006(8)	3791(12)	1839(8)	153(10)
F4	909(7)	6993(10)	882(8)	144(9)
F5	1354(7)	8450(11)	896(7)	127(8)
F6	519(6)	7955(10)	-37(7)	120(7)
N2	0	8388(25)	2500	145(10)
C20	415(20)	6871(35)	2454(22)	222(19)
C21	534(8)	7482(14)	2304(9)	51(4)
C22	470(10)	7860(16)	2085(11)	79(6)

a) Equivalent isotropic U defined as 1/3 of the trace of the orthogonalized U_{ij} tensor.

Table 5.9c Bond lengths (Å) for the compound



Rh1-Rh2	2.522(2)	Rh1-O1	2.016(7)
Rh1-O2	2.026(11)	Rh1-O3	2.012(13)
Rh1-O4	1.995(8)	Rh1-N1	2.134(10)
Rh2-O5	2.026(9)	Rh2-O6	2.025(12)
Rh2-O7	2.007(11)	Rh2-O8	1.999(8)
O1-C1	1.259(18)	O2-C3	1.236(19)
O3-C5	1.300(17)	O4-C7	1.235(20)
O5-C1	1.253(18)	O6-C3	1.273(17)
O7-C10	1.229(15)	O8-C12	1.265(16)
N1-C15	1.361(20)	N1-C19	1.324(17)
C1-C2	1.491(18)	C3-C4	1.501(28)
C5-C6	1.369(23)	C5-C9	1.530(33)
C6-C7	1.375(30)	C7-C8	1.505(19)
C9-F1	1.222(26)	C9-F2	1.356(21)
C9-F3	1.316(27)	C10-C11	1.393(23)
C10-C13	1.499(33)	C11-C12	1.429(25)
C12-C14	1.491(19)	C13-F4	1.356(31)
C13-F5	1.300(25)	C13-F6	1.325(22)
C15-C16	1.376(22)	C16-C17	1.363(22)
C17-C18	1.369(27)	C18-C19	1.369(22)

Table 5.9d Bond angles (°) for the compound



Rh2-Rh1-O1	86.1(3)	Rh2-Rh1-O2	85.3(3)
O1-Rh1-O2	92.0(4)	Rh2-Rh1-O3	99.6(3)
O1-Rh1-O3	87.9(4)	O2-Rh1-O3	175.0(4)
Rh2-Rh1-O4	94.6(3)	O1-Rh1-O4	178.1(4)
O2-Rh1-O4	86.3(4)	O3-Rh1-O4	93.8(4)
Rh2-Rh1-N1	173.9(3)	O1-Rh1-N1	89.9(4)
O2-Rh1-N1	90.2(4)	O3-Rh1-N1	84.8(4)
O4-Rh1-N1	89.2(4)	Rh1-Rh2-O5	85.1(3)
Rh1-Rh2-O6	85.7(3)	O5-Rh2-O6	88.9(4)
Rh1-Rh2-O7	96.7(3)	O5-Rh2-O7	90.4(4)
O6-Rh2-O7	177.4(4)	Rh1-Rh2-O8	97.6(30)
O5-Rh2-O8	175.3(5)	O6-Rh2-O8	87.5(4)
O7-Rh2-O8	93.1(4)	Rh1-O1-C1	121.5(8)
Rh1-O2-C3	121.8(9)	Rh1-O3-C5	117.5(11)
Rh1-O4-C7	125.8(11)	Rh2-O5-C1	122.2(9)
Rh2-O6-C3	120.3(11)	Rh2-O7-C10	122.3(11)
Rh2-O8-C12	125.6(10)	Rh1-N1-C15	120.0(9)
Rh1-N1-C19	123.7(10)	C15-N1-C19	116.0(12)
O1-C1-O5	124.4(11)	O1-C1-C2	117.5(13)
O5-C1-C2	118.1(13)	O2-C3-O6	125.3(16)
O2-C3-C4	120.1(14)	O6-C3-C4	114.7(15)
O3-C5-C6	130.8(19)	O3-C5-C9	109.7(14)
C6-C5-C9	119.3(15)	C5-C6-C7	126.0(16)

Table 5.9d cont'd

O4-C7-C6	124.7(13)	O4-C7-C8	116.0(17)
C6-C7-C8	119.2(15)	C5-C9-F1	115.7(19)
C5-C9-F2	111.91(16)	F1-C9-F2	109.7(19)
C5-C9-F3	109.7(18)	F1-C9-F3	106.3(18)
F2-C9-F3	102.7(18)	O7-C10-C11	129.4(17)
O7-C10-C13	114.8(16)	C11-C10-C13	115.7(13)
C10-C11-C12	125.4(12)	O8-C12-C11	123.5(12)
O8-C12-C14	115.9(15)	C11-C12-C14	120.6(13)
C10-C13-F4	108.8(17)	C10-C13-F5	111.6(18)
F4-C13-F5	106.5(21)	C10-C13-F6	116.9(20)
F4-C13-F6	106.2(19)	F5-C13-F6	106.1(17)
N1-C15-C16	122.6(14)	C15-C16-C17	118.6(15)
C16-C17-C18	120.0(16)	C17-C18-C19	117.6(14)
N1-C19-C18	125.0(15)		

Appendix One.
Cyclic Voltammetry.

A1.1	Introduction.	230
A1.2	Instrumentation.	230
A1.3	The basic experiment.	233
A1.4	The characteristics of a cyclic voltammogram.	233

A1.1 Introduction.

Cyclic voltammetry is one of the most versatile electroanalytical techniques. Its effectiveness results from its capability for rapid observation of the redox behaviour of an electro-active species over a wide range of solvents. This provides a simple and direct method for the measurement of a half reaction when both the reduced and oxidised forms are stable on the timescale of the experiment.

The experiment involves cycling the potential at the working electrode while monitoring the current flow. The potential is controlled with respect to a reference electrode (*eg.* S.C.E. or Ag/AgCl). The potential applied across these two electrodes can be considered to be an exciting signal and the current measured at the working electrode to be its response. The exciting signal can be illustrated graphically as a linear potential scan with a triangular wave form (Figure A1.1). The cyclic voltammogram is a plot of current vs. potential. A reversible reaction gives rise to a voltammogram similar to that illustrated in Figure A1.2.

A1.2 Instrumentation.

Cyclic voltammetry requires a waveform generator, a potentiostat, and current/voltage converter which are usually incorporated into a single electronic device, and an X-Y recorder (Figure A1.3). The wave form generator produces the exciting signal which is then applied to the electrochemical cell by the potentiostat. The current/voltage converter is used to measure the resulting current and finally the X-Y recorder is used to display the voltammogram obtained.

Figure A1.1 A graphical representation of the exciting signal for a cyclic voltammetric experiment.

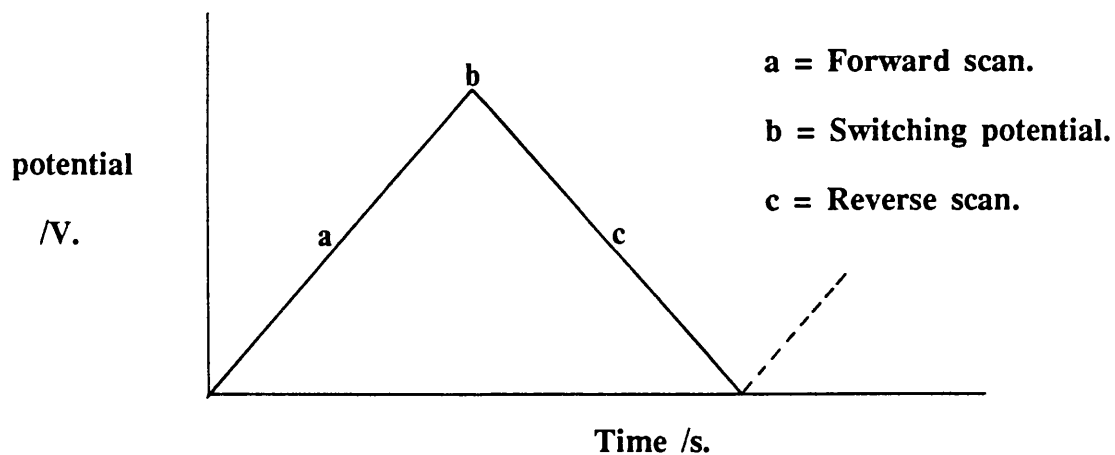


Figure A1.2 A cyclic voltammogram illustrating a reversible one-electron reduction.

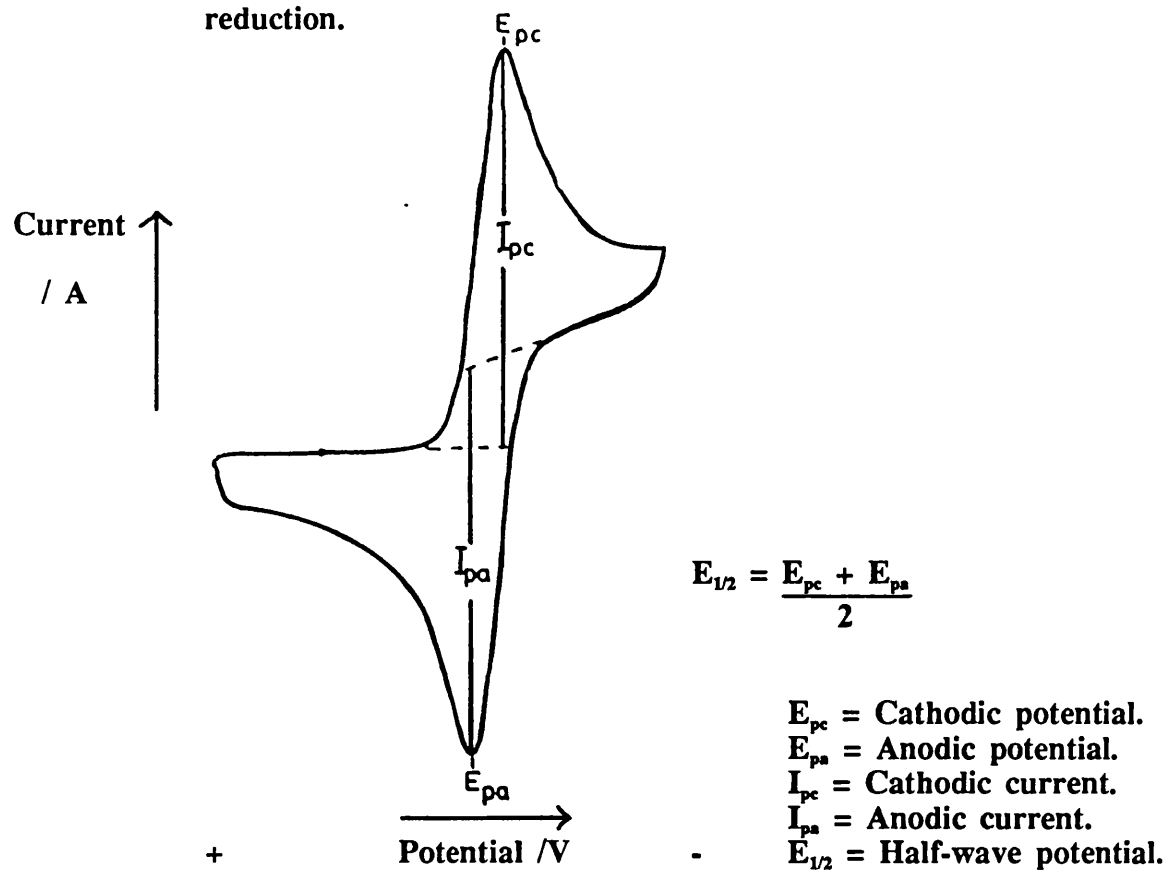
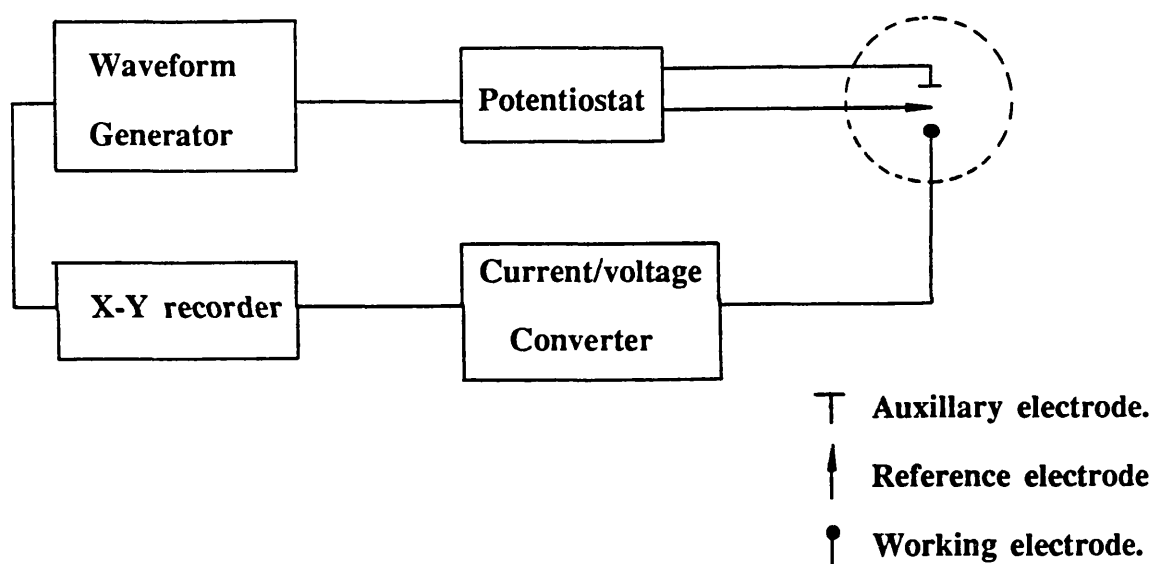


Figure A1.3 A diagrammatic representation of the instrumentation for a cyclic voltammetric experiment.



A1.1.3 The basic experiment.

In order to simplify the discussion a reduction process will be described. The forward scan of the cyclic voltammetric experiment commences at a point where there is no current response. As the potential is increased the material begins to be reduced and the current response starts to increase. The current continues to increase as the rate of reduction increases at more negative potential until a maximum is reached. The current then decreases at a steady rate as the potential continues to be increased. The peak observed is the result of two competing factors, 1) The increase in the net rate of reaction as the potential is made more negative and, 2) The development of a thickening depletion layer across which the reactant must diffuse. When the applied potential reaches the switching potential the direction of the scan is reversed and the potential decreased. As the potential decreases the reduced material will be re-oxidised resulting in a second peak for reasons analogous to those described above.

A1.4 The characteristics of a cyclic voltammogram.

The characteristics of the voltammogram can be used to determine the nature of the reaction. The formal potential, E° can be described by Equation A1.1.

$$E^\circ = \frac{E_{pc} + E_{pa}}{2} = E_{1/2} \quad \text{.....[A1.1]}$$

The number of electrons transferred can be determined by the separation of the forward and return waves E_{pc} and E_{pa} as illustrated by Equation A1.2.

$$\Delta E_p = E_{pc} - E_{pa} = 59/n \text{ mV} \dots\dots[\text{A1.2}]$$

n = no. of electrons transferred.

The Randles-Sevik Equation (Equation A1.3) indicates that I_p is proportional

$$I_p = (2.69 \times 10^5) n^{3/2} A D C \nu^{1/2} \dots\dots[\text{A1.3}]$$

C = concentration.

ν = Scan rate.

A = electrode surface area.

D = diffusion co-efficient.

to the $\nu^{1/2}$ and hence a graph of peak height against $\nu^{1/2}$ will give a straight line with the gradient equal to $(2.69 \times 10^5) n^{3/2} A D C$ and passing through the origin.

For a reversible reaction the above observations will be true under all conditions. The ratio of the peak heights I_{pc}/I_{pa} will be equal to unity and this along with the formal potential, and peak separation will remain constant at all scan rates. For a quasireversible reaction the above characteristics will hold under some conditions, but will vary with the scan rate, and with the conditions within the electrochemical cell (*eg* temperature). As scan rate increases the separation of the cathodic and anodic peaks will increase. Finally for an irreversible reaction only the Randles-Sevik relationship will hold. The most striking characteristic of an irreversible reaction is the absence of a return wave.

Appendix Two.**Linear free energy relationships - Substituent parameters.**

A2.1	Hammett substituent parameters.	236
A2.2	Taft substituent parameters.	236
A2.3	The use of substituent parameters in this study.	237

A2.1 Hammett substituent parameters.

The Hammett equation is a linear free energy relationship defined by Equation A2.1

$$\log (k/k_0) = p\sigma \quad \text{.....[A2.1]}$$

k = equilibrium constant for a substituted species.

k_0 = equilibrium constant when the substituent is H.

p = constant for a particular reaction.

σ = Hammett parameter for a particular substituent.

The original derivation of the equation resulted from work carried out on the dissociation of benzoic acid as illustrated in scheme A2.1. Separate values for Hammett parameters are quoted for substituents co-ordinated to the phenyl ring at the *para*-carbon and *meta*-carbon. These substituent parameters can be defined as a measure of the total electronic effects of a substituent group, when attached to a benzene ring. Positive values are indicative of a substituent group more electron withdrawing than the hydrogen atom while negative values indicate a group more electron donating than hydrogen (Table A2.1).

A2.2 Taft substituent Parameters.

Taft parameters are linear free energy parameters which can be used as a measure of the electron withdrawing (positive values) or electron donating (negative values) of a particular substituent group. These parameters were developed

using rates of reaction for acid and base catalysed hydrolysis of esters (Scheme A2.2). The assumption was made that resonance and steric effects would be equal for both pathways. This allowed a scale to be defined, using Equation A2.2, that

$$\log(k/k_0)_B - \log(k/k_0)_A = \rho\sigma^* \dots[A2.2]$$

k_0 = rate for R=CH₃

σ^* = Taft substituent parameter.

was dependent only on inductive effects. Values of Taft parameters for a range of substituents are given in Table A2.1.

A2.3 The use of substituent parameters in this study.

Hammett substituent parameters are used in Chapter 2 as a measure of the electron donating/withdrawing ability of the substituents R and R' attached to the amidate ligands [RC₆H₄NOCCH₃], and [HNOCC₆H₄R']. Taft parameters are used in Chapter 4 as a measure of the electron donating ability of the substituents R, R', and R'' in the compounds [Rh₂(O₂CR)_n(R'NOCR'')_{4-n}]. The use of these parameters in this way is quite remote from their more usual use in calculating reaction rates. The ease of oxidation/reduction of these compounds is likely to be effected by the electron donating/withdrawing ability of the substituents attached to the bridging ligands and therefore their use does appear to be justified.

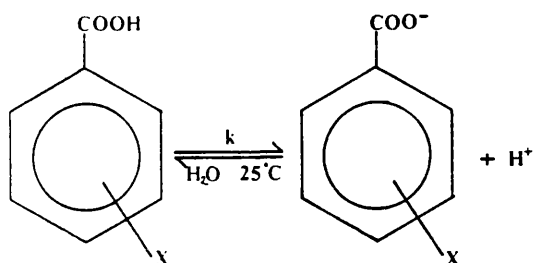
Table A2.1 Values of Taft and Hammett parameters for various substituent groups.

Substituent group	Taft parameter σ^* ^a	<i>p</i> -Hammett parameter σ_p^b	<i>m</i> -Hammett parameter σ_m^b
H	+0.490	0.00	0.00
CH ₃	0.00	-0.170	-0.069
C ₂ H ₅	-0.100	-0.151	-0.043
C ₃ H ₇	-0.115	-	-
C(CH ₃) ₃	-0.300	-0.197	-0.120
C ₆ H ₅	+0.600	+0.009	+0.06
Cl	-	+0.226	+0.355
CF ₃	-	+0.551	+0.415

a) See reference 124.

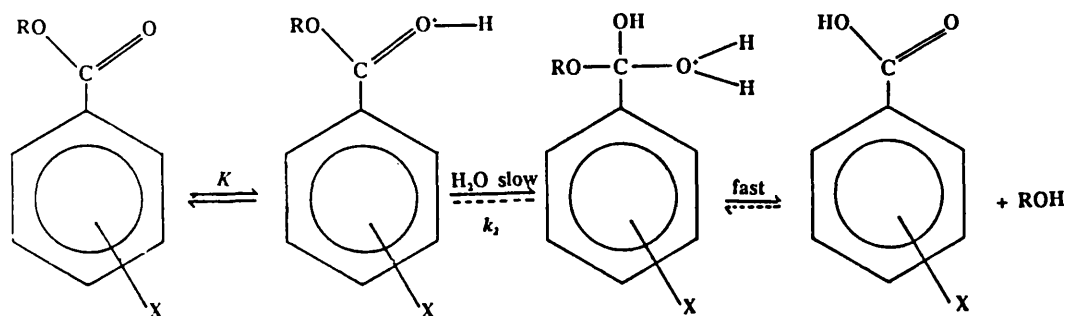
b) See reference 125.

Scheme A2.1 Scheme illustrating the dissociation reaction of benzoic acid.

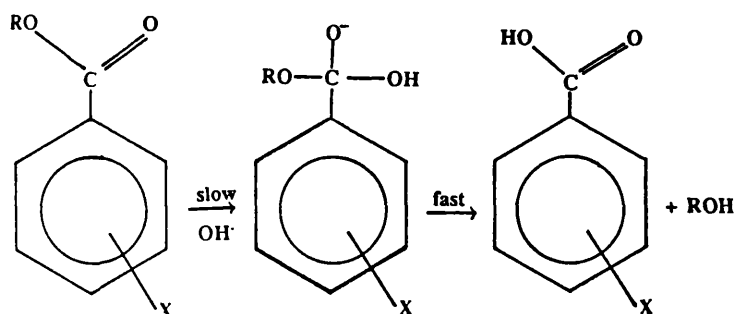


Scheme A2.2 Scheme illustrating the acid (a) and base (b) catalysed hydrolysis of substituted esters.

a) Acid catalysed.



b) Base catalysed.



References.

1. J.A. Bertrand, F.A. Cotton, and W.A. Dollase, a) *Inorg. Chem.*, 1963, **2**, 1166. b) *J. Am. Chem. Soc.*, 1963, **85**, 1349.
2. W.T. Robinson, J.E. Fergusson, and B.R. Penfold, *Proc. Chem. Soc.*, 1963, 116.
3. F.A. Cotton, and T.E. Hass, *Inorg. Chem.*, 1964, **3**, 10.
4. V.G. Kuznetsov, and P.A. Koz'min, a) *Zh. Strukt. Khim.*, 1963, **4**, 55. b) *J. Struct. Chem.*, 1963, **4**, 49.
5. F.A. Cotton, N.F. Curtis, C.B. Harris, B.F.G. Johnson, S.J. Lippard, J.T. Mague, W.R. Robinson, and J.S. Wood, *Science*, 1964, **145**, 1305.
6. F.A. Cotton, *Inorg. Chem.*, 1965, **4**, 334.
7. F. Taha, and G. Wilkinson, *J. Chem. Soc.*, 1963, 5406.
8. M.J. Bennett, W.K. Bratton, F.A. Cotton, and W.R. Robinson, *Inorg. Chem.* 1968, **7**, 1570.
9. D. Lawton, and R. Mason, *J. Am. Chem. Soc.*, 1965, **87**, 921.
10. F.A. Cotton, Z.C. Mester, and T.R. Webb, *Act. Cryst.*, 1974, **B30**, 2768.
11. W.K. Bratton, and F.A. Cotton, *J. Am. Chem. Soc.*, 1965, **87**, 921.
12. W.K. Bratton, and F.A. Cotton, *Inorg. Chem.*, 1970, **9**, 789.
13. M.J. Bennett, F.A. Cotton, and R.A. Walton, a) *J. Am. Chem. Soc.*, 1966, **88**, 3866. b) *Proc. R. Soc.*, 1968, **A303**, 175.
14. F.A. Cotton, *Quarterly Reviews*, 1966, **20**, 389, and references therein.
15. T.A. Stephenson and G. Wilkinson, *J. Inorg. Nucl. Chem.*, 1966, **28**, 2285.
16. M.J. Bennett, K.G. Caulton, and F.A. Cotton, *Inorg. Chem.*, 1969, **8**, 1.
17. I.I. Chernyaev, E.V. Shenderetskaya, and A.A. Koryagina, a) *Zh. Neorg. Khim.*, 1960, **5**, 1163. b) *Russ. J. Inorg. Chem.*, 1960, **5**, 559.
18. I.I. Chernyaev, E.V. Shenderetskaya, A.A. Koryagina, and A.G. Maisrova, a) *Zh. Neorg. Khim.*, 1965, **10**, 537. b) *Russ. J. Inorg. Chem.*, 1965, **10**, 290.

19. I.I. Chernyaev, E.V. Shenderetskaya, A.A. Koryagina, and A.G. Maisrova, a) *Zh. Neorg. Khim.*, 1966, **11**, 2575. b) *Russ. J. Inorg. Chem.*, 1966, **11**, 1383.
20. M.A. Porai-Koshits, and A.S. Antsyshkina, a) *Dokl. Akad. Nauk. S.S.S.R.*, 1962, **146**, 1102. b) *Prod. Acad. Sci. U.S.S.R. Chem. Sect.*, 1962, **146**, 902.
21. F.A. Cotton, B.G. DeBoer, M.D. La Prade, J.R. Pipal, and D.A. Ucko, a) *J. Am. Chem. Soc.*, 1970, **92**, 2926. b) *Acta Cryst.*, 1971, **B27**, 1664.
22. L. Pauling, *Proc. Acad. Sci. U.S.A.*, 1975, **72**, 3799.
23. L. Pauling, *Proc. Acad. Sci. U.S.A.*, 1975, **72**, 4200.
24. F.A. Cotton, and E. Pedersen, *Inorg. Chem.*, 1975, **14**, 388.
25. J.G. Norman, G.E. Renzoni, and D.A. Case, *J. Am. Chem. Soc.*, 1979, **101**, 5256.
26. L. Dubicki, and R.L. Martin, *Inorg. Chem.*, 1970, **9**, 673.
27. K.G. Caulton, and F.A. Cotton, a) *J. Am. Chem. Soc.*, 1969, **91**, 6517. b) *J. Am. Chem. Soc.*, 1971, **93**, 1914.
28. F.A. Cotton, *Acc. Chem. Res.*, 1969, **2**, 240.
29. J.G. Norman Jr., and H.J. Kolari, *J. Am. Chem. Soc.*, 1978, **100**, 791.
30. A. Bino, F.A. Cotton, and T.R. Felthouse, *Inorg. Chem.*, 1979, **18**, 2599.
31. T. Togano, M. Mukaida, and T. Nomura, *Bull. Chem. Soc. Japan.*, 1980, **53**, 2085.
32. D.S. Martin, R.A. Newman, and L.M. Vlasnik, *Inorg. Chem.*, 1980, **19**, 3404.
33. A.J. Lindsay, R.P. Tooze, M. Motevalli, M.B. Hursthouse, and G. Wilkinson, *J. Chem. Soc. Chem. Commun.*, 1984, 1383.
34. A.J. Lindsay, G. Wilkinson, M. Motevalli, and M.B. Hursthouse, *Chem. Soc. Dalton Trans.*, 1985, 2321
35. M.G.B. Drew, P. Higgins, and G.M. McCann, *J. Chem. Soc. Chem. Commun.*, 1987, 1385.

36. P. Higgins, and G.M. McCann, *J. Chem. Soc. Dalton Trans.*, 1988, 661.
37. F.A. Cotton, M. Matusz, and B. Zhong, *Inorg. Chem.*, 1988, **27**, 4368.
38. T. Malinski, D. Chang, F.N. Feldmann, J.L. Bear, and K.M. Kadish, *Inorg. Chem.*, 1983, **22**, 3225.
39. M.Y. Chevan, F.N. Feldmann, X.Q. Lin, J.L. Bear, and K.M. Kadish, *Inorg. Chem.*, 1984, **23**, 2373.
40. K. Ryde, and D.A. Tocher, *Inorg. Chim Acta.*, 1986, **118**, L49.
41. A.R. Chakravarty, and F.A. Cotton, *Polyhedron*, 1985, **4**, 1957.
42. A.R. Chakravarty, F.A. Cotton, and D.A. Tocher, *Polyhedron*, 1985, **4**, 1097.
43. A.R. Chakravarty, F.A. Cotton, and D.A. Tocher, *Inorg. Chem.*, 1985, **24**, 1263.
44. A.R. Chakravarty, F.A. Cotton, and W. Schwotzer, *Polyhedron*, 1986, **5**, 1821.
45. A.R. Chakravarty, F.A. Cotton, and D.A. Tocher, *Inorg. Chem.*, 1985, **24**, 172.
46. D.A. Tocher, *Inorg. Chim. Acta.*, 1986, **115**, 51.
47. A.R. Chakravarty, F.A. Cotton, and D.A. Tocher, *Inorg. Chem.*, 1985, **24**, 2857.
48. A.R. Chakravarty, and F.A. Cotton, *Inorg. Chim. Acta.*, 1986, **113**, 19.
49. A.R. Chakravarty, F.A. Cotton, D.A. Tocher, and J.H. Tocher, *Polyhedron*, 1985, **4**, 1475.
50. Y.B. Yoh, and G.G. Christoph, *Inorg. Chem.*, 1978, **17**, 2590.
51. Y.B. Yoh, and G.G. Christoph, *Inorg. Chem.*, 1979, **18**, 1122.
52. F.A. Cotton, and T.R. Felthouse, *Inorg. Chem.*, 1980, **19**, 323.
53. F.A. Cotton, and T.R. Felthouse, *Inorg. Chem.*, 1981, **20**, 600.
54. K. Aoki, and H. Yamazaki, *J. Chem. Soc. Chem. Commun.*, 1980, 186.

55. F.A. Cotton, and T.R. Felthouse, *Inorg. Chem.*, 1980, **19**, 2347.
56. F.A. Cotton, and J.L. Thompson, *Acta. Cryst.*, 1981, **B37**, 2235.
57. F.A. Cotton, and T.R. Felthouse, *Inorg. Chem.*, 1981, **20**, 2703.
58. G.G. Christoph, J. Halpern, G.P. Khare, Y.B. Yoh, and C. Romanowski, *Inorg. Chem.*, 1981, **20**, 3029.
59. F.A. Cotton, T.R. Felthouse, and S. Klein, *Inorg. Chem.*, 1981, **20**, 3037.
60. G.G. Christoph, and Y.B. Yoh, *J. Am. Chem. Soc.*, 1979, **101**, 1422.
61. F.A. Cotton, and J.L. Thompson, *Inorg. Chim. Acta.*, 1984, **81**, 193.
62. A.M. Dennis, R.A. Howard, J.L. Bear, J.D. Bear, J.D. Korp, and I. Bernal, *Inorg. Chim. Acta.*, 1979, **37**, L561.
63. M.A. Porai-Koshits, L.M. Dikareva, G.G. Sadikov, and I.B. Baranovski, a) *Zh. Neorg. Khim.*, 1979, **24**, 1286. b) *Russ. J. Inorg. Chem.*, 1979, **24**, 716.
64. C.J. Simmons, A. Clearfield, and Y. Sun, *Inorg. Chim. Acta.*, 1986, **121**, L3.
65. T.R. Felthouse, *Prog. in Inorg. Chem.*, 1983, **29**, 73 and references therein..
66. E.B. Boyer, and S.D. Robinson, *Coord. Chem. Revs.*, 1983, **50**, 109 and references therein.
67. K. Das, K.M. Kadish, and J.L. Bear, *Inorg. Chem.*, 1978, **17**, 930.
68. L.A. Bottomley, and T.A. Hallberg, *Inorg. Chem.*, 1984, **23**, 1584.
69. A.M. Dennis, R.A. Howard, D. Lançon, K.M. Kadish, and J.L. Bear, *J. Chem. Soc. Chem. Commun.*, 1982, 399.
70. A.R. Chakravarty, F.A. Cotton, D.A. Tocher, and J.A. Tocher, *Inorg. Chim. Acta.*, 1985, **101**, 185.
71. T.P. Zhu, M.Q. Ahsan, T. Malinski, K.M. Kadish, and J. L. Bear, *Inorg. Chem.*, 1984, **23**, 2.
72. J. Duncan, T. Malinski, T.P. Zhu, Z.S. Hu, K.M. Kadish, and J. L. Bear, *J. Am. Chem. Soc.*, 1982, **104**, 5507.

73. A.M. Dennis, J.D. Korp, I. Bernal, R.A. Howard, and J.L. Bear, *Inorg. Chem.*, 1983, **22**, 1522.
74. R.S. Lifsey, X.Q. Lin, M.Y. Chavan, M.Q. Ahsan, K.M. Kadish, and J.L. Bear, *Inorg. Chem.* 1987, **26**, 830.
75. M. Q. Ahsan, I. Bernal, and J.L. Bear, *Inorg. Chem.*, 1986, **25**, 260.
76. K.M. Kadish, D. Lançon, A.M. Dennis, and J.L. Bear, *Inorg. Chem.*, 1982, **21**, 2987.
77. J.L. Bear, T.P. Zhu, T. Malinski, A.M. Dennis, and K.M. Kadish, *Inorg. Chem.*, 1984, **23**, 674.
78. M.Y. Chavan, T.P. Zhu, X.Q. Lin, M.Q. Ahsan, J.L. Bear, and K.M. Kadish, *Inorg. Chem.* 1984, **23**, 4538.
79. M. Berry, C.D. Garner, I.H. Hillier, A.A. Macdowell, and W. Clegg, *J. Chem. Soc. Chem. Commun.*, 1980, 494.
80. M. Berry, C.D. Garner, I.H. Hillier, and W. Clegg, *Inorg. Chim. Acta.*, 1980, **45**, L209.
81. F.A. Cotton, and T.R. Felthouse, *Inorg. Chem.*, 1981, **20**, 584.
82. F.A. Cotton, S. Han. And W. Wang, *Inorg. Chem.*, 1984, **23**, 4762.
83. D.A. Tocher, and J.H. Tocher, *Inorg. Chim. Acta.*, 1987, **131**, 69.
84. D.A. Tocher, and J.H. Tocher, *Inorg. Chim. Acta.*, 1985, **104**, L15.
85. D.A. Tocher, and J.H. Tocher, *Polyhedron*, 1986, **5**, 1615.
86. J.L. Bear, C.L. Yao, L.M. Liu, F.J. Capdevielle, J.D. Korp, T.A. Albright, S.K. Kang, and K.M. Kadish, *Inorg. Chem.*, 1989, **28**, 1254.
87. A.R. Chakravarty, F.A. Cotton, D.A. Tocher, and J.H. Tocher, *Organomet.*, 1985, **4**, 8.
88. A.R. Chakravarty, F.A. Cotton, and D.A. Tocher, *J. Chem. Soc. Chem. Commun.*, 1984, 501.

89. F.A. Cotton, and K.R. Dunbar, *J. Am. Chem. Soc.*, 1987, **109**, 3142.
90. F.A. Cotton, F. Barcelo, P. Lahuerta, R. Llusar, J. Paya, and M.A. Ubeda, *Inorg. Chem.*, 1988, **27**, 1010.
91. F.A. Cotton, and M. Matusz, *Inorg. Chim. Acta.*, 1988, **143**, 45.
92. E.C. Morrison, and D.A. Tocher, *Inorg. Chim. Acta.*, 1989, **157**, 139.
93. E.C. Morrison, and D.A. Tocher, *Inorg. Chim. Acta.*, 1989, **156**, 99.
94. W.R. Tikkanen, E. Binamira-Soriga, W.C. Kaska, And P.C. Ford, *Inorg. Chem.*, 1984, **23**, 141.
95. W.R. Tikkanen, E. Binamira-Soriga, W.C. Kaska, And P.C. Ford, *Inorg. Chem.*, 1983, **22**, 1147.
96. M.Q. Ahsan, I. Bernal, and J.L. Bear, *Inorg. Chim. Acta.*, 1986, **115**, 135.
97. P. Piraino, G. Bruno, G. Tresoldi, S. Lo Schiavo, and P. Zanello, *Inorg. Chem.*, 1987, **26**, 91.
98. A.K. Chakravarty, F.A. Cotton, and D.A. Tocher, *J. Am. Chem. Soc.*, 1984, **106**, 6409.
99. A.R. Chakravarty, F.A. Cotton, M.P. Diebold, D.B. Lewis, and W.J. Roth, *J. Am. Chem. Soc.*, 1986, **108**, 971.
100. A.R. Chakravarty, F.A. Cotton, and D.A. Tocher, *Inorg. Chem.*, 1984, **23**, 4030.
101. T. Behling, G. Wilkinson, T.A. Stephenson, D.A. Tocher, and M.D. Walkinshaw, *J. Chem. Soc. Dalton Trans.*, 1983, 2109.
102. R.W. Mitchell, A. Spencer, and G. Wilkinson, *J. Chem. Soc. Dalton Trans.*, 1973, 846.
103. A.R. Chakravarty, and F.A. Cotton, *Inorg. Chim. Acta.*, 1985, **105**, 19.
104. W. Clegg, *Acta. Cryst.*, 1980, **B36**, 3112.
105. M. Berry, C.D. Garner, I.H. Hillier, A.A. MacDowell, and W. Clegg, *Inorg.*

- Chim. Acta.*, 1981, 53, 161.
106. H.J. McCarthy, and D.A. Tocher, *Inorg. Chim. Acta.*, 1989, 158, 1.
107. G.M. Sheldrick, "SHELXTL Plus" an integrated system for the solving, refining, and displaying crystal structures from diffraction data University of Göttingen F.R.G. 1986.
108. G.A. Rempel, P. Legzdins, H. Smith, and G. Wilkinson, *Inorg. Synth.*, 1971, 13, 90.
109. S. Cenini, R. Ugo, and F. Bonati, *Inorg. Chim. Acta.*, 1967, 1, 443.
110. C.D. Garner, S. Parkes, I.B. Walton, and W. Clegg, *Inorg. Chim. Acta.*, 1978, 31, L451.
111. J. Halpern, E. Kimura, J. Molin-Case, and C.S. Wong, *J.Chem. Soc. Chem. Commun.*, 1971, 1207.
112. H. Pasternak, and F. Pruchnik, *Inorg. Nucl. Chem. Letts.*, 1976, 12, 591.
113. M. Calligaris, L. Campana, G. Mestroni, M. Tornatore, and E. Alessio, *Inorg. Chim. Acta.*, 1987, 127, 103.
114. G.T. Behnke, and K. Nakamoto, *Inorg. Chem.*, 1967, 6, 433.
115. G.T. Behnke, and K. Nakamoto, *Inorg. Chem.*, 1967, 6, 440.
116. H.F. Holtzclaw Jr., and J.P. Collman, *J. Am. Chem. Soc.*, 1957, 79, 3318.
117. J Lewis, R.F. Long, and C. Oldham, *J. Chem. Soc.*, 1965, 6740.
118. H.J. McCarthy, and D.A. Tocher, *Inorg. Chim. Acta.*, 1988, 145, 171.
119. H.J. McCarthy, and D.A. Tocher, *Polyhedron*, 1989, 8, 1117.
120. F.A. Cotton, G.W. Rice, *Nouv. J. Chim.*, 1977, 1, 301.
121. W. Depmeier, K. Dietrich, K. König, H. Musso, and W. Weiss, *J. Organomet. Chem.*, 1986, 314, C1.
122. N. Mehmet, MSc. Thesis, University of London, 1989.
123. N. Mehmet, and D.A. Tocher work in progress.

- 124 R.W. Taft, Jr. in *Steric Effects in Organic Chemistry*, M.S. Newman (ed.), J. Wiley and Sons, New York, 1956 page 619.
- 125 H.H. Jaffe, *Chem. Revs.*, **53**, 191 (1953).

Publications.

- 1) Crystal and molecular structure of
 $[\text{Rh}_2(\text{O}_2\text{CCH}_3)_2(\text{OC}(\text{CF}_3)\text{CH}(\text{CO}(\text{CF}_3)_2)\text{C}_5\text{H}_5\text{N})]$.
H.J. McCarthy, and D.A. Tocher, *Inorg. Chim. Acta.*, 1988, **145**, 171.

- 2) An unusual example of intermolecular coupling between metal-metal bonded dimers: Crystal and molecular structure of
 $[\text{Rh}_2(\text{O}_2\text{CCH}_3)_2(\text{CF}_3\text{C}(\text{O})\text{CHC}(\text{O})\text{CH}_3)_2\text{C}_5\text{H}_5\text{N}]$
H.J. McCarthy, and D.A. Tocher, *Polyhedron*, 1989, **8**, 1117.

- 3) Observations of an $[\text{Ru}_2]^{n+}$ unit (n=3,4,5,6) Electrochemical studies into the molecule $[\text{Ru}_2(\text{MeC}_5\text{NH}_3\text{NH})_3(\text{O}_2\text{CCH}_3)\text{Cl}]$ in dimethylsulphoxide.
H.J. McCarthy, and D.A. Tocher, *Inorg. Chim. Acta.*, 1989, **158**, 1.

Crystal and Molecular Structure of Rh₂(O₂CCH₃)₂(OC·CF₃·CH·CO·CF₃)₂·2C₅H₅N

HOLLY J. McCARTHY and DEREK A. TOCHER*

Department of Chemistry, University College London,
20 Gordon Street, London WC1H 0AJ, U.K.

(Received December 14, 1987)

Introduction

Some twenty years ago the reaction of Rh₂(O₂CCH₃)₄ with β-diketones was reported to give complexes with the stoichiometry [Rh(O₂CCH₃)(β-diketonato)L]₂, where L is the neutral donor ligand, H₂O or pyridine [1]. Several structures were proposed for these molecules. However, the most likely one contained a [Rh₂]⁴⁺ core, two cisoid bridging acetato ligands, one chelating β-diketonato ligand on each metal ion, and one donor ligand L on each metal ion *trans* to the metal-metal bond. We have a substantial interest in the redox chemistry of the [Rh₂]⁴⁺ unit [2-4] and decided to prepare further examples of these molecules and explore their electrochemical properties. Before embarking on such a programme we believed it was important to determine unequivocally the structure of at least one representative compound. The compound which we chose to study crystallographically was Rh₂(O₂CCH₃)₂(OC·CF₃·CH·CO·CF₃)₂·2C₅H₅N. The results of that structure determination are now reported here.

Experimental

The compound Rh₂(O₂CCH₃)₂(OC·CF₃·CH·CO·CF₃)₂·2C₅H₅N was prepared as reported previously [1]. Single crystals suitable for X-ray crystallographic measurement were grown by slow evaporation from a 1:1 mixture of dichloromethane and hexane.

A suitable crystal of C₂₄H₁₈N₂O₈F₁₂Rh₂ (*M* = 896, triclinic, *a* = 10.397(5), *b* = 12.620(7), *c* = 12.764(8) Å, α = 88.63(5), β = 70.61(4), γ = 74.20(4)°, *U* = 1515(1) Å³, space group *P*1̄, *Z* = 2, *D*_e = 1.96 g cm⁻³, μ(Mo Kα) = 11.5 cm⁻¹, λ = 0.71073 Å, *F*(000) = 876) was examined using a Nicolet R3m/V diffractometer. Of the 5690 independent reflections measured 3447 were observed ($|F_o| > 3\sigma|F_o|$). The position of the two rhodium atoms in the asymmetric unit were derived from a three-dimensional Patterson map and the remainder of the

structure obtained using least-squares refinement and difference electron density maps. No attempt was made to locate the hydrogen atoms in the structure. All other atoms were refined anisotropically. We note that the -CF₃ groups on the β-diketonato ligands are undergoing rapid rotation and that consequently the isotropic equivalent temperature factors associated with the twelve fluorine atoms are high. Refinement was by full-matrix least-squares methods to give *R* = 0.081, *R*_w = 0.071 (*w*⁻¹ = σ²(*F*) + 0.00015 *F*²). The maximum residual electron density was 1.1 e Å⁻³ which was close to *F*(4). The maximum shift/error in the final refinement was 0.012. Computations were carried out on a Microvax II computer using the SHELXTL Plus program system [5] and published scattering factors [6]. Table I lists the fractional atomic coordinates, while Table II contains important bond distances and angles.

TABLE I. Fractional Atomic Coordinates (x10⁴) for Rh₂(O₂CCH₃)₂(OC·CF₃·CH·CO·CF₃)₂·2C₅H₅N

	<i>x</i>	<i>y</i>	<i>z</i>
Rh(1)	293(1)	2098(1)	3329(1)
Rh(2)	2956(1)	1653(1)	2441(1)
N(1)	-2012(11)	2287(9)	4372(9)
N(2)	5302(11)	1043(9)	1851(9)
O(1)	669(10)	1870(7)	4785(7)
O(2)	2989(10)	1176(7)	3950(8)
O(3)	582(10)	452(7)	3092(8)
O(4)	2843(10)	164(7)	2001(8)
O(5)	-26(9)	3719(7)	3597(8)
O(6)	-155(9)	2244(7)	1893(7)
O(7)	3032(10)	2095(8)	903(8)
O(8)	3149(10)	3080(8)	2933(8)
F(1)	-870(13)	3961(9)	-77(8)
F(2)	-2354(11)	3163(10)	853(9)
F(3)	-283(12)	2216(8)	-96(8)
F(4)	-72(24)	6118(11)	2594(12)
F(5)	-249(26)	5728(10)	4101(15)
F(6)	-1893(16)	6080(12)	3712(27)
F(7)	4988(12)	4530(9)	2666(11)
F(8)	2931(15)	5023(10)	3783(13)
F(9)	3406(16)	5674(9)	2210(13)
F(10)	4440(18)	2365(15)	-1275(10)
F(11)	3516(23)	4011(14)	-1007(12)
F(12)	2315(18)	3006(18)	-850(11)
C(1)	1889(15)	1430(10)	4792(11)
C(2)	2069(17)	1139(13)	5922(12)
C(3)	1727(14)	-145(10)	2439(12)
C(4)	1785(16)	-1317(11)	2134(13)
C(5)	-395(14)	4405(10)	2944(11)
C(6)	-641(15)	4198(11)	1965(12)
C(7)	-519(14)	3156(11)	1532(10)
C(8)	-998(18)	3108(13)	526(12)
C(9)	-619(20)	5570(13)	3324(17)
C(10)	3283(15)	2991(13)	560(13)

(continued)

* Author to whom correspondence should be addressed.

TABLE I. (continued)

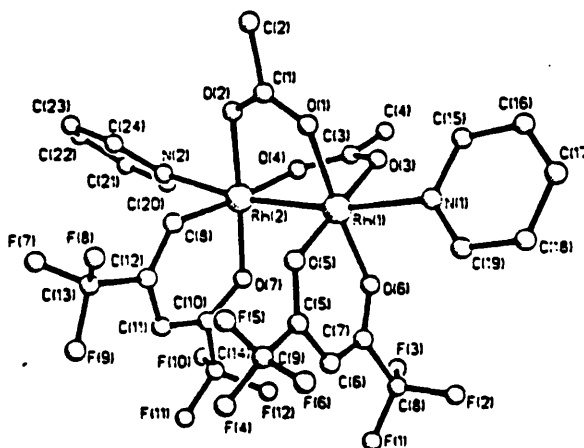
	x	y	z
C(11)	3443(17)	3847(14)	1123(15)
C(12)	3363(15)	3822(12)	2243(16)
C(13)	3649(23)	4757(15)	2776(22)
C(14)	3422(21)	3075(21)	-635(16)
C(15)	-2301(15)	1546(11)	5135(12)
C(16)	-3654(16)	1615(14)	5840(13)
C(17)	-4729(16)	2479(13)	5802(13)
C(18)	-4504(18)	3262(15)	5049(17)
C(19)	-3119(17)	3137(12)	4358(14)
C(20)	6073(16)	363(14)	914(12)
C(21)	7520(17)	-76(15)	592(14)
C(22)	8211(17)	167(13)	1266(14)
C(23)	7474(15)	860(12)	2203(11)
C(24)	6018(14)	1276(12)	2487(11)

TABLE II. Selected Bond Lengths and Angles for $\text{Rh}_2(\text{O}_2\text{CCH}_3)_2(\text{OC}\cdot\text{CF}_3\cdot\text{CH}\cdot\text{CO}\cdot\text{CF}_3)_2\cdot 2\text{C}_5\text{H}_5\text{N}$

Bond lengths (Å)			
Rh(1)-Rh(2)	2.523(2)	Rh(2)-O(2)	2.013(8)
Rh(1)-O(1)	2.022(8)	Rh(2)-O(4)	2.019(9)
Rh(1)-O(3)	2.032(8)	Rh(2)-O(7)	2.009(9)
Rh(1)-O(5)	1.999(8)	Rh(2)-O(8)	2.003(9)
Rh(1)-O(6)	2.028(8)	Rh(2)-N(2)	2.212(10)
Rh(1)-N(1)	2.271(11)		
Bond angles (°)			
N(1)-Rh(1)-Rh(2)	169.3(3)		
O(1)-Rh(1)-N(1)	85.3(4)		
O(3)-Rh(1)-N(1)	89.2(4)		
O(5)-Rh(1)-Rh(2)	95.5(3)		
O(5)-Rh(1)-O(1)	88.7(4)		
O(6)-Rh(1)-Rh(2)	96.7(3)		
O(6)-Rh(1)-O(1)	176.0(4)		
O(6)-Rh(1)-O(5)	94.4(3)		
O(2)-Rh(2)-Rh(1)	84.8(3)		
O(4)-Rh(2)-Rh(1)	85.0(3)		
O(4)-Rh(2)-O(2)	91.6(4)		
O(7)-Rh(2)-N(2)	89.8(4)		
O(7)-Rh(2)-O(4)	88.2(4)		
O(8)-Rh(2)-N(2)	87.4(4)		
O(8)-Rh(2)-O(4)	176.3(4)		
O(1)-Rh(1)-Rh(2)	85.4(3)		
O(3)-Rh(1)-Rh(2)	85.5(3)		
O(3)-Rh(1)-O(1)	90.5(4)		
O(5)-Rh(1)-N(1)	89.6(4)		
O(5)-Rh(1)-O(3)	178.6(4)		
O(6)-Rh(1)-N(1)	92.3(4)		
O(6)-Rh(1)-O(3)	86.3(4)		
N(2)-Rh(2)-Rh(1)	170.6(3)		
O(2)-Rh(2)-N(2)	87.2(4)		
O(4)-Rh(2)-N(2)	90.3(4)		
O(7)-Rh(2)-Rh(1)	98.1(3)		
O(7)-Rh(2)-O(2)	177.1(4)		
O(8)-Rh(2)-Rh(1)	96.9(3)		
O(8)-Rh(2)-O(2)	85.4(4)		
O(8)-Rh(2)-O(7)	94.7(4)		

Results and Discussion

The molecular structure of $\text{Rh}_2(\text{O}_2\text{CCH}_3)_2(\text{OC}\cdot\text{CF}_3\cdot\text{CH}\cdot\text{CO}\cdot\text{CF}_3)_2\cdot 2\text{C}_5\text{H}_5\text{N}$ is depicted in Fig. 1. The molecule contains structural features in common with those described for $\text{Rh}_2(\text{O}_2\text{CCH}_3)_2(\text{dmg})_2\cdot 2\text{PPh}_3$ [7]. The two rhodium atoms are bridged by two acetate ligands and each rhodium is also coordinated by a chelating $[\text{OC}\cdot\text{CF}_3\cdot\text{CH}\cdot\text{CO}\cdot\text{CF}_3]^-$ ligand. The coordination sites *trans* to the Rh-Rh bond are occupied by pyridine molecules. The Rh-Rh bond length, 2.523(2) Å, is much greater than that observed in the tetracarboxylate complex $\text{Rh}_2(\text{O}_2\text{CCH}_3)_4\cdot 2\text{C}_5\text{H}_5\text{N}$, 2.396(1) Å [8], as would have been expected. The Rh-Rh bond distance is very similar to that found in $[\text{Rh}_2(\text{O}_2\text{CCH}_3)_2(\text{phen})_2]$ complexes (mean: 2.558(3) Å) [9], but is significantly less than that found for $\text{Rh}_2(\text{O}_2\text{CCH}_3)_2(\text{dmg})_2\cdot 2\text{PPh}_3$, 2.618(5) Å, [7]. The mean Rh-N distance 2.242(11) Å is comparable with that found in $\text{Rh}_2(\text{O}_2\text{CCH}_3)_4\cdot 2\text{C}_5\text{H}_5\text{N}$, 2.227(3) Å [8]. The geometry at the rhodium atoms is distorted octahedral with the internal angles involving the chelating ligands being significantly greater than 90° ($\angle\text{O}(5)\text{-Rh}(1)\text{-O}(6)$, 94.4(3)°; $\angle\text{O}(7)\text{-Rh}(2)\text{-O}(8)$, 94.7(4)°). The Rh-Rh and Rh-N bonds are not colinear ($\angle\text{Rh}(2)\text{-Rh}(1)\text{-N}(1)$ = 169.3(3)°; $\angle\text{Rh}(1)\text{-Rh}(2)\text{-N}(2)$ = 170.6(3)°). The latter observation can almost certainly be attributed to unfavourable steric interactions between the -CF₃ groups on the chelating β-diketonates and the axial ligands. Unfavourable steric interactions also occur between the substituent groups on the different chelating ligands, with the dihedral angle between the least-squares planes defined by the atoms Rh(1)-O(5)-C(5)-C(6)-C(7)-O(6) and Rh(2)-O(7)-C(10)-C(11)-C(12)-O(8) being 23.9°. In addition the β-diketonate ligands are rotated about the Rh-Rh axis by *ca.* 14° from the eclipsed configuration (torsion angles O(5)-Rh(1)-

Fig. 1. Molecular structure of $\text{Rh}_2(\text{O}_2\text{CCH}_3)_2(\text{OC}\cdot\text{CF}_3\cdot\text{CH}\cdot\text{CO}\cdot\text{CF}_3)_2\cdot 2\text{C}_5\text{H}_5\text{N}$, showing the atom labelling scheme.

Rh(2)–O(8) 14.9°; O(6)–Rh(1)–Rh(2)–O(7) 14.2°. The two bridging acetate ligands are also distorted with torsion angles about the Rh–Rh bond of 11.3° and 12.5°.

Supplementary Material

Tables of thermal parameters and observed and calculated structure factors are available from the authors on request.

Acknowledgements

We wish to thank Johnson Matthey plc for generous loans of rhodium trichloride and the S.E.R.C. for the provision of the X-ray equipment.

References

- 1 S. Cenini, R. Ugo and F. Bonati, *Inorg. Chim. Acta*, **1**, 443 (1967).
- 2 D. A. Tocher and J. H. Tocher, *Inorg. Chim. Acta*, **104**, L15 (1985).
- 3 D. A. Tocher and J. H. Tocher, *Polyhedron*, **5**, 1615 (1986).
- 4 D. A. Tocher and J. H. Tocher, *Inorg. Chim. Acta*, **131**, 69 (1987).
- 5 G. M. Sheldrick, 'SHELXTL Plus', an integrated system for solving, refining and displaying crystal structures from diffraction data, University of Göttingen, F.R.G., 1986.
- 6 'International Tables for Crystallography', Vol. 4, Kynoch Press, Birmingham, U.K., 1974, pp. 99–149.
- 7 J. Halpern, E. Kimura, J. Molin-Case and C. S. Wong, *J. Chem. Soc., Chem. Commun.*, 1207 (1971).
- 8 Y.-B. Koh and G. G. Christoph, *Inorg. Chem.*, **17**, 2590 (1978).
- 9 M. Calligaris, L. Campana, G. Mestroni, M. Tornatore and E. Alessio, *Inorg. Chim. Acta*, **127**, 103 (1987).

AN UNUSUAL EXAMPLE OF INTERMOLECULAR
COUPLING BETWEEN METAL-METAL BONDED DIMERS:
CRYSTAL AND MOLECULAR STRUCTURE OF
 $\text{Rh}_2(\text{O}_2\text{CCH}_3)_2(\text{CF}_3\text{C}(\text{O})\text{CHC}(\text{O})\text{CH}_3)_2 \cdot \text{C}_5\text{H}_5\text{N}$

HOLLY J. McCARTHY and DEREK A. TOCHER*

Department of Chemistry, University College London, 20 Gordon Street,
London WC1H 1AJ, U.K.

(Received 24 October 1988; accepted 24 November 1988)

Abstract—The reaction of $\text{Rh}_2(\text{O}_2\text{CCH}_3)_4$ with 1,1,1-trifluoro-2,4-pentanedionate in water, gives two isomers of $\text{Rh}_2(\text{O}_2\text{CCH}_3)_2(\text{CF}_3\text{C}(\text{O})\text{CHC}(\text{O})\text{CH}_3)_2 \cdot 2\text{H}_2\text{O}$. Addition of pyridine and elution from a silica column gives isomerically pure $\text{Rh}_2(\text{O}_2\text{CCH}_3)_2(\text{CF}_3\text{C}(\text{O})\text{CHC}(\text{O})\text{CH}_3)_2 \cdot \text{C}_5\text{H}_5\text{N}$. The structure of the crystalline product was obtained by X-ray diffraction. The crystals belong to the monoclinic space group $P2_1/n$ with $a = 9.660(2)$, $b = 19.976(3)$, $c = 13.202(2)$ Å, $\beta = 106.54(2)^\circ$, $V = 2442(1)$ Å³ and $z = 4$. The structure was refined on 2708 independent reflections to $R_w = 0.0604$. The asymmetric unit contains a single dinuclear unit in which only one rhodium atom is bound by an axial pyridine molecule. The Rh—Rh bond is 2.534(1) Å and the Rh—N bond, 2.133(10) Å. Surprisingly, pairs of dinuclear units are linked together in the solid state via two long, 3.106 Å, Rh—C interactions, between the axial site on the metal and the γ -carbon atom of the β -diketonate ligand.

The vast majority of the classical metal-metal bonded dimers of the type $\text{M}_2(\text{XYZ})_4$ (where XYZ is a monoanionic three-atom bridging ligand) exist as discrete dinuclear units, or simple bis-adducts $\text{M}_2(\text{XYZ})_4\text{L}_2$ (L = pyridine, H_2O , PR_3 etc.), both in the solid state and in solution. Relatively few of these compounds exist as polymeric materials, the best characterized examples being the ruthenium compounds $\text{Ru}_2(\text{O}_2\text{CR})_4\text{Cl}$ and $\text{Ru}_2(\text{HN}(\text{O})\text{CR})_4\text{Cl}$, in which dinuclear cations are linked in chains by bridging axial chloride ions,¹⁻⁴ and the so-called "unsolvated" $\text{Cr}_2(\text{O}_2\text{CR})_4$ molecules, which associate in the solid state via oxygen bridge bonding.^{5,6} In the course of our studies into the products formed on reaction of dirhodium(II) tetracarboxylate molecules with a number of β -diketone ligands, we have encountered an unusual molecule $\text{Rh}_2(\text{O}_2\text{CCH}_3)_2(\text{CF}_3\text{C}(\text{O})\text{CHC}(\text{O})\text{CF}_3)_2 \cdot \text{C}_5\text{H}_5\text{N}$, which in the solid state dimerizes through a pair of weak rhodium-carbon interactions.

EXPERIMENTAL

Synthesis

$\text{Rh}_2(\text{O}_2\text{CCH}_3)_4 \cdot 2\text{CH}_3\text{OH}$ (0.156 g, 0.31 mmol) was refluxed in H_2O (20 cm³) with $\text{CF}_3\text{C}(\text{O})\text{CH}_2\text{C}(\text{O})\text{CH}_3$ (0.5 cm³) for 6 h. The green precipitate formed was filtered off and air-dried. The solid was suspended in CH_3OH (10 cm³) to which $\text{C}_5\text{H}_5\text{N}$ (0.1 cm³) was added. The mixture was stirred for 1 h, in which time a red solution was obtained. The CH_3OH was removed under reduced pressure and the red gum redissolved in CH_2Cl_2 (5 cm³). This was loaded onto a silica gel (60-120 mesh) column and a green band eluted with a mixture of CH_2Cl_2 (80%), *n*-hexane (12%) and diethyl ether (8%). Slow evaporation of this solution resulted in the deposition of a homogeneous mass of green crystalline material. Yield 0.167 g, 70%. Found: C, 32.2; H, 2.7; N, 1.8. Calc. for $\text{C}_{19}\text{H}_{19}\text{NO}_8\text{F}_6\text{Rh}_2$: C, 32.2; H, 2.7; N, 2.0%. IR spectrum (KBr disc): 3449(w), 1607(m), 1542(s), 1512(m), 1481(m), 1443(s), 1420(w), 1340(m).

* Author to whom correspondence should be addressed.

1267(s), 1210(s), 1198(s), 1152(s), 1137(s), 1095(m), 1064(w), 1003(w), 946(w), 819(w), 789(m), 754(w), 697(s), 624(w), 598(w), 530(w), 350(w) cm^{-1} (key: s, strong; m, medium; w, weak). Mass spectrum: $m/z = 630$, $[\text{Rh}_2(\text{O}_2\text{CCH}_3)_2(\text{CF}_3\text{C}(\text{O})\text{CHC}(\text{O})\text{CH}_3)_2]^-$. Proton NMR (CD_2Cl_2 solvent, $(\text{CH}_3)_4\text{Si}$ reference): 17 C, pyridine, δ 8.48, 7.96, 7.52 ppm; $\text{CF}_3\text{C}(\text{O})\text{CHC}(\text{O})\text{CH}_3$, 5.54 ppm; O_2CCH_3 , 2.08 ppm; $\text{CF}_3\text{C}(\text{O})\text{CHC}(\text{O})\text{CH}_3$, 1.90 ppm; -79 C, pyridine, δ 8.41, 7.97, 7.53 ppm; $\text{CF}_3\text{C}(\text{O})\text{CHC}(\text{O})\text{CH}_3$, 5.63 and 5.44 ppm; O_2CCH_3 , 2.10 and 2.06 ppm; $\text{CD}_3\text{C}(\text{O})\text{CHC}(\text{O})\text{CH}_3$, 1.89 and 1.84 ppm.

X-ray studies

Green needle crystals were obtained as described above.

Crystal data. $\text{C}_{19}\text{H}_{19}\text{NO}_8\text{F}_6\text{Rh}_2$, monoclinic, space group $P2_1/n$, $a = 9.660(2)$, $b = 19.976(3)$, $c = 13.202(2)$ Å, $\beta = 106.54(2)^\circ$, $U = 2442$ Å³, $z = 4$, $M = 709.20$, $D_c = 1.93$ g cm^{-3} , $\mu(\text{Mo-K}\alpha) = 13.8$ cm^{-1} , $F(000) = 1392$.

Measurements. Refined unit cell parameters were obtained by centring 50 reflections on a Nicolet R3mV diffractometer. A total of 4322 unique data were measured in the range $5^\circ \leq 2\theta \leq 50^\circ$ with Mo-K α radiation (graphite monochromator). Of these, 2708 reflections had $I > 2.0\sigma(I)$ and were considered to be observed. Three standard reflections were remeasured every 97 scans and showed no significant loss (< 2%) in intensity during the data collection. The data were corrected for Lorentz and polarization factors, and an empirical absorption correction was applied.

Structure analysis. The positions of the two rhodium atoms were derived using direct methods and the remaining non-hydrogen atoms were found by iterative application of difference Fourier synthesis and least-squares refinement. The fluorine atoms are disordered over two sites. A satisfactory model for the disorder was found by assuming a 75% occupancy of one site [fluorines F(1a)—F(6a) attached to C(9) and C(14)] and a 25% occupancy of the alternative site [fluorines F(1b)—F(6b) attached to C(8) and C(13)]. No attempt was made to locate the hydrogen atoms. All atoms [except F(3b)] were refined anisotropically. The final cycle of refinement included 374 parameters and converged to give $R = 0.0776$ and $R_w = 0.0604$ ($w^{-1} = \sigma^2(F) + 0.00088F^2$), and did not shift any parameter by more than 0.026 times its estimated standard deviation. The final difference Fourier map was featureless with the largest peak being 1.01 e Å⁻³. Computations

were carried out on a Microvax II computer using the SHELXTL PLUS program package.

Final atomic coordinates, thermal parameters and structure factor tables have been deposited with the Editor and with the Cambridge Crystallographic Data Centre, as supplementary material.

RESULTS AND DISCUSSION

Some 20 years ago, the reaction of $\text{Rh}_2(\text{O}_2\text{CCH}_3)_4$ with β -diketones was reported to give complexes with the stoichiometry $[\text{Rh}(\text{O}_2\text{CCH}_3)(\beta\text{-diketonato})\text{L}]_2$, where L is the neutral donor ligand, H_2O or pyridine.⁷ Several structures were proposed for these molecules. However, the most likely one contained a $[\text{Rh}_2]^{4+}$ core, two cisoid bridging acetato ligands, one chelating β -diketonato ligand on each metal ion, and one donor ligand, L, on each metal ion in the coordination site *trans* to the rhodium—rhodium single bond. We have recently confirmed this geometry for the molecule $\text{Rh}_2(\text{O}_2\text{CCH}_3)_2(\text{CF}_3\text{C}(\text{O})\text{CHC}(\text{O})\text{CF}_3)_2 \cdot 2\text{C}_5\text{H}_5\text{N}$.⁸

When $\text{Rh}_2(\text{O}_2\text{CCH}_3)_4$ is treated with an aqueous solution of the unsymmetrical β -diketone, $\text{CH}_3\text{C}(\text{O})\text{CH}_2\text{C}(\text{O})\text{CF}_3$, two isomers of the compound $\text{Rh}_2(\text{O}_2\text{CCH}_3)_2(\text{CF}_3\text{C}(\text{O})\text{CHC}(\text{O})\text{CH}_3)_2 \cdot 2\text{H}_2\text{O}$ are formed.⁷ Although these isomers were not separated by Cenini *et al.* they were identified by ¹H NMR spectroscopy. In the *cis* isomer the β -diketonate ligands are arranged such that the $-\text{CF}_3$ substituents are approximately eclipsed, leading to inequivalent acetato ligands, while in the *trans* isomer each $-\text{CF}_3$ group is eclipsed with the $-\text{CH}_3$ substituent on the other β -diketonate, giving rise to an equivalence of the two acetato ligands in the NMR spectrum.

If the crude reaction mixture described earlier is treated with pyridine, which displaces the axially coordinated water molecules, and is then eluted from a silica column, an efficient separation of the two isomers can be effected.

The first fraction to be eluted from the column was shown, by ¹H NMR spectroscopy, to be the *trans* isomer. Surprisingly however, integration of the ¹H NMR spectrum was in the ratio pyridine—acetate— β -diketonate of 1:2:2. Given the propensity for the $[\text{Rh}_2]^{4+}$ unit to interact strongly with two axial ligands, this observation could not be easily rationalized and therefore we deemed it necessary to determine unequivocally the structure of this molecule in the solid state by X-ray crystallography.

Green needle crystals of $\text{Rh}_2(\text{O}_2\text{CCH}_3)(\text{CF}_3\text{C}(\text{O})\text{CHC}(\text{O})\text{CH}_3)_2 \cdot \text{C}_5\text{H}_5\text{N}$ are readily obtained

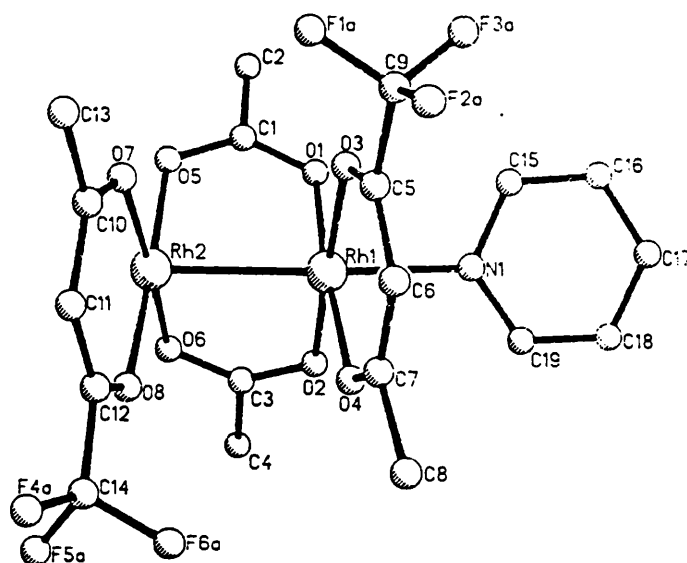
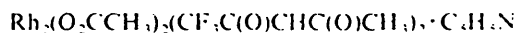


Fig. 1. Molecular structure of $\text{Rh}_2(\text{O}_2\text{CCH}_3)_2(\text{CF}_3\text{C}(\text{O})\text{CHC}(\text{O})\text{CH}_3)_2 \cdot \text{C}_5\text{H}_5\text{N}$ defining the atom labelling scheme.

by the slow evaporation of the solvent mixture used to elute the chromatography column. Data collection, structure solution and refinement used routine procedures described previously.⁹

The molecular structure of $\text{Rh}_2(\text{O}_2\text{CCH}_3)_2(\text{CF}_3\text{C}(\text{O})\text{CHC}(\text{O})\text{CH}_3)_2 \cdot \text{C}_5\text{H}_5\text{N}$ is shown in Fig. 1, while the coupling of the dinuclear units is illustrated in Fig. 2. Selected bond lengths and angles are presented in Table 1. The two rhodium atoms in the dinuclear core are bridged by two acetate ligands and each rhodium is also coordinated by a chelating $[\text{CF}_3\text{C}(\text{O})\text{CHC}(\text{O})\text{CH}_3]^-$ ligand. The coordination site on Rh(1) *trans* to the Rh—Rh bond is occupied by a pyridine molecule.

The Rh—Rh bond length, 2.534(1) Å, is very similar to the one observed in $\text{Rh}_2(\text{O}_2\text{CCH}_3)_2(\text{CF}_3\text{C}(\text{O})\text{CHC}(\text{O})\text{CF}_3)_2 \cdot 2\text{C}_5\text{H}_5\text{N}$, 2.523(2) Å,⁸ and is much greater than that observed for the tetracarboxylate complex, $\text{Rh}_2(\text{O}_2\text{CCH}_3)_4 \cdot 2\text{C}_5\text{H}_5\text{N}$, 2.396(1) Å.¹⁰ This Rh—Rh bond distance is not dissimilar to that observed in $\text{Rh}_2(\text{O}_2\text{CCH}_3)_2(\text{phen})_2$ complexes (mean: 2.558(3) Å), which also contain only two acetate ligands bridging the metal—metal single bond.¹¹ One closely related molecule, $\text{Rh}_2(\text{O}_2\text{CCH}_3)_2(\text{dmg})_2 \cdot 2\text{PPh}_3$, has been observed to have a significantly longer Rh—Rh bond, 2.618(5) Å.¹² The Rh—Rh and Rh—N bonds are not colinear: angle Rh(2)—Rh(1)—N(1) =

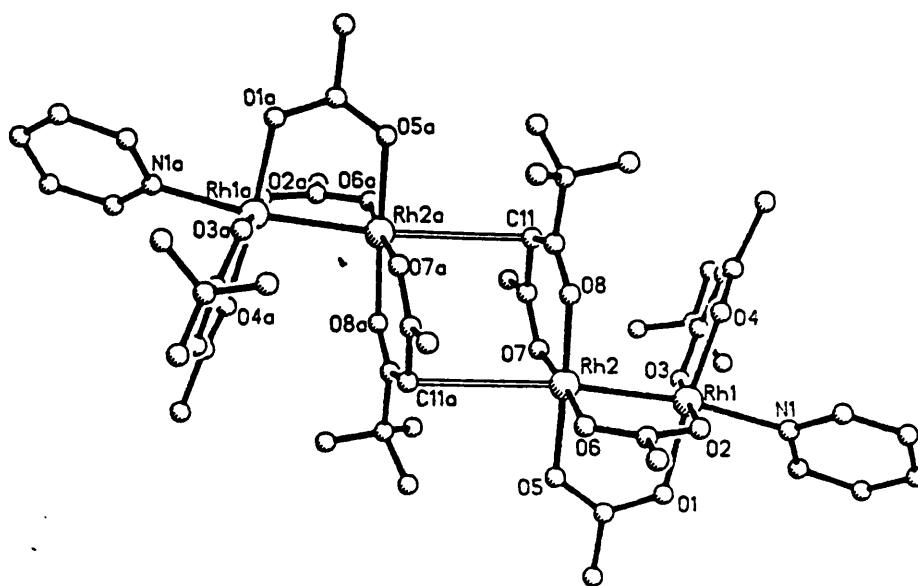


Fig. 2. Coupling of the dinuclear units (atoms labelled "a" are generated by an inversion centre).

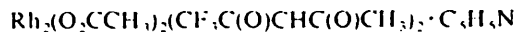
Table 1. Selected bond lengths (Å) and bond angles (°) for $\text{Rh}_2(\text{O}_2\text{CCH}_3)_2(\text{CF}_3\text{C}(\text{O})\text{CHC}(\text{O})\text{CH}_3)_2 \cdot \text{C}_5\text{H}_5\text{N}$

Rh(1)—O(1)	2.022(8)	Rh(1)—Rh(2)	2.534(1)
Rh(1)—O(2)	2.023(8)	Rh(2)—O(5)	2.039(9)
Rh(1)—O(3)	2.008(9)	Rh(2)—O(6)	2.033(9)
Rh(1)—O(4)	1.998(8)	Rh(2)—O(7)	2.001(9)
Rh(1)—N(1)	2.133(10)	Rh(2)—O(8)	1.993(9)
O(1)—C(1)	1.272(15)	O(2)—C(3)	1.268(16)
C(1)—O(5)	1.262(15)	C(3)—O(6)	1.249(15)
C(1)—C(2)	1.500(19)	C(3)—C(4)	1.532(18)
O(3)—C(5)	1.266(18)	O(7)—C(10)	1.241(16)
C(5)—C(9)	1.547(19)	C(10)—C(13)	1.505(19)
C(5)—C(6)	1.395(21)	C(10)—C(11)	1.413(19)
C(6)—C(7)	1.414(19)	C(11)—C(12)	1.415(18)
C(7)—C(8)	1.527(21)	C(12)—C(14)	1.487(18)
C(7)—O(4)	1.258(15)	C(12)—O(8)	1.238(15)
O(1)—Rh(1)—Rh(2)	86.1(2)	O(2)—Rh(1)—Rh(2)	86.4(3)
O(2)—Rh(1)—O(1)	91.7(4)	O(3)—Rh(1)—Rh(2)	95.5(2)
O(3)—Rh(1)—O(1)	86.9(4)	O(3)—Rh(1)—O(2)	177.5(4)
O(4)—Rh(1)—Rh(2)	98.2(2)	O(4)—Rh(1)—O(1)	175.0(4)
O(4)—Rh(1)—O(2)	86.1(4)	O(4)—Rh(1)—O(3)	95.2(4)
N(1)—Rh(1)—Rh(2)	171.8(3)	N(1)—Rh(1)—O(1)	86.9(4)
N(1)—Rh(1)—O(2)	89.5(4)	N(1)—Rh(1)—O(3)	88.4(4)
N(1)—Rh(1)—O(4)	88.7(4)	O(5)—Rh(2)—Rh(1)	84.9(3)
O(6)—Rh(2)—Rh(1)	84.5(3)	O(6)—Rh(2)—O(5)	90.2(4)
O(7)—Rh(2)—Rh(1)	99.8(2)	O(7)—Rh(2)—O(5)	88.8(4)
O(7)—Rh(2)—O(6)	175.5(4)	O(8)—Rh(2)—Rh(1)	97.8(2)
O(8)—Rh(2)—O(5)	176.0(4)	O(8)—Rh(2)—O(6)	87.1(4)
O(8)—Rh(2)—O(7)	93.6(4)		

171.8(3)°. This angle is similar to those observed in $\text{Rh}_2(\text{O}_2\text{CCH}_3)_2(\text{CF}_3\text{C}(\text{O})\text{CHC}(\text{O})\text{CF}_3)_2 \cdot 2\text{C}_5\text{H}_5\text{N}^8$ and $\text{Rh}_2(\text{O}_2\text{C}(\text{CH}_3)_3)_2(\text{CF}_3\text{C}(\text{O})\text{CHC}(\text{O})\text{CF}_3)_2 \cdot 2\text{C}_5\text{H}_5\text{N}^{13}$ and can almost certainly be attributed to unfavourable steric interactions between the axial ligands and the $-\text{CF}_3$ substituent(s) on the chelating β -diketonate ligands. Although the deviation from linearity is significant, it is markedly less than that observed in $\text{Rh}_2(\text{O}_2\text{CR})_2[(\text{C}_6\text{H}_4)\text{PR}'\text{R}']_2 \cdot 2\text{L}$ molecules, which also exhibit similarly distorted structures.^{14,15} The rhodium-carboxylate-oxygen bonds are longer than those to the β -diketonate oxygen atoms (mean values of 2.029 and 2.000 Å, respectively). In addition, the Rh—Rh—O(carboxylate) angles average 85.5°, while those involving the β -diketonate ligands average 97.8°. The dihedral angle between the least-square planes defined by the atoms Rh(1)—O(3)—C(5)—C(6)—C(7)—O(4) and Rh(2)—O(7)—C(10)—C(11)—C(12)—O(8) is 29.3°. These distortions from the idealized octahedral geometry about the metal ions must be attributed to the unfavourable steric interactions between the substituent groups on the two chelating β -diketonate ligands. The two β -diketonate ligands

are rotated about the Rh—Rh axis by *ca* 7° from the eclipsed configuration (torsion angles O(3)—Rh(1)—Rh(2)—O(7) 7.6°; O(4)—Rh(1)—Rh(2)—O(8) 6.6°). Similarly, the two bridging acetate ligands are distorted with torsion angles about the Rh—Rh bond of 6.2 and 7.4°. This twisting of one end of the dinuclear molecule with respect to the other is much reduced from that observed in $\text{Rh}_2(\text{O}_2\text{CCH}_3)_2(\text{CF}_3\text{C}(\text{O})\text{CHC}(\text{O})\text{CF}_3)_2 \cdot 2\text{C}_5\text{H}_5\text{N}^8$ where the four independent torsion angles fall in the range 11–15°.

Initial inspection of the molecular structure indicated that one rhodium atom per molecule was coordinatively unsaturated. However, when the crystal packing was examined, it became apparent that in the solid state the binuclear units are associated in pairs, see Fig. 2. The open site on Rh(2) is blocked by a γ -carbon atom of a β -diketonate ligand on an adjacent molecule. The rhodium-to-carbon distance, 3.106 Å, is too long to be considered as a formal bond. However, the interaction must be relatively strong, otherwise we would expect to observe the axial ligation of a second pyridine molecule. Similar long metal-carbon interactions have been observed in the homoleptic β -diketonate com-



1121

pounds of mercury(II) and iron(II).^{16,17} We believe that the separation between the two metallocyclic rings is principally a function of the unfavourable steric interactions. There is no evidence of metal-metal interactions between the dinuclear units, the Rh(2)—Rh(2a) distance being $> 4.8 \text{ \AA}$.

The ^1H NMR spectra recorded in CD_2Cl_2 at 290 K (see Experimental), show only averaged β -diketonate and acetate ligands. When spectra were recorded at 194 K, each class of ligand has two sets of resonances consistent with a steady-state structure in which only one rhodium ion is ligated by pyridine. The low temperature NMR data do not conclusively establish that binuclear units are linked in pairs in solution. However, even though neither signal due to the proton on the γ -carbon atom exhibits resolved coupling to rhodium, we believe that the chemical shift difference, which is much larger than that for any other pair of proton environments, may be attributed to a structure in solution closely similar to that which is observed in the crystal lattice.

Acknowledgements—We thank Johnson Matthey plc for their generous loans of rhodium trichloride and the SERC for provision of the X-ray equipment.

REFERENCES

1. M. J. Bennett, K. G. Caulton and F. A. Cotton, *Inorg. Chem.* 1969, **8**, 1.
2. A. Bino, F. A. Cotton and T. R. Felthouse, *Inorg. Chem.* 1979, **18**, 2599.
3. A. R. Chakravarty, F. A. Cotton and D. A. Tocher, *Polyhedron* 1985, **4**, 1097.
4. A. R. Chakravarty and F. A. Cotton, *Polyhedron* 1985, **4**, 1957.
5. F. A. Cotton, M. W. Extine and G. W. Rice, *Inorg. Chem.* 1978, **17**, 176.
6. F. A. Cotton, C. E. Rice and G. W. Rice, *J. Am. Chem. Soc.* 1977, **99**, 4704.
7. S. Cenini, R. Ugo and F. Bonati, *Inorg. Chim. Acta* 1967, **1**, 443.
8. H. J. McCarthy and D. A. Tocher, *Inorg. Chim. Acta* 1988, **145**, 171.
9. E. C. Morrison, C. A. Palmer and D. A. Tocher, *J. Organomet. Chem.* 1988, **349**, 405.
10. Y.-B. Koh and G. G. Christoph, *Inorg. Chem.* 1978, **17**, 2590.
11. M. Calligaris, L. Campana, G. Mestroni, M. Tornatore and E. Alessio, *Inorg. Chim. Acta* 1987, **127**, 103.
12. J. Halpern, E. Kimura, J. Molin-Case and C. S. Wong, *J. Chem. Soc., Chem. Commun.* 1971, 1207.
13. H. J. McCarthy and D. A. Tocher, to be published.
14. A. R. Chakravarty, F. A. Cotton, D. A. Tocher and J. H. Tocher, *Organometallics* 1985, **4**, 8.
15. E. C. Morrison and D. A. Tocher, *Inorg. Chim. Acta* 1989, **157**, 139.
16. W. Depmeier, K. Dietrich, K. König, H. Musso and W. Weiss, *J. Organomet. Chem.* 1986, **314**, C1.
17. F. A. Cotton and G. W. Rice, *Nouv. J. Chim.* 1977, **1**, 301.

Observations of an $[\text{Ru}_2]^{n+}$ Unit ($n = 3, 4, 5, 6$):
Electrochemical Studies into the Molecule
 $\text{Ru}_2(\text{MeC}_5\text{NH}_3\text{NH})_3(\text{O}_2\text{CCH}_3)\text{Cl}$ in Dimethyl
Sulphoxide

HOLLY J. McCARTHY and DEREK A. TOCHER*

Department of Chemistry, University College London,
20 Gordon St., London WC1H 0JA, U.K.

(Received November 8, 1988)

The redox chemistry of dinuclear molecules containing metal-metal bonds is an area of rapidly growing interest. The metals rhenium, rhodium and ruthenium particularly lend themselves to this type of study as many of their compounds undergo complicated electron-transfer reactions to generate new molecules in which the formal metal-metal bond order has been altered. Our particular concern is with the redox properties of the dinuclear ruthenium(II/III) complexes in which the metals are connected by a bond of the order 2.5. Complexes containing this $[\text{Ru}_2]^{5+}$ unit have been the subject of numerous electrochemical reports [1-11]. Several compounds, for example the carboxylates $\text{Ru}_2(\text{O}_2\text{CR})_4\text{Cl}$ [1] and $\text{Ru}_2(\text{HNCOCF}_3)_4\text{Cl}$ [2], have been observed to undergo one-electron reductions to give diruthenium(II/II) compounds, while others, e.g. $\text{Ru}_2(\text{Me}_3\text{CCONH})_4\text{Cl}$ [11], undergo oxidation to the related diruthenium(III/III) compounds. In a limited number of cases a single compound can be both oxidised and reduced in reversible one-electron steps. For example, the series of complexes $\text{Ru}_2(\text{RNpyr})_4\text{Cl}$ can be oxidised to the cations $[\text{Ru}_2(\text{RNpyr})_4\text{Cl}]^+$ and reduced to the anions $[\text{Ru}_2(\text{RNpyr})_4\text{Cl}]^-$ [6, 10]; the former contain a ruthenium-to-ruthenium triple bond while the latter contain a double bond between the metal ions. Thus it is the dinuclear cores $[\text{Ru}_2]^{4+}$, $[\text{Ru}_2]^{5+}$ and $[\text{Ru}_2]^{6+}$ which have been recorded for this class of molecule. We now wish to report the electrochemical behaviour of a new diruthenium molecule $\text{Ru}_2(\text{MeC}_5\text{NH}_3\text{NH})_3(\text{O}_2\text{CCH}_3)\text{Cl}$. This molecule is unusual in that it cannot only be oxidised to the diruthenium(III/III) cation but can also be sequentially reduced in two one-electron steps to yield what is formally a diruthenium(II/I) complex ion, containing an $[\text{Ru}_2]^{3+}$ core and a bond of the order 1.5 between the metal ions.

Results and Discussion

The new compound $\text{Ru}_2(\text{MeC}_5\text{NH}_3\text{NH})_3(\text{O}_2\text{CCH}_3)\text{Cl}$ was prepared using a general method de-

* Author to whom correspondence should be addressed.

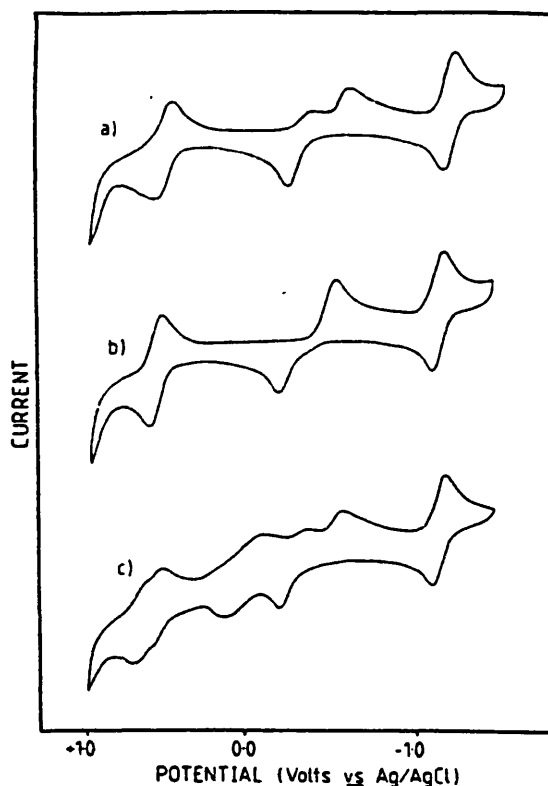


Fig. 1. Cyclic voltammograms of $\text{Ru}_2(\text{MeC}_5\text{NH}_3\text{NH})_3(\text{O}_2\text{CCH}_3)\text{Cl}$ in DMSO: (a) no added ions; (b) excess of Cl^- ions added; (c) less than one equivalent of Ag^+ ions added.

scribed previously [10]. The dinuclear structure was confirmed by an X-ray diffraction study [12].

The complex was sufficiently soluble in dimethyl sulphoxide for its redox behaviour to be studied by cyclic voltammetry. In a solution containing 0.1 M $[\text{N}(\text{C}_4\text{H}_9)_4][\text{BF}_4]$ as supporting electrolyte there are three well-defined responses in the potential range +1.0 to -1.6 V^\dagger , as shown in Fig. 1a. The electron-transfer reactions at *ca.* -0.5 and -1.5 V can be assigned as reductions of the dinuclear molecule, while that at *ca.* $+0.55 \text{ V}$ is due to oxidation. The one-electron nature of the reduction processes was confirmed by comparison of the diffusion-limited currents in the stirred voltammograms with those obtained from known quantities of ferrocene.

The first reduction process contains two components, at -0.41 and -0.64 V . This observation is not altogether surprising and can be rationalised by invoking the establishment of equilibria between different axially solvated dinuclear units in solution.

[†] All potentials were measured with respect to an Ag/AgCl reference electrode against which ferrocene was oxidised at a potential of $+0.60 \text{ V}$.

Such equilibria have been described previously [2, 3, 10, 11]. Although there are three components in equilibrium, only two waves are observed and therefore two of the components must be in rapid equilibrium. Surprisingly, only a single reoxidation wave is observed at -0.27 V (Fig. 1a), implying that the three reduced species $[\text{ClRu}^{\text{II}}(\text{MeC}_5\text{NH}_3\text{NH})_3(\text{O}_2\text{CCH}_3)\text{Ru}^{\text{II}}\text{Cl}]^{2-}$, $[(\text{DMSO})\text{Ru}^{\text{II}}(\text{MeC}_5\text{NH}_3\text{NH})_3(\text{O}_2\text{CCH}_3)\text{Ru}^{\text{II}}\text{Cl}]^{1-}$ and $[(\text{DMSO})\text{Ru}^{\text{II}}(\text{MeC}_5\text{NH}_3\text{NH})_3(\text{O}_2\text{CCH}_3)\text{Ru}^{\text{II}}(\text{DMSO})]^0$ are in rapid equilibrium. On scanning to more negative potentials, a second reduction wave is observed at ca. -1.3 V. The current carried by this reversible wave is equal to that of its precursor. The observation of only a single wave confirms that the various mono-reduced species are in rapid equilibrium. Although the observation of a second reduction wave is not entirely unprecedented, previously such waves have either been highly irreversible or alternatively assigned to the reduction of coordinated ligands [4]. Addition of the free ligand to the electrochemical solution does not affect the reversibility of the process and argues for the reduction of the dinuclear unit to one which formally contains a diruthenium(II/I) centre. Although both reduction products are stable on the cyclic voltammetric timescale, spectroelectrochemical measurements in dimethyl sulphoxide show that the reduced complexes undergo slow chemical decomposition.

The oxidation wave at $+0.56$ V is uncomplicated although a slight broadness in the peaks may be consistent with the equilibrium between differently axially substituted molecules occurring on a time-scale comparable to that of the electrochemical experiment.

Addition of an excess of chloride ions to the electrochemical cell results in a sharpening of the voltammetric peaks and the loss of the reduction wave at -0.41 V (Fig. 1b). The three waves observed each carry an identical current (within 2%) and are assigned to reductions or the oxidation of the bis-chloride adduct $[\text{ClRu}(\text{MeC}_5\text{NH}_3\text{NH})_3(\text{O}_2\text{CCH}_3)\text{RuCl}]^-$, as appropriate.

Addition of less than one equivalent of Ag^+ ions to the electrochemical cell displaces the equilibrium between the different axially ligated species in the direction of the bisdimethyl sulphoxide adducts. In the cyclic voltammogram (Fig. 1c), new reduction and oxidation waves are observed at -0.15 and $+0.75$ V, respectively, which must be assigned to the bis solvent adduct $[(\text{DMSO})\text{Ru}(\text{MeC}_5\text{NH}_3\text{NH})_3(\text{O}_2\text{CCH}_3)\text{Ru}(\text{DMSO})]^+$. Surprisingly, neither the addition of Cl^- ions nor Ag^+ ions has any significant observable effect on the character of the second reduction process, under the experimental conditions which were employed.

Further studies into the kinetics of axial ligand exchange are in progress.

Acknowledgement

We wish to thank Johnson Matthey plc for generous loans of ruthenium trichloride.

References

- 1 F. A. Cotton and E. Pedersen, *Inorg. Chem.*, **14** (1975) 388.
- 2 T. Malinski, D. Chang, F. N. Feldman, J. L. Bear and K. M. Kadish, *Inorg. Chem.*, **22** (1983) 3225.
- 3 M. Y. Chavan, F. N. Feldman, X. Q. Lin, J. L. Bear and K. M. Kadish, *Inorg. Chem.*, **23** (1984) 2373.
- 4 A. R. Chakravarty, F. A. Cotton and D. A. Tocher, *J. Am. Chem. Soc.*, **106** (1984) 6409.
- 5 A. R. Chakravarty, F. A. Cotton and D. A. Tocher, *Inorg. Chem.*, **24** (1985) 2857.
- 6 A. R. Chakravarty, F. A. Cotton, D. A. Tocher and J. H. Tocher, *Polyhedron*, **4** (1985) 1475.
- 7 A. R. Chakravarty, F. A. Cotton and W. Schwotzer, *Polyhedron*, **5** (1986) 1821.
- 8 L. F. Warren and V. L. Goedken, *J. Chem. Soc., Chem. Commun.*, (1978) 909.
- 9 A. R. Chakravarty and F. A. Cotton, *Inorg. Chim. Acta*, **113** (1986) 19.
- 10 D. A. Tocher, *Inorg. Chim. Acta*, **115** (1986) 51.
- 11 K. Ryde and D. A. Tocher, *Inorg. Chim. Acta*, **118** (1986) L49.
- 12 In preparation.